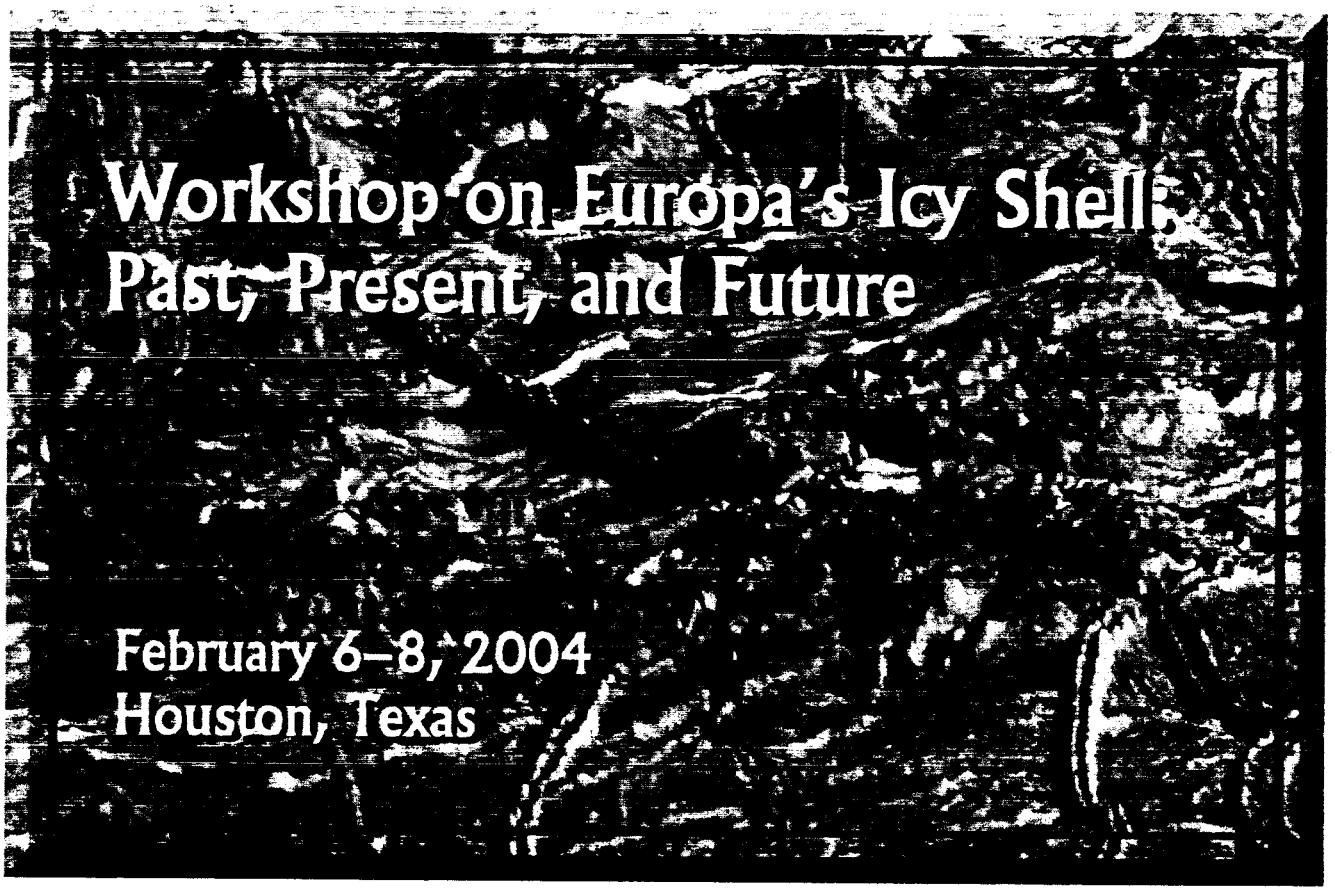

WORKSHOP PROGRAM AND ABSTRACTS

Workshop on Europa's Icy Shell: Past, Present, and Future

February 6–8, 2004
Houston, Texas

— Sponsored by —

Lunar and Planetary Institute
National Aeronautics and Space Administration

— Scientific Organizing Committee —

Adam Showman, *University of Arizona*
William McKinnon, *Washington University*
Simon Kattenhorn, *University of Idaho*
Jeffrey Kargel, *U.S. Geological Survey*
Paul Schenk, *Lunar and Planetary Institute*
Francis Nimmo, *University College, London*
Louise Prockter, *Johns Hopkins University, APL*

— Conveners —

Paul Schenk, Lunar and Planetary Institute
Francis Nimmo, University of London
Louise Prockter, Johns Hopkins University, APL

Lunar and Planetary Institute 3600 Bay Area Boulevard Houston TX 77058-1113

LPI Contribution No. 1195

Compiled in 2004 by
LUNAR AND PLANETARY INSTITUTE

The Institute is operated by the Universities Space Research Association under Agreement No. NCC5-679 issued through the Solar System Exploration Division of the National Aeronautics and Space Administration.

Abstracts in this volume may be cited as

Author A. B. (2004) Title of abstract. In *Workshop on Europa's Icy Shell: Past, Present, and Future,* p. XX. LPI Contribution No. 1195, Lunar and Planetary Institute, Houston.

This volume is distributed by

ORDER DEPARTMENT
Lunar and Planetary Institute
3600 Bay Area Boulevard
Houston TX 77058-1113, USA
Phone: 281-486-2172
Fax: 281-486-2186
E-mail: order@lpi.usra.edu

Mail orders requestors will be invoiced for the cost of shipping and handling.

ISSN No. 0161-5297

Preface

This volume contains abstracts that have been accepted for presentation at the workshop on Europa's Icy Shell: Past, Present, and Future, February 6–8, 2004, Houston, Texas.

Administration and publications support for this meeting were provided by the staff of the Publications and Program Services Department at the Lunar and Planetary Institute.

Contents

Program

Friday, February 6, 2004

INTRODUCTION
8:30 a.m. Lecture Hall

Chair: **P. M. Schenk**

8:30 a.m. Schenk P. M.
Welcoming Remarks

8:40 a.m. McKinnon W. B. * [INVITED]
Overview of Europa's Icy Shell: Questions of Thickness, Composition, Rheology, Tectonics, and Astrobiological Potential **[#7048]**

COMPOSITION
9:20 a.m. Lecture Hall

Chairs: **W. B. McKinnon**
R. T. Pappalardo

9:20 a.m. Kargel J. S. * [INVITED]
Composition and Geochemical Evolution of Europa's Icy Shell **[#7006]**

10:00 – 10:10 a.m. **Break**

10:10 a.m. McCord T. B. * Orlando T. M. Hansen G. B. Hibbitts C. A.
Hydrated Materials on Europa's Surface: Review of Current Knowledge and Latest Results **[#7044]**

10:25 a.m. Carlson R. W. *
Distribution of Hydrogen Peroxide, Carbon Dioxide, and Sulfuric Acid in Europa's Icy Crust **[#7031]**

10:40 a.m. Clark R. N. *
Surface Composition of Europa: Mixed Water, Hydronium, and Hydrogen **[#7057]**

10:55 a.m. Dalton J. B. * Jamieson C. S. Quinn R. C. Prieto-Ballesteros O. Kargel J.
Highly Hydrated Sulfate Salts as Spectral Analogs to Disrupted Terrains on Europa **[#7049]**

11:10 a.m. Gomis O. * Satorre M. A. Leto G. Strazzulla G.
Molecules Produced on the Surface of Europa by Ion Implantation in Water Ice **[#7002]**

11:25 a.m. Moore M. H. Hudson R. L. * Carlson R. W. Ferrante R. F.
Formation and Stability of Radiation Products in Europa's Icy Shell **[#7009]**

11:40 a.m. Prieto-Ballesteros O. * Kargel J. S. Fernández-Sampedro M. Hogenboom D. L.
Clathrate Hydrates in Jupiter's Satellite Europa and Their Geological Effects **[#7010]**

11:55 – 12:20 p.m. **Discussion**

12:20 – 1:30 p.m. **Lunch**

Friday, February 6, 2004

PHYSICAL PROPERTIES
1:30 p.m. Lecture Hall

Chairs: **S. A. Kattenhorn**
J. R. Spencer

1:30 p.m. Kohlstedt D. L. * [INVITED]
Deformation of Ice **[#7054]**

2:00 p.m. Blankenship D. D. * Morse D. L. [INVITED]
Earth's Ice Sheets and Ice Shelves as an Analog for Europa's Icy Shell **[#7053]**

[Canceled] Duval P. * Montagnat M.
The Rheology of Ice at Low Stresses; Application to the Behavior of Ice in the Europan Shell **[#7001]**

2:25 p.m. Barr A. C. * Pappalardo R. T.
Numerical Implementation of Ice Rheology for Europa's Shell **[#7018]**

2:40 p.m. Nimmo F. *
What is the Young's Modulus of Ice? **[#7005]**

2:55 p.m. Sandwell D. T. *
Limits on the Strength of Europa's Icy Shell from Topographic Spectra **[#7043]**

3:10 – 3:45 p.m. **Break**

3:45 p.m. Turtle E. P. * [INVITED]
What Europa's Impact Craters Reveal: Results of Numerical Simulations **[#7020]**

4:10 p.m. Phillips C. B. * Chyba C. F.
Impact Gardening, Sputtering, Mixing, and Surface-Subsurface Exchange on Europa **[#7036]**

4:25 p.m. Spencer J. R. * [INVITED]
Thermal Properties of Europa's Ice Shell **[#7040]**

4:50 p.m. Eluszkiewicz J. *
Assessing Porosity Structure in Europa's Crust **[#7014]**

5:05 – 5:35 p.m. **Discussion**

Friday, February 6, 2004

POSTERS
5:40 p.m. Great Room

Konesky G. A.
Can the Electronic Tongue be Given a Taste for Life? **[#7007]**

Lipps J. H.
Europa's Icy Crust as a Habitat and Repository of Life **[#7015]**

Myrick T. Frader-Thompson S. Wilson J. Gorevan S.
Development of an Inchworm Deep Subsurface Platform for in Situ Investigation of Europa's Icy Shell **[#7041]**

Cooper J. F. Johnson R. E. Waite J. H.
Remote Sensing of Europa Surface Composition with Ions, Neutral Atoms, and X-Rays in the Local Space Environment **[#7019]**

Biele J. Ulamec S. Parpart A.
Melting Probe Tests in Thermal Vacuum **[#7013]**

Wurz P. Rohner U. Whitby J. A.
A Highly Miniaturised Laser Ablation Time-of-Flight Mass Spectrometer for Planetary Exploration **[#7003]**

Collier M. R. Sittler E. Chornay D. Cooper J. F. Coplan M. Johnson R. E.
Remote Sensing of Icy Galilean Moon Surface and Atmospheric Composition Using Low Energy (1 eV–4 keV) Neutral Atom Imaging **[#7022]**

Hand K. P. Carlson R. W. Chyba C. F.
Empirical Determination of Radiolytic Products in Simulated Europan Ices **[#7029]**

Markus T. Gogineni S. P. Green J. L. Fung S. F. Cooper J. F. Taylor W. W. L. Garcia L.
Reinisch B. W. Song P. Benson R. F. Gallagher D.
Surface Penetrating Radar Simulations for Europa **[#7016]**

Crawford Z. A. Pappalardo R. T. Collins G. C.
Creating a Georeferenced Digital Image Library of Europa **[#7035]**

Schenk P. Moore J. M.
High-Resolution Mapping of Europa's Impact Craters: Comparison with Ganymede **[#7051]**

Qin R. Buck W. R. Pappalardo R. T.
Europan Bands Formed by Stretching the Icy Crust: A Numerical Perspective **[#7030]**

Kereszturi A.
Implication on Possible Submarin Biosignatures at Chaotic Terrains **[#7011]**

Saturday, February 7, 2004

AGES AND STRATIGRAPHY
8:30 a.m. Lecture Hall

Chairs: **E. P. Turtle**
P. E. Geissler

8:30 a.m. Zahnle K. * Schenk P. Dones L. Levison H. [INVITED]
Cratering Rates in the Jovian System **[#7052]**

8:55 a.m. Prockter L. M. * Figueredo P. H. [INVITED]
Geological Features and Resurfacing History of Europa **[#7056]**

9:35 a.m. Schenk P. M. *
Sinking to New Lows & Rising to New Heights: The Topography of Europa **[#7046]**

10:15 – 10:35 a.m. **Break**

TIDAL DEFORMATION
10:35 a.m. Lecture Hall

Chairs: **P. E.Geissler**
E. P. Turtle

10:35 a.m. Moore W. B. * [INVITED]
Tidal Deformation and Tidal Dissipation in Europa **[#7055]**

11:05 a.m. Bills B. G. *
Long Period Variations in Tidal and Librational Forcing of Europa **[#7025]**

11:20 a.m. Figueredo P. H. * [INVITED]
Geological Constraints on Tidal and Rotational Deformation on Europa **[#7045]**

11:50 a.m. Kattenhorn S. A. *
What is (and Isn't) Wrong with Both the Tension and Shear Failure Models for the Formation of Lineae on Europa **[#7023]**

12:05 p.m. Marshall S. T. * Kattenhorn S. A.
Analysis of Europan Cycloid Morphology and Implications for Formation Mechanisms **[#7026]**

12:20 – 12:50 p.m. **Discussion**

12:50 – 1:50 p.m. **Lunch**

Saturday, February 7, 2004

THERMAL EVOLUTION AND TECTONICS
1:50 p.m. Lecture Hall

Chairs: **A. P. Showman**
P. H. Figueredo

1:50 p.m. Nimmo F. * [INVITED]
Lateral and Vertical Motions in Europa's Ice Shell **[#7004]**

2:20 p.m. Hussmann H. * Spohn T.
Europa's Ice Shell Thickness Derived from Thermal-Orbital Evolution Models **[#7012]**

2:35 p.m. Sotin C. * Choblet G. Head J. W. Mocquet A. Tobie G.
Thermal Evolution of Europa's Icy Crust **[#7017]**

2:50 p.m. Stempel M. M. * Barr A. C. Pappalardo R. T.
Constraints on the Opening Rate of Bands on Europa **[#7027]**

3:05 p.m. Manga M. * Sinton A.
Wax Models of Europan Tectonics **[#7008]**

3:20 p.m. Patterson G. W. * Head J. W. III
Numerical Modeling of Plate Motion: Unraveling Europa's Tectonic History **[#7038]**

3:35 – 3:55 p.m. **Break**

3:55 p.m. Geissler P. E. * [INVITED]
Origin of Chaos Terrain **[#7050]**

4:25 p.m. Tobie G. * Choblet G. Lunine J. Sotin C.
Interaction Between the Convective Sublayer and the Cold Fractured Surface of Europa's Ice Shell **[#7033]**

4:40 p.m. Pappalardo R. T. * Barr A. C.
Domes on Europa: The Role of Thermally Induced Compositional Diapirism **[#7047]**

4:55 p.m. Zolotov M. Yu. * Shock E. L. Barr A. C. Pappalardo R. T.
Brine Pockets in the Icy Shell on Europa: Distribution, Chemistry, and Habitability **[#7028]**

5:10 – 5:40 p.m. **Discussion**

6:00 p.m. **Dinner in Galveston via bus (advance reservations required)**

Sunday, February 8, 2004

OCEANS AND EXPLORATION
8:30 a.m. Lecture Hall

Chairs: **G. C. Collins**
D. D. Blankenship

8:30 a.m. Makris N. C. * Lee S. Pappalardo R. T.
Probing Europa's Interior with Natural Sound Sources **[#7024]**

8:45 a.m. Peters M. E. * Blankenship D. D. Morse D. L.
Radar Sounding Studies for Quantifying Reflection and Scattering at Terrestrial Air-Ice and Ice-Ocean Interfaces Relevant to Europa's Icy Shell **[#7034]**

9:00 a.m. Winebrenner D. P. * Blankenship D. D. Campbell B. A.
Physical Basis for the Radar Observation of Geological Structure in the Ice Shell on Europa **[#7037]**

9:15 a.m. Vance S. D. * Brown J. M. Spohn T. Shock E.
Subsurface Action in Europa's Ocean **[#7039]**

9:30 a.m. Collins G. C. * Goodman J. C.
Hydrothermal Plumes and Heating Europa's Ice Shell from Below **[#7032]**

9:45 a.m. Niebur C. * [INVITED]
JIMO Status

10:00 – 10:20 a.m. **Break**

PANEL DISCUSSION
10:20 a.m. Lecture Hall

Chair: **G. Schubert**

10:20 a.m. Johnson T. V. McKinnon W. B. Melosh H. J. Moore J. M. Schubert G.
Experts (Graybeard) Panel and Workshop Discussions

11:45 a.m. **Closing Remarks**

NUMERICAL IMPLEMENTATION OF ICE RHEOLOGY FOR EUROPA'S SHELL. A. C. Barr, R. T. Pappalardo, *Laboratory for Atmospheric and Space Physics, Campus Box 392, University of Colorado, Boulder, CO 80309, (amy.barr@colorado.edu).*

We present a discussion of approximations to the temperature dependent part of the rheology of ice. We have constructed deformation maps using the superplastic rheology of *Goldsby & Kohlstedt, 2001*, and find that the rheologies that control convective flow in the Europa's are likely grain boundary sliding (Q*=49 kJ/mol, n=1.8, p=1.4) and basal slip (Q*=60 kJ/mol, n=2.4) for a range of grain sizes 0.1 mm $< d <$ 1 cm. We compare the relative merits of two different approximations to the temperature dependence of viscosity and argue that for temperature ranges appropriate to Europa, implementing the non-Newtonian, lab-derived flow law directly is required to accurately judge the onset of convection in the ice shell and temperature gradient in the near-surface ice.

Deformation Maps: Deformation maps for ice I were constructed using the rheology of *Goldsby & Kohlstedt, 2001*, which expresses a composite flow law for ice I as the sum of four individual flow laws with different dependence upon temperature, strain-rate and grain size. The deformation map shows the locus of points in $\sigma - T$ space where the strain rate from each pair of flow laws are equal. The flow law that contributes the largest strain rate is judged to be dominant in that region. Maps for $d = 0.1$ mm and $d = 1$ cm, which bracket common estimates of the grain size within Europa's ice shell [*McKinnon, 1999*], are shown in Figure 1 a,b. For the low (~ 0.01 MPa) convective stresses in an ice shell 10's of km thick, the controlling rheology of the ice shell is grain boundary sliding, but basal slip can become important if the grain size is small.

Implementing Temperature Dependence: There is a common method of approximating temperature-dependent rheology used by the Earth mantle convection community [e.g. *Solomatov, 1995*] and applied to icy satellite convection [*McKinnon, 1999*; *Nimmo & Manga, 2002*] which approximates the lab-derived flow law ($\eta \sim exp(Q^*/RT)$) as $\eta \sim exp(-\gamma T)$ where γ is the Frank-Kamenetskii (FK) parameter:

$$\gamma = \left.\frac{\partial(\ln \eta)}{\partial T}\right|_{T_i}. \quad (1)$$

Here T_i is the interior temperature of the ice shell, which is not known *a priori*, but is typically close to the melting point (T_m) so it is assumed that $\gamma = Q^*/nRT_m^2$. The viscosity contrast across the convecting layer $\Delta\eta = \exp(E\Delta T)$. Use of this approximation results in lower surface viscosities than predicted by the lab-derived flow law. This does not affect the outcome of stagnant-lid (large $\Delta\eta$) convection simulations, provided the resulting $\Delta\eta$ is high enough that the surface ice remains immobile ($\Delta\eta > 10^4$). For grain boundary sliding within Europa's ice shell, $\gamma\Delta T \sim 7.75$ and $\Delta\eta = 5 \times 10^3$. This relatively low $\Delta\eta$ results in a sluggish lid convection, where the top-most layer of cold ice has a low enough viscosity to particpate in convective flow by being dragged along the surface of the convecting region.

An alternative way to approximate the temperature dependence of ice viscosity to use a best-fit, temperature-linearized flow law of form [*Reese, et al., 1999*]:

$$\eta(T) = b\exp(-\bar{E}T) \quad (2)$$

where the parameters $\bar{E}$ and b are determined from a least-squares fit to the lab-derived flow law. For grain boundary sliding in the Europan temperature range T_s=100 K to T_m=260 K, the best-fit line underestimates the lab-derived flow law by a factor of $\sim 10 - 100$ at the base of the ice shell. This does not change the physics of the stagnant lid convection within the ice shell, which is most sensitive to the viscosity at the base of the rheological lithosphere, not at the base of the ice shell [*Reese, et al., 1999*]. It does have a large effect the critical thickness at which the ice shell begins to convect. For example, an artifical underestimate of viscosity at T_m by a factor of ~ 100 results in an underestimate of critical shell thickness for the onset of convection of order $(100)^{1/3} \sim 5$.

A plot comparing these approximations to $\eta(T)$ and the lab-derived flow law is shown in Figure 1c.

Comparison Between Rheological Approximations and Lab-Derived Law: We performed three numerical simulations using the Citcom finite element software [*Moresi and Gurnis, 1996; Zhong, et al., 1998; Zhong, et al., 2000*] in order to compare the accuracy of these two approximations. All three simulations had a Rayleigh number of 2×10^6 and constant temperature boundary conditions with T_s=100 K and T_m=260 K, appropriate for Europa's ice shell. For grain boundary sliding with a grain size of 1 mm and strain rate of 10^{-10}s^{-1}, this corresponds to an ice shell thickness of $\sim$ 20 km. Since the temperature dependence of ice rheology is of key interest in this test, we did not implement the strain-rate dependence of viscosity.

Results from implementing the lab-derived flow law directly are shown in Figure 1d. An effective $\gamma\Delta T$ for this rheology was calculated using the T_i value obtained in this simulation, $T_i = 245$ K, which implies $\gamma\Delta T = 8.68$.

Results from implementing a temperature-linearized simulation with $\gamma\Delta T = 8.68$ are shown in Figure 1e. The viscosity contrast across the convecting layer implied by this rheology $\Delta\eta \sim 6 \times 10^3$, low enough to permit sluggish lid convection. As a result, the heat flow through the ice shell (Nu) in this simulation was 50% higher than the value obtained implementing the lab-derived flow law. The thickness of the stagnant lid δ_o, which scales roughly as $1/Nu$, is underestimated by 40% compared to the lab-derived law.

Results from implementing the best-fit linearized flow law are shown in Figure 1f. The viscosity contrast across the ice shell implied by the best-fit line is $\Delta\eta \sim 10^8$, predicting stagnant lid behavior. The heat flow through the ice shell agrees with the lab-law at the 10% level. Estimates of the interior temperature (T_i) are correct to within >5% in either approximation.

Discussion: If a temperature-linearized rheology must be

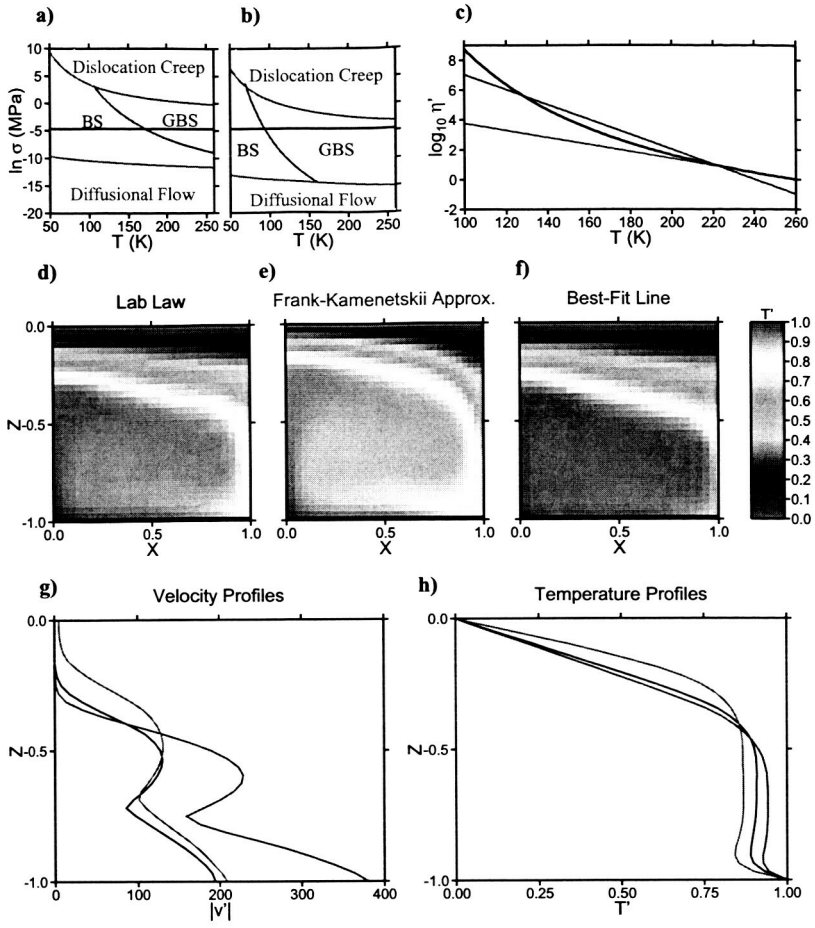

Figure 1: a) Deformation map for Ice I with grain size $d = 0.1$ mm. b) Deformation map for Ice I with grain size d=1 cm. Based on the rheology of *Goldsby & Kohlstedt, 2001*. BS=basal slip, GBS=grain boundary sliding. Purple horizontal line indicates approximate level of convective stress in Europa's ice shell, ~ 0.01 MPa. c) Approximations to the temperature dependent portion of the GBS rheology for d=1 mm within Europa's ice shell. Black: lab-derived flow law; Red: Frank-Kamenetskii approximation (FK) (eq. 1); Blue: best-fit, temperature-linearized law (eq. 2). Relative viscosity values (η') are scaled to the viscosity at the melting point of ice at T =260 K predicted by the GBS flow law. d) Isotherms calculated using the lab-derived GBS rheology with $Ra = 2 \times 10^6$. e) Isotherms calculated using an effective FK parameter (eq. 1) to approximate the GBS rheology. f) Isotherms calculated using a best-fit, temperature-linearized approximation of GBS rheology. g) Velocity profiles from the above simulations. The simulation employing an effective FK parameter has a non-zero surface velocity and is therefore in the sluggish lid regime of behavior due to the low $\Delta\eta$ predicted by this approximation. h) Temperature profiles from the above simulations. Both approximations to the lab-law predict the value of T_i to within a few percent.

used for numerical reasons, or to calculate bulk parameters of the ice shell using pre-existing scaling laws, using a best-fit linear flow law rather than the standard Frank-Kamenetskii approximation can provide more accurate values for the heat flux (Nu) and the stagnant lid thickness (δ_o). In order to accurately caputure the overall behavior of the ice shell, the appropriate creep regime of the lab-derived flow law should be implemented directly in numerical simulations. We are currently in the process of implementing this form of temperature dependence in conjunction with a fully strain-rate dependent ice rheology to understand the geological and astrobiological consequences of convection within Europa's ice shell.

Acknowledgements: Support for this work is provided by NASA GSRP grant NGT5-50337 and NASA Exobiology grant NCC2-1340.

References: Goldsby, D. L. and D. L. Kohlstedt, *JGR* v. 106, p. 11,017-11,030, 2001; Solomatov, V. S., *Ph. Fluids*, v. 7, p.266-274, 1995; Reese, C. C., et al., *Icarus* v. 139, p. 67-80, 1999; McKinnon, W. B. *GRL* v. 26, p. 951-954; Nimmo, F. and M. Manga, *JGR*; Zhong, S. M, et al., *JGR* v. 103, p. 15255-15268, 1998; Moresi, L. and M. Gurnis, *Earth and Planet. Sci. Lett.* v. 138, p. 15-28, 1996; Zhong, S. M. et al., *JGR* v. 105, p. 11,063-11,082, 2000.

MELTING PROBE TESTS IN THERMAL VACUUM. J. Biele[1], S. Ulamec[1] and A. Parpart[1],
[1]Institute for Space Simulation, German Aerospace Center (DLR), Linder Höhe, D 51147 Köln, Germany; jens.biele@dlr.de, stephan.ulamec@dlr.de, andre.parpart@dlr.de

Introduction: One of the most fascinating aspects of the Europa relevant science is the putative subglacial ocean. To probe this ocean in situ, only melting probes seem to be feasible. The principle of the technology has successfully been proven e.g. in Antarctica [6]. However, a principle difference (at least in the initial penetration) is the low pressure on Europa leading to sublimation rather than melting of the ice layer. Our measurements confirmes an extended theory that includes this effect and demonstrates the feasibility of the method. We how how the transition of sublimation to melting can take place after the "borehole" behind the probe has closed and sufficient pressure has been built up to sustain liquid water.

Theoretical background: In a simple energy balance approximation, neglecting all losses, we can approximate the heat needed to progress a distance l as;

$$\Delta W = Al\rho\,[c_p\,(t_F - t) + L_v] \qquad (1)$$

If the heating power is P, then the melting speed is

$$V = l\,P / \Delta W \qquad (2)$$
$$= P / A\rho\,[c_p\,(t_F - t) + L_v] \qquad (3)$$

where

A is the probe's cross-section (m^2), l is the probes length (m), c_p the specific heat capacity of ice (ranging from 1.5 kJ kg^{-1} K^{-1} to 2.2 kJ kg^{-1} K^{-1}), ρ the density of the ice (~920 kg m^{-3}), L_V the heat of fusion of the ice (~330 kJ kg^{-1}) resp. the heat of sublimation of ice (~2500 kJ kg^{-1}), t_F the melting/sublimation temperature of the ice (K) and t is the local ice temperature (K)

Eq. (3) easily shows that the penetration velocity under sublibmation conditions should be ~7.6 times slower than under melting condition.
An important point here is that the melting velocity scales with the inverse of the cross-sectional area of the probe. Hence the usual design is a cylindrical tube with a large (>10) aspect ratio (length/diameter).

A more sophisticated theory was laid out by [5] and confirmed by [1-4]. Briefly, with an optimal design, about 20% more power has to be expended for a given melting velocity than is suggested by eq. 5. This is because a hole with a slightly bigger cross-section than the probe has to be melted to permit the flow of melt water resp. steam and the conductive heat losses in the surrounding ice have to be accounted for. Great care has to be taken, particularly in cold ice, to ensure that the re-freezing of the ice is slow compared to the melting velocity, in order not to block the probe. Alternative proposals for melting probes foresee heating elements distributed along the length of the probe for that reason.

Experimental setup: Fig. 1 shows the experimental melting probe used here. Its copper melting head can be heated with 200, 400 or 600 W (230V AC) and bears a Pt100 to control the head's temperature. The cylindrical body is hollow yet watertight; the tether is for now externally spooled by a motor, controlled by a force sensor in the tether so the probe is automatically lowered whenever it has sufficiently advanced. An optical counter on the tether wheel senses the depth of the probe.

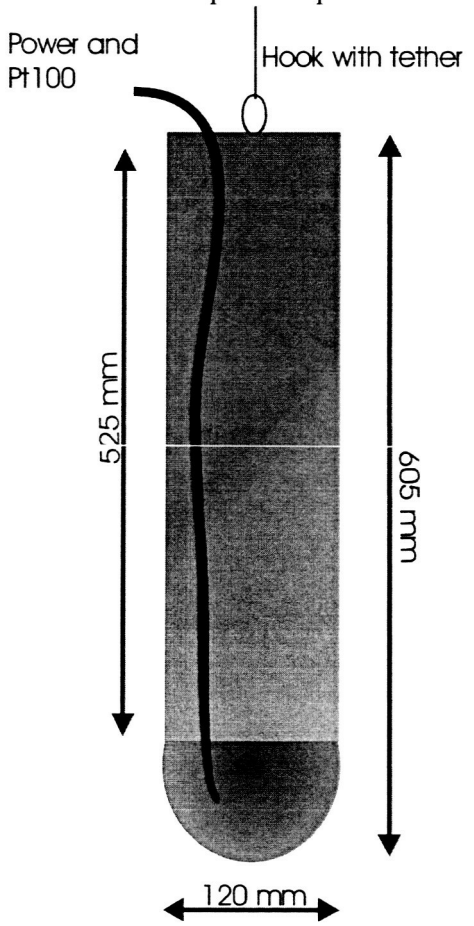

Fig.1: Melting probe (AWI design with refurbishments)

For the thermal vacuum experiments, we use the existing planetary simulation chamber at DLR Cologne Technical data of this chamber is shown in fig.2. The size of the experimental space is as follows: diameter 1.4m, height 1.8m. Cooling system: LN2 (77K)

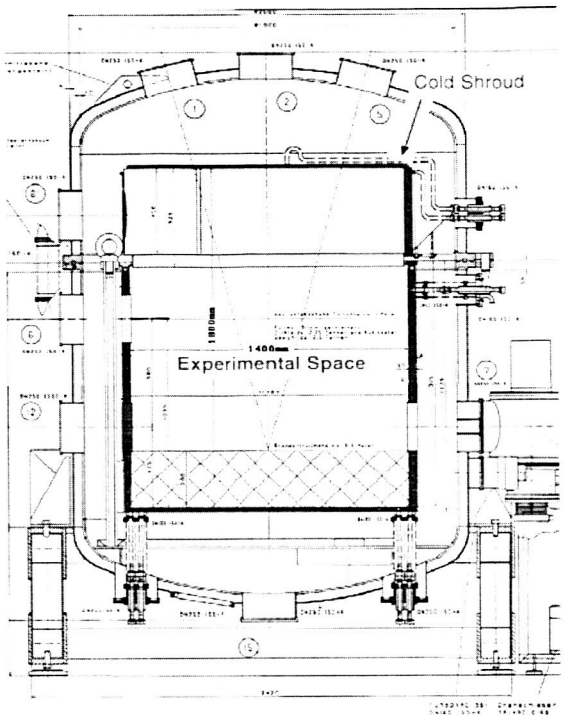

Fig. 2: Thermal vacuum chamber

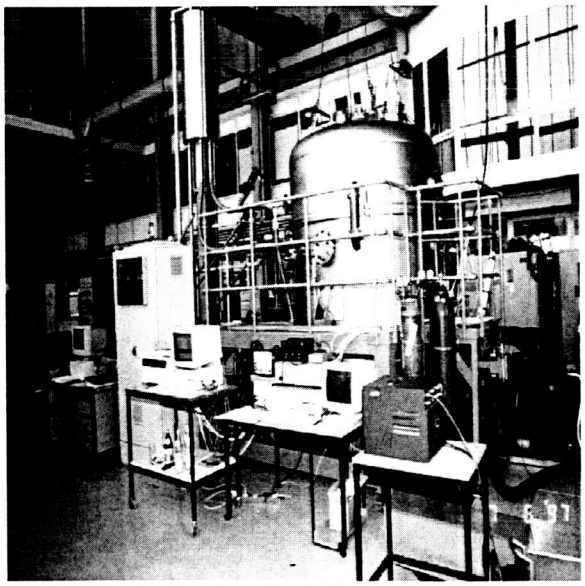

Fig. 3: The Planetary Simulation Facility.

Results: First experiments of melting in ice of -20°C under atmospheric pressure have confirmed that eqn (2) holds,with some 20% losses to be taken into account. In vacuum (ca. 1 mbar, mostly water vapour), however, the penetration velocity after first results appears to be drastically lower. Experiments with different ice temperatures (down to 77 K) and different heater powers (200-600 W) are in progress. Due to freezing of the tether behind the probe once a sufficient depth had been reached, the full process of closing the borehole under vacuum conditions could not yet be fully observed. We plan to refurbish the probe with an internal tether spooler mechanism in the next step.

References: [1] Aamot H.W.C.(1967a) J. Glaciol. Vol 6, 935-939. [2] Aamot H.W.C. (1967b) CRREL Special Report 119, Cold Regions Research & Engineering Laboratory, Hanover, New Hamphire. [3] Aamot H.W.C. (1967c) CRREL Special Report 194, Cold Regions Research & Engineering Laboratory, Hanover, New Hamphire. [4] Aamot H.W.C. (1968) CRREL Special Report 210, Cold Regions Research & Engineering Laboratory, Hanover, New Hamphire. [5] Shreve R.L. (1962) J. Glaciol. 4, 151-160, 1962. [6] Biele, J., Ulamec, S, Garry, J. et al. (2002) Proceedings of the Second European Workshop on Exo/Astrobiology Graz, Austria, 16-19 September 2002 (ESA SP-518, November 2002), 253-260

LONG PERIOD VARIATIONS IN TIDAL AND LIBRATIONAL FORCING OF EUROPA

Bruce G. Bills NASA/GSFC, Greenbelt, MD 20771 Bruce.G.Bills@nasa.gov

Introduction: The gravitational field of Jupiter exerts a profound influence on the energy balance, thermal evolution, and stress regime of Europa. It is widely appreciated that dissipation associated with the spheroidal tidal deformation is a major source of heat [1, 2, 3, 4]. Another possibly important source of dissipation is the toroidal deformation field associated with forced librations [5, 6, 7]. Both tidal and librational deformations depend on the distance and direction to Jupiter, as seen from Europa. These quantities vary with time as a result of the finite values of orbital eccentricity and spin pole obliquity, though the obliquity effects have been ignored in most previous studies.

Variations in eccentricity and obliquity of the Galilean satellites occur on a very wide range of time scales, as angular momentum is exchanged among the orbital and rotational components of the coupled system. The orbital periods are only a few days in length, and the secular changes in orbital period associated with tidal and librational dissipation have characteristic time scales of 10^9 years or longer [8, 9, 10]. On intermediate time scales, the satellites perturb each other, and the Sun and Saturn make additional contributions.

The present values of satellite orbital inclinations and obliquities are not particularly representative of their respective longer term variations. As a result, the tidal stress and dissipation regimes at present may not provide adequate explanation of the sources of surface features seen on the satellites.

Obliquity: On relatively short time scales ($<10^4$ years), the satellite inclinations and obliquities can be approximated by a model which treats the spin pole of Jupiter as inertially fixed. In that case, each satellite orbit plane responds to torques from the oblate figure of Jupiter, mutual interaction with the other satellites, and a weak solar torque. The free oscillation periods of this system are (7.358, 29.63, 139.97, and 547.89) years. Motions of the satellite spin poles are driven by torques from Jupiter, acting on the oblate figures of the satellites. The spin pole precession periods are (0.66, 5.16, 31.9, and 320) years for Io, Europa, Ganymede and Callisto, respectively.

In order to understand longer term variations in forced obliquities of the Galilean satellites, and the resulting variations in tidal forcing, we have investigated the response of the system composed of four satellite orbits and the spin of Jupiter to varying solar torques. The solar torque varies as the orbital inclination of Jupiter varies, on time scales of 10^5-10^6 years. The dominant source of orbital variation is exchange of angular momentum between the orbits of Jupiter, Saturn, Uranus, and Neptune. In the secular variation model of Laskar [11] there are 50 Fourier terms representing the orbit pole of Jupiter.

The response of each of the objects (Jupiter's spin and satellite orbits) is a weighted sum of normal mode responses, with weights proportional to the forcing amplitude but also determined by proximity of the forcing period to the normal mode period. The free oscillation periods of the 5-body system are (7.365, 29.635, 139.56, 546.16, and 536,500) years. The spin pole precession period of Jupiter, without satellites, would be 980 kyr, but solar torques on the satellite orbits, coupled to Jupiter via its oblateness, shorten that period to 536 kyr. The largest source of uncertainty in this estimate is the polar moment of inertia of Jupiter, which has a 4% uncertainty.

One of the larger terms in Laskar's secular orbital model is nearly in resonance with the lowest frequency term in the 5-body system. This allows substantial variations in the obliquity of Jupiter and the satellite orbital inclinations on 10^5 year time scales. As the satellite orbits evolve under tidal influence, the strength of resonant forcing will vary.

Eccentricity: A similar secular variation model can be applied to estimate changes in orbital eccentricity within the Galilean satellite system. The principle difference is that mean motion resonances among the satellites pump up the eccentricity values and increase the rates of apsidal advance. The free oscillation periods of this system are (6.121, 21.21, 138.35, and 535.84) years [12]. As was seen above for the spin and orbit poles, the eccentricities are also subject to longer period perturbations associated with changes in the orbit of Jupiter.

If the only mechanisms at work were a competition between tidal dissipation, which tends to circularize orbits, and mean motion resonances, which increases eccentricity, then a steady state could conceivably be achieved, or oscillations might arise from the feedback between dissipation rate and internal heating [13]. In that case, the only interesting time scales would be the orbital periods of the satellites (a few days) and the heat transport time across the lithospheric thermal

boundary layer (highly uncertain, but likely millions of years) [13,14,15].

The presence of dynamical forcing at intermediate time scales of 10^1-10^2 years (from mutual perturbations of the satellite orbits) and 10^4-10^6 years (from changes in the orbit of Jupiter), suggests that formation of surface features on Europa might occur on some of these longer time scales.

Tides and Librations: An arbitrary displacement field in an incompressible material can be uniquely expressed as a sum of spheroidal and toroidal components. In an isotropic body, tidal deformation is purely spheroidal and that due to differential libration is purely toroidal.

The source of tidal dissipation is the stress and strain rate induced by changes in the gravitational potential at Europa as the distance and direction from Europa to Jupiter change over an orbital period, due to finite orbital eccentricity [1, 2, 3] and obliquity [16]. The ultimate source of librational dissipation is radial variation in the amplitude of forced librations [5, 6, 7], or small departures from steady rotation, which arise from torques exerted by Jupiter on the tidally deformed body of Europa.

The spatial patterns of dissipative heating and near-surface stress associated with tides and librations depend on both the internal structure of the body and on the external forcing. Simplistic models of the external forcing may lead to erroneous inferences about internal structure from observed surface features.

Cycloidal fractures may be due to tides (and/or librations) without being formed in a single orbit [17, 18]. Likewise, many other tectonic features attributed to non-synchronous rotation [19, 20, 21] may have an origin related to shorter period cycles of stress and strain.

References:

[1] Peale, S.J. et al. (1979) Science, 203,892-894. [2] Ross, M. and G. Schubert (1987) Nature, 325, 132-134. [3] Ojakangas, G.W. and D.J. Stevenson (1989) Icarus, 81, 220-241. [4] Peale, S.J. (2003) Celest. Mech., 87, 129-155. [5] Eckhardt, D.H. (1981) Moon, 25, 3-49. [6] Comstock, R.L., and B.G. Bills (2003) JGR, 108, 5100. [7] Bills, B.G. (1999), JGR, 104, 2653-2666. [8] Aksnes, K. and F.A. Franklin (2001) Astron.J., 122, 2734-2739 [9] Lieske, J.H. (1987) Astron. Astrophys. 176, 146-158. [10] Peale, S.J., and M.H. Lee (2002) Science, 298, 593-597. [11] Laskar, J. (1988) Astron. Astrophys., 198, 341-362. [12] Lieske, J.H. (1998) Astron. Astrophys. Supp. 129, 205-217. [13] Ojakangas, G.W. and D.J. Stevenson (1986), Icarus, 66, 341-358. [14] Moore, W.B. (2001) Icarus, 154,548-550. [15] Moore, W.B. (2003) JGR, 108, 5096. [16] Bills, B.G. and R.D. Ray, (2000), JGR, 105, 29277-29282. [17] Hoppa, G. et al. (1999) Science, 285, 1899-1902. [18] Greenberg, R. et al., (2003) Celest. Mech.,87, 171-188. [19] Greenberg, R. and S.J. Weidenschilling, (1984) Icarus, 58, 186-196. [20] Helfenstein, P. and E.M. Parmentier (1983) Icarus, 61, 175-184. [21] Hoppa, G. et al. (1999) Icarus 137, 341-347.

EARTH'S ICE SHEETS AND ICE SHELVES AS AN ANALOG FOR EUROPA'S ICY SHELL. D. D. Blankenship[1] and D. L. Morse[1], [1]Institute for Geophysics, John A. and Katherine G. Jackson School of Geosciences, The University of Texas at Austin, 4412 Spicewood Springs Rd, Bldg 600, Austin, TX, 78759 (blank@ig.utexas.edu).

Introduction: Earth's ice sheets and ice shelves could be viewed as poor analogs for understanding physical states and the processes governing these states within Europa's icy shell because their formation is dominated by atmospheric processes. However below the top few tens of meters, the atmosphere ceases to dominate their physical state so they become increasingly relevant as analogs for Europa. Our intent is to examine the thermal, structural and compositional states of Earth's ice sheets and ice shelves from the perspective of their governing processes, then to relate these processes to those hypothesized for Europa. Our ultimate goal is to elucidate possible observable physical states within Europa's icy shell based on these analogous processes.

Thermal State: Earth's polar ice sheets in East Antarctica, West Antarctica and Greenland are up to five km in thickness and have surface temperatures ranging from 213 – 273 K. In many cases, their internal temperature profiles are nearly isothermal in the upper half, where vertical advection of cold material from above (snow) dominates, and linearly increasing with depth in the lower half where upward conduction of geothermal and latent heat dominates. Strain heating, horizontal advection and spatially- or temporally-varying boundary conditions all contribute to deviations from this simplified description. A significant deviation from this temperature structure exists for polythermal ice caps (e.g., Svalbard) where significant thicknesses of temperate ice (isothermal at the pressure melting point) are found at the base, overlain by a linearly-varying layer. These profiles generally result from the vertical advection of heat by surface melt draining through the colder upper layer of these ice caps. The temperature profiles for ice shelves are widely varied as the profile inherited from the present ice sheet continues to be modified by downward advection of accumulating material and melt/freeze processes become dominant at the base. Advected heat either from surface melt or ocean infiltration can substantially modify these profiles.

Many processes analogous to those responsible for the thermal state of Earth's ice sheets and ice shelves have been proposed for Europa's icy shell. These include an overlying kilometers-thick brittle shell where thermal conduction is thought to dominate but with added tidally driven strain heating or possibly substantial melting and freezing at depth. In addition, the vertical advection of heat by the redistribution of surface material by sputtering (frost) and gardening, downslope motion or the draining of brines may be thermally analogous. Finally, it should be noted that there are no known Earth analogs for thermal convection within a deep ductile layer that has been proposed for Europa although the thermal processes in Earth's polythermal glaciers may yet prove analogous if tidally driven heating is distributed throughout Europa's icy shell.

Structural State: Here we characterize the structural state of Earth's ice sheets and ice shelves considering the density variations and the distribution of fracture associated with ice streams, which are fast-flowing regions within Earth's ice sheets that are many tens of kilometers in width and hundreds of kilometers in length. Ice streams are also the dominant contributor to ice shelf volume.

Density layering in the upper few tens of meters of Earth's ice sheets and ice shelves is pervasive. This is because ice sheet surfaces on Earth are continually generated by deposition and densification processes that vary temporally but on independent timescales. Tension fractures dominate the ice sheet surface where ice streaming (i.e., basal sliding) begins, whereas tension fractures dominate both the surface and base of the ice where grounded ice sheets (or ice streams) transition to floating ice shelves. The process that controls the distribution of these fractures is the balance between the strain rate gradient (i.e., the acceleration of the ice) and the ability to accommodate this strain through annealing (which is a function of temperature). Similarly, pervasive and nearly chaotic shear fractures characterize the lateral boundaries of the ice streams over regions that are many times the ice thickness in width. The ice streaming process that controls the position and width of these zones is dominantly stress concentrations at the boundaries of gravity-driven slab flow. Other characteristics of Earth's ice sheets that are rare but possibly relevant include "collapse structures" and ice "blistering". Collapse structures are circular fracture zones several ice thicknesses in width associated with elevated geothermal flux at the base of the ice. Ice "blisters" are zones of vertical uplift, typically meters in width, that are caused by partial melting and refreezing of exposed sub-ice meltwater.

Analogous structural processes on Europa may include vertical density variations in the shallow subsurface caused by the interplay between deposition of sputtering byproducts (e.g., frost) and deposition/erosion associated with gardening/mass-wasting. In addition, the tension-fracture and shear-zone evolu-

tion proposed for the hemisphere-scale ridges (with bands) on Europa are a result of tidal flexure and non-synchronous rotation that may have analogs in the onset, shear-margin and grounding-line evolution of the sub-continental scale Antarctic ice streams. Finally, many of the hypotheses for the formation of pits and spots on Europa parallel those for "collapse" and ice "blister" structures on Earth and it may be possible to extend the hypothesized processes for the slab flow of ice streams to the motion of blocks within larger zones of chaos on Europa.

Compositional State: The compositional state of Earth's ice sheets and ice shelves is dominated by subtle debris and impurity layering. The process driving the layering is surface deposition and vertical advection of material resulting from transient events. The material may be transported atmospherically (e.g., volcanic ash) or through the process of mass wasting (debris fall). The other primary compositional states are represented by units of impure ice found both at the base of and within ice shelves. The process causing these bodies is associated with freezing of sea water either in the low temperature gradient at the ice-water interface (so-called marine-ice units) or in the sharper temperature gradients within cracks that penetrate a substantial portion of the ice shelf. The steepness of the temperature gradient modulates the rate of impurity rejection as the ice freezes. An ice shelf dominated by marine ice formation is the Filchner-Ronne ice shelf of West Antarctica; crack-fill is associated both with tidal flexure at grounding lines and ice berg calving. Often, sub-ice cracks extend into the upper regions of the ice shelf allowing sea water to infiltrate the poorly compacted material and migrate laterally giving horizontally extensive bodies of very impure ice well above any marine ice layer.

Processes on Europa that may be analogous to those described above include the modulation of the deposition of sputtering by-products by transient gardening and mass wasting events resulting in layering of impurities (somewhat analogous to density layering processes). A slow freezing of sub-ice sea water is commonly proposed in association with the infilling of transient melt zones for spot/chaos formation as well as crack infilling for ridge/band formation. Analogous to Earth, a likely implication of these crack infilling hypotheses for Europa would be laterally extensive units of impure ice at the base of any zone of compaction penetrated by the crack.

Conclusion: The ultimate goal of any comparison of processes governing the physical state of Earth's ice sheets and ice shelves with processes operating within Europa's icy shell must be to help define a state space that can be used to evaluate and prioritize experiments for the next mission to Europa. The somewhat naïve associations made here are introduced primarily to initiate discussions on the most effective path to accomplishing this through additional terrestrial investigations.

DISTRIBUTION OF HYDROGEN PEROXIDE, CARBON DIOXIDE, AND SULFURIC ACID IN EUROPA'S ICY CRUST. R. W. Carlson, Jet Propulsion Laboratory, California Institute of Technology, Pasadena, CA 91109 (rcarlson@lively.jpl.nasa.gov)

Introduction: *Galileo's* Near Infrared Mapping Spectrometer (NIMS) detected hydrogen peroxide [1], carbon dioxide [2, 3] and a hydrated material on Europa's surface, the latter interpreted as hydrated sulfuric acid ($H_2SO_4 \cdot nH_2O$) [4] or hydrated salts [5]. Related compounds are molecular oxygen [6], sulfur dioxide [7], and two chromophores, one that is dark in the ultraviolet (UV) and concentrated on the trailing side, the other brighter in the UV and preferentially distributed in the leading hemisphere [8]. The UV-dark material has been suggested to be sulfur [9].

Hydrogen Peroxide: H_2O_2, a photolytically unstable molecule, is continuously formed on Europa by energetic charged particle bombardment and its presence demonstrates the importance of radiolysis on Europa [1]. H_2O_2 is present in equatorial and mid latitudes on Europa's leading hemisphere. The peroxide and CO_2 distributions are correlated, consistent with experiments showing enhanced H_2O_2 production in the presence of electron scavengers such as CO_2 [10]. The presence of H_2O_2 on the leading side and its non-detection on the trailing hemisphere may be due to the greater abundance of pure ice (i. e., less hydrated material) on the leading side compared to the trailing hemisphere. Hemispherical differences in chemical impurities and the resulting radiation chemistry pathways may also be involved.

Carbon Dioxide: CO_2 is present in the equatorial region of the leading hemisphere but is not apparent on the trailing hemisphere. Band strength maps show a non-uniform distribution that correlates with dark regions on the leading hemisphere that contain the UV-bright material mentioned above. Since meteoritic infall is greatest on this hemisphere, Europa's CO_2 is suggested to be radiolytically produced in dark carbonaceous meteoritic deposits. A tenuous CO_2 atmosphere, similar to Callisto's atmosphere [11], will be produced from molecules diffusing out of the surface. Atmospheric loss rates of CO_2 are consistent with radiolytic production and meteoritic infall.

Sulfuric acid: Europa's hydrated material, assumed to be sulfuric acid hydrate that is continuously produced and destroyed by radiolysis [4,12,13] was mapped using spectral fits and measured optical constants of $H_2SO_4 \cdot 8H_2O$ and H_2O. Radiative transfer calculations for intimate granular mixtures were used to find the fraction of hydrate and the radii of ice and hydrated acid grains (Fig. 1). The distribution exhibits a strong trailing side enhancement with maximum hydrate concentrations of about 80% (by number). The hydrate concentration correlates with ultraviolet-dark material and the SO_2 concentration [14], consistent with the radiolytic sulfur cycle [4, 12]. High-resolution maps show patterns that correlate with geological features. Lineae resolved by NIMS show hydrate concentrations on the flanks, with reduced or null hydrate concentrations in the upwelled lineae material. Sublimation of water during diapiric heating of the surrounding crust can enhance sulfur and sulfuric acid concentrations and produce such correlation. The trailing side enhancement of sulfurous material suggests Iogenic sulfur ion implantation as the source. Over the 10-My age of the surface, more sulfur is deposited than is observed (as sulfate, SO_2, and sulfur) but the concentration is consistent with burial by gardening and asynchronous rotation. Endogenic sources of sulfurous material may also contribute.

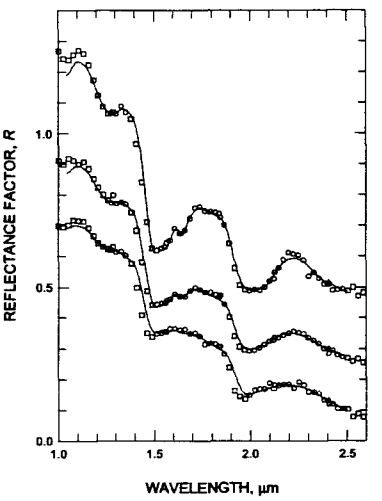

Fig. 1. Example fits to NIMS spectra. The fractional H_2SO_4 hydrate concentrations are: ~ 30% (top), ~ 50% (middle), ~ 80% (bottom).

Acknowledgement: This work was supported by NASA's Planetary Geology and Geophysics Program.

References: [1] Carlson, R. W., et al. (1999) *Science* **283**, 2062-2064. [2] Smythe, W. D. et al. (1998) *LPS XXIX*. [3] Carlson, R. W. (2001) *Bull. Amer. Astron. Soc.* **33**, 1125. [4] Carlson et al. (1999) *Science* **280**, 97-99. [5] McCord, T. B. et al. (1998) *Science* **280**, 1242-1245. [6] Spencer, J. R. and Calvin, W. M. (2002) *Astron. J.* **202**, 3400-3403. [7] Noll, K. S. et al. (1995) *J. Geophys. Res.* **100**, 19057-19059. [8] McEwen, A. S. (1986) *J. Geophys. Res.* **91**, 8077-8097. [9] Johnson, R. E. et al. *Icarus* **75**, 423-436. [10] Moore, H. H. and Hudson, R. L (2000) *Icarus* **145**, 282-288. [11] Carlson, R. W. (1999) *Science* **283**, 820-821. [12] Carlson, R. W. et al. (2002) *Icarus* **157**, 456-463. [13] Moore, M. H. et al.(2004) this conf. [14] Hendrix, A. et al. (2002) *Eurojove Conf.*

THE SURFACE COMPOSITION OF EUROPA: MIXED WATER, HYDRONIUM, AND HYDROGEN PEROXIDE ICE. R. N. Clark, U. S. Geological Survey, Denver, CO (rclark@usgs.gov).

Interpretations of the composition of the surface of Europa have been controversial, with different identifications resulting in correspondingly different implications for the origin and evolution of the satellite. The surface of Europa has an unusual water spectrum that has previously been interpreted as resulting from sulfate and carbonate salt minerals. However, the spectra of such minerals at the temperatures of Europa's surface have features which preclude their presence. This has led some investigators to postulate an unspecified hydrated mineral as the cause, and the term "non-icy" is now generally used to describe the Europa material. Europa's "non-icy" spectrum has also been interpreted as a sulfuric acid hydrate. Sulfuric acid hydrate spectral features are not unique to sulfuric acid, because other acids show similar features. These features are interpreted here as being due to hydronium, H3O, in the ice structure. Thus, Europa's "non-icy" material is interpreted as being due to hydronium. Hydronium ice may be caused by ionization defects in regular ice due to bombardment by magnetospheric particles, implantation of protons in the ice surface, or endogenic processes indicating an acidic ocean, or all three. Hydrogen peroxide also has been identified on Europa, and hydrogen peroxide-acid mixtures provide close matches to Europa's "non-icy" material. This too may be caused by ionization defects from the particle bombardment, or may indicate an ocean of acid and hydrogen peroxide.

Spectra of Ganymede and Callisto show spectral characteristics of the Europa water-hydronium-peroxide ice, but with less intensity and are consistent with an exogenic modification of the surfaces by particle bombardment, rather than decreasing amounts of salt and oceanic processes as one moves away from Jupiter.

Europa's "non-icy" spectra may be composed of >99% ordinary ice that has been disrupted by the particle bombardment, or an acid-hydrogen peroxide mixture composed of about 2/3 water. Liquid acid-hydrogen peroxide mixtures readily attack organic molecules, metals, and other compounds. If a lander melted this surface during its operations, the liquid could attack lander components and destroy experiments. An ocean composed of an acid-hydrogen peroxide mixture is a hostile environment for life as we currently know it.

REMOTE SENSING OF ICY GALILEAN MOON SURFACE AND ATMOSPHERIC COMPOSITION USING LOW ENERGY (1 eV- 4 keV) NEUTRAL ATOM IMAGING.

M. R. Collier[1], E. Sittler, D. Chornay, J. F. Cooper, M. Coplan, R. E. Johnson
[1]NASA/GSFC Building 21 Room 246, Code 692, Greenbelt, MD 20771 United States
mcollier@pop600.gsfc.nasa.gov

We describe a low energy neutral atom imager suitable for composition measurements at Europa and other icy Galilean moons in the Jovian magnetosphere. This instrument employs conversion surface technology and is sensitive to either neutrals converted to negative ions, neutrals converted to positive ions and the positive ions themselves depending on the power supply. On a mission such as the Jupiter Icy Moons Orbiter (JIMO), two back-to-back sensors would be flown with separate power supplies fitted to the neutral atom and ion/neutral atom sides. This will allow both remote imaging of 1 eV $< E <$ 4 keV neutrals from icy moon surfaces and atmospheres, and in situ measurements of ions at similar energies in the moon ionospheres and Jovian magnetospheric plasma. The instrument provides composition measurements of the neutrals and ions that enter the spectrometer with a mass resolution dependent on the time-of-flight subsystem and is capable of resolving molecules. The lower energy neutrals, up to tens of eV, arise from atoms and molecules sputtered off the moon surfaces and out of the moon atmospheres by impacts of more energetic (keV to MeV) ions from the magnetosphere. Direct Simulation Monte Carlo (DSMC) models are used to convert measured neutral abundances to compositional distributions of primary and trace species in the sputtered surfaces and atmospheres. The escaping neutrals can also be detected as ions after photo- or plasma-ionization and pickup. Higher energy, keV neutrals come from charge exchange of magnetospheric ions in the moon atmospheres and provide information on atmospheric structure. At the jovicentric orbits of the icy moons the presence of toroidal gas clouds, as detected at Europa's orbit, provide further opportunities to analyze both the composition of neutrals and ions originating from the moon surfaces, and the characteristics of magnetospheric ions interacting with neutral cloud material. Charge exchange of low energy ions near the moons, and directional distributions of the resultant neutrals, allow indirect global mapping of magnetic field structures around the moons. Temporal variation of the magnetic structures can be linked to induced magnetic fields associated with subsurface oceans.

HYDROTHERMAL PLUMES AND HEATING EUROPA'S ICE SHELL FROM BELOW. G. C. Collins[1] and J. C. Goodman[2], [1]Wheaton College, Norton MA (gcollins@wheatoncollege.edu), [2]Woods Hole Oceanographic Institution, Woods Hole MA (jgoodman@whoi.edu).

Introduction: Chaotic terrain disrupts the icy surface of Europa at a variety of scales, from large chaos areas over 100 km across to an abundance of small features less than 10 km in diameter. Models proposed for the formation of chaotic terrain [1-3] invoke some type of localized thermally-driven modification of the ice shell. Localization of heat may be caused by thermal diapirism within the ice shell [1,4], or focusing of heat from Europa's rocky interior, through a liquid layer, to the base of the ice shell. This latter possibility has been previously investigated from the perspective of how heat can be transmitted through the ocean via hydrothermal plumes [3,5], and from the perspective of how a plume could melt through the ice shell to produce chaotic terrain [2,10]. In this abstract we address hydrothermal plume behavior and ice shell melting, in an attempt to better understand how these processes may operate on Europa, and ultimately we wish to know if they leave visible evidence in Europa's surface geology.

Hydrothermal Plumes: Radiogenic heat and possibly tidal dissipation keep the temperature of the rocky interior of Europa above the temperature of the overlying ocean. The interior heat must be transmitted through the ocean and ice shell to be radiated into space. If heat sources are sufficiently localized at the top of the rocky interior, they will drive hydrothermal plumes in the ocean. Since the ocean is heated from below and cooled from above, it will convect, which will keep it well mixed and unstratified (unless the salinity is lower than 25 g/kg, see [6]). Thus to understand how heat can be concentrated at the base of Europa's ice shell, we need to understand the behavior of hydrothermal plumes in a rotating unstratified environment. Previous discussions of hydrothermal plumes in a Europan ocean have considered a rotating stratified environment [5] or a nonrotating environment [3].

We have performed a detailed scaling analysis of plumes in a rotating unstratified environment, and then carried out laboratory experiments of plumes in a rotating tank to verify our analysis and find unknown constants (summary in [7], full details in [8]). Based on this analysis, we can predict the behavior of hydrothermal plumes for a range of ocean depths and heat outputs. We consider a range of ocean depths from 50-170 km, based on gravity data [9] and an ice shell thickness less than 30 km. The appropriate range of heat output to consider is less constrained, so we adopt the values considered by previous authors [5,10] plus a margin, to give us a range of heat sources from 0.1 to 100 GW. Within this broad parameter space, we find very little variation in plume diameter. The diameter varies from 20 km at the thin ocean, low heat flux corner of our parameter space, to over 60 km at the thick ocean, high heat flux corner. There is also little variation in the maximum velocity of Coriolis-driven currents (3-8 mm/s), and these currents are too weak to drive ice raft motion in a melt-through model of chaotic terrain formation if a small amount of ice or slush remains at the surface [8]. Heat flux delivered by a plume to the base of the ice shell varies between 0.1-10 W/m^2.

Plume Scale vs. Chaos Scale: If chaotic terrain is formed by hydrothermal plumes melting through the ice shell, then the most common diameter of chaotic terrain areas will be the same as the diameter of the plume (or slightly larger, as eddies shed from the plume will carry heat away from the center), so we should expect that most chaos areas would be several tens of km in diameter. To understand why this is the case, we must examine how the ice shell melts in response to heat applied to its base. O'Brien et al. [10] have modeled this problem using an axisymmetric heat source at the base of the ice shell that is stronger at the center than the edges. This setup has the potential to make any diameter of melt-through between zero and the diameter of the heat source, since the ice shell will first be penetrated at the center of the heat source. However, they find that once the ice is penetrated, the diameter of the melted patch rapidly grows to equal the diameter of the heat source. This happens because there is a large amount of energy that goes into melting the subsurface ice, and once this is melted only a small amount of additional energy is needed to expand the edges of the melted surface patch. The area of the melted patch is proportional to the total energy delivered by the plume, minus a constant (to account for subsurface melting before penetration). For example, O'Brien et al. calculate that a 60 km wide heat source with a heat source of 50 GW can melt through 5.8 km of ice in ~1800 years, then after another 400 years the melt patch has grown to over a sixth of the heat source diameter. To make a melt-through patch smaller than 10 km, the plume would have to shut off between 1800 years and 2200 years.

The observed size distribution of chaotic terrain shows that the vast majority have diameters less than

15 km, and the observed number of areas keeps increasing down to ~8 km in diameter [11] or even smaller [12]. Is there a distribution of plume energies that could lead to the observed distribution of chaotic terrain diameters? If we assume that the energy of plumes, like many other geophysical systems, follows a power-law distribution, we find that we can match the size distribution of large chaos areas with the O'Brien model, but the model distribution asymptotes to a constant value at a diameter less than the plume diameter. All non-pathological distributions show this asymptotic behavior at small diameters, in opposition to the observations that the number of chaos areas increases with decreasing diameter. The only way to have the energy distribution of hydrothermal plume sources produce the observed size distribution of chaotic terrain areas is to include an infinite spike in the energy distribution function precisely at the energy required to melt through all the subsurface ice. Such an energy distribution for hydrothermal plumes on Europa is highly unlikely - why would volcanoes on the seafloor regularly vent for precisely the amount of time required to barely melt through the ice shell? Most likely there is some process other than melt-through which is controlling the size distribution of chaotic terrain.

Effect of Plumes on Ice Shell: Thus far our discussion has assumed that complete melt-through of the ice shell is a possible consequence of heating the base of the shell with a hydrothermal plume. However, complete melt-through is inconsistent with a simple energy balance between thermal emission from the surface and heating from below. To maintain melt at Europa's surface requires at least 300 W/m^2 [13], far more than the predicted heat fluxes from hydrothermal plumes in the parameter space outlined above. For the maximum heat fluxes predicted for plumes, tens of meters of ice remain unmelted at the surface in the equilibrium case. Previous calculations which predicted total melt-through at these same heat fluxes [10] suffered from insufficient vertical model resolution, see [13].

Hydrothermal plumes can supply heat to the base of the ice shell and perhaps significantly thin the ice. What effects could this have on the shell and the surface geology? We have argued that plumes and melt-through are unlikely to explain small chaos areas and the motion of ice rafts. Thinning the ice could drive ice raft motion if the rafts are carried on viscous basal ice which is flowing into the hole at the bottom of the shell. Isostatic adjustment of thinned ice could be observed as depressions in the surface. An example of this could be the E14 dark spot which is depressed by hundreds of meters [14], and is filled with low albedo material which could originate by cryovolcanism or by driving off frost due to enhanced heat flow in the thinned shell. The enhanced heat flux at the base of the ice shell from a hydrothermal plume could also trigger or enhance thermal diapirism, which has been proposed to form several surface features on Europa [1,4,15]. Heat from plumes could also produce localized areas of brine mobilization [16] which could contribute to the formation of chaotic terrain.

If there are localized heat sources at the base of the unstratified ocean, they will locally deposit that heat at the base of the ice shell above, at a characteristic scale. Do they have an effect on the observed geology of Europa? It appears that the scale of plumes cannot be reconciled with the melt through model to produce the observed population of chaotic terrain features. Perhaps plumes have a more indirect effect on the surface geology, by enhancing heat flow and by locally thinning the ice shell.

References: [1] Pappalardo R. T. et al. (1998) *Nature* 391, 365-368; [2] Greenberg R. et al. (1999) *Icarus* 141, 263-286; [3] Collins, G. C. et al. (2000) *JGR* 105, 1709-1716; [4] Nimmo, F., and M. Manga (2002) *GRL* 29, 2109; [5] Thomson, R. E., and J. R. Delaney (2001) *JGR* 106, 12,335-12,365; [6] Melosh, H. J. et al. (2002) *LPSC XXXIII*, #1824; [7] Goodman, J. C. et al. (2003) *LPSC XXXIV*, #1834; [8] Goodman, J. C. et al. (2003) *JGR*, submitted; [9] Anderson, J. D. et al. (1998) *Science* 281, 2019-2022; [10] O'Brien, D. P. et al. (2002) *Icarus* 156, 152-161; [11] Spaun, N. A. et al. (2001) *LPSC XXXII*, #2132; [12] Riley, J. et al. (2000) *JGR* 105, 22,599-22,615; [13] Collins, G. C. et al. (2003) *LPSC XXXIV*, #1430, Goodman, J. C. et al. (2003) *Icarus*, submitted; [14] Prockter, L. M. and P. M. Schenk (2002) *LPSC XXXIII*, #1732; [15] Figueredo, P. H. et al. (2002) *JGR* 107, 5026; [16] Head, J. W., and R. T. Pappalardo (1999), *JGR* 104, 27,143-27,155.

REMOTE SENSING OF EUROPA SURFACE COMPOSITION WITH IONS, NEUTRAL ATOMS, AND X-RAYS IN THE LOCAL SPACE ENVIRONMENT. J. F. Cooper[1], R. E. Johnson[2], and J. H. Waite[3], [1]Raytheon Technical Services Company LLC, SSDOO Project, Code 632, NASA Goddard Space Flight Center, Greenbelt, MD 20771, jfcooper@pop600.gsfc.nasa.gov, [2]Engineering Physics, University of Virginia, Thornton Hall B103, Charlottesville, VA 22904, rej@virginia.edu, [3]Atmospheric, Oceanic and Space Sciences, University of Michigan, 2455 Hayward, Ann Arbor, MI 48109, hunterw@umich.edu.

The surface chemistry of Europa is a mixture of material in unknown proportions from multiple sources: (1) early accretion from the protoplanetary nebula, (2) accretion from comet impacts during heavy and later bombardment, (3) emergence of subsurface (e.g., oceanic, hydrothermal) materials during resurfacing events related to tidal heating, (4) implantation of ions from the magnetospheric plasma, and (5) molecular evolution from radiolysis driven by magnetospheric particle irradiation energy. Observations of the oxygen exosphere and surface trace components including H_2O_2 and CO_2 can easily be attributed to products of magnetospheric interactions with little if any input from Europa's interior. However, whether the observed sulfate hydrates are from endogenic or exogenic sources is related also to the uncertainties about the existence of a liquid water ocean within Europa.

The challenge of future compositional measurements, e.g. by in-situ and remote sensing instruments on the planned Jupiter Icy Moons Orbiter (JIMO), is to separate the intrinsic elemental composition of Europa's surface and subsurface regions from the background components induced by magnetospheric interactions. Remote sensing observations from Earth suggest a net Na source at Europa, based on comparison of Na/K abundance ratios in neutral clouds around Io and Europa, and Na_2SO_4 hydrate is a candidate component for Europa's non-ice materials. Since $MgSO_4$ and H_2SO_4 are also candidates, identification of Europa's non-ice sulfates will require at minimum the separate in-situ and/or remote sensing measurements of abundances for Na, K, Mg, S, and other elemental species in the magnetospheric and surface environments.

Oxygen is of course universally abundant from H_2O ice, but the critical need is to determine ratios for abundances of other species to O. For astrobiology it is crucial to survey magnetospheric and surface abundances of other biogenic elements such as C, N, and P. The ratio Fe/O could provide information on the oxidation state of the putative ocean, for example since this ratio was high in an oxygen-poor ocean like that of the Archean Earth but fell as concentrations of dissolved oxidants increased with the rise of biogenic O_2.

In previous missions from Pioneer to Galileo the in-situ measurement of magnetospheric composition has been marginal even for elemental species, but the potential capabilities of JIMO could extend to measurement of isotopic abundances. Europa presumably accreted from material with standard solar isotopic abundances, but both magnetospheric interactions and biological processes produce isotopic fractionation which could be diagnostic of origin. Elemental species escaping via sputtering from Europa's surface into the local magnetospheric environment, and those found within materials of biological origin, would have preferentially lighter isotopes than for standard solar abundances. Isotopic ratios could serve to measure the age of surface regions, since older regions subject to sputtering should show heavier isotopic fractions than younger regions. Age is also suggested by the emplacement of younger features on older features. Hot spots for biological materials could show unusually low isotopic masses. In either case such regions would become high-priority candidates for landed expeditions to search for molecular evidence of a subsurface ocean and for biochemical signs of life.

A wide variety of instrumental techniques are potentially available to measure Europa surface composition remotely from orbits around Europa and Jupiter, and in-situ on the surface of Europa. The latter would likely provide the highest mass resolution, e.g. for biomolecules and isotopes, but obviously the least information on global distributions. Orbital instruments that directly image sputtered neutrals and x-ray excitation line emission from the surface could provide global geologic context but may have limited mass resolution. On the trailing hemisphere of Europa both the incident fluxes of energetic electrons, and the observed concentrations of sulfates, are higher than elsewhere, so remote imaging of x-ray lines from the irradiated surface materials there might yield compositional data on elemental abundances. Neutral sputtering is driven by keV-to-MeV energetic ions with more global impact distributions on the moon's surface, so low-energy neutral imaging would also cover the leading hemisphere of Europa.

With 2-D/3-D atmospheric and ionospheric models now in development, abundances of neutrals and ions sampled with high mass resolution for elements, iso-

topes, and molecules by an orbiter in the Europa atmosphere may be correlated to abundances of underlying surface regions. Detectability of heavier molecules could be improved with in-situ sampling at lower altitudes, e.g. for eccentric orbits with periapses at tens of kilometers. A unique capability of JIMO might be to use the Xe ion propulsion beam to create artificially-induced plumes of sputtered material from targeted regions. JIMO cruise measurements of ion and neutral magnetospheric particle composition could also indirectly yield surface composition data, since sputtered neutrals become ionized and are picked up by the corotating magnetospheric field, and a neutral toroidal cloud of alkalis and, likely, hydrogen or oxygen has been observed at Europa's orbit.

Magnetospheric ions originating from the Jovian moons and other sources (interplanetary solar wind, Jupiter's atmosphere) are accelerated to energies of tens of MeV per nucleon and higher during diffusive transport within the Jovian magnetosphere. Instrumental techniques are available to make precise measurements of energy, isotopic mass, and directional distributions for such ions. Phase space density analysis can in some cases be used to trace measured distributions of energetic ions of specific composition (e.g., Na) to points of origin (e.g., Europa). Knowledge that some types of ions, such as Na from Europa and S from Io, originate from discrete sources can in turn be used to investigate the dynamics of ion transport and acceleration in the large-scale magnetosphere. Precision ion spectrometers on JIMO could be used to determine ion charge states from measurements of the anisotropic interactions of high-energy, large-gyroradius ions with moons such as Europa. Since ion gyroradius is inversely proportional to the local magnetic field magnitude, such measurements can also be used to probe induced magnetic fields associated with Europa's putative subsurface ocean and intrinsic magnetic fields as found at Ganymede.

Finally, full characterization of energy and anisotropy distributions for major ion and electron species in the Jovian magnetosphere at the orbits of the icy Galilean moons is required to accurately model the position-dependent yields of magnetospheric irradiation products (neutrals and x-rays) from the moon surfaces. In the case of sputtering at Europa's surface, low energy sulfur and oxygen ions from the Io plasma torus dominate the number density but sputtering yields per unit energy from electronic ionization maximize for these ions at MeV energy. The incident energy distribution also affects the global surface patterns of sputtering, since high energy ions affect larger regions of the moon surface than lower energy ions, the latter having effects more concentrated in the trailing hemisphere like those of energetic electrons.

The energy distributions of incident magnetospheric particles, particularly for more penetrating protons and electrons as compared to short-range iogenic heavy ions, are also important to the resultant density distributions of irradiation products as functions of surface depth on Europa and elsewhere. The relative proportions of products from direct sputtering at sub-micron depths and from volume radiolysis down to meter depths partly determine the altitude distributions of these products in the moon atmosphere. 'Hot' atoms from sputtering initially produce larger scale heights of atmospheric neutrals than 'cold' atoms from leakage of radiolysis products through volume ice at 100 K. Eventually, all atmospheric atoms not reentering, and sticking to, the surface are lost to the magnetosphere due to atmospheric sputtering and dissociation reactions. For radiolytic product measurements it may be preferable to carry out in-situ atmospheric composition measurements of cold (sub-eV) atoms at low altitudes, while neutral imaging samples the hot (~ 10 eV) sputtered atoms at higher altitudes.

CREATING A GEOREFERENCED DIGITAL IMAGE LIBRARY OF EUROPA. Z. A. Crawford[1], R. T. Pappalardo[1], G. C. Collins[2], [1]Laboratory for Atmospheric and Space Physcis (LASP), University of Colorado at Boulder, UCB 392, Boulder CO, 80309 (zane.crawford@colorado.edu, robert.pappalardo@colorado.edu), [2]Physics and Astronomy Department., Wheaton College, Norton, MA 02766 (gcollins@wheatonma.edu).

Introduction: Geographic Information Systems (GIS) software has been used extensively in Earth-based quantitative mapping as the means for tying computational models to field and satellite observations of the surface. However, it has not yet become the standard method of mapping and manipulating geographic data in extraterrestrial settings. Currently, mapping is commonly done on a frame-by-frame basis in applications unaware of georefrencing, making large-scale generalizations and data-sharing between research groups difficult.

In the hopes of reducing duplicated efforts, enhancing collaboration between researchers, and facilitating quantitative geological analyses, we are creating a digital library of the Galileo SSI images of Europa which are processed uniformly, and consistently georeferenced so as to be ready for use in several popular GIS software packages (e.g. ESRI's ArcGIS 8.3)

Processing Methodology: We begin with the planetary data system (PDS) imaging archives and use the USGS Integrated Software for Imagers and Spectrometers (ISIS) to update pointing and calibrate the images. Bad lines and ragged edges are removed. The corrected USGS 1 km Europa basemap defines the coordinate system and hence our georefrencing. We manually tie higher resolution images to the basemap images in order to ensure consistent positioning. Using only the spacecraft pointing data, positioning errors of tens of km exist in high resolution images. We plan to make the images available on the internet and to the PDS both as ISIS cubes and as projected, georeferenced TIFF files.

Potential Applications: With correctly georeferenced images and a capable GIS software package, it is simple to measure true distances, areas, and orientations regardless of the map projection used. Mapped features can be output in a digital format and their content analyzed quantitatively in comparison with predictions made by computational models.

Computer-assisted stratigraphic sorting: It is essential that mapping of structures on Europa be performed in GIS for the following reasons. First, the feature locations and orientations will then be inherently referenced to the coordinate system of the body. Second, the resulting structures map will exist in the form of a database, which can be searched and shared, and on which quantitative analyses can be performed. Third, ancillary information about each structure (e.g., morphology) can be stored within the database. Finally, the enormous number of structures to be analyzed on Europa demands that we take a database approach to analyzing the data if we are to make significant progress in understanding their patterns, relationships, stratigraphy, and origins.

One analysis the database will allow is the sorting of lineaments by age. Even when the stratigraphic relationships are locally clear, there is too much data to comprehend if one looks at a broad region. As a result, manual stratigraphic sorting of the structures within the database is possible [1], but slow and errorprone.

We are developing a GIS module to assist the stratigraphic sorting process, by tracking each local stratigraphic relationship as input by the user, then sorting the resulting database to produce the sequence of structures that best matches the observations. These techniques can also be applied Ganymede, Callisto, and other planetary bodies.

Correlating surface stresses and lineaments: Nonsynchronous rotation and diurnal tidal stresses contribute to a stress pattern that affects the surface of Europa, each on a very different time scale. Over the 85- hour orbital period, the diurnal stress pattern acts on the surface, with a maximum magnitude of ~40 kPa [2]. The nonsynchronous stress pattern sweeps over the surface due to a slow rotation of the icy shell over the tidally locked interior of the moon, and occurs with a period of >10,000 years [3]. Polar wander (reorientation of the icy shell with respect to the axis of rotation) may also contribute to the surface stress pattern on Europa [4]. These three candidate stress mechanisms can combine additively.

In order to compare the observed pattern of lineaments with many possible combinations of these stress fields as calculated by quantitative stress modeling [5], we will use a computer to aid in the comparisons, and determine the parameter space in which the best fits lie. For this to work lineament mapping must be performed with a consistent coordinate system across the globe, thus making digital mapping far preferable to mapping without GIS.

References: [1] McBee and Collins (2002) LPSC XXXIII abstract #1449. [2] Hoppa et al. (1999a) *Science, 285*, 1899-1902. [3] Hoppa et al. (1999) *Icarus, 137*, 341-347. [4] Leith and McKinnon (1996) *Icarus, 120*, 387-398. [5] Stempel and Pappalardo (2003)

HIGHLY HYDRATED SULFATE SALTS AS SPECTRAL ANALOGS TO DISRUPTED TERRAINS ON EUROPA.
J.B. Dalton[1], C.S. Jamieson[2], R.C. Quinn[3], O. Prieto-Ballesteros[4] and J. Kargel[5], [1]SETI Institute, MS 245-3, NASA Ames Research Center, Moffett Field, CA 94035-1000 email: dalton@mail.arc.nasa.gov, [2]University of Hawaii, Manoa, 2545 McCarthy Hall, Honolulu, HI 96822-2275. email: csjamieso@hawaii.edu. [3]SETI Institute, MS 239-12, NASA Ames Research Center, Moffett Field, CA 94035-1000 email: rquinn@mail.arc.nasa.gov. [4]Centro de Astrobiologia, (CSIC/INTA), Torrejón de Ardoz, Madrid (España) e-mail: prietobo@inta.es. [5]Astrogeology Team, U.S. Geological Survey, 2255 N. Gemini Dr., Flagstaff, AZ 86001 e-mail: jkargel@usgs.gov.

Introduction: Asymmetric and distorted near-infrared absorption features indicate the presence of hydrated materials on the surface of Europa [1,2]. A number of species have been proposed as the material which plays host to the waters of hydration. The most promising class of these may well be the ones which retain high numbers of water molecules. Earlier work [2,3] has shown discrepancies between near-infrared spectra of disrupted terrains on Europa gathered by the Galileo NIMS instrument and the spectral behavior of hydrated salts of low hydration states. Other work [4,5,6,7] indicates that these discrepancies are reduced at higher levels of hydration. Here we report additional laboratory measurements which strengthen the case for highly hydrated materials on Europa.

Europa Compared to Water Ice: Figure 1 depicts the spectrum of dark plains units on the trailing hemisphere of Europa compared to a spectrum of ordinary water ice. The primary water absorption features near 1.0, 1.25, 1.5 and 2.0 microns (μm) are shifted and distorted in the Europa spectrum. The broad absorptions near 1.5 and 2.0 μm in the water ice spectrum are composed of several smaller absorptions which combine to produce the broader features. Narrower absorptions such as the crystalline water ice absorption feature at 1.65 μm can be discerned in the Europa spectrum, particularly between 1.5 and 2.0 μm.

Absorption features of hydrated salts: Note also the well-rounded shoulders at the right of the 1.0- and 1.25-μm features in the water ice and Europa spectra of Figure 1. These are affected by minor absorptions in the hydrated salt spectra of Figure 2. Many of the minor absorptions become more pronounced in the hydrates because the host molecule obstructs the interactions between individual H_2O molecules which cause molecular vibrations to occur over a broader frequency range. At low temperatures such as those found on the icy satellites, further reduction in interaction between energy states results in enhanced separation of these spectral features [2,6,9]. This effect is subdued in molecules of higher hydration state because the increased number of water molecules are able to interact more directly.

Effect of Increasing Hydration: Epsomite ($MgSO_4 \cdot 7H_2O$) displays the asymmetric absorption features endemic to the hydrates. However, it contains a number of additional features not seen on Europa. Sodium sulfide nonahydrate ($Na_2S \cdot 9H_2O$) has broader absorption at 2.0 microns due to the greater number of water molecules, but the orientation of the hydrated waters about the sulfide gives rise to several absorptions at very different energies than those seen in the sulfate hydrates; note the center positions of the 1.5- and 2.0-μm absorptions as compared to the sulfate hydrates. Mirabilite ($Na_2SO_4 \cdot 10H_2O$) begins to more closely approximate the Europa feature shapes, but again exhibits additional features, notably at 1.75 and 2.2 μm.

Magnesium Sulfate Dodecahydrate: We have successfully synthesized magnesium sulfate dodecahydrate ($MgSO_4 \cdot 12H_2O$) using a compressed-helium cryostat with programmable temperature controller at NASA-Ames Research Center. We began with a mixture of $MgSO_4 \cdot 7H_2O$ and H_2O, in stoichiometric proportions, which was placed in the environment chamber under dry nitrogen atmosphere. The temperature was programmed to oscillate about the eutectic and peritectic of the 3-phase system with a gradually decreasing amplitude over 16 hours. Each cycle resulted in solvation of a higher proportion of H_2O, until the entire mixture had become dodecahydrite. The identity has been verified using differential scanning calorimetry. Because the dodecahydrate decomposes at temperatures above ~267 K, the sample was maintained at subfreezing temperatures using a liquid nitrogen bath during transfer to the calorimeter. A spectrum of the dodecahydrate is shown in Figure 2. The absorption features at 1.5 and 2.0 μm display the same asymmetry as the Europa features, with fewer additional absorptions as seen in the lower hydration state samples. However, as with the other hydrates, a cation-OH stretch at 1.35 μm [8] is apparent cutting into the shoulder of the transition between the 1.25- and 1.5-μm bands, in contrast to the well-rounded shoulders seen in the Europa and water ice spectra.

$MgSO_4$ and Na_2CO_3 Brines: When sufficient water is present to create a brine, many of these small spectral features become subdued [7]. This is partly due to the interactions between the numerous water molecules, and partly due to scattering between salt

and water grains within the frozen brine mixture [2]. However, the additional water also tends to broaden the 2.0-μm and deepen the 1.65-μm features, while failing to completely eliminate the 1.35-μm cation-OH stretch. Flash-freezing of brines or other solutions limits crystal growth times, creating many small crystals which act as scattering centers. These scattering centers can decrease spectral contrast, reducing the influence of individual spectral features [2,9].

Mixtures: While no single material has yet provided a satisfactory match to the Europa spectrum, none have been conclusively ruled out on the basis of spectral arguments, either, and several may be present in low abundances. Neglecting stability considerations, many of these materials could be present at 5 to 60 percent levels by weight. A mixture of several materials with coincident features at 1.5 and 2.0 μm could produce a spectral match without any one material contributing a strong enough absorption to contradict the NIMS data. While this has been tried with limited success using materials of low hydration state [1,2,3], new spectral measurements of highly hydrated materials [4,5] offer the potential to significantly improve upon these earlier studies.

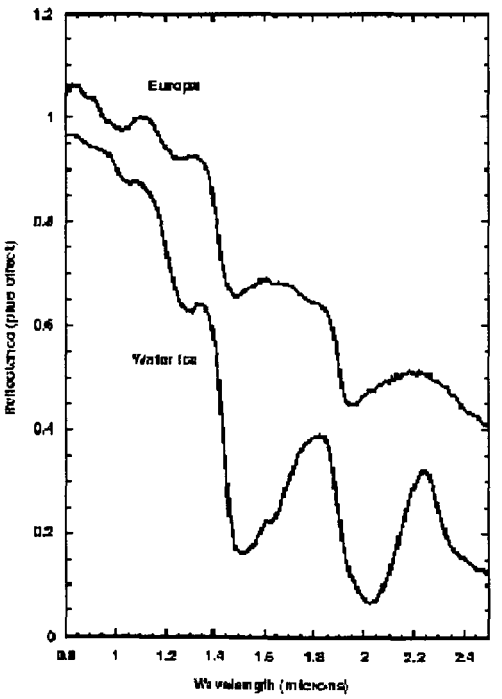

Figure 1. Galileo NIMS spectrum of dark terrain on Europa compared to water ice. Europa spectrum is from observation C3ENLINEA and represents a 26-pixel average. The water ice spectrum contains 1-5 μm quartz crystals as neutral scattering elements.

Conclusions: As the number of waters of hydration increases, the near-infrared spectra of hydrated salt compounds begin to more closely approximate the Galileo NIMS results. Magnesium sulfate dodecahydrate exhibits uncannily close yet imperfect similarities to the NIMS observations. Discrepancies remaining in the fine structure of brine and hydrate spectra (such as at 1.35 μm) could be exploited by a properly designed instrument to determine not only the materials, but also the relative proportions of materials, that make up the surface layer. Further laboratory measurements of as-yet unexamined compounds in the hydrate family may reveal even better correspondences.

References: [1] McCord, T.B. *et al.* (1998) *Science, 280,* 1242-1245. [2] Dalton, J.B. (2000) Ph.D. Dissertation, Univ. Colo., Boulder. [3] McCord T.B. *et al.* (1999) *JGR, 104,* 11,824-11,852. [4] Carlson R.W. *et al.* (2002) *Icarus 157,* 456-463. [5] Prieto-Ballesteros, O. *et al.* (1999) *LPS XXX,* Abstract #1762. [6] Dalton, J.B. (2003) *Astrobiology, 3, v. 4.* (in press). [7] McCord, T.B. *et al.* (2002) *JGR, 107,* 4-1, 4-6. [8] Dalton, J.B. and Clark R.N. (1999) *LPS XXX,* Abstract #2064. [9] Dalton, J.B. and Clark R.N. (1998) *Bull. Am. Astron. Soc., 30,* 1081.

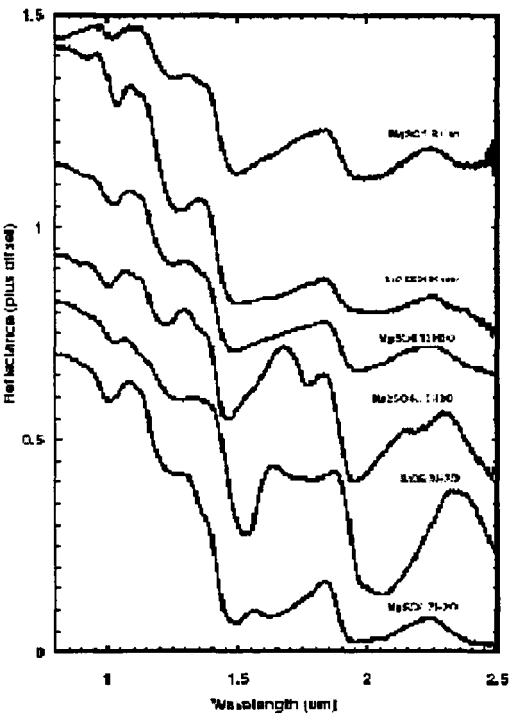

Figure 2. Spectra of highly hydrated compounds and frozen brines. From bottom: Epsomite, $MgSO_4 \cdot 7H_2O$, 100K; Sodium sulfide nonahydrate, $Na_2S \cdot 9H_2O$, 200K; Mirabilite, $Na_2SO_4 \cdot 10H_2O$, 200K; Dodecahydrite, $MgSO_4 \cdot 12H_2O$, 250K; $NaHCO_3$ and $MgSO_4$ saturated brines, flash-frozen at 77K.

THE RHEOLOGY OF ICE AT LOW STRESSES; APPLICATION TO THE BEHAVIOR OF ICE IN THE EUROPAN SHELL. P. Duval[1] and M. Montagnat[2], [1]Laboratoire de Glaciologie et Géophysique de l'Environnement/CNRS, B.P. 96, 38402 St. Martin d'Hères cedex, France, duval@lgge.obs.ujf-grenoble.fr, [2]LTPCM/INPG, B.P. 75, 38402 St. Martin d'Hères cedex, France, maurine. montagnat@ltpcm.inpg.fr

Introduction: The existence of an ocean in Europa is attributed to tidal heating [1], [2]. The thickness of the ice shell is poorly constrained. Surface features are in agreement with the occurrence of thermally induced solid-state convection within the lowest part of the ice shell [3]. The ice shell would be therefore composed of a thick brittle conductive layer overlying a convective sublayer [4],5]. Tidal heating would be located in the bottom of the convective layer. These results are obviously largely dependent on the viscosity of the ice. Tidal stresses are estimated of the order of 0.04 MPa with a strain rate of about 10^{-10} s^{-1} whereas convective stresses would be substantially lower. These mechanical conditions are found in polar ice sheets for which the lower bound for strain rates is about 10^{-13} s^{-1} near the surface of the East Antarctic ice sheet.

The rheological behavior of ice at low stresses is subjected to extensive studies to improve ice sheet flow models. In situ and laboratory measurements are needed for a better knowledge of the ice flow law at these low strain rates and for the construction of polycrystals models used to simulate the mechanical behavior of isotropic and anisotropic ices. A review of recent results on the behavior of pure ice is given here with emphasis placed on the physical deformation mechanisms which control the deformation of ice at low stresses. Particular attention is paid to the variation of the viscosity with stress, temperature and grain size in the deformation conditions of the Europan ice shell.

The ice flow law: From several laboratory studies, the flow law for deviatoric stresses lower than 0.1 MPa, is associated with a stress exponent lower than 2 [6, 7, 8]. Results can be questioned because of the long time needed to obtain reliable data. But, a clear indication of the decrease of the stress exponent below 0.1 MPa is found from the analysis of field data. A stress exponent of about 2 is found from boreholes deformation measurements in Greenland [9]. Convincing results on the flow law at low stresses were obtained from bubbly ice density and bubbles pressure measurements [10]. Data support a flow law with a stress exponent lower than 2 at low stresses.

The deformation modes: Indication of deformation mechanisms is obtained by comparing the deformation of ice single crystals well oriented for basal slip and the deformation of isotropic polycrystals [8]. The relatively low strain rates of polycrystals cannot be explained by a geometric effect related to the random orientation of crystals. Basal slip is put forward as the main deformation mode [11]. Basal slip providing two slip systems, two other slip systems should be activated to respect the stress compatibility and the continuity of the deformation across grain boundaries [12]. Slip on prismatic and pyramidal planes are generally suggested as additional slip systems. But, the activity of these slip systems given by several polycrystals models keeps a value lower than 10% for isotropic ice [11] and the occurrence of such slip is not proved. Dislocation climb can be assumed as a complementary deformation mode [13]; but, the dissociation of dislocations in the basal plane and the relatively low diffusion rate of oxygen atoms make uncertain this assumption. Grain boundary sliding (GBS) can be also suggested. But, there is no evidence of the occurrence of such process in the flow conditions of ice sheets. This mechanism was put forward as the predominant deformation mode of polar ice by Goldsby and Kohlstedt [14]. This assertion was reached from laboratory experiments carried out on very fine grained-ices. Extrapolation to conditions found in ice sheets was questioned by Duval and Montagnat [15]. The microstructure and the development of the preferential orientation of ice crystals is clearly no in accordance with GBS as the dominant deformation mode in polar ice sheets. GBS could be invoked to accommodate basal slip; this deformation mode has nothing doing with the behavior of superplastic materials. With regard to the accommodation of basal slip, it is significant to discuss all physical processes which occur in ice sheets. Grain boundary migration (GBM) associated with the normal grain growth and continuous recrystallization appears to be an efficient recovery process [16], [17]. By sweeping dislocations located in the front of moving grain boundaries, GBM prevents kinematics hardening caused by the incompatibility of the deformation

between grains. It is not a deformation mode, but it contributes to keep high the activity of basal slip systems. The analysis of the microstructure of single crystals from deep ice cores by X-ray diffraction has revealed a significant distortion of the lattice accommodated by geometrically necessary dislocations [18]. These strain heterogeneities are related to the strong anisotropy of the ice crystal inducing a significant mismatch of slip at grain boundaries. The role of strain gradients in the plastic behavior of ice polycrystals appears to be significant. In conclusion, by accommodating basal slip, several physical processes, identified in ice sheets, must contribute to the large activity of the basal slip systems. The preponderance of intracrystalline slip is moreover in agreement with the simulation of the development of fabrics by micro/macro approaches [11].

Application to the Europan ice shell: Deformation conditions in the assumed convective layer of Europa are very similar to those described above for polar ice sheets. By assuming pure water ice, the deformation mechanism with a stress exponent slightly lower than 2 is likely. But, considering that convective stresses are significantly less than the fluctuating tidal stresses, a newtonian viscosity should be assumed for this process [4]. An important point is the effect of grain size and water content since temperate ice could be present in the convective layer. There is a clear indication from in situ measurements that strain rate is depending on grain size in polar ice sheets [19], [20]. The exact relationship between strain rate and grain size is not well defined. But, it seems clear that strain rate is increasing with decreasing grain size. This result is not in contradiction with physical processes put forward to accommodate basal slip in ice sheets. The efficiency of GBM to reduce the internal stress field induced by the incompatibility of deformation between grains is depending on grain size [18]. Grain boundary sliding and strain gradients seen as accommodation processes are also depending on grain size. Concerning the effect of temperature near melting point, extensive studies were developed by the glaciological community [21], [22]. The viscosity of ice containing some percents of water can be ten times lower than that containing a negligible melt phase [21]. It is significant to point out that the viscosity of ice containing 7% of melt is of the order of 10^{13} Pa.s [22]. The first role of the liquid phase would consist of attenuation of the internal stress field which develops during the primary creep [22].

References : [1] Cassen P. et al. (1979), *GRL, 6,* 731-734. [2] Spohn T. and Schubert G. (2003) *Icarus, 161,* 456-467. [3] Pappalardo R. T. et al. (1988) *Nature, 391,* 365-367. [4] McKinnon W. B. (1999) *GRL, 26,* 951-954. [5] Tobie G. et al. (in press) JGR. [6] Mellor M. and Testa R. (1969) *J. of Glaciology, 8,* 147-152. [7] Duval P. (1976) C. R. Acad. Sc. Paris, 277, 703-706. [8] Duval P. and Castelnau O. (1995) *J. de Phys. C3, 5,* C3-197-C3-205. [9] Dahl-Jensen D. and Gundestrup N. S. (1987) *AIHS Publication, 170,* 31-43. [10] Lipenkov V. Ya. et al. (1997) *J. of Glaciology, 43,* 397-407. [11] Castelnau O. et al. (1996) *JGR, B6,* 13,851-13,868. [12] Hutchinson J. W. (1976) *Met. Trans. 8A,* 1465-1469. [13] Duval P. et al. (1983) *J. Phys. Chem., 87,* 4066-4074. [14] Goldsby D. L. and Kohlstedt W. B. (1997) *Scripta Mat., 37,* 1399-1406. [15] Duval P. and Montagnat M. (2002) *JGR, B107,* ECV14 1-2. [16] De La Chapelle S. et al. (1998) *JGR, B3,* 5091-5105. [17] Duval P. and Montagnat M. (2000) *EPSL, 183,* 179-186. [18] Montagnat M. et al. (2003) *EPSL, 214,* 369-378. [19] Cuffey K. M. et al. (2000) *JGR, B12,* 27,889-27,894. [20] Cuffey K. M. et al. *JGR, B12,* 27,895-27,915. [21] Colbeck, S. C. and Evans R. J. *J. of Glaciology, 12,* 71-86. [22] De La Chapelle S. et al. *GRL, 26,* 251-254.

ASSESSING POROSITY STRUCTURE IN EUROPA'S CRUST. J. Eluszkiewicz, Atmospheric and Environmental Research, Inc., 131 Hartwell Ave., Lexington, MA 02421, jel@aer.com.

Introduction: Knowledge of the density structure (i.e., porosity) in Europa's outer shell is very important in evaluating the prospects of a sounding radar in detecting a subsurface ocean [1] and in studies of the origin of geological structures [2]. Density structure is also likely to affect the rate at which minor constituents, including those that affect the radar signal, as well as possible biological markers, diffuse from the interior to the surface. The primary process affecting the density structure (and the closely-coupled thermal structure) of Europa's subsurface layers is self-gravitational compaction. The depth of a porous regolith on an Europa-size icy satellite has previously been estimated to exceed 1 km [1, 3]. In view of the critical importance of the density structure in the design and interpretation of upcoming JIMO/Europa mission (especially a radar instrument), the time has come to re-examine that estimate, including an assessment of the associated error budget.

Ice Metamorphism on Europa: In addition to affecting the density structure in the dry regolith, compaction will influence the depth of the transition zone between ice and liquid characterized by a network of brine pockets. In this transition zone, compaction is likely to proceed as a two-phase flow, with liquid being squeezed out from the collapsing pore space. Once the pore space loses interconnectivity, the elimination of the remaining brine pockets will be limited by the solubility of the brine constituents in the surrounding ice matrix. As the radar attenuation is expected to increase rapidly in this transition zone [4], an estimate of the depth of this zone will provide an upper limit to the depth of penetration of the radar signal (the actual penetration depth is likely to be smaller and determined by volumetric scattering in the dry regolith [1]). Another metamorphic process operating at depth on Europa is grain growth in the ice matrix. Grain growth will affect the concentration gradients of minor constituents, as the latter tend to diffuse more rapidly along grain boundaries than through the crystal interior [5].

Approach: Uncertainties in ice rheology under Europan conditions are the largest source of error in evaluating the density structure, although the p-T conditions in Europa's regolith are closer to those in terrestrial ice than conditions in the smaller and/or more-distant-from-the-Sun icy satellites. Consequently, an investigation of compaction on Europa can to some extent make use of rheological data for terrestrial ice, especially as the ice/liquid boundary is approached. In its most general form, calculating the density structure of Europa's subsurface layers presents a coupled microphysical/thermal/chemical problem that is best addressed via an integrated approach based on the multi-phase flow formalism [6]. In such an approach the heat and mass transfer equations are solved self-consistently, using material data for ice extrapolated to Europa from terrestrial conditions. A first-order estimate of the regolith depth can be obtained by applying equations describing compaction driven by dislocation creep, applied both to a dry regolith [1, 7] and to a regolith filled with liquid [6]. This initial estimate of density and thermal gradients should be followed by an evaluation of salt concentration gradients (taking into account grain growth and its impact on the salt diffusion coefficient) and their impact on the radar return. The density and thermal structure of Europa's regolith should be computed on a variety timescales corresponding to the geological processes that are likely to generate significant porosity.

References: [1] Eluszkiewicz J. Presentation at 35th DPS Meeting [2] Nimmo et al. (2003) *Icarus, 166,* 21. [3] Eluszkiewicz J. and Stevenson D. J. (1990) *LPSC XX,* 264. [4] Moore J. C. (2000) *Icarus, 147,* 292. [5] Wolff E. W. et al. (1989) *Geophys. Res. Lett., 16,* 487. [6] McKenzie G. H. (1984) *J. Petrol. 25,* 713. [7] Eluszkiewicz, J. (1990) *Icarus, 84,* 215.

GEOLOGICAL CONSTRAINTS ON TIDAL AND ROTATIONAL DEFORMATION ON EUROPA. P. H. Figueredo, Department Geological Sciences, Arizona State University, Tempe, AZ 85287-1404, figueredo@asu.edu.

1. Introduction: Orbital resonances with Io and Ganymede maintain a permanent eccentricity in Europa's orbit around Jupiter [1]. This situation produces a) 'diurnal' variations in the tidal figure of Europa during its 85 hr orbit, leading to dissipative heating as well as surface stresses, and b) a non-zero average tidal torque, which can drive nonsynchronous rotation (NSR) of the satellite [2, 3]. In addition, any mass concentration away from the equator could trigger episodes of polar wander of the outer cryosphere, if detached from the interior by a liquid layer [4]. Over the past few years, researchers have modeled the stress fields associated with these processes and their variation with space and time, from which they predicted specific orientations and trends in the lineament record of Europa [e.g., 3, 5-7]. In this review, I summarize the geological evidence for tidal and rotational processes on Europa as reflected in Voyager and (especially) Galileo images of the satellite. I address the constraints they place in the conditions and rates of deformation, the ongoing discrepancies in the interpretation of the data and their implications, and some ways of resolving outstanding issues.

2. Nonsynchronous rotation (NSR): The average gravitational torque of Jupiter on Europa's misaligned tidal figure tends to make Europa's rotation rate faster than synchronous [2], even in a completely solid body. An internal ocean would allow the decoupled outer shell to rotate nonsynchronously, drifting eastward over the tidally deformed interior. NSR stresses in the cryosphere are cumulative (until relieved by failure) and can match the magnitude of diurnal stresses with just ~1° of rotation [e.g., 3]. Therefore NSR likely constitutes the main source of stress for tectonic activity on Europa.

2.1. Fracturing: Fracturing of the cryosphere by tidal stresses (<0.4 kPa) requires the ice to be thin and weak. Widespread fracturing of Europa is in itself evidence of either an extremely thin shell, inconsistent with most thickness estimates (e.g., [8]), or an extra source of stress in the cryosphere. The pattern of global fractures on Europa and its offset with respect to the tidal stress pattern is consistent with NSR stresses [3, 5-7]. Stress models achieve better matches with the lineament record when both sources of stress, tidal and NSR, are combined [e.g., 3]. As discussed in section 3.1, the propagation of cycloidal fractures was likely controlled by diurnal stresses [9]; features that are not cycloidal possibly resulted from rapid propagation or were driven by NSR stresses.

2.2. Translation of features: As the outer ice shell moves eastward, surface features are expected to migrate from their original longitude of formation. The major lineaments on Europa can be explained as tensile cracks within a stress field with diurnal and NSR components only after translating these features westward a few tens of degrees or more [e.g., 6, 7, 10, 11]. In the same way, the orientation and sense of shear of strike-slip features in some areas fit better global stress models if they formed west of their current locations [3, 10]. It is generally considered that during the eastward migration of the cryosphere, fractures progressively relieve the accumulated NSR stress; this scenario could be confirmed when a global stratigraphic framework is established. The number of fractures formed during each rotation could constrain the number of rotations recorded in the visible geologic record (i.e., the last 30-80 Myr [12]) from which we can put an upper limit to the rate of NSR. On this basis, the NSR rate was estimated as <240,000 yr [10] from displacements of cycloids in one locality (and >12,000 yr from the lack of displacements of features between Voyager and Galileo images [13]), assuming a constant rate of 1-2 fractures per cycle. However, indications of repeated fracturing per cycle [11, 14-16, section 2.3] and of a rapid drop in the rate of tectonic resurfacing during the visible geologic record [17, cf. 18] challenge these assumptions.

As the outer shell of Europa moved eastward with respect to the deformed interior, it would become stretched where it moves over the tidal bulges, and compressed as it moves away from them [3]. Thus an area around the equator should have experienced cycles of extension and compression. The geologic record shows no widespread evidence of such alternation of stress conditions, although structural trends suggestive of shear failure at low latitudes have been reported [19]. In this sense, the evidence for compressional low-albedo bands, ridges, or folds [20-23] remains limited, and their relationship to tidal and rotational processes has not been addressed in detail. If the NSR rate was relatively fast, as implied by some studies [10], one would expect longitudinal 'smearing' of units formed under specific stress conditions (notably at low latitudes), with activity migrating westward with time. Despite the current lack of uniform coverage and a global stratigraphic network on Europa, there seems to be no obvious indication of such a progression or of smearing [24]. While the few impact craters on Europa show no leading/trailing asymmetries in their distribution [12], supporting rapid NSR, the distribution of other units appears to vary strongly with longitude. Chaos regions roughly match the location of the equatorial zones of NSR isotropic compression [25] and maximum tidal dissipation [11, 26, cf. 27]; the extensional wedges of Argadnel Regio are located roughly over one equatorial zone of isotropic extension [28], without an antipodal counterpart. If these units originated from global stresses, then the late NSR rate seems to have been very slow; alternatively, the units could have resulted from endogenic activity, with possible influence from tidal processes [29, 30].

2.3. Lineament rotation: One of the NSR model predictions is the systematic rotation of lineaments with time, if they originated as tensile fractures [8, 28]. Consistent with this prediction, and strengthening the case for both NSR and tensile fracturing of the cryosphere, several researchers have reported progressive clockwise and counterclockwise lineament rotations in the northern and southern hemispheres, respectively [e.g., 11, 15, 16, 28, 31]. The amount of rotation recorded by the most prominent lineaments varies considerably, from 25° to more than 700°. These results and their interpretation are complicated by the possibility of shear failure in some areas [19], the formation of only a few fractures per cycle [10], ambiguities in the sense of rotation [32], and the possibility of polar wander [4, 20]. Definitive evidence for the rotation of lineaments with time should come from detailed (i.e., lineament-by-lineament) stratigraphic studies in more locations and the development of a global stratigraphic framework for Europa.

3. Diurnal tides: The periodic reorientation of the tidal figure of Europa during each orbit causes oscillations in the

global diurnal stress field. During each cycle, stresses in a given region change from tensile to compressional as they rotate and change amplitude [3]. The magnitude of the tidal stresses, which depends on the thickness of the cryosphere, is estimated to be <40 kPa. The effects of diurnal tides seem reflected in several tectonic features on Europa:

3.1. Cycloidal fractures: The origin of Europa's conspicuous chains of curved segments, or cycloids, has been successfully explained by Hoppa et al. [9] in the framework of diurnal tidal stresses. During an orbit and under sufficient tensile stress, a fracture will propagate in a curved path in response to the rotation of the local stress field, producing an arc segment. Subsequent orbits will add continuous arc segments as long as the crack remains active. The length of each arc, their radius and sense of curvature, and the 'pointiness' of the cusps between arcs can be reproduced by varying the ice strength and the speed and direction of fracture propagation. Tidal stresses predict the formation of concentric sets of tight, 'boxy' arcs around the sub- and antijovian points of Europa, with more linear cycloids extending between them [9, 14]. Such a pattern seems consistent with the formation of Argadnel Regio (the "wedges" region) in the past, although no equivalent is found at the antipode.

3.2. Strike-slip features: Models of fault 'walking' by diurnal tidal stresses predict sinistral and dextral strike-slip displacements to dominate in the northern and southern hemispheres, respectively; at latitudes £30°, the sense of displacement is also a function of the fault azimuth and longitude of formation [20, 33]. Overall, these trends are consistent with the geologic record of strike-slip features [11, 20, 33]. Some inconsistencies exist, although they are generally attributed to the effects of NSR [33] and polar wander [20]. Details on the mechanism, however, await more thorough studies on issues such as a) the reasons why not all fractures underwent walking, even in polar regions; b) the along-strike variations in offset; c) the effectiveness of walking for very long faults; and d) the relationship between the amount of offset and the structure accommodating it. In this sense, the existence of simple fractures associated with significant lateral offset [15] is inconsistent with most ridge-building mechanisms, as discussed in section 3.3. Strike-slip is assumed in most analyses to result from primary tidal walking, although many of them could be secondary features accommodating deformation elsewhere. Structural studies are needed to identify morphological distinctions between the two processes, which could provide alternative explanations for some of the mentioned uncertainties.

3.3. Ridge-building: While tidal stresses most likely are combined with NSR stresses to fracture the brittle cryosphere (section 2.1), diurnal processes can operate in the enlargement of a crack into ridges or more developed morphologies [3]. According to some models, tidal working of fractures builds ridges by diurnal 'pumping' of crushed ice and slush from an ocean [3] and/or shear at more shallow levels [34]. It is argued that tidal pumping and strike-slip motions require fractures to extend through a relatively thin cryosphere [3, 10], despite issues with overburden pressure and ductile ice. This is not necessarily the case; for example, melts generated by shear could be pumped through fractures. Only dilational bands seem to involve a more intimate connection with the ocean as well as other sources of stress like secular variations, NSR, ocean currents, or convection cells [e.g., 29, 35-37]. Alternative 3-D structures of faults and geomorphological studies assessing systematically the intersections between ridges, variations at cycloid cusps and areas of sharp change in fault azimuth are necessary to refine models of ridge-building by diurnal tides.

4. Polar wander: Polar wander of a detached outer cryosphere was proposed as a possible consequence of the centrifugal displacement towards the equator of any mass concentration originally at higher latitudes [4]. Polar wander has been invoked to explain essentially any departure in the distribution of features (e.g., lineaments, chaos, wedges, and strike-slip features [7, 15, 20, 28]) from the equatorial symmetry of the tidal and NSR models. Interpretation of the evidence becomes uncertain, as the reported amounts of displacement and possible pivoting points differ considerably, which could be an expected effect of polar wander events in a nonsynchronously rotating Europa. It is worth noting, however, that if polar wander occurred relatively late (as suggested by [20]), it would render invalid most of the detailed correlations between lineaments and global stress fields [e.g., 3, 9-11, 16] that are considered in support of the tidal and NSR models.

5. Conclusions and outstanding issues: The geologic record indicates that tidal and rotational deformations are likely the main driver for geologic activity on Europa. To assume the initiation of lineaments as tensile cracks provides good matches with tidal and rotational stress patterns; the possibility of failure by shear and especially bending stresses should be considered for certain locations and times. Diurnal tidal stresses successfully explain the origin and characteristics of Europan cycloids, strike-slip displacements, and possibly ridges, but they involve fractures to form under very weak tensile stresses and to propagate through the entire cryosphere. In this sense, alternative fault geometries, dislocation scenarios, and sources of melt should be explored in order to determine if these conditions are indeed a requirement. NSR can accumulate adequate amounts of stress for failure and tends to match the overall pattern and sequence of lineaments on Europa. Fundamental constraints on this process, like the amount and rate of rotation, should become clearer from future results from lineament-by-lineament stratigraphy, terminator observations, and geophysical measurements. The evidence for polar wander, especially on recent times, should be considered with caution until supported in combination with global stress models or observations of actual displacement.

References: **[1]** Peale et al. 1979, *Science* 203: 892; **[2]** Greenberg and Weidenschilling 1984, *Icarus* 58: 186; **[3]** Greenberg et al. 1998, *Icarus* 135: 64; **[4]** Ojankangas and Stevenson 1989a, *Icarus* 81: 220; **[5]** Helfenstein and Parmetier 1985, *Icarus* 61: 175; **[6]** McEwen 1986, *Nature* 321: 49; **[7]** Leith and McKinnon 1996, *Icarus* 120: 387; **[8]** Pappalardo et al. 1999, JGR 104: 24015; **[9]** Hoppa et al. 1999a, *Science* 285: 1899; **[10]** Hoppa et al. 2001, *Icarus* 153: 208; **[11]** Figueredo and Greeley 2000, *JGR* 105: 22629 ; **[12]** Zahnle et al. 2003, *Icarus* 163: 263; **[13]** Hoppa et al. 1999b, *Icarus* 137: 341; **[14]** Bart el al. 2003, *LPSC* 34: #1396; **[15]** Figueredo and Greeley 2003, *LPSC* 34: #1017; **[16]** Kattenhorn 2002, *Icarus* 159: 490; **[17]** Figueredo and Greeley, *Icarus*, in press; **[18]** Basilevsky and Head 2002, *Geology* 30: 1015; **[19]** Spaun et al. 2003, *JGR* 108: JE001499; **[20]** Sarid et al. 2002, *Icarus* 158: 24; **[21]** Greenberg et al. 2003, *LPSC* 34: #1861; **[22]** Patterson and Pappalardo 2002, *LPSC* 33: #1681; **[23]** Prockter and Pappalardo 2001, *Science* 289: 941; **[24]** Figueredo 2002, *PhD dissert.*, ; **[25]** Pappalardo et al. 1998, *LPSC* 29: #1732; **[26]** Riley et al. 2000, *JGR* 105: 22599; **[27]** Ojakangas and Stevenson 1989b, Icarus 81: 242; **[28]** Geissler et al. 1998, *Nature* 391: 368; **[29]** Pappalardo and Head 2001, *LPSC* 32: #1866; **[30]** McKinnon 1999, *GRL* 26: 951; **[31]** Geissler et al. 1999, *LPSC* 30: #1743; **[32]** Sarid et al.. 2003, *LPSC* 34: #1445; **[33]** Hoppa et al. 1999c, *Icarus* 141: 287; **[34]** Nimmo and Gaidos 2002, *JGR* 107: JE001476; **[35]** Tufts et al. 2000, *Icarus* 146: 75; **[36]** Greenberg et al. 2002, *Rev. Geophys* 40: RG000096; **[37]** Prockter et al. 2002, *JGR* 107: JE001458.

ORIGIN OF CHAOS TERRAIN. Paul E. Geissler, Astrogeology Program, U.S. Geological Survey, Flagstaff Field Center, 2255 N. Gemini Dr., Flagstaff, AZ 86001 USA. (pgeissler@usgs.gov).

A NASA press conference in April, 1997 heralded the "discovery of an ocean on Europa" based upon the initial interpretation of crustal fragments within Conamara Chaos as ice "rafts" that had floated on a near-surface layer of liquid water. Although later imaging and more detailed analyses turned up a variety of surface features that were likely formed by diverse mechanisms, subsequent Galileo data provided ample confirmation that Europa's ice shell has been disrupted many times by large bodies of near-surface liquid water. This talk will review the characteristics of chaos terrain, the photogeological evidence for ice rafting, and the implications of liquid water near the surface of Europa.

Chaos regions share several characteristics, including an irregular, rough matrix that has replaced the ridged terrain common on Europa. This matrix material is commonly dark brown in color and often occupies the floor of irregularly shaped depressions that are 200 to 300 meters lower than the surrounding ridged terrain and are generally bounded by steep scarps. Within the matrix are often found fragments of intact crust with ridges still visible on their upper surfaces. The orientations and locations of some of these fragments demonstrate that they shifted in position (rotated, translated, or tilted) when the surface was disrupted, indicating that the fragments were underlain by a mobile substrate such as liquid water or ductile ice. Because the last remaining crustal fragments within chaos regions often incorporate relatively large and heavy ridges, the substrate must be denser than the solid ice crust, i.e. liquid water. From shadow measurements we can determine that the height of the fragments above the matrix is typically 200 to 300 m, suggesting that these ice "bergs" are 2 to 3 km thick according to Archimedes' Principle. Fragment thicknesses estimated in this way are equal to their minimum lateral dimensions, consistent with their interpretation as floating ice rafts.

Chaos regions range in size from a few kilometers to several hundreds of kilometers across. The dimensions of the largest examples are greater than the maximum possible thickness of the solid ice shell. There are no indications that chaos regions formed in stages like the nested paterae of Io, although there are several instances of younger chaos that overprinted older, inactive chaos terrain. Hence, the bodies of liquid underlying the chaos must have been at least as extensive as the chaos regions themselves, and at least 2 to 3 km deep in order to float ice rafts of the thicknesses inferred. Such large bodies of water would be unstable as sills sandwiched within a thick ice shell, and would sink through the lower density ice or quickly drain through faults and fractures in the solid ice shell. More likely, the liquid layer beneath chaos terrain is a global subsurface sea that melted through the solid ice shell and thermally disrupted the surface (Greenberg et al., 1999, Icarus 141, 263). A mechanism of brine mobilization (Head and Pappalardo, 1999, JGR 104, 27143) has been suggested for creating a transient layer of liquid within a thick ice crust, but such a process ought to expend itself early in Europa's geologic history, as soon as the ice shell differentiated.

The youngest chaos regions are among the most recent features on Europa's surface, suggesting that chaos terrain could be forming even today. Chaos formation is not a new phenomenon, however. Ancient chaos terrain can be recognized that dates back to the beginning of Europa's (short) geological record. Chaos in various stages of degradation can be seen that is overprinted with tectonic fractures and ridges and sometimes younger chaos, which can lead to the curious situation of chaos atop ice rafts. The processes by which chaos is obscured are identical to the means by which impact craters are erased, and the difficulty of recognizing older features of either type does not imply that chaos or crater formation are new phenomena.

Two other mechanisms modify chaos regions after thermal disruption has ended. First, the newly formed features represent zones of weakness in the ice shell that are subject to horizontal compression as the shell accommodates expansion elsewhere. Second, the melted area must refreeze to the thickness of the surrounding ice shell, perhaps aided by infill via viscous flow of the ice below, while preserving the high frequency component of the surface topography. These processes probably account for the puzzling variations in chaos morphology, such as the elevated matrix material reported by Schenk and Pappalardo (LPSC 2002).

Chaos terrain is ubiquitous on Europa. It is somewhat more prevalent along the equator, but large chaos regions have been found even at the poles, suggesting either extensive heating at high latitudes (where the ice shell is expected to be thick) or that polar wander has taken place. Riley et al. (2000, JGR 105, 22599) estimate that ~30% of the surface of Europa is occupied by younger chaos, while another ~10% may be covered by

older, partially obscured chaos regions. Chaos formation is thus an important resurfacing mechanism, competing with resurfacing by tectonism and ridge formation.

The presence of liquid water near the surface of Europa has important implications for exobiology and future spacecraft exploration. Melt-through provides a means of mixing surface materials into the interior, supplying oxidants and exogenic compounds that could help sustain life in the subsurface sea. It also exposes seawater at the surface of the satellite, yielding a means to determine the composition of the ocean hidden within. Active or recently formed chaos regions could one day provide a portal for access to Europa's ocean for direct exploration, an expedition that will be inevitable (if it is possible), given the nature of human curiosity.

MOLECULES PRODUCED ON THE SURFACE OF EUROPA BY ION IMPLANTATION IN WATER ICE. O. Gomis[1], M. A. Satorre[1], G. Leto[2] and G. Strazzulla[2], [1]Dpto. de Física Aplicada, Escuela Politécnica Superior de Alcoy (UPV), Placeta Ferrándiz Carbonell 2, 03801 Alcoy (Spain); osgohi@fis.upv.es, msatorre@fis.upv.es, [2]INAF-Osservatorio Astrofisico, via S. Sofia 78, I-95123 Catania, Italy; gle@ct.astro.it, gianni@ct.astro.it.

Abstract: Europa surface spectra reveal that its main constituents are in the form of ices. Between them frost H_2O [1] is dominant although traces of CO_2 [2], SO_2 [3][4], O_2 [5] and H_2O_2 [6] have also been found. Other compounds found mainly in the darker regions are hydrated materials [7][8]. Europa is located inside the intense magnetosphere of the giant Jupiter. The magnetosphere is populated by protons and ions such as S^{n+} and O^{n+}, and energetic electrons [9]. In fact, one of the mechanisms suggested to be responsible for the formation of the icy molecules present on Europa is the interaction of the magnetospheric plasma with the surface of the satellite. When an energetic ion collides with the icy surface, part of the deposited energy destroys molecular bonds in the target producing radicals that can then react to synthesize new molecules. In the case of a thick satellite surface, in which ions are implanted, the possibility exists that the new produced molecules contain the incident ion [10].

We have carried out implantation experiments of ions relevant to the Jovian system in water ice and mixtures. We focused on studying and characterizing the molecules formed by ion implantation and to analyze if this mechanism can quantitatively account for some of the species found on the surface of the satellite. Also of our interest is the study of likely chemical pathways that could give rise to the new molecules. The used experimental technique has been in-situ infrared spectroscopy. Our results are also relevant to other Galilean satellites and to other places inside the Solar System.

In this work we present the results of experiments of ion implantation in pure water ice by using five different types of ions (H^+, C^+, N^+, O^+ and Ar^+). We have first focused on the study of the production of the hydrogen peroxide molecule. The energy of the used ions is 30 keV and the experiments have been carried out at 16 and 77 K. Our experiments show that H_2O_2 is produced at both temperatures and by all the different ions. We have found that the quantity of produced H_2O_2 is greater for ions with a higher stopping power, being protons the ions that produce the smallest quantity [11]. We have also observed that oxygen is the ion that at 77 K produces the greatest quantity of H_2O_2. More precisely, an asymptotic value of about 4% of H_2O_2 (into respect to H_2O) in number of molecules has been found for O^+ implantation. Because this value of H_2O_2 concentration is much greater than the 0.13% inferred by the NIMS feature on Europa, we suggest that hydrogen peroxide could be, on the surface of the satellite, distributed only in patches. This result could be useful to support the suggested possibility of a radiation-driven ecosystem on Europa based on the availability of organic molecules and oxidants such as hydrogen peroxide. Also of great interest is the possibility that the H_2O_2 could reach the putative subsurface ocean [12].

We have also found that C implantation into water ice produces CO_2; the production yield (molec ion^{-1}) has been measured [13]. For the case of Europa a better estimation of the C^{n+} ion fluxes that impinge on the satellite is needed in order to estimate if carbon implantation could be in fact responsible for the quantity of CO_2 found on the satellite.

Future planned experiments are the implantation of sulfur ions into water ice to study the production of SO_2 and sulfates. Sulfur implantation has been in fact suggested to be responsible for the formation of SO_2 found on the surface of Europa [3][8][14].

References: [1] Calvin W. M. et al. (1995) *JGR, 100*, 19041–19048. [2] Smythe W. D. et al. (1998) *BAAS, 30*, 1448. [3] Lane A. L. et al. (1981) *Nature, 292*, 38–39. [4] Noll K. S. et al. (1995) *BAAS, 27*, 1339. [5] Spencer J. R. and Calvin W. M. (2002) *AJ, 124*, 3400–3403. [6] Carlson R. W. et al. (1999) *Science, 283*, 2062–2064. [7] McCord T. B. et al. (1998) *Science 280*, 1242–1245. [8] Carlson R. W. et al. (1999) *Science 286*, 97–99. [9] Cooper J. F. et al. (2001) *Icarus, 149*, 133–159. [10] Strazzulla et al. (2001) *Spectrochim. Acta A57*, 825–842. [11] Gomis et al. (2003) *Planet. Space Sci.*, in press. [12] Chyba C. F. (2000) *Nature 403*, 381–382. [13] Strazzulla et al. (2003) *Icarus, 164*, 163–169. [14] Sack et al. (1992) *Icarus, 100*, 534–540.

This research is supported through Italian Space Agency (ASI), Italian Ministero dell'Istruzione, Università e Ricerca (MIUR) and Spanish Ministerio de Ciencia y Tecnología (MCyT)/Project AYA2001-2385 and EC FEDER funding.

EMPIRICAL DETERMINATION OF RADIOLYTIC PRODUCTS IN SIMULATED EUROPAN ICES. K. P. Hand[1], R. W. Carlson[2], and C. F. Chyba[1,3] [1]Dept. Geological & Environmental Sciences, Stanford University, 450 Serra Mall, Building 320 Stanford, CA 94305, (khand@stanford.edu), [2]Jet Propulsion Laboratory, California Institute of Technology, Pasadena, CA 91109 (rcarlson@lively.jpl.nasa.gov), [3]The SETI Institute, 2035 Landings Drive, Mountain View, CA, 94303 (chyba@seti.org).

Introduction: The chemical composition of Europa's surface is strongly influenced by energetic charge particle bombardment from Jupiter's magnetosphere. Here we report on progress in experimental work designed to address: 1) The production of radiolytic products in thermodynamic disequilibrium that could be utilized by known terrestrial microorganisms, and 2) The modification of complex organic molecules and degradation of biological material by the simulated Europan surface radiation environment.

Methods: The experimental facility includes a 500 eV – 20 keV electron gun in a vacuum chamber coupled to a continuous flow cryostat capable of maintaining temperatures in the range of 4 K – 320 K. The configuration of the electron gun chamber allows for simultaneous mass spectroscopy, Fourier transform IR-spectroscopy, UV flourescence, and UV transmission and reflectance. Water vapor and compound mixtures (e.g. propane, formaldehyde, alcohols...) are deposited on the cryostat plate and the resulting ice mixture is then bombarded with high energy electrons, simulating the Europan surface environment. Irradiations are performed at temperatures that simulate Europan conditions and chemical evolution of the samples is determined using mass spectroscopy and infrared spectroscopic measurements, both obtained throughout the exposure. High doses are achieved in order to establish equilibrium species.

Results: The most recent results from our work are presented. In particular, two sets of experimental results are considered.

Disequillibrium products: We have undertaken an experimental determination of the chemicals that are produced by high-dose irradiation of ice containing impurities relevant to Europa. Radiolysis produces molecular species in thermodynamic disequilibrium [1, 2, 3], and these may in turn be used by organisms in energy-producing reactions, forming a radiation-driven ecosystem as hypothesized by Chyba [4] and Chyba and Hand [5]. Here we determine the production rates and equilibrium concentrations for products such as formaldehyde, methane, oxygen, organic molecules, and thiols from irradiated ice containing compounds of carbon, sulfur, and silicate. Delivery of such compounds to the putative ocean and the metabolic utility of these radiolytic products is also considered.

Modification of biosignatures: The second component of this work is an analysis of the radiolytic modification of chemical biosignatures. High-energy radiation decomposes molecules on Europa, even to depths of several meters. A rough mean dose for material in the upper 10 cm of the ice shell is on the order of 10^4-10^5 eV per 16 amu, enough to ionize and dissociate all molecular species several times over [6, 7].

A prime measurement goal for an astrobiology mission orbiting or landing on Europa is determination of the surface and subsurface, searching for complex organic molecules that may serve as biosignatures. Determining the depth required for obtaining useful biosignature molecules requires a systematic study of candidate molecules, irradiated in ice at Europa-like temperatures. Here we examine the products of such exposure on a variety of organic molecules, biological compounds, and some microorganisms contained within the simulated Europan ice matrix. By varying dose rate we simulate various depths below the ice shell surface and yield results for survivability of biosignatures in the ice shell.

Acknowledgements: This work is supported by NASA's Exobiology program.

References: [1] Carlson R. W. et al. (1999) Science *283, 2062.* [2] Carlson R. W. et al. (1999) Science *286, 97.* [3] Spencer and Calvin (2002), *Astron. J. 124, 3400.* [4] Chyba C. F. (2000) *Nature, 403,* 381–382. [5] Chyba C. F. and Hand K. P. (2001) *Science. 292, 2026-2027.* [6] Carlson, R. W. *DPS 2003.* [7] Cooper et al. (2001) *Icarus, 149, 133.*

EUROPA'S ICE SHELL THICKNESS DERIVED FROM THERMAL-ORBITAL EVOLUTION MODELS. H. Hussmann, T. Spohn, *Universität Münster, Institut für Planetologie, Wilhelm-Klemm-Str. 10, 48149 Münster, Germany, (hhussman@uni-muenster.de).*

Introduction

Images of Europa obtained by the *Galileo* spacecraft show a variety of surface features that are generally believed to be related to the thermal state and thickness of Europa's H_2O-layer. A substantial part of this layer is expected to be liquid, forming a subsurface ocean of up to about 100 km thickness. This is suggested by the detection of an induced magnetic field at shallow depth [1], by equilibrium models of the heat production and heat transport rates through the ice shell (e.g.,[2, 3]), and by the interpretation of geological surface features (e.g.,[4]). The latter show evidence for both a thick ice shell of a few tens of kilometers and a thin ice shell with a thickness of only a few km, or even just a few hundreds of meters. The absolute ages of these surface features are unknown. Therefore, we calculated thermal orbital evolution models in order to determine Europa's ice thickness as a function of time. Different phases of ice thickness may be related to different kinds of surface features. Another important question addressed in this study is the following: Can the ocean exist for several Ga?

Since the inner three Galilean satellites are locked in the Laplace resonance, the history of Europa cannot be understood without considering the evolutions of its neighbouring satellites Io and Ganymede. Due to the resonance, the orbital periods of Io, Europa, and Ganymede are close to the ratio of 1:2:4 and their forced eccentricities are maintained over long periods of time. A part of the orbital energy gained by Io due to tidal interaction with Jupiter is dissipated as heat in Io's and Europa's interior (e.g.,[5]). Ganymede's dissipation rate is negligible during the evolution in the Laplace resonance. It may have been important though during formation of the resonance. The gravitational interactions between Io and Jupiter tend to drive the satellites deeper into resonance and to increase their mean motions. Dissipation in the satellites tends to drive them out of resonance and thereby to decrease their eccentricities and mean motions. Due to these opposing effects oscillations are possible, where the orbital elements and the dissipation rates vary considerably [6, 7]. These variations of Europa's (and Io's) thermal state may serve as an explanation for different kinds of surface features on Europa.

The Model

Basically, our model consists of four parts:

1. *Interior structure*: We assume that Io and Europa are differentiated into an iron-rich core and a silicate shell. Additionally, there is the H_2O-layer on Europa. These models are consistent with the moments of inertia of the satellites derived from *Galileo* data [8, 9].

2. *Tidal heating*: The rheology of the viscoelastic layers is cast in terms of a Maxwell model with temperature dependent viscosity and rigidity. In case of Io tidal dissipation occurs in the silicate shell. For Europa we consider two different models. In model 1 dissipation is restricted to the silicate layer. In model 2 dissipation within the ice layer is assumed. The tidal forces are determined by the potential Love number k_2, which is a function of rheology and thus temperature. The dissipation rate Q_{diss} is then given by [10]

$$Q_{diss} = -\frac{21}{2}\frac{R^5 n^5 e^2}{G}\mathrm{Im}(k_2), \qquad (1)$$

where R is the satellite's radius, n the mean motion, e the eccentricity, and G the gravitational constant.

3. *Heat transfer*: To calculate the heat transfer rate through the silicate shells and Europa's ice layer a parameterized model of convection is used. The time dependence of the thickness of the conductive stagnant lid is determined from energy balance equations. As heat sources we take into account the tidal dissipation rates and radiogenic heating from the rocky layers.

4. *Orbital evolution*: The satellites evolve in the Laplace resonance. Ganymed is included as a point mass in the orbital equations, which are based on the models described in [5] and [7]. Dissipation in Jupiter is parameterized by the dissipation coefficient Q_J. This value and the initial mean motions are chosen such that the present-day orbital configuration of Io, Europa, and Ganymede is reproduced at 4.6 Ga.

The link between all four parts of the model is provided by the dissipation rate depending on the orbital elements as well as on structure, rheology and temperature (Eq.1).

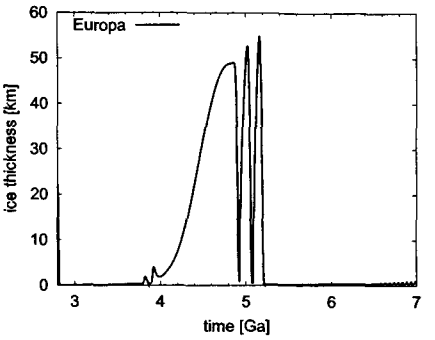

Figure 1: Equilibrium ice thickness according to heat production of model 1 (dissipation within Europa's silicate shell).

Results

The orbital evolution of Io and Europa can be devided into different phases, which are closely related to the ice thickness due to the different dissipation rates and corresponding heat productions. The phases, which are discussed in detail in [11], include equilibrium phases as well as oscillatory phases. Here we focus on the implications for Europa's ice shell thickness. Examples are shown in Figs.1–3. The current state, is obtained at 4.6 Ga in all models. In Fig.1 the result is shown for model

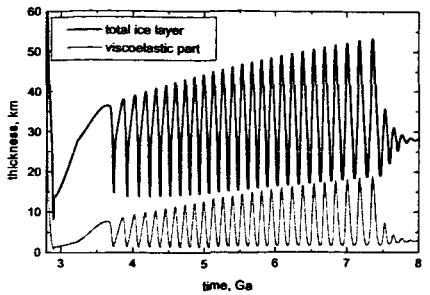

Figure 2: Ice thickness according to model 2 (dissipation within Europa's ice layer).

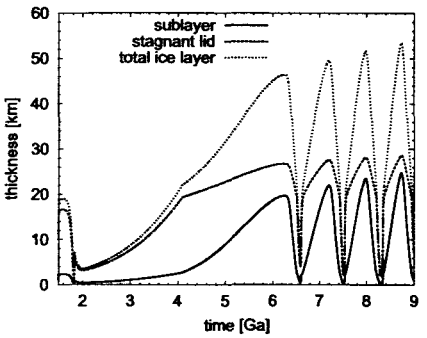

Figure 3: Ice thickness according to model 2 including lithospheric evolution in Io.

1, where dissipation in Europa is restricted to the silicate shell. The thickness of the ice layer is estimated from the heat flow out of the silicate shell using equilibrium conditions for the ice shell. The present-day thickness of the ice shell is about 30 km. Europa is in this case in a phase of increasing ice thickness. The eccentricity is decreasing, while the mean motion is increasing implying that the satellites move away from Jupiter (not shown here). However, there are thin-ice phases with thicknesses smaller than 1 km about 600 Ma b.p. Oscillations are initiated at about 4.8 Ga. After the oscillations there is another phase where Europa is in a high temperature state accompanied by small ice thicknesses.

In Figs.2 and 3 the evolution is shown for model 2, where dissipation in Europa is restricted to the ice layer. In Fig.2 the total thickness of the ice layer and the thickness of its viscoelastic part are shown. The difference between these values equals the thickness of the upper conductive lid. The current state is obtained during the oscillatory phase. Again, the thickness is about 30 km. However, there are variations in total ice thickness in the range of about 10–40 km on a period of about 200 Ma. In this case there are no phases with ice thicknesses smaller than 10 km.

In Fig.3 the thermal model of Io is changed. In Fig.2 it is assumed that convection within Io occurs in the whole mantle and that it is driven by the temperature difference between interior mantle temperature and surface temperature. In Fig.3, a conductive lithosphere is included in the Io-model. In this case the satellites evolve more slowly. The present state is obtained before oscillations are initiated. The current thickness of Io's lithosphere is about 12 km (not shown here). Using this Io-model it is not possible to satisfy Io's heat flux constraint of at least 2 Wm^{-2} [12, 13]. The value derived from these models is 0.1 Wm^{-2}. This suggests that other heat transfer mechanisms instead of thermal conduction through the lithosphere are more important for the present Io.

In all the models the thickness of Europa's ice layer is less than about 60 km. Since the total thickness of the H_2O-layer exceeds 70 km with most likely values of more than 100 km, our results suggest, that the ocean is present over geological timescales. Different surface features on Europa may be related to different phases of ice thickness. This implies that the chaos terrain, which is generally believed to be one of the youngest features on Europa was formed more than 100 Ma b.p. However, according to our derived present-day ice thickness of 30 km, domes formed by upwelling plumes in the convecting ice are better candidates for the most recent features. Note, that the present-day value of ice thickness is independent of the chosen model.

The formation of features in a thin ice layer of only a few km or less, requires substantial tidal heating within the silicate shell. This additionally requires relatively high eccentricities, which will ecceed the currently observed values. This is further evidence for an ice shell thickness of a few tens of km for the present Europa.

References

[1] Kivelson, M. G. *et al.* 2000. *Science* **289**, 1340–1343.

[2] Hussmann, H. *et al.* 2002. *Icarus* **156**, 143–151.

[3] Spohn, T. and G. Schubert 2003. *Icarus* **161**, 456–467.

[4] Pappalardo, R. T. *et al.* 1999. *J. Geophys. Res.* **104**, 24,015–24,055.

[5] Yoder, C. F. and S. J. Peale 1981. *Icarus* **47**, 1–35.

[6] Ojakangas G. W. and D. J. Stevenson 1986. *Icarus* **66**, 341–358.

[7] Fischer, H.-J. and T. Spohn 1990. *Icarus* **83**, 39–65.

[8] Anderson, J. D. *et al.* 1998. *Science* **281**, 2019–2022.

[9] Anderson, J. D. *et al.* 2001. *J. Geophys. Res.* **106**, 32,963–32,969.

[10] Segatz, M. *et al.* 1988. *Icarus* **75**, 187–206.

[11] Hussmann, H. and T. Spohn 2003. *Icarus*, submitted.

[12] Veeder, G. J. *et al.* 1994. *J. Geophys.Res.* **99**, 17095–17162.

[13] Matson, D. L. *et al.* 2001. *J. Geophys. Res.* **106**, 33,021–33,024.

COMPOSITION AND GEOCHEMICAL EVOLUTION OF EUROPA'S ICY SHELL. J.S. Kargel, U.S. Geological Survey, 2255 N Gemini Dr., Flagstaff, AZ 86001, U.S.A. (email: jkargel@usgs.gov).

Introduction: The *Galileo* project's discovery of imaging, spectroscopic, and geophysical evidence pointing to the existence of an ice-covered ocean on Europa stands among the most stunning scientific and philosophical achievements of the Space Age. Europa, a geologically dynamic water world, runs even with Mars as a place where life may now or have once existed. In one respect, Europa is a better bet than Mars for current life: Europa presently has an ocean, whereas the longevity of vigorous hydrologic systems on Mars is still subject to debate. However, aside from the fairly certain conclusion that Europa now has an ocean, our knowledge of Europa remains scanty by comparison to what we know of Mars. The floating shell's composition is not reliably known. Each of several geochemical models has vast implications for Europan shell dynamics. I shall review divergent compositional interpretations of spectroscopic/imaging data and models of compositional evolution, and draw logical implications for shell structure and dynamics.

Some big controversies

The bizarre beauty of Europa arises from the coupled geological and geochemical dynamics of the icy shell and ocean. How this coupling is achieved and what processes occur unknown; ideas are plentiful. Two far-reaching current debates concern: (1) the physical dynamics of the floating shell (thick shell vs. thin shell debate and solid-state convection versus melt-through), and (2) the geochemical dynamics of the floating shell (including interpretations of the non-ice material: is it hydrated sulfate salts, hydrated sulfuric acid, or hydronium ice?). Probably nobody understands Europa's reality very well; the reality may encompass some of what each group has supported. The debates are not going to be solved until we have a new Jupiter/Europa mission designed to resolve the disputes. In the mean time, further work is warranted, because the observations, models, and arguments will shape the experiments and observational capabilities needed for future missions and will better frame the interpretations once we obtain new observations.

Imaging clearly indicates that Europa's physical shell dynamics are coupled to geochemistry; but nothing so far has proven how this coupling is accomplished. I review some published ideas below and offer some new ones about the coupling. *Each idea upholds a significance of the mysterious non-ice "red stuff."*

To deflect unintended impressions that anybody actually understands Europa, I offer the following schedule of ideas. My sense is that we know as much about Europa now as we knew of Mars after *Mariner 9* (not so much, except how exciting it is).

Dynamic daily thinking

Monday's exogenous thought: the cell stain hypothesis. The icy shell of Europa is nearly pure ice. A red stain comes externally by implantation of magnetospheric plasma into ice and UV and particle radiation damage of ice. Staining is controlled by geologic structures and geography. Factors include: (i) heterogeneous distribution of mineral grain size and grain fabric (such as anisotropy), (ii) microtectonic fabric (such as ice strain and microfracturing), (iii) cumulative radiation damage (and age) of the ices, (iv) partial local topographic shielding and regional (latitude/longitude) control of the magnetospheric flux, and (v) temperature variations related to latitude and albedo. These factors cause differential retention and processing, loss to space, burial, or concentration of the products of exogenic alteration of ice and implanted exogenous species. Thus, Europa's structured surface is like a structured cell, which absorbs stains differentially, thus making visible cellular organelles and other subcellular structures. If Europa's icy shell is nearly pure ice, it may have originated by heterogeneous accretion or by efficient fractional crystallization of an ocean and brine drainage from ice.

Tuesday's endogenous thought: The invisible ink hypothesis. The floating shell may be nearly all H_2O, but the red stuff is emplaced as uncolored trace impurity. The stain, like invisible ink written onto the surface from below, has an endogenic origin. Diapiric structures, partial melting, intrusions, brine drainage, fractional crystallization, and explosive gassy eruptions redistribute and fractionate the stain and partly segregate it from ice. Charged particles, UV, and cosmic rays color the stain, which may be a trace sulfate (salt or acid); it may be related to the ocean or not.

Wednesday's hump thought: we might never make it to the end of the week. Without in-situ data we will not resolve exogenous and endogenous sources of the red stain, because it is chemically disequilibrated material. With both high-temperature suboceanic processing or radiation processing it all looks the same.

Thursday's humbling truth revealed? The "it's not just red barn paint" hypothesis. The red substance looks so bold on the surface because it is fundamentally a major component of a chemically complex floating shell. Whether intrinsically red or dyed by exogenic alteration, the physics of the icy shell and

viability of the ocean as a habitat is affected. It is probably a sulfate (hydrated sulfate salts or hydrated sulfuric acid). But that is not all. It is a heterogeneous mixture, perhaps short-chain sulfur, sulfuric acid, and sulfate salts; maybe add to that traces of arsenic minerals (e.g., realgar and orpiment), selenium, and sulfur phosphides. Sulfates and other soluble components may have been derived either from low-temperature or high-temperature aqueous alteration of the rocky interior of Europa. Solutes affect the melting point, density, viscosity, and thermal conductivity of the icy shell. It is central to issues of melt-through, diapirism, and tidal heating. Reaction products may have accumulated on the seafloor, and others may have floated to the base of the icy shell. Little about Europa can be understood without understanding this material.

Friday's party thought: Europa has an "Io" lurking below its ocean. The red substance comes up from below and is intrinsically red. Europa vents sulfur dioxide and Pele-plume-like red stuff into the ocean, where it quenches and eventually vents onto the surface or upwells through the ice. We can learn much about Europa by understanding Io.

Saturday's escape to the mountains: Whatever the red substance may be, the surface elemental, molecular, and mineralogical composition of Europa's surface can be tightly constrained by Earth- and Earth-orbit-based astronomical observations. We can then better constrain and model *Galileo's* observations. Top priority should be astronomical studies of charged ionic and neutral atomic/molecular particles emanating from Europa. Such studies may provide the only fundamental, new Europa observations for a long time.

Sunday's hope: Any Europa orbiter ought to be capable of (1) multispectral discrimination of sulfurous chromophores, and (2) neutral and ion spectroscopic determinations of elements from hydrogen through the masses at least of arsenic and selenium. The mission design should allow Europan and Ionian emanations to be distinguished.

BIBLIOGRAPHY:

Carlson, R.W., R. E. Johnson, and M. S. Anderson 1999. Sulfuric acid on Europa and the radiolytic sulfur cycle. *Science* 286, 97-99.

Clark, R.N., 2003, The surface composition of Europa: Mixed water, hydronium, and hydrogen peroxide ice, *Eos*, Trans. AGU, 84(46), Fall Meet. Suppl., Abstract P51B, F971

Fanale, F. P., and 22 colleagues 1999. Galileo's multi-instrument spectral view of Europa's surface composition, *Icarus* 139, 179-188.

Fanale, F.P., Y. H. Li, E. Decarlo, N. Domergue-Schmidt, S. K. Sharma, K. Horton, J. C. Granaham and Galileo NIMS team 2001. An experimental estimates of Europa's ocean composition independent of Galileo orbital remote sensing. *J. Geophys. Res.* 106, 14,595-14,600.

Greenberg, R. G., G. V. Hoppa, B. R. Tufts, P. Geissler, J. Riley, and S. Kadel 1999. Chaos on Europa, *Icarus* 141, 263-286.

Head, J. W. III, and R.T. Pappalardo, 1999. Brine mobilization during lithospheric heating on Europa: Implications for formation of chaos terrain, lenticula texture, and color variations, *J. Geophys. Res.* 104, 27,143-27,156.

Hogenboom, D.L., J. S. Kargel, J. P. Ganassan, and L. Lee 1995. Magnesium sulfate –water to 400 MPa using a novel piezometer: densities, phase equilibria, and planetological implications. *Icarus* 115, 258-277.

Kargel, J. S., J. Z. Kaye, J. W. Head III, G. M. Marion, R. Sassen, J. K. Crowley, O. Prieto-Ballesteros, and D. L. Hogenboom 2000. Europa`s crust and ocean: origin, composition and the prospects for life. *Icarus* 148, 226-265.

Kargel, J.S., J.W. Head, III, D. L. Hogenboom, K.K. Khurana, and G. Marion, 2001, The System Sulfuric Acid-Magnesium Sulfate-Water: Europa's Ocean Properties Related to Thermal State. *Lun. Planet. Sci.* XXXII, abstract 2138 (CD-ROM).

McCord, T. B., and 11 others 1999. Hydrated salt minerals on Europa's surface from the Galileo near-infrared mapping spectrometer (NIMS) investigation. *J. Geophys. Res.* 104, 11,827-11,851.

McCord, T. B., T. M. Orlando, G. Teeter, G. B. Hansen, M. T. Sieger, N. G. Petrik, and L. Van Keulen, 2001. Thermal and radiation stability of the hydrated salt minerals epsomite, mirabilite, and natron under Europa environmental conditions. *J. Geophys. Res.* 106, 3311-3319.

McKinnon, W.B. and M.E. Zolensky, 2003, Sulfate content of Europa's ocean: Evolutionary considerations, 35th Meeting of the Div. Planet. Sci, (abstract 6.02), *Bull., Amer. Astronom. Soc.*, 35, 919.

O'Brian, D. P., Geissler, P. and R. Greenberg, 2002. A melt-through model for chaos formation on Europa. *Icarus* 156, 152-161.

Pappalardo, R. T., and 10 colleagues 1998. Geological evidence for solid-state convection in Europa's ice shell, *Nature* 391, 365-368.

Pappalardo, R. T., and 31 colleagues 1999. Does Europa have a subsurface ocean? Evaluation of the geologic evidence. *J. Geophys. Res.* 104, 24015-24056.

Prieto, O., and J.S. Kargel, 2002, Thermal conductivity and thermal diffusivity of some hydrated salts at low temperature: Implications of Jupiter's satellite, Europa. Abstract 1726, *Lun. Planet. Sci.* XXXIII (CD-ROM).

Spaun, N.A. and J.W. Head 2001. Modeling Europa's crustal structure: Recent Galileo results and implications for an ocean. *J. Geophys. Res.*106, 7567-7576.

Spaun, N. A., J.W. Head, G.C. Collins, L.M. Prockter, and R.T. Pappalardo, 1998. Conamara Chaos Region, Europa: Reconstruction of Mobile Ice Polygons. *Geophys. Res. Lett.* 25, 4277-4280.

Zolotov, M.Y. and E.L. Shock, 2003, Energy for biological sulfate reduction in a hydrothermally formed ocean on Europa. *J. Geophys. Res.*, 108, E4, 5022, doi:10.1029/2002JE001966.

WHAT IS (AND ISN'T) WRONG WITH BOTH THE TENSION AND SHEAR FAILURE MODELS FOR THE FORMATION OF LINEAE ON EUROPA. S. A. Kattenhorn, Department of Geological Sciences, University of Idaho, PO Box 443022, Moscow, ID 83844-3022; simkat@uidaho.edu.

Introduction: An unresolved problem in the interpretation of lineae on Europa is whether they formed as tension- or shear-fractures. Voyager image analyses led to hypotheses that Europan lineaments are tension cracks induced by tidal deformation of the ice crust [1]. This interpretation continued with Galileo image analyses, with lineae being classified as crust-penetrating tension cracks [2]. Tension fracturing has also been an implicit assumption of nonsynchronous rotation (NSR) studies [e.g. 1-4]. However, recent hypotheses invoke shear failure to explain lineae development [5-6]. If a shear failure mechanism is correct, it will be necessary to re-evaluate any models for the evolution of Europa's crust that are based on tensile failure models, such as NSR estimates. For this reason, it is imperative that the mechanism by which fractures are initiated on Europa be unambiguously unraveled. A logical starting point is an evaluation of the pros and cons of each failure model, highlighting the lines of evidence that are needed to fully justify either model.

Types of Lineae: Numerous classification schemes have been developed to describe the range of lineae morphologies observed on Europa's surface [2-4, 7]. It is generally accepted that there is an evolutionary sequence of lineae development from fractures/isolated troughs, to proto-ridges/raised-flank troughs, to double ridges, and finally complex ridges.

Strike-Slip Faults. Many lineae on Europa show lateral offsets of relatively older structures. These strike-slip faults vary considerably in both morphology and size. Many resemble double ridges [6, 8] having small offsets (~100s of m); others are hundreds of km long and occur as several km-wide, internally deformed, dilational bands with offsets of up to 10s of km [9-10]. These features attest to the fact that shear failure is a major deformation mechanism on Europa.

Formation Mechanisms: A number of mechanisms have been proposed to explain the origin of lineae [11]. The two most prominent models are the tension and the shear failure models; however, neither model is undeniably more acceptable than the other.

Tension Models. Tension fracturing is assumed to be the result of stretching of the ice crust in response to the combined effects of diurnal tides and NSR (Fig. 1). Tensile stresses of <1 MPa are predicted to occur [2]. Orientations of fractures are dictated by principal tidal stress orientations. For such a model, there is only one preferred orientation of fractures forming at any one point in time.

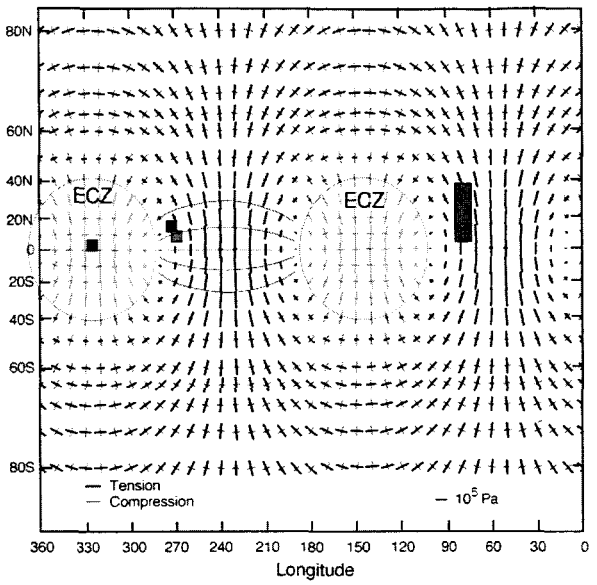

Figure 1. Principal tidal stresses at 1/8 orbit after apojove with 1° of NSR [2]. Gray areas are equatorial compressive zones. Red lines show expected locations and orientation ranges of tension fractures. Mapped regions: orange: [3], red: [4], blue and green: [6].

Shear Models. Shear failure is hypothesized to occur in equatorial compressive zones (ECZs), where tidal stresses are predicted to be compressive (Fig. 1). Frictional heating during shearing causes melting and possibly extrusion that gradually builds up ridges [5]. The Coulomb criterion for shear failure allows for a conjugate set of shear fractures. In the shear failure model, there are thus two potential orientations of fractures forming at any one point in time.

In Support of Tensile Failure Models: Other than in ECZs, tensile tidal stresses are common. Brittle materials are characteristically weaker in tension than in compression and ice on Europa is hypothesized to have a low tensile strength (<1 MPa) [2]. Orientations of major lineae agree remarkably well with orientations of tidal stresses (adjusting for NSR reorientation of the ice shell). Fracture mapping in both the leading and trailing hemispheres has shown a consistent rotation of fracture orientations through time [3-4], and no ambiguous cross-cutting relationships, agreeing with NSR model predictions for tensile fracturing.

Problems with Tensile Failure Models: There are also many aspects of lineae that are not supported by tensile failure models. The most obvious problem arises with lineae having orientations that could only

have occurred in the ECZs. In several mapped regions affected by ECZs (Fig. 1), lineae should have orientations within ~30° of E-W. However, such orientations are rare (Fig. 2), except for smooth bands, which are typically ~E-W oriented, extensional features [3-4]. Also unclear is how surface fractures evolve into ridges. Models for ridge development that invoke tapping into an underlying ocean have been criticized because they implicitly require a thin ice shell, which is inconsistent with mounting evidence for convection-driven diapirism in the crust, implying an ice thickness of at least 15km [12].

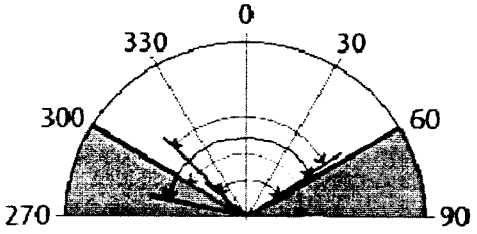

Figure 2. Expected range of orientations of tension cracks (light blue shaded areas) in the regions of the boxes in Fig. 1. Colored arrows show actual ranges of lineae in these regions (color scheme as in Fig. 1).

In Support of Shear Failure Models: The obvious appeal of shear failure models is that they can account for lineae development in the absence of tensile stresses in the crust. Furthermore, lineae orientations (Fig. 2) seem to agree with predicted conjugate set orientations in the ECZs (NW-SE and NE-SW) rather than those predicted by tension models [6]. Shear activity is supported by the existence of major strike-slip faults. If slip events are rapid, frictional heating along the fault walls provide a source for ridge-building material without the need to tap into an underlying ocean.

Problems with Shear Failure Models: At present, there is no convincing geological evidence that conjugate sets of similar-aged lineae exist in near-equatorial regions. This may be a reflection of a lack of explicit identification of such features rather than a lack of the features themselves. In a conjugate set, neither fault is more or less likely to form than the other; therefore, conjugate sets should show ambiguous cross-cutting relationships. Evidence of this has not been documented. Furthermore, inconsistent shear sense along features with identical orientations [6] is inconsistent with Coulomb failure predictions. The typical lack of offsets along most double ridges is also difficult to reconcile with lineae evolving as shear fractures. Finally, lineae at latitudes $\geq\pm40°$, where tensile stresses occur, are not morphologically different from ECZ lineae, raising the possibility that they have identical formation mechanisms (whether in tension or shear).

Discussion: Detailed mapping from Galileo images must continue across all latitudes and longitudes to clarify fracture sequences, cross-cutting relationships, the mechanics of fracture propagation, and contrary fracture behaviors in different locations. For example, [6] suggest that there is no clear sequence of rotating fracture orientations through time in the E4 and E6 regions, but rather superposed conjugate sets. In contrast, I have found no ambiguous cross-cutting relationships or evidence of conjugate fracture sets in the Bright Plains (BP) region, very near the E6 region of [6]. The BP shows a clear time progression of resolved shear sense on fractures in different orientations, in response to the rotating NSR stress field. The angles between BP double ridges with stratigraphically similar ages are not constant, ranging from 19-86°. The angle, θ, between conjugate faults is purely a function of the coefficient of sliding friction of Europan ice, μ, such that $\theta = \tan^{-1}(1/\mu)$. For a reasonable range of μ [13], θ should be restricted to 60-90°, suggesting that BP double ridges are not conjugate sets (but not disproving that they may be shear fractures). Fracture orientations in the BP (red in Fig. 2) do not fall within a stress field that permits tension fracturing, which may either imply shear fracturing, or may entail the existence of a stress component (such as fluid pressure) that superimposes tidal stresses. Finally, assuming that all fractures in the BP are tension fractures, the amount of NSR is estimated to be as much as 900° [4]. But if BP double ridges are conjugate shear fractures, NSR estimates must be reduced by at least 180°. This discrepancy clearly indicates that our inferences about the rotational history of Europa are inherently flawed by our lack of certainty about the origin of lineae.

References: [1] Helfenstein, P. and Parmentier, E.M. (1985) *Icarus*, 61, 175-184. [2] Greenberg, R. et al. (1998) *Icarus*, 135, 64-78. [3] Figueredo, P.H. and Greeley, R. (2000) *JGR*, 105, 22,629-22,646. [4] Kattenhorn, S.A. (2002) *Icarus*, 157, 490-506. [5] Nimmo, F. and Gaidos, E. (2002) *JGR*, 107, E4, 10.1029/2000JE001476. [6] Spaun, N.A. et al. (2003) *JGR*, 108, E6, 10.1029/2001JE001499, 1-21. [7] Head, J.W. et al. (1999) *JGR*, 104, E10, 24,223-24,236. [8] Hoppa, G. et al. (2000) *JGR*, 105, 22,617-22,627. [9] Schenk, P.M. and McKinnon, W.B. (1989) *Icarus*, 79, 75-100. [10] Sarid, A.R. et al. (2002) *Icarus*, 158, 24-41. [11] Pappalardo, R.T. et al. (1999) *JGR*, 104, 24,015-24,056. [12] Barr, A.C. and Pappalardo, R.T. (2002) GSA Abs. Progs. 34, (6), 36-37. [13] Rist, M.A. et al. (1994) *Annal. Glaciol.*, 19, 131-137.

Acknowledgements: Supported by NASA grant NAG5-11495 and NASA Idaho EPSCoR NCC5-577.

IMPLICATION ON POSSIBLE SUBMARIN BIOSIGNATURES AT CHAOTIC TERRAINS. A. Kereszturi (Department of Physical Geolography, Eotvos Lorand University of Sciences, Pázmány sétány 1/C, Budapest, H-1088, Hungary, E-mail: krub@freemail.hu)).

Introduction: Observations and theories suggest Europa is interesting object for astobiology [1,2,3]. For future radar and cryobotic missions we have to know the best locations for analysis. Here we summarize aspects of some processes and structures in the icecrust interesting for astrobiology. We suggest the best locations are great chaotic terrains with signs of internal activity [4,5] which may hold information on the submarin geothermal centers too.

Ice crust: Based on the Galileo's images we estimated the relative height of "icebergs" inside at a 48x38 km part of the famous Conamara Chaos with errors of measurements below of 20%. We analysed the real shape of rafts by Airy isostasy taken the crust to be in mechanical, hydrostatical equilibrium and composed of ice with density of 0.9175 g/cm^3. On *Fig. 1.* the theoretical process of terrain breaking is visible: during the formation that blocks which were broken into pieces with greater height than width, rotate into more stable drifting position. Based on the size and shape distribution we can find the isometric shaped blocks which diameter is equal to the thickness were present before the terrain breaking.

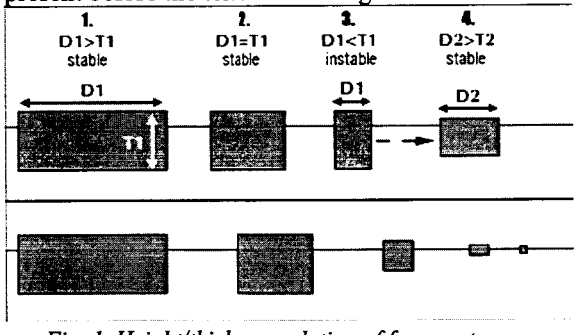

Fig. 1. Height/thickness relation of fragments

On *Fig. 2. A* the shadow based average relative heigth of certain blocks versus the blocks' maximal diameter is visible. The relative height distribution turns off around 75 m height and 2000 m diamater. Based on isostatic drifting, the absolute ice thickness of the original blocks were 2 km, of the matrix is about 0.5 km (*Fig. 2. B*) based on the "block rotation method". Before terrain breaking probably ice thinning took place until the onset of instable situation. This may be the reason that estimations from other authors prefer higher value near to 20 km [6].

Processes during ice thinning: Below the thinning ice we have decreasing hydrostatic pressure and gases become less soluble. Depending on the solubled gas composition and temperature of the warm plume, gases with high enough vapor pressure (like some carbohydrates) can "boil" and change into the form of gas bubbles. The best locations for bubble formation are along tectonic lineaments between rafts where water can get very near to the surface. Here we have not only concentration of gas bubbles but strong brine migration too. Based on the orientation of rafts' straight edges the breaking took place along previous linear weakening zones parallel to the lineaments of surrounding terrain (*Fig. 3*). Based on our calculation the low level matrix could be as thin as 500 m, at the faults even thinner with even lower overburden pressure. Gas bubbles freezed into the ice can give information on chemistry, possible nutrients at submarin volcanic centers.

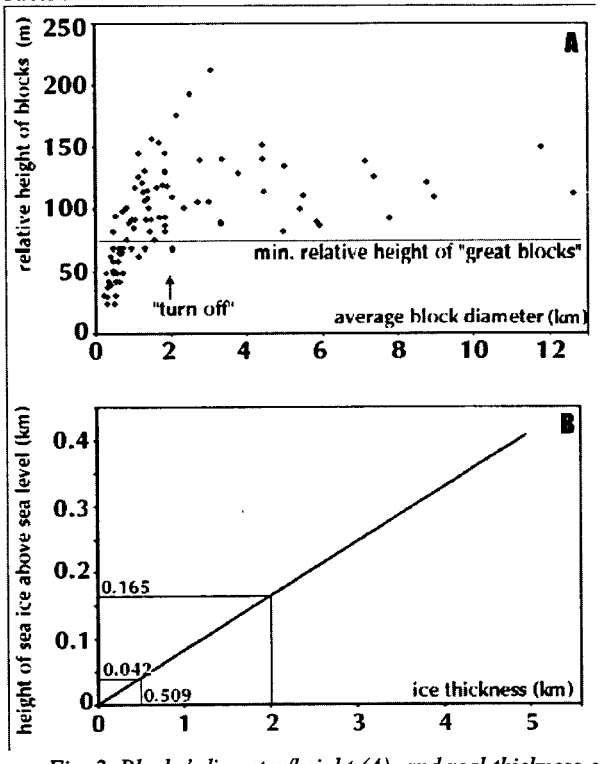

Fig. 2. Blocks' diameter/height (A), and real thickness of blocks (2 km) and matrix (0.509 km) (B)

Processes during ice thickening: Important precesses take place during thickening of the crust during the cease of submarin geothermal activity. The ice's thickening speed slows exponentially in an ideal case with the most imortant period at the beginning when obverburden ice is thin (hydrostatic pressure is low), and thermohalin water plume is still present. During the freezing of new ice we have the following

possibilities: *1. Freezing of floating particles into ice* originated from submarin volcanic center. The settling speed of solid particles in water depends on the density difference and upward speed of water plumes and described by Stokes law. Under thermadynamic equilibrium at the base of the ice crust at chaotic terrain we have freezing and thawing together. Inside freezing parts solid particles can freeze into the ice. Based on estimations of [7] vertical water flow can be in the order of mm/s. With the average density of common weathered and hydrated silicates, spherical particles with diameter smaller than 1 mm can be carried to the top of the ocean with plumes [8]. During a cryobotic mission we can observe them if their settling velocity is lower than the cryobot's sinking speed. (In the case of faster setlling particles accumulate at the bottom tip of water filled cave around the cryobot.). *2. Chemical layering* because of vertical changes in the physical parameters. During the thickening of ice under growing hydrostatic pressure water can solve more material. As a result the thinner the ice is, the more material condense out from the solution. After the end of the refreeze we have decreasing ratio of solid condensates in downward direction and growing ratio of possible solubled and refreezed materials depening on phase changes inside the ice.

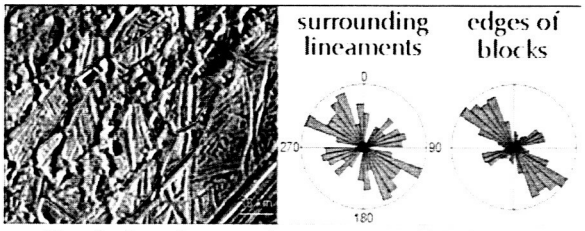

Fig. 3. Distribution of orientation of blocks' edge and surrounding lineaments

Structures are probably present today: Estimating the ratio of original and changed surface (with and without pre-breaking lineaments) we can have the recycled area and volume too. The former is nearly 50% at the analysed chaos and the later is 18000 km^3 if 2 km would have been the original thickness. In the case of 20 km of original thickness the same later is around of 160000-200000 km^3.

Implication for future probes: The best possible targets for in-situ analysis of the upper mentioned processes are: 1. young chaotic terrains (the older the terrain is the more extensive decomposition could took place by brine migration and other processes), 2. high ratio of matrix/original rafts (for much new and recycled refrozen material), 3. great size of chaotic terrains (higher level of geothermal activity rises more possible biosignatures and melts/refreezes more ice). Possible layering (chemical and physical) could be observed with sophisticated penetrating radar technology not only at fresh but at overprinted chaotic terrains. In the case of a cryobotic mission [9] without the ability of precise landing we have statistical chance to land and thaw through new and not old ice. But connecting our results with other estimations for original crustal thickness before terrain breaking, our probe have to meet with new ice deeper than 2 km. The best location would be in the low level matrix, we can land there with chance of 50% in the upper analysed case when the landing ellipse covers the central part of the chaos.

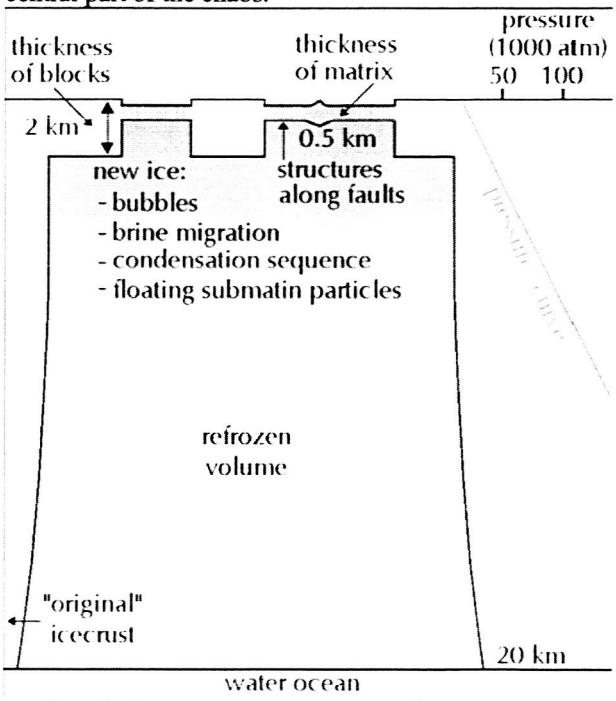

Fig. 4.: Important structures in reforzen ice

References: [1] Brack A. (ed.) (1998) Potential non-martian sites for extraterrestrial life, in Exobiology in the Solar System & the search of life on Mars, pp. 65-67. [2] McCord, T. B. et al., Salts on Europa"s surface detected by galileo near infrared mapping spectrometer, Science 280, pp. 1242-1245. [3] Carr M. H. et al. (1998) Evidence for a subsurface ocean on Europa, Nature 391, pp. 383-365. [4] Greenberg, R. et al. (1999) Tectonic processes on Europa: Tidal stresses, mechanical response, and visible features, Icarus 135, pp. 64-78. [5] Greenberg R. at al. (1998) Icarus 135, 64-78. [6] Schenk, P. M. (2002), Nature 417, pp. 1341-1345. [7] Goodman J. C., Collins, G. C., Marshall, J. (2002) JGR in press, [8] Thomson, R. E., Daleney J. R. (2001) (2001)Evidence for a weakly stratified European ocean sustained by seaflor flux,, JGR 106, 12335-12365. [9] Biele J., Ulmanec S., Barber S. J., Wright, I. P. (2003) Proc. Of the Second European Conference on Exo/Astrobiology

DEFORMATION OF ICE. D. L. Kohlstedt, University of Minnesota (Department of Geology and Geophysics, Pillsbury Hall, Minneapolis, MN 55455; dlkohl@umn.edu)

Introduction: Ice, like other materials, deforms by brittle, ductile, or a combination of brittle and ductile processes. The dominant mechanism of deformation is determined by the conditions to which the mass of ice is subjected. At low temperatures and high differential stresses, deformation occurs predominantly by brittle processes, while at high temperatures and low stresses, ductile process govern flow behavior. As pressure increases with increasing depth, brittle deformation gives way to ductile flow. The transition occurs roughly at a depth at which the lithostatic pressure reaches the level of the differential stress.

In my talk, I will first review aspects of brittle deformation, emphasizing mechanisms of crack nucleation and propagation. I will then focus on ductile deformation or creep of ice, concentrating on recent progress arising from laboratory experiments that provide new insights into mechanisms of plastic flow. Field observations on flow of glaciers and ice sheets provide a direct test of the applicability of laboratory results to large-scale flow of ice. In addition, I will address the role of water on the rheological properties of ice.

Creep of Ice: Creep of most crystalline materials, at least if steady-state flow is attained, is reasonably well described by a flow law of the form:

$$\dot{\varepsilon} = A\frac{\sigma^n}{d^p}\exp\left(-\frac{E+PV}{RT}\right) \qquad (1)$$

where $\dot{\varepsilon}$ is strain rate, A a materials parameter, σ differential stress, d grain size, E activation energy, V activation volume, P pressure, T temperature, and R the gas constant. The values of the stress exponent n and the grain size exponent p are characteristic of the mechanism of deformation.

In the dislocation creep regime, $n = 4.0$ and $p = 0$ for ice; that is, at relatively large grain sizes and/or high differential stresses, deformation is grain-size insensitive [1]. At smaller grain sizes and/or lower stresses, grain-size sensitive flow processes become important. In most materials, diffusion creep dominates at lower stress and finer grain sizes, characterized by $n = 1$ and $p = 2$-3. However, in ice, diffusion creep is not readily accessible. Nonetheless, a significant grain-size sensitive regime exists for ice.

To explore grain-size sensitive creep under laboratory conditions (i.e., strain rates greater than $\sim 10^{-8}$ s^{-1}) fine-grained samples are essential. Laboratory results obtained on samples with small grain sizes can be extrapolated to larger grain sizes appropriate for flow of glaciers and icy satellites using flow laws such as that in Eq. (1). One grain-size sensitive creep regime has been identified for ice. At constant grain size and temperature, a transition occurs with decreasing stress from dislocation creep to a regime in which grain boundary sliding and basal slip operate in concert to yield $n = 1.8$ and $p = 1.4$ [2].

The constitutive equation describing flow of ice over a wide range of stress, grain size, and temperature conditions can then be expressed as the sum of the contributions from dislocation (dis) creep, with $n = 4.0$ and $p = 0$, and grain-boundary sliding (gbs) accommodated basal slip, with $n = 1.8$ and $p = 1.4$:

$$\dot{\varepsilon}_{tot} \approx \dot{\varepsilon}_{dis} + \dot{\varepsilon}_{gbs} \qquad (2)$$

In Eq. (2), the subscript tot indicates total strain rate, and the approximately equal to symbol suggests that other creep mechanisms (such as diffusion creep) may contribute under yet unexplored deformation conditions. Historically, creep of ice has been described by a single flow law $n = 3$ [3], which is now understood to reflect deformation experiments carried out at the transition between dislocation creep ($n = 4.0$) and grain-boundary sliding accommodated basal slip ($n = 1.8$).

One direct test of laboratory-derived flow laws is comparison with field observations of flow of glaciers and ice sheets. Based on a field experiment on the Barnes Ice Cap, both the microstructure and the stress exponent ($n = 1.7$) observed at low shear stresses of ~0.02 MPa on relatively coarse-grained ice [4] are similar to those obtained in laboratory experiments in the grain-size sensitive creep regime [2]. Likewise, with decreasing stress, a transition from $n = 4.5$ to $n = 1.9$ was reported for flow of ice with a grain size $d > 1$ mm in the Meserve Glacier [5]. More recent field studies also observe grain-size sensitive flow [6]. Hence, the laboratory-derived constitutive equation for ice appears to provide a robust framework for modeling the rheological behavior of Europa.

References:

[1] Durham W. B.. and Stern L. A.(2001) *Annu. Rev. Earth Planet. Sci.*, 29 295-330. [2] Goldsby D. L. and Kohlstedt D. L., (2001) *J. Geophys. Res., 106,* 11017-11030. [3] Glen J. W. (1955) *Proc. Roy. Soc., A228* 111-114. [4] Hooke R. L. (1973) *J. Glac., 12,* 423-438. [5] Holdsworth G. and Bull C. (1968) *Int. Symp. Antarcic Glaciological Exploration, 86* 204. [6] Cuffey K. M., Thorsteinsson, T. and Waddington, E. D. (2000) *J. Geophys. Res., 105,* 27889-27894.

CAN THE ELECTRONIC TONGUE BE GIVEN A TASTE FOR LIFE? G. A. Konesky, Bovie Medical Corp., 3 Rolling Hill Rd, Hampton Bays, NY 11946-3716, g.konesky@att.net

Introduction: An integrated array of electrochemical sensors, termed the "electronic tongue," has been developed for in-situ determination of extraterrestrial geochemistry [1]. By noting the ability of a microorganism to modify its environment, but also making minimal assumptions otherwise, such a sensor array can be used as an electrochemically-based growth sensor [2].

A complimentary approach relies on the collection and detection of respiratory electrons [3], again without relying on any specific terminal electron acceptor.

Both approaches, unfortunately, are susceptible to local geochemistry posing as biochemistry. By combining strategies, along with techniques of variable sample size influence on time-resolved activity, a robust and reproducible system results for the remote detection of microbial life. Spaceflight hardware realizations benefit form small size, low weight, low power requirements, low data rates, and simple construction which is tolerant to shock and vibration. Experimental results are discussed.

References: [1] Kounaves, S. P. et al. (2002) *Environmental Electrochemistry*, ACS, Symp. 811, 306-319. [2] Kounaves, S. P. et al. (2001) *SPIE Proc. 4495,* 137-144. [3] Konesky, G. A. (2003) *IEEE Aerospace*, Vol. 2.07, 2.0704.

EUROPA'S ICY CRUST AS A HABITAT AND REPOSITORY OF LIFE. Jere H. Lipps. Department of Integrative Biology and Museum of Paleontology, University of California, Berkeley, California 94720, jlipps@uclink4.berkeley.edu.

Life, if it exists or existed on Europa, could be abundant and varied [1-3], as well as preservable in the surface ice. Europa's probable sub-ice ocean would provide a large number of habitats. By analogy with Earth's icy habitats, many ecologic settings are likely in and on the ice, as well as the on the ocean's floor and in the water column [4-8]. All of these could have been preserved in place or transported to the icy crust through oceanographic, geologic, glaciologic or biologic processes.

Habitats in the ice include the large fissures and refrozen areas, areas below clear ice that transmits light, tiny cracks, brine channels, inter-crystal water films, ice surfaces in the water, and oases caused by impact, volcanic heat, or surface meltwater. Some of these places might be inhospitable to life because of extreme chemical, radiation or other conditions, but are included here for more careful consideration, given the tenacity of life in Earth's ice-influenced environments.

The ice would likely preserve current life and fossil organisms, traces or biomarkers once they were incorporated into it. Later geologic processes may have brought them close to, or exposed them, at the surface where they could be imaged and sampled. Europa's geology indicates a relatively young, dynamic crust that created many terrains and exposures [9] that could be targeted for further exploration. These sites include the areas of refrozen ocean, the ridges and rills associated with fissures, low areas where water may have collected, and "dirty" ice that may include benthic material floated to the surface by bottom anchor ice or gouged by ice, as well as the wide variety of ice habitats. Pelagic life might be preserved abundantly. Because the ice on Europa varies in age and a stratigraphy can be assembled, a history of life may also be reconstructed.

Thus, a sampling strategy for life and its history on Europa should include paleontological and molecular biological objectives that would clearly document the present and former existence of life on Europa. The strategy should include pre-landing detailed imaging of sites with probable preserved or extant ice habitats, followed by surface exploration with impactors, penetrators, ice clippers, or rovers to outcrop and surface materials.

References: **[1]** Chyba, C. F. 2000. Energy for microbial life on Europa - A radiation-driven ecosystem on Jupiter's moon is not beyond the bounds of possibility. Nature 403(6768): 381-382. **[2]** Chyba, C. F. and C. B. Phillips. 2001. Possible ecosystems and the search for life on Europa. Proc. National Acad. Sciences USA 98(3): 801-804. **[3]** Chyba, C. F. and C. B. Phillips. 2002. Europa as an abode of life. Origins of Life and Evol. Biosphere 32(1): 47-68. **[4]** Krebs, W. N., J. H. Lipps, and L. H. Burckle. Ice diatom floras, Arthur Harbor, Antarctica. Polar Biology. 7:163-171. **[5]** Lipps, J. H. W. N. Krebs. 1974. Planktonic foraminifera associated with Antarctic sea ice. Jour. Foraminiferal Research. 4:80-85. **[6]** Lipps, J. H., W.N. Krebs, and N. K. Temnikow. 1977. Microbiota under Antarctic ice shelves. Nature. 265:232-233. **[7]** Lipps, J.H., T. E. Ronan, Jr., and T. E. DeLaca. 1979. Life below the Ross Ice Shelf, Antarctica. Science. 203:447-449. **[8]** Lizotte, M. P., and K. R. Arrigo (Eds.). 1998. Antarctic sea ice: biological processes, interactions and variability. Antarctic Research Series 73: 1-198. **[9]** Pappalaroo, R. T., J. W. Head, and R. Greeley. 1999. The hidden ocean of Europa. Scientific American. 281(4):54-63.

PROBING EUROPA'S INTERIOR WITH NATURAL SOUND SOURCES. Nicholas C. Makris, *Massachusetts Institute of Technology, Cambridge, MA 02139, USA, (makris@mit.edu)*, Sunwoong Lee, *Massachusetts Institute of Technology, Cambridge, MA 02139, USA*, Robert T. Pappalardo, *University of Colorado, Boulder, CO 80309-0392, USA.*

The exploration of Jupiter's icy moon Europa is of paramount interest to astrobiology. Since Europa may harbor a vast liquid ocean below the surface, it is considered one of the most likely places in the solar system for extraterrestrial life to exist. However, there is still no conclusive evidence that a subsurface ocean exists on Europa, and great uncertainties remain on the thickness of the outer ice shell and depth of the potential ocean. Seismo-acoustic surveys are necessary techniques to provide ground truth information on these substantial uncertainties.

Our goal is to use both seismo-acoustic echo-sounding and tomographic techniques to determine Europa's interior structure. Echo-sounding reveals the depth and composition of terrestrial seafloor and sub-bottom layers by analysis of the arrival time and amplitude of acoustic reflections from these interfaces. Tomography reveals the temperature structure of terrestrial oceans by the way sound waves are perturbed along forward propagation paths. We plan to exploit natural cracking events on Europa's surfaces as sound sources of opportunity. Recent work shows that cycloidal cracks on the surface of Europa likely form on a daily basis due to stresses induced by Europa's eccentric orbit which has a period of roughly 3.5 days [1]. We estimate that the acoustic waves radiated from these cracks will be in the $0.1 \sim 100$ Hz range with typical wavelengths exceeding 1 km. In contrast to ice-penetrating radar, such long wavelength disturbances suffer minimal attenuation from mechanical relaxation mechanisms in ice an water and are relatively insensitive to anomalies such as ice fractures. Meteor impacts typically occur at a monthly rate and also have potential use as sound sources.

The Jupiter Icy Moons Orbiter may carry a triaxial seismometer capable of measuring seismo-acoustic displacements in three spatial dimensions at a single point on Europa's surface. Many valuable measurements can be made with a single seismometer. For example, an initial task for this sensor would be to determine the overall level of seismo-acoustic activity on Europa by time series and spectral analysis [2]. This would provide a simple and direct method for determining the level of current surface activity. Correlations could be made of ambient noise versus environmental stress level to determine whether noise levels respond directly to orbital eccentricities. Such an analysis was conducted for the Earth's Arctic Ocean where roughly two meters of nearly continuous pack ice cover an ocean that is typically between $0.1 \sim 5$ km in depth. These terrestrial results show a near perfect correlation between underwater noise level and environmental stresses and moments applied to the ice sheet from wind, current, and drift [3]. Additionally, in the Antarctic, tidally driven ice cracking events and the subsequent tidally driven opening and closing motion of these cracks have long been incidentally observed in ice shelves, and the level of seismicity due to tidally induced ice-fracturing events are shown to be strongly correlated with the sea tides [4, 5].

Robust estimates can be made of Europa's ice layering structure and potential ocean depth with a single acoustic sensor if the signal-to-noise ratio is sufficiently high [2]. On Europa, an isolated cracking event from a cycloidal feature will lead to numerous echoes emanating from multiple reflections of compressional, shear and combined compressional-shear waves from the various layers of Europa's ice-water interior. Using 3-D seismo-acoustic propagation models developed for the Arctic Ocean on Earth, we find that the spacing of arrivals in time can be used to robustly estimate source range as well as ice and ocean layering parameters. To investigate signal-to-noise ratio issues, we have developed a Europan waveguide noise model that is based on classical ocean acoustic noise models [2, 6]. Our present simulations indicate that possible "Big Bang" cracking events lead by the interplay of diurnal stresses with inhomogeneities in the outer ice shell or Europa's potential asynchronous rotation due to an ocean layer below will emanate significant amount of seismo-acoustic waves that can stand robustly above Europan ambient noise. We also show that impacts of even small meteors fall into the Big Bang category that may be frequent enough to be used as sources of opportunity.

The regions in which ice faulting are active can be identified with multiple sensors. The identification of active faulting regions are especially important to astrobiological studies on Europa since faults provide a rapid mechanism for transport of materials from the surface to the ocean and vice-versa. These active regions could form potential habitats for life since the transport of materials may provide necessary ingredients for life. Seismo-acoustic measurements can identify and localize these active faulting regions without ambiguity.

References

[1] Hoppa, G. V., Tufts, R., Greenberg, R., Geissler, P. E., 1999, *Science*, **285**, 1899-1902.

[2] Lee, S., Zanolin, M., Thode, A. M., Pappalardo, R. T., Makris, N. C., 2003, *Icarus*, **165**, 144-167.

[3] Makris, N. C., Dyer, I., 1986, *J. Acoust. Soc. Am.*, **79**, 1434-1440.

[4] Robin, G., 1958, Glaciology III, Norsk Polarinstitut, Oslo.

[5] Anandakrishnan, S., Alley, R. B., 1997, *J. Geophy. Res.*, **102**, 15183-15196.

[6] Kuperman, W. A, Ingenito, F., 1980, *J. Acoust. Soc. Am.*, **67**, 1988-1996.

Wax models of Europan tectonics. Michael Manga[1] and Antoine Sinton[2], [1]Department of Earth and Planetary Science, University of California, Berkeley, 94720, USA (manga@seismo.berkeley.edu) [2] Magistere des Science de la Matiere, Ecole Normale Superieure de Lyon, FRANCE (asinton@ens-lyon.fr).

Introduction: The Europan surface preserves a wide range of features that suggest extension [1], compression [2] and strike-slip motion [3]. Understanding the origin and dynamics that result in these surface features may ultimately provide insight into the rheological and thermal structure of the Europan ice shell, and its evolution through time.

Developing theoretical and numerical models for Europan tectonics is challenging because they should involve coupled brittle failure and (nonlinear) viscous flow. The mathematical complexity of the problem but geometric simplicity of phenomena on the Earth that involve plates (e.g., plate tectonics, solid crusts on lava lakes) has motivated several studies of transform and microplate dynamics using wax analoguess [4-5]. We thus built an experimental apparatus to simulate Europan ice tectonics, and performed a set of experiments with model parameters appropriate for Europa.

Experimental approach: Our experimental approach follows that of previous studies [4-5] but also allows for periodic surface deformations that arise, for example, from tidal deformation. In these experiments, solid wax simulates the brittle, elastic layer and the molten wax simulates the region that deforms as a viscous fluid, either warm ice [6] or liquid water [7]. The solid layer of wax actually consists of two sublayers – a brittle layer that can break and a ductile layer that deforms viscously.

Figure 1 shows the experimental apparatus. The wax container (right) is heated by a resistance heater until the wax is entirely molten. The surface of the wax is then cooled with the fan shown in the upper right. A layer of solid wax develops at the surface, and the steady-state thickness of the solid wax layer is controlled by adjusting the heat flux provided by the resistance heater. Once the solid wax layer has thickened to its steady-state value, the motor (left) is turned on. The various signal generators, amplifiers, and power supplies shown on the left control the horizontal motion of the vertical plate that is immersed in the wax tank. We can control the rate of secular extension (or compression), and the period and amplitude of any time-dependent or oscillatory deformation.

Scaling: The use of waxes as analogues for geological materials has perhaps been most successful in studies of lava flow morphology and emplacement [see review in 8]. Wax models of lava flows exhibit the full range of morphologies, from pillows, to rifted flows, to folded flow and finally sheet flows with increasing extrusion rate.

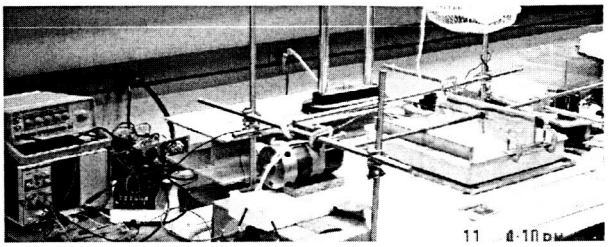

Figure 1: Photo of experimental apparatus.

The dimensionless parameter that governs lava flow morphology (at least in the lab experiments), and allows the analogue experiments to be scaled to real lava flows, was found to be ψ = cooling time scale / deformation time scale.

A second parameter is needed to characterizes the relative magnitudes of secular dilation and tidal cycling. This is denoted γ and is defined in [7].

For a brittle ice layer thickness of 1 km and using a tidal strain rate to estimate the deformation time scale, we obtain $\psi \sim 54$ for Europa. Given the uncertainties of the various parameters that affect ψ, we consider $10 < \psi < 300$ and $0 < \gamma <$ infinity in our experiments.

Results and conclusions: Our wax experiments can produce a wide range of surface features that, at least qualitatively, resemble many of the surface features on Europa including bands and ridges. We do not, however, create and preserve features that clearly resemble chaos and double ridges. Interestingly many of the patterns more closely resemble images of Ganymede's surface [9]

A typical experiments is shown in Figure 2. The overall width of this band is about twice the total amount of extension. The individual ridges that make up this band are folds (half a wavelength long) that form during the compression phase of the periodic deformation. Each fold and ridge are bounded by what was once a fault in the brittle wax layer. The complex pattern of these ridges arises when, due to shear localization, rifting jumps from one location to another.

We were able to perform a total of 26 experiments (before the first author accidentally allowed the apparatus to self-destruct) for different values of ψ, γ and thickness of the solid wax layer. Our preliminary conclusions are

- Band-like features can form if $\gamma > 0$. Small scale folds (Figure 3) within the bands are not always parallel to each other as a result of shear localization [10]. Bands may have

complex morphologies, as illusratedd in Figure 2 and 4.

- The width of band-like features can in some cases be quite a bit greater than the total amount of extension (see Figure 4 where there is no net extension).
- Features resembling class 2 structures [7] form for γ < about 0.2 and ψ less than about 100.
- Features that most closely resemble double ridges form only where strike-slip motion dominates and where γ is small.
- The wavelength of small scale structures (folds) is similar to the total thickness of the solid wax layer.Figure 2: Band-like feature (γ = 0.1, ψ = 30)

Figure 2: Band-like feature (γ=0.1, ψ=30).

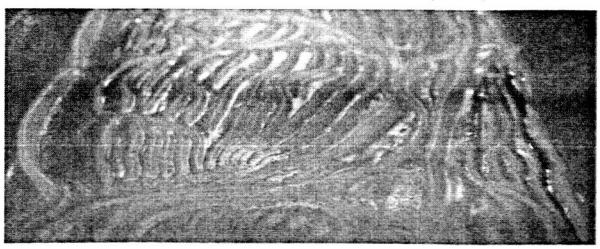

Figure 3. Band containing nonparallel ridges that form from strain localization (γ = 0.4 and ψ = 20)

Finally, we also performed some experiments in which the thickness of the brittle layer was variable. Figure 4 shows an example of the structures that develop. Where the brittle layer is thinnest (middle of photo, box 2, where ψ = 0.01) structures extend radially from the region where the brittle layer is thinnest. On the sides of the photo, ψ = 30 and the band structure is similar to that in Figure 2.

If the processes that occur in the lab experiments are indeed similar to those that produce bands, the morphology of bands and features within bands can be used to infer the thickness of the brittle layer, and identify regions where the brittle layer is thinnest.

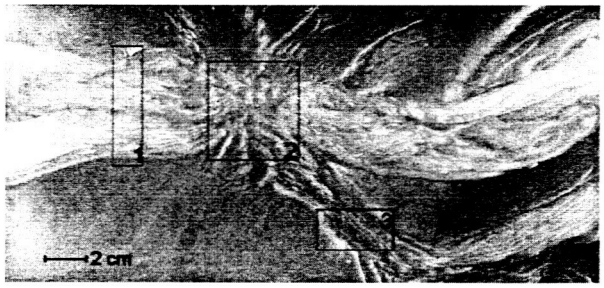

Figure 4: Solid layer has a variable thickness (ψ~ 0.01 in box 2 and 30 near the sides of the photo; γ = 0).

References: [1] Prockter LM et al (2002) *JGR, 107*, 10.1029/2002JE001458. [2] Prockter LM and Pappalardo RT (2000) *Science, 289*, 941-943. [3] Nimmo F and Gaidos E (2002) *JGR, 107*, 10.1029/2000JE001476. [4] Olderburg DW and Brune JN (1972) *Science, 178*, 301-304. [5] Ragnarsson R et al (1996) *Phys Rev Lett, 76*, 3456-3459. [6] Sullivan R et al (1998) Nature, 391, 371-373. [7] Tufts R et al. (2000) Icarus, 146, 75-97. [8] Griffiths RW (2000) *Ann Rev Fluid Mech, 32*, 477-51. [9] Head JW et al (2002) *GRL, 29*, 10.1029/2002GL015961. [10] Wylie JJ and Lister JR (1998) *J Fluid Mech, 365*, 369-381.

SURFACE PENETRATING RADAR SIMULATIONS FOR EUROPA. T.Markus, *NASA Goddard Space Flight Center, Code 975,Greenbelt, MD 20771, USA (Thorsten.Markus@nasa.gov)*, S.P. Gogineni, *University of Kansas, Lawrence, KS 66045*, J.L. Green, S.F. Fung, J.F. Cooper, W. W. L. Taylor, L. Garcia, *NASA Goddard Space Flight Center, Code 630, Greenbelt, MD 20771, USA*, B.W. Reinisch, P.Song, *University of Mass. Lowell, Lowell, MA 01854, USA*, R. F. Benson, *NASA Goddard Space Flight Center, Code 692, Greenbelt, MD 20771, USA*, D. Gallagher, *NASA Marshall Space Flight Center, Huntsville, AL 35812, USA.*

Of the icy moons of Jupiter, Europa is thought to be the best candidate for having a liquid ocean underneath a relatively small layer of ice. Estimates put the thickness of the ice shell anywhere between 2-30 km, with a few models predicting up to 100 km. Much of the uncertainties are due to the largely unknown temperature gradients and levels of water impurities across different surface layers. One of the most important geological processes is the possible transportation of heat by ice convection. If the ice is convecting, then an upper limit of about 20 km is set for the depth of the ocean underneath. Convection leads to a sharp increase in temperature followed by a thick region of nearly constant temperature. If ice is not convecting, then an exponentially increasing temperature profile is expected. The crust is thought to be a mixture of ice and rock. Although the exact percentage of rock is not known, it is expected to be low. Additionally, the ice crust could contain salt, similar to sea ice on Earth. The exact amount of salt and how that amount changes with depth is also unknown. In preparation for the Jupiter Icy Moons Orbiter (JIMO) mission, we performed simulations for a surface-penetrating radar investigating signatures for different possible surface and sub-surface structures of these moons in order to estimate the applicability of using radar with a frequency range between 1 and 50 MHz. This includes simulations of power requirements, attenuation losses, layer resolutions for scenarios with and without the presence of a liquid ocean underneath the ice, cases of convecting and non-convecting ice, different impurities within the ice, and different surface roughnesses.

The figure shows simulations of a received subsurface sounding signal at 10 MHz for a typical Europa scenario. In this case, we treated the 7-km ice as a layered medium consisting of a 2 km-thick icy crust with 5% impurities and 5 km-thick pure ice with bedrock or an ocean underneath. The 5-km layer of pure ice is assumed to be convecting or non-convecting with resulting differences in the temperature profile. The results show that we will be able to differentiate between a) ice covering bedrock from b) ice covering an ocean, as well as between convecting and non-convecting ice. The ice/rock-ice interface is at a depth of 2 km in both cases. The ice-ocean or ice-bedrock interface is at a depth of 7 km in both cases (the data beyond 7-km in are a) due to the foldover effect of the FFT).

The space environment above the icy surface of Europa is a source of radio noise in this frequency range from natural sources in the Jovian magnetosphere. The ionospheric and magnetospheric plasma environment of Europa affects propagation of transmitted and return signals between the spacecraft and the solid surface in a frequency-dependent manner. The ultimate resolution of the subsurface sounding measurements will be determined, in part, by a capability to mitigate these effects. We discuss an integrated multi-frequency approach to active radio sounding of the Europa ionospheric and local magnetospheric environments, based on operational experience from the Radio Plasma Imaging (RPI) experiment on the IMAGE spacecraft in Earth orbit, in support of the subsurface measurement objectives.

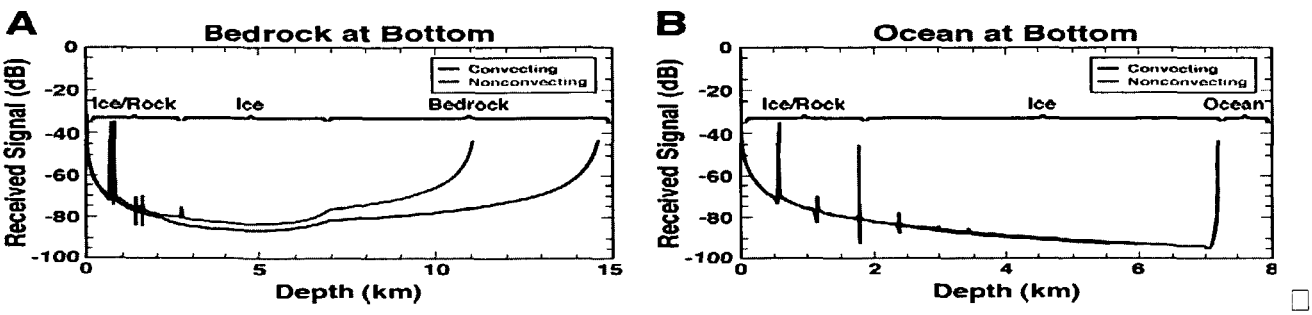

ANALYSIS OF EUROPAN CYCLOID MORPHOLOGY AND IMPLICATIONS FOR FORMATION MECHANISMS. S. T. Marshall and S. A. Kattenhorn, Department of Geological Sciences, University of Idaho, Moscow, ID 83844-3022. (mars0776@uidaho.edu; simkat@uidaho.edu)

Introduction: Europa's highly fractured crust has been shown to contain features with a range of differing morphologies [1,2]. Most lineaments on Europa are believed to have initiated as cracks, although the type of cracking (e.g. tensile vs. shear) remains unclear and may vary for different morphologies. Arcuate lineaments, called cycloids or flexi, have been observed in nearly all imaged regions of Europa and have been modeled as tensile fractures that were initiated in response to diurnal variations in tides [3,4]. Despite this hypothesis about the formation mechanism, there have been no detailed analyses of the variable morphologies of cycloids. We have examined Galileo images of numerous locations on Europa to develop a catalog of the different morphologies of cycloids. This study focuses on variations in morphology along individual cycloid segments and differences in cusp styles between segments, while illustrating how morphologic evidence can help unravel formation mechanisms. In so doing, we present evidence for cycloid cusps forming due to secondary fracturing during strike-slip sliding on pre-existing cycloid segments.

What Qualifies a Cycloid: A cycloid (Fig. 1) is defined as an arcuate fracture that contains at least two segments and one cusp. Cycloids have previously been noted to be variably manifested as fractures, double ridges, and smooth bands [3-5].

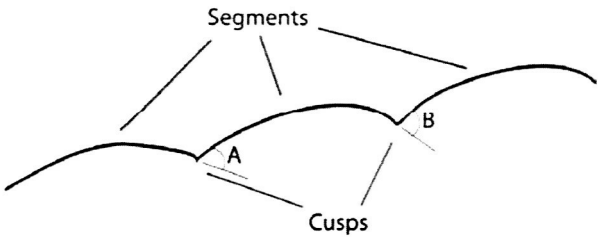

Figure 1. A cartoon of a typical cycloid consisting of segments and cusps with, in this case, differing cusp angles A and B.

Previous Models: Previously, cycloids were interpreted to have formed by thrust faulting [5] or as a result tensile fracturing in a diurnal stress field [3,6]. The diurnal model follows from rotation of principal tidal stress orientations during each Europan day (counter-clockwise in the northern hemisphere and clockwise in the southern hemisphere) [3]. In this model, cycloids are interpreted to be tensile fractures which form perpendicular to the maximum tensile stress and grow in a curved path following the rotating stress field. This implies the cycloid cartooned in Fig. 1 would have propagated towards the left in the northern hemisphere and towards the right in the southern hemisphere. This model agrees remarkably well with the distribution of cycloidal features on Europa [3,6].

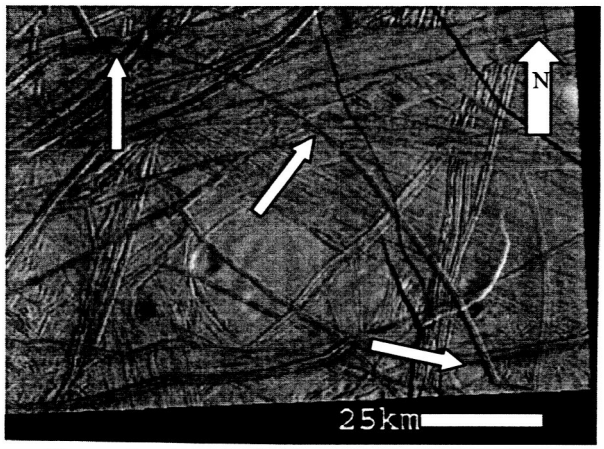

Figure 2. Arrows indicate a complex cycloid segment with changing morphology along strike. The NW end is a proto-ridge (using the nomenclature of [2]) and gradually changes towards the SE into a double ridge (image center ~ 21° N, 133° E).

Segment Morphology: Some cycloids change morphology along individual segments, usually with an abrupt change in morphology at the cusp of a segment followed by a gradual change along strike of the adjacent segment. Fig. 2 shows one such segment that is a well-developed double-ridge at its SE tip with a gradually changing morphology into a proto-ridge [2] towards its NW tip. This variability illustrates the notion that cycloids cannot always be defined by a single morphology, and may also imply that cycloid segments are subject to different loading conditions along strike.

Interpretation of Complex Segments. Previous work has modeled double ridge formation from shear heating [7], diurnal opening and closing [8], or linear diapirism [9]. The diapir model [9] does not address curved ridges, while the other two models [7,8] lead to differing interpretations of cycloids with complex morphologies. If double ridges form as the result of shear heating [7], one would expect double ridges to be more prominent in areas that have undergone more shear and less prominent in areas of less shear. If this model is accurate, the complex segment shown in Fig.

2 would have been subject to more shear near its SE tip and gradually less shear towards the NW. Conversely, if double ridges form as tension fractures that are re-worked by repeated diurnal opening and closing [8], the segment in Fig. 2 can be interpreted to have been subject to the most diurnal working in the SE and gradually less towards the NW.

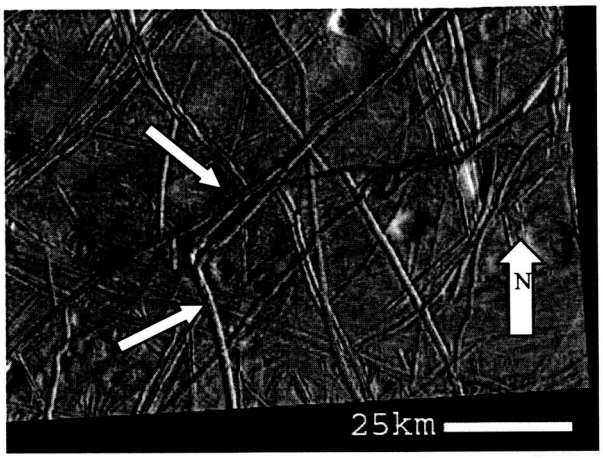

Figure 3. Arrows indicate a complex cusp where a segment from the south meets two segments from the northeast. The two northeast trending segments merge into one ridge towards the northeast (image center ~ 28° N, 140° E).

Cusp Morphology: Previous work has not detailed the styles and angles of cusps of cycloids. Many cycloids have cusps that are simple intersections between two segments (Fig. 2) while others are more complex (Fig. 3). There appears to be no characteristic angle (angles A and B in Fig. 1) between cycloid segments or dependence on trend direction of segments at cusps. Nonetheless, all measured angles are acute and typically fall between 50-70°. High resolution Galileo images (e.g. Fig. 3) have revealed that many cycloids have more complex cusps than what can be resolved at lower, Voyager-like resolutions. As described below, these complex cusps may provide insight into growth directions of similar cycloids, and hence their morphologic evolution in the tidal stress field.

Formation of Complex Cusps. We interpret complex cusps to form by secondary fracturing related to strike-slip motion on a pre-existing feature [e.g. 10,11]. According to the tidal walking theory [12], throughout one Europan day, a pre-existing crack is subject to an ever-changing stress field in which it will be subject to a repeating cycle of opening, sliding, closing and then frictional back-sliding. During the time when a crack is subject to shearing, it may develop secondary tensile fractures (also known as tail cracks, wing cracks, kinks, or horsetail fractures depending on their shape) in its extensional quadrants [5,10,13]. Tail cracks are predicted to form at about 70° to the trend of the crack for pure strike-slip sliding, but have been shown to form at lower angles for instances of mixed strike-slip/dilational motions [10]. This result agrees with the observation that cusp angles are commonly between 50-70°. Secondary fracturing, like that seen near the SE end of Agenor Linea [10,14], typically occurs as multiple fractures, but has also been shown to occur as a single secondary fracture [10,11]. If cusps form by utilizing secondary fractures created during the sliding portion of the diurnal cycle on pre-existing cycloid segments, it would not be unexpected for some cusps to be simple and some to be more complex. Complex cusps could potentially be used to infer growth direction of cycloids since the side of the cusp with multiple ridges would have formed as secondary fracturing and would thus be younger. Offsets may not be visible across cycloids since the amount of slip required to create secondary fracturing is much less than what can be resolved even in high resolution Galileo images.

Discussion: Based on the tidal walking theory, the northern hemisphere should be subject to right-lateral frictional back-sliding ("pure" strike-slip motion) on pre-existing lineaments. We thus interpret that in Fig. 3, the southern segment is oldest and the cycloid grew to the NE using multiple secondary fractures created during right-lateral motion during the tidal walking of the southern segment. This interpretation agrees with growth direction implied by the diurnal model which would also predict this northern hemisphere cycloid to grow in a counter-clockwise manner, however we present a slightly different, but compatible, mechanism for formation of cusps.

References: [1] Greeley, R. et al. (2000) *JGR, 105,* 22,559-22,578. [2] Kattenhorn, S.A. (2001) *Icarus, 157,* 490-506. [3] Hoppa, G.V. et al. (1999) *Science, 285,* 1899-1902. [4] Greenberg, R. and Geissler, P., (2002) *Meteoritics and Planetary Science, 37,* 1685-1710. [5] Schenk, P.M. and McKinnon, W.B. (1989) *Icarus, 79,* 75-100. [6] Bart, G.D. et al. (2003) *LPSC XXXIV abstract #1396.* [7] Nimmo, F. and Gaidos, E. (2002) *JGR, 107,* 10.1029/2000JE001476. [8] Greenberg, R. et al. (1998) *Icarus, 135,* 64-78. [9] Head, J.W. et al. (1999) *JGR, 104,* 24,223-24,236. [10] Kattenhorn, S.A. (2003) *LPSC XXXIV abstract #1977.* [11] Schulson, E.M. (2002) *JGR, 107,* 10.1029/2001JE001586. [12] Hoppa, G.V. et al. (1999) *Icarus, 141,* 287-298. [13] Cruikshank, K.M. et al. (1991) *J. Struct. Geol., 13,* 865-886. [14] Prockter, L.M. et al. (2000) *JGR, 105,* 9483-9488.

Acknowledgements: This work was supported by NASA grant number NAG5-11495.

HYDRATED MATERIALS ON EUROPA'S SURFACE: REVIEW OF CURRENT KNOWLEDGE AND LATEST RESULTS. T. B. McCord[1], T. M. Orlando[2], G. B. Hansen[1] and C. A. Hibbitts[2], [1]Planetary Sci. Inst., NW Div., Box 667, Winthop WA 98862, mccordtb@aol.com, [2]School of Chemistry and Biochemistry and School of Physics, Georgia Institute of Technology, Atlanta, GA 30332-0400.

Introduction: The reflectance spectra of Europa, returned by the Galileo Mission's Near Infrared Mapping Spectrometer (NIMS), very early in the investigation, showed H_2O absorptions that were interpreted by many as due to hydrated minerals. McCord et al. [1,2] showed that these absorptions were associated with material that is concentrated in the liniments and chaotic terrain, later confirmed by Fanale et al. [3], and proposed that these were due to hydrated salt minerals, mostly $MgSO_4$ hydrate, probably associated with the ocean below. They proceeded to demonstrate that $MgSO_4$ hydrate is stable over the age of the solar system on Europa's surface [4] and showed that rapidly frozen brines, as might occur when liquid is exposed on Europe or be simulated by radiation damage to crystalline material, even more closely resembled the optical properties of the Europa material [5]. $MgSO_4$ is thought to be a reasonable material to be found on Europa, given that it is a common product of low temperature aqueous alteration of carbonaceous chondrite material, such as occurs in the thermal evolution of bodies like the icy Galilean satellites, and is found commonly in primitive meteorites [6]. The disturbed regions on Europa seem likely places for subsurface ocean briny materials to reach the surface.

Carlson et al. [7] then suggested that a simpler explanation is that the material is sulfuric acid (H_2SO_4) created by radiolysis of sulfur with ice and they suggested a chemical cycle driven by radiation from the Jupiter magnetosphere. They presented reflectance spectra of frozen sulfuric acid hydrate that closely resembled the NIMS Europa spectrum. The source of the sulfur they suggested is probably exogenic, from sulfur ions entrained in the Jupiter magnetic field, although they allowed that sulfur in material from the ocean below might be sufficient.

Recently, Clark (Personal communication, 2003) proposed that the hydronium ion (H_3O^+) is really what is creating the spectral signature and that this ion is present for most acids with water ice and could be due to radiation damage in water ice alone. His explanation does not require sulfates or perhaps any anionic material, but only needs water ice and radiation. He presented a spectrum of a mixture of water ice with HCL with H_2O_2 (earlier reported by Carlson et al. on Europa) and a spectrally neutral black material (carbon) that is a close match to the Europa spectrum. Our laboratory results also indicate that the cation and its solvation, not just the solvated anion, is important in affecting the spectral signatures for these materials, and that the hydronium Ion may be involved along with other effects.

It appears, from these three apparently very different explanations, that it is difficult to determine from the NIMS data available the identity of the material on Europa responsible for the NIMS spectral signature. All three types of materials seem to have reflectance spectra that closely resemble the Europa spectrum. There are small differences between the spectra presented with each of the three explanations and that for Europa, and explanations offered for these differences. A major problem is that, in spite of its major discoveries, the NIMS Europa spectra are noisy and mostly of very low spatial resolution (mostly hundreds of km per pixel, although a few postage-stamp observations of a few km per pixel were made). Further, the spectral resolution and perhaps the spectral coverage are insufficient (about 27 nm and 0.7-5 μm) to define all the spectral features that might be helpful.

We might consider arguments other than spectral interpretations to argue plausibility. The material associated with the unusual spectral signature appears strongly concentrated in the disrupted regions on Europa—lineaments and chaotic terrain. These regions are clearly associated with processes involving the subsurface and are therefore endogenic in nature. Thus, it appears that the responsible material is from below. However, this material could be modified differently than the surrounding material by irradiation, and this modification might cause the spectral signature to change. As stated, magnesium sulfate is to be expected, even required, from thermal-chemical evolution models, along with lesser quantities of other salts, specifically Na_2SO_4. McCord et al. [4] pointed out that, while Mg (doubly bonded) is stable to radiolysis, Na (singly bonded) in sulfate is not. In fact, Na is seen coming off Europa. Abundant H^+ may substitute for the lost Na^+ and create H_2SO_4 (sulfuric acid). Thus, some sulfuric acid is expected if salts are present.

Both the Carlson and Clark explanations for the Europa NIMS spectral signature concern exogenically driven processes. Radiolysis of ice is expected on Europa, although clearly water ice in crystalline form persists. It is difficult to see how the spatial distribution of the spectral signature is created unless materials associated with endogenic processes are associated. Thus, all three explanations may be correct to some extent. This may be one of those "blind people feeling the elephant" situations where we don't yet have the full picture.

Clearly, we do not sufficiently understand either the suite of materials presented to the surface of Europa (from below or above) or the chemical processes that might alter them. The laboratory studies required are difficult in that the environment of Europa's surface must be simulated. Attempts are being made, however, by all three teams so far involved, and inputs from others can be expected. This question is more general than Europa and may be fundamental to the evolution and state of objects that formed with water and suffered low-temperature alteration, such as Ceres [8].

It is certainly true that better measurements of Europa are required. Fortunately, NASA recently announced a major mission back to the Icy Satellites, the Jupiter Icy Moons Orbiter (JIMO). It is likely that a more capable spectrometer and perhaps other relevant instruments will be on board and that these new data will settle the question. In the meantime, and to prepare for JIMO, studies of the chemistry of these materials are clearly required.

A review of the status of this controversy will be presented along with the latest results available at the time of the workshop. The implications for the JIMO mission science and instrument requirements will be discussed.

References:

[1] McCord, T. B., G. B. Hansen, F. P. Fanale, R. W. Carlson, D. L. Mat-son, T. V. Johnson, W. D. Smythe, J. K. Crowley, P. D. Martin, A. Ocampo, C. A. Hibbitts, J. C. Granahan, and The NIMS team, (1998) Salts on Europa's surface detected by Galileo's near infrared mapping spectrometer, *Science, 280*, 1242-1245.

[2] McCord, T. B., G. B. Hansen, D. L. Matson, T. V. Johnson, J. K. Crowley, F. P. Fanale, R. W. Carlson, W. D. Smythe, P. D. Martin, C. A. Hibbitts, J. C. Granahan, and A. Ocampo, (1999) Hydrated salt minerals on Europa's surface from the Galileo near-infrared mapping spectrometer (NIMS) investigation, *J. Geophys. Res.*, 104, 11824-11852.

[3] Fanale, F. P., et al., (2000) Tyre and Pwyll: Galileo orbital remote sensing of mineralogy versus morphology at two selected sites on Europa, *J. Geophys. Res., 105*, 22647-22655.

[4] McCord, T. B., T. M. Orlando, G. Teeter, G. B. Hansen, M. T. Sieger, N. G. Petrik and L. Van Keulen, (2001) Thermal and radiation stability of the hydrated salt minerals epsomite, mirabilite and natron under Europa environmental conditions, *J. Geophys. Res.*, 106, 3311-3319.

[5] McCord, T. B., G. Teeter, G. B. Hansen, M. T. Sieger and T. M. Orlando (2002) Brines exposed to Europa surface conditions, *J. Geophys. Res., 107*, 10.1029/2000JE001453.

[6] Fanale, F. P., Y. H. Li, E. Decarlo, N. Domergue-Schmidt, S. K. Sharma, K. Horton, J. C. Granahan, and the Galileo NIMS team, (1998) Laboratory simulation of the chemical evolution of Europa's aqueous phase (abstract), *Lunar Planet. Sci.*, XXIX, 1248, [CD-ROM].

[7] Carlson, R. W., R. E. Johnson and M. S. Anderson, (1999) Sulfuric acid on Europa and the radiolytic sulfur cycle. *Science, 286*, 97-99.

[8] McCord, T. B. and C. Sotin, (2003) Ceres: Evolution and Current state, submitted to *J. Geophys. Res.*

OVERVIEW OF EUROPA'S ICY SHELL: QUESTIONS OF THICKNESS, COMPOSITION, RHEOLOGY, TECTONICS, AND ASTROBIOLOGICAL POTENTIAL. William B. McKinnon, Dept. of Earth and Planetary Sciences and McDonnell Center for the Space Sciences, Washington University, Saint Louis, MO 63130, mckinnon@wustl.edu.

Introduction: Europa possesses an icy shell; this much has been clear since *Voyager*. That Europa's shell is also floating is now generally accepted as well, thanks to *Galileo*. Much attention has been focused on determining the thickness of the shell, but as a goal in itself this is not enough! We also need to know what the shell is made of, what its rheological, mechanical, & structural properties are, how these govern and respond to tectonic forces and impacts, how the shell has evolved through geologic time, and what, if any, astrobiological potential the shell and ocean below possess.

Some Historical Perspective: Why is Europa's icy shell thought to be "ungrounded?" Four close passes by *Galileo* determined Europa's second-degree gravity term C_{22}, which in turn yielded a normalized moment-of-inertia (MOI) of 0.346 ± 0.005 (1 σ) [1]. This MOI *assumes* that the tidal and hydrostatic figure is hydrostatic. Nevertheless, even factoring in generous systematic uncertainty, the MOI implies a differentiated Europa, and for cosmochemically plausible rock+metal compositions, a deep ice (and/or water) layer [1,2]. For solar rock+metal, the icy layer is ~135 km thick [3].

The induced magnetic field clearly indicates a conducting layer within or close to Europa. Because the ionosphere of Europa is insufficiently conductive to carry the required currents, the conductive layer must be within the body of Europa [4]. A metallic core is too deep to account for the magnitude of the induced field, so the conducting layer must lie within the icy shell or outermost mantle. Barring an exotic composition for the latter, Europa must possess a conductive ocean beneath the ice or sufficiently hot outer mantle that an ocean, conductive or not, is implied [2,4].

The gravity and magnetic data rule out earlier hypotheses for a thin (≤25-km) solid ice shell directly coupled to a hydrated silicate interior [e.g., 5]. In this concept Europa's lineaments were due to stresses arising from convection in the rocky interior and propagated upward into the ice. This is not to cast aspersions on historical models but to point out that such thinking represented a barrier to accepting or even considering a "mobilist" Europa [e.g., 6]. The lesson for today is not to become so enamored of one's own preferred hypotheses for Europa's icy shell (e.g., "thick" vs. "thin") that one cannot see the logic and value of alternatives.

Composition: Europa's shell is mostly water ice, but there are other components, especially in areas of recent tectonic activity or impact exhumation. The near-infrared absorption bands are distorted in a manner characteristic of highly hydrated sulfates. Radiation processed $MgSO_4 \cdot nH_2O$ is arguably the leading candidate [2], but an alternative is $H_2SO_4 \cdot nH_2O$ [7]. In the latter case, the sulfur could be exogenic (Iogenic) in origin. Exospheric Na and K are seen as well, and in a ratio that implies they are not dominantly Iogenic [7], but the source minerals on Europa (presumably chlorides and/or sulfates) have not been identified.

The composition of the ice shell reflects the composition of the ocean below, albeit after geophysical and radiolytic processing. Theoretical models favor an oxidized, sulfate-bearing ocean [8-10] with low (compared with terrestrial) concentrations of alkali salts [8,9]. Europa's *primordial* ocean, however, was most likely reduced and sulfidic and only later evolved to be oxidized and modestly sulfate bearing [10]; this is in strong contrast to the hypersaline (~saturated) CI-analogue model [8]. The conductivity limits implied by the Galileo magnetometer data unfortunately do not provide useful constraints on sulfate concentration. For ocean depths consistent with the gravity data, the minimum conductivity necessary to account for the induced field is ~0.1 S m^{-1}, which is ~1/25 that of terrestrial seawater [2,4]. The implied NaCl salinity scales accordingly, and can be met by even the partial extraction model of [9]. In this case the minimum sulfate concentration needed is zero. If the conductivity is due to sulfate alone, ~1 wt% is the minimum implied.

Improved spectral analyses, either from existing or future data, will be critical to progress. For although the thermomechanical properties (diffusivity, viscosity, etc.) of pure water ice are very well understood, those of highly hydrated sulfate salts (for example) are not, and are likely quite different from those of water ice (owing to, among other things, the large unit cells of the sulfate minerals [11]).

Rheology: Experimental studies have made such progress that a fairly complete understanding of the steady-state viscous creep of pure water ice exists [12,13]. For most temperature and stress regimes of interest for Europan geology, nearly Newtonian grain-size-sensitive GBS creep (GSS in [13]) is the dominant flow law. Only for higher stress levels and larger grain sizes (>1 cm) is power-law creep law dominant (see deformation maps in [13]). For very fine grain sizes and very low stresses, diffusional creep may become important [12], but such creep has yet to be observed

experimentally. Given the importance of grain size (d), a good understanding of what controls grain growth under planetary conditions is necessary [13]. Largely untapped glaciological understanding should help, notwithstanding current rheological controversies [14].

Tectonics: *To convect or not to convect?* Using a tidally linearized GBS rheology and the convection theory of Solomatov and coworkers, Europa's shell was shown to be unstable to convection for shell thicknesses >20 km or so (for d = 1 mm), with thinner shells unstable for smaller grain sizes (>10 km or so for d = 100 μm) [15]. Using an older, generic Newtonian rheology and a modified parameterized convection scheme, [16] argued that Europa's shell is less likely to convect (i.e., the shell must be thicker in comparison with [15]). As [15,16] both treat the shell as bottom heated, the difference in results stems from the rheologies and convection formalisms employed.

Tidal heating is a harsh mistress. There are two different problems, when does convection initiate (~bottom heated) and what is the steady-state condition (~internally heated)? In the latter case, tidal heating is important in the convecting sublayer but may be neglected (with care) in the stagnant lid [16-18], which differs from standard treatments of internally heated convection. Using tidally linearized rheologies and a modified parameterized convection scheme for internal heating, [17] found steady-state solutions with shell thicknesses ranging from ~50 km (GBS & d = 0.1 mm) to ~15-20 km (GBS & d = 1 mm as well as power-law ductile A [13]). They favored the high heat flows from the GBS & d = 1 mm case on geological grounds, but it is notable that a steady-state solution for ductile A creep dominance was found with a substantially thinner shell than stability (initiation) conditions indicate [15,17]. This either implies that the evolution of the shell when convection begins is quite interesting (it thins) or, of course, that more analysis is necessary.

It has been hypothesized that grain-size evolution in hot, straining ice will lead to ~equal contributions from GBS and power-law creep [13]. For present-day tidal amplitudes, this implies $d \sim 1$ mm and basal viscosities near 10^{14} Pa-s [15]. These conditions are very close to those for maximum tidal heating in the sublayer [15,17]. Is there a "Europanthropic" principle?

Pits and uplifts. Numerous uplifts, breached uplifts, regular and irregular domes, small chaos regions, and apparently genetically related depressions (pits) are seen across Europa, ranging in size from the very large Murias Chaos [19] to features no more than a few km across [e.g., 20]. The structural relations clearly indicate a dominant role for solid-state diapirism [19,21] and for the pits volume loss due to subsurface melting [22]. Features the scale of Murias may be due to upwelling in an ice shell marginally unstable to convection [23]. The far more numerous, small scale features are more likely due to diapiric instability in a bottom thermal boundary layer (the traditional source of plumes in the terrestrial planets). The smallest uplifts imply the smallest diapirs, which imply a bottom boundary layer thickness of ~1 km or less [18]. For such a thin layer to be unstable requires a low viscosity, which in [18] is due to diffusional creep at very fine grain sizes (~20-60 μm). Alternatively, tidally linearized GBS creep at similar grain sizes will suffice, especially if weakened by grain-boundary melting [14]. Are such grain sizes possible for hot ice? Perhaps impurities from the ocean impede grain growth, or perhaps convective strain fines grain size after all [15].

At minimum, existence of the boundary layer provides evidence for (and constrains) core heat flow. The ability of small diapirs to rise a sufficient distance through the sublayer has been questioned [20] based on [24]. Getting diapirs to pierce the stagnant lid and elastic lithosphere is the real problem. Ascent may be aided by tidal heating [15,25], low viscosity due to partial melt or low grain size, or compositional effects (melting and drainage of brine) [18,26].

Cycloid ridges. The evolution of cycloid ridges from cycloid cracks, and the diurnal stress cycle needed to generate them, are powerful geologic arguments for a floating ice shell [2,27]. Movement on deep (>1 km) faults at 0.1 MPa stresses remains problematic, however. These and other aspects of shell tectonics will be discussed as time allows.

References: [1] Schubert G. et al. (2004) in *Jupiter – Planet, Satellites & Magnetosphere,* Cambridge Univ. Press, in press. [2] Greeley R. et al. (2004) in *Jupiter–PS&M,* CUP, in press. [3] McKinnon W.B. and Desai S.S. (2003) *LPS XXXIV*, #2104. [4] Zimmer C. et al. (2000) *Icarus, 147,* 329-347. [5] Ransford G.A. et al. (1981) *Nature, 289*, 21-24. [6] Schenk P.M. and McKinnon W.B. (1989) *Icarus, 79*, 75-100. [7] Johnson R.E. et al. (2004) in *Jupiter–PS&M,* CUP, in press. [8] Kargel J.S. et al. (2000) *Icarus, 148*, 226-265. [9] Zolotov, M.Y. and Shock E.L. (2001) *JGR, 106*, 32,815-32,827. [10] McKinnon W.B. and Zolensky M.E. (2003) *Astrobiology, 3*, in press. [11] Hawthorne F.C., et al. (2000) *Rev. Min. Geochem., 40*, 1-112. [12] Goldsby D.L. and Kohlstedt D.L. (2001) *JGR, 106*, 11,017-11,030. [13] Durham W.B. and Stern L.A. (2001) *AREPS, 29*, 295-330. [14] Goldsby D.L. and Kohlstedt D.L. (2002) *JGR, 107(B11)*, ECV-17. [15] McKinnon W.B. (1999) *GRL, 26*, 951-954. [16] Hussmann H. et al.. (2002) *Icarus, 156*, 143-151. [17] Ruiz J. and Tejero R. (2003) *Icarus, 162*, 362-373. [18] Nimmo F. and Manga M. (2002) *GRL, 29(23),* 24. [19] Figueredo, P.H. et al. (2002) *JGR, 107(E5),* 2. [20] Greenberg R. et al. (2003) *Icarus, 161,* 102-126. [21] Pappalardo, R.T. et al. (1998) *Nature, 391,* 365-368. [22] McKinnon W.B. and Schenk P.M. (2004), in prep. [23] McKinnon W.B. and Gurnis M. (1999) *LPS XXX*, #2058. [24] Rathbun J.A. et al. (1998) *GRL, 25*, 4157-4160. [25] Sotin C. et al. (2002) *GRL, 29(8)*, 74. [26] Pappalardo, R.T. and Barr A.C. (2003), submitted. [27] Hoppa et al. (1999) *Science, 285*, 1899-1902.

FORMATION AND STABILITY OF RADIATION PRODUCTS IN EUROPA'S ICY SHELL M. H. Moore[1], R. L. Hudson[2], R. W. Carlson[3], and R. F. Ferrante[4] ([1]NASA/Goddard Space Flight Center, Greenbelt, MD 20771; Marla.H.Moore@nasa.gov, [2]Eckerd College, St Petersburg, FL 33733; hudsonrl@eckerd.edu, [3]JPL, Pasadena, CA 91109; tassie@earthlink.net, US Naval Academy, Annapolis, MD 21402; ferrante@usna.edu)

Introduction: Spectra of Europa reveal a surface dominated by water-ice [1] along with hydrated materials [2,3] and minor amounts of SO_2 [4,5], CO_2[6], and H_2O_2 [7]. Jovian magnetospheric ions (protons, sulfur, and oxygen) and electrons produce significant chemical modifications of the surface on time scales of a few years at micrometer depths [8]. Our laboratory studies examine the formation and stability of radiation products in H_2O-rich ices relevant to Europa. Infrared (IR) spectra of ices before and after irradiation reveal the radiation destruction of molecules and the formation of products at 86 – 132 K. In addition, spectra of ices during warming track thermal evolution due to chemical changes and sublimation processes.

IR-identified radiation products in 86 - 132 K irradiated $H_2O + SO_2$ ices are the bisulfate ion, HSO_4^-, sulfate ion, SO_4^{2-}, and the hydronium ion, H_3O^+. Warming results in the formation of a residual spectrum similar to liquid sulfuric acid, H_2SO_4, for H_2O:SO_2 ratios of 3:1, whereas hydrated sulfuric acid, H_2SO_4 4 H_2O, forms for ratios of 30:1. Radiation products identified for irradiated $H_2O + H_2S$ ices at 86 K are H_2S_2 and SO_2. When irradiated at 110 and 132 K, ices with H_2O:H_2S ratios of either 3:1 or 30:1 show the formation of H_2SO_4 4 H_2O on warming to 175 K. We have also examined the radiation stability of H_2SO_4.

Addition of CO_2 to $H_2O + SO_2$ ices results in the formation of CO_3 at 2046 cm^{-1} (4.89 m). This is the strongest band from a carbon-containing product in the mid-IR spectral region, and it is also seen when either pure CO_2 or $H_2O + CO_2$ ice is irradiated. Experiments with CH_4 added to $H_2O + SO2 + CO_2$ ices addressed the question of methane's use as a marker of methanogens in an irradiated ice environment.

New results on the near-IR spectrum of pure H_2O_2 will be included in this presentation. Interpretations of near-IR water bands, with H_2O_2 present, will be discussed. Irradiations of H_2O_2 and $H_2O + H_2O_2$ mixtures, to examine the possibility of O_2 and O_3 formation [9], are currently under investigation and new results will be discussed.

These laboratory studies provide fundamental information on likely processes affecting the outer layer of Europa's icy shell. This layer has the coldest, most heavily bombarded material in which radiation chemical markers of H_2O_2 and O_2 have already been detected. Through downward mixing, gardening, and subduction, these surface species may become available for subsurface activity.

This research is supported through NASA/ Planetary Geology and Geophysics

References: [1] Calvin, W.M. *et al.* (1995) *JGR, 100,* 19041-19048.[2] McCord, T.B. *et al.* (1998) *Science, 280;* 1242. [3] Carlson, R.W. *et al.* (1996) *Science, 274,* 385-388. [4] Lane, A.L. *et al.* (1981) *Nature, 292,* 38-39. [5] Noll, K.S. *et al.* (1995) *JGR, 100,* 19057-19059. [6] Smythe, W.D. *et al.* (1998) *LPSC*; [7] Carlson, R.W. *et al.* (1999) *Science, 283,* 2062-2064. [8] Cooper *et al.* (2001) *Icarus, 149,* 133-159. [9] Cooper, P.D., Johnson, R.E., and Quickenden, T.I. (2003) Icarus (submitted).

TIDAL DEFORMATION AND TIDAL DISSIPATION IN EUROPA. W. B. Moore, *Department of Earth and Space Sciences, University of California, Los Angeles, Los Angeles, CA 90095-1567, USA.*

Tidal forces have played a dominant role in the evolution of the inner three Galilean satellites of Jupiter. From the assembly of the Laplace resonance to the volcanic activity of Io, tidal forces orchestrate the dynamics and evolution of Io, Europa, and Ganymede. In Europa's ice shell, tidal deformation may directly drive surface tectonics, while tidal dissipation within the shell may indirectly lead to surface modification. Tidal forces may also lead to non-synchronous rotation of the shell or even true polar wander through torques acting on asymmetries in the shape of the shell.

Tidal Deformation of Europa's Ice Shell

The presence of a liquid ocean beneath Europa's ice shell essentially determines the tidal response of the shell. Since the ocean has no mechanical strength, it flows in response to the tide, attempting to match the changing shape of the equipotentials. Unless the shell is very thick and strong, it cannot effectively limit the motion of the underlying liquid, therefore the deformation of the shell very nearly matches that of the liquid, and is independent of the thickness or strength of the shell to within a few percent, for shells less than about 100 km thick. The stresses in the shell are primarily dependent on the strength of the shell, since the deformation is determined by the fluid response. Since we do not know the rigidity of ice under Europan conditions to within a factor of 10, the stresses in the shell are equally uncertain.

The tidal deformation of Europa's ice shell is determined by solving the equations of motion for a layered Maxwell-viscoelastic body in a time varying gravitational potential [*Moore and Schubert*, 2000]. The interior of Europa is modeled as several uniform layers and is completely specified by the radii of the layers and the values of density, viscosity and shear modulus in each layer. Liquid layers have zero shear modulus and are treated as inviscid since the viscosities of liquid iron and liquid water are very small. A liquid core is assumed in the calculations presented here. The effect of a solid core is to reduce deformation by several percent. The parameters of the basic model are given in Table 1. The densities

Table 1: Europa Interior Model.

Layer	thickness [km]	density [kg m^{-3}]
core	704	5150
mantle	742	3300
ice/ocean	119	1000

are constrained by the hydrostatic models which best fit the observed gravitational field of Europa [*Anderson et al.*, 1998].

In a Europan reference frame, the time-varying potential

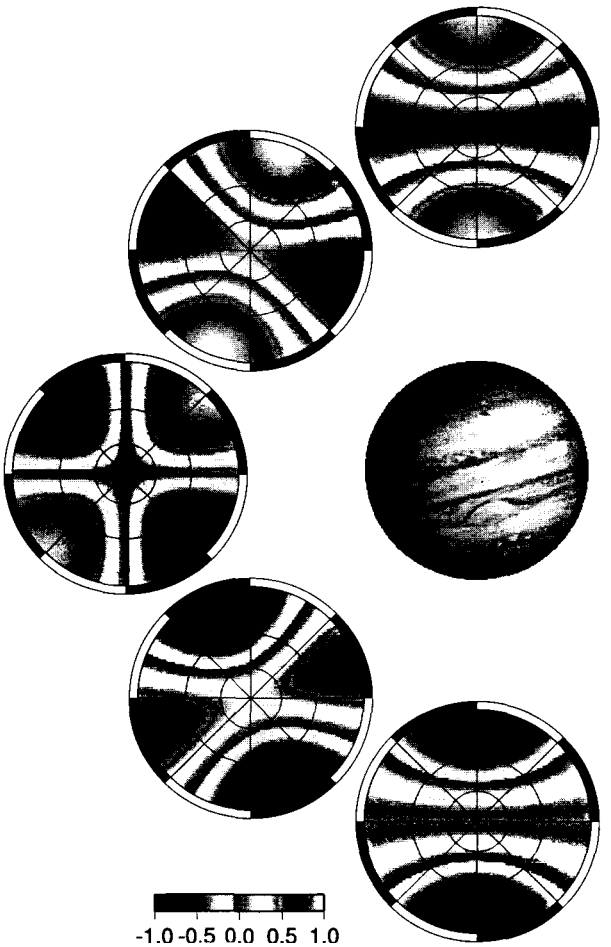

Figure 1: Φ from (1) normalized to ± 1 plotted over the northern hemisphere of Europa beginning at perijove (top) and proceeding counter-clockwise to apojove. The direction to Jupiter is indicated by the image.

to first order in the eccentricity is given by [*Kaula*, 1964]:

$$\Phi = r^2\omega^2 e\left\{-\frac{3}{2}P_2^0(\cos\theta)\cos\omega t + \frac{1}{4}P_2^2(\cos\theta)\left[3\cos\omega t\cos 2\phi + 4\sin\omega t\sin 2\phi\right]\right\} \quad (1)$$

where r is radius from the center of Europa, ω is the orbital angular frequency (2.05×10^{-5} rad s^{-1}), e is the orbital eccentricity (0.0093), θ and ϕ are the colatitude and longitude with zero longitude at the sub-Jovian point, t is time, and P_2^0 and P_2^2 are associated Legendre polynomials.

Figure 1 is a normalized map of Φ as given by (1) over one half of a Europan orbit starting at perijove (top left) and proceeding counter-clockwise. The remainder of the orbit is a reflection of the first half. Except for a scale factor (usually

given as Love numbers) and a possible phase lag, Figure 1 also represents the radial surface displacement u_r and the perturbation to the force of gravity Δg. Table 2 gives the maximum

Table 2: Love numbers and peak radial deflection.

D [km]	μ [Pa]	h_2	k_2	u_r [m]
0	0	1.26	0.261	29.6
1	10^9	1.26	0.261	29.6
10	10^9	1.25	0.259	29.3
100	10^9	1.16	0.241	27.2
1	10^{10}	1.25	0.259	29.3
10	10^{10}	1.16	0.241	27.2
100	10^{10}	0.669	0.141	15.7
		no ocean		
119	10^9	0.0271	0.0149	0.636
119	10^{10}	0.0252	0.0144	0.591

values of u_r as well as the surface Love numbers h_2 and k_2 for models of Europa's rheological structure with varying ice thickness D and shear modulus μ. The surface Love numbers are defined by:

$$h_2 = \frac{g_0 u_r}{\Phi} \quad and \quad k_2 = \frac{\Phi_{tidal}}{\Phi} \tag{2}$$

where g_0 is the acceleration of gravity at the surface, and Φ_{tidal} is the potential that results from the deformation of Europa. For the fluid/elastic models in Table 2 there are no phase lags. Visco-elastic behavior can cause the tidal response of Europa to lag the disturbing potential.

Tidal Dissipation

Phase lags in the tidal response due to visco-elastic behavior also lead to dissipation of tidal energy in the form of heat within Europa's ice shell. Using the same solutions presented above, the dissipation rate can be computed from

$$\frac{dW}{dt} = \sum_{ij} \sigma_{ij}(t)\, \dot{e}_{ij}(t-\tau) \tag{3}$$

where dW/dt is the power dissipation rate, σ is the stress tensor, $\dot{e}$ is the strain rate tensor, and τ is the phase lag. If the phase lag is zero (purely elastic response), the sum goes to zero because σ and $\dot{e}$ are perfectly out of phase. From the constitutive relation for a Maxwell visco-elastic body:

$$\dot{e}_{ij} = \frac{1}{\mu}\dot{\sigma}_{ij} + \frac{1}{\eta}\sigma_{ij} \tag{4}$$

it is clear that the viscosity η is the critical parameter controlling dissipation. Since the viscosity of ice is very dependent on temperature, the heat production in the ice shell cannot be decoupled from the heat transport, and the two processes must be modeled in a self-consistent way.

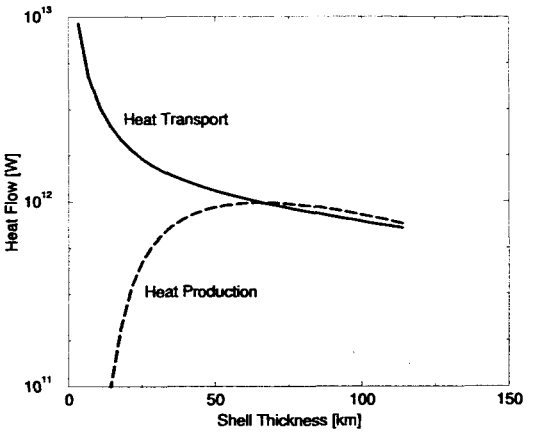

Figure 2: Heat transported by convection (solid line) vs. heat produced by tidal dissipation (dashed line) for a set of self-consistent temperature profiles in a Europan ice shell.

One means of achieving a self-consistent model is to use a convective parameterization to establish the temperature structure in a shell of a given thickness. The heat transported by convection can then be compared with the heat produced by tidal dissipation in a shell with the same temperature structure. An example of such a calculation is shown in figure where the heat transport is given by the solid line and the heat production by the dashed line for ice shells of different thickness on Europa, using the temperature- and stress-dependent grain boundary sliding rheology of *Goldsby and Kohlstedt* [2001], and the convective parameterization of *Solomatov and Moresi* [2002]. There exists an equilibrium between heat production and heat loss in this case for a shell thickness of about 70 km.

References

Anderson, J. D., G. Schubert, R. A. Jacobsen, E. L. Lau, and W. B. Moore, Europa's differentiated internal structure: Inferences from four Galileo encounters, *Science*, *281*, 2019–2022, 1998.

Goldsby, D. L., and D. L. Kohlstedt, Superplastic deformation of ice: Experimental observations, *J. Geophys. Res.*, *106*, 11017–11030, 2001.

Kaula, W. M., Tidal dissipation by solid friction and the resulting orbital evolution, *Rev. Geophys.*, *2*, 661–685, 1964.

Moore, W. B., and G. Schubert, The tidal response of Europa, *Icarus*, *147*, 317–319, 2000.

Solomatov, V. S., and L. N. Moresi, Scaling of time-dependent stagnant lid convection: Application to small-scale convection on Earth and other terrestrial planets, *J. Geophys. Res.*, *105*, 21795–21817, 2000.

DEVELOPMENT OF AN INCHWORM DEEP SUBSURFACE PLATFORM FOR IN SITU INVESTIGATION OF EUROPA'S ICY SHELL. T. Myrick[1], S. Frader-Thompson[2], J. Wilson[3], S. Gorevan[4], [1]Honeybee Robotics, 204 Elizabeth Street, New York, NY, 10012, Myrick@HoneybeeRobotics.com, [2]Honeybee Robotics, 204 Elizabeth Street, New York, NY, 10012, Frader@HoneybeeRobotics.com, [3]Honeybee Robotics, 204 Elizabeth Street, New York, NY, 10012, Wilson@HoneybeeRobotics.com, [4]Honeybee Robotics, 204 Elizabeth Street, New York, NY, 10012, Gorevan@HoneybeeRobotics.com.

Introduction: Honeybee Robotics is presently developing a drill system that may be well suited for a landed Europa exploration mission due to its currently estimated penetration depth, size, power requirements, and payload capabilities. The Inchworm Deep Subsurface Platform moves in a locomotive fashion, advancing one section of the drill while the other is anchored to the borehole wall. This system has the potential to drill hundreds of meters to several kilometers below the surface of Europa, depending on whether the system is tethered or untethered. Interesting subsurface targets on Europa such as the liquid ocean below the icy shell and bacteria potentially imbedded within the shell can be studied in situ using an Inchworm Platform. Ice shell thickness estimates range from a few kilometers [1] to tens of kilometers thick [2] and bacteria location estimates range from the bottom of the Europan ocean floor [3] to the near surface. The Inchworm Platform is an ideal candidate for accessing these sites for in situ investigations.

Drill Technology and Development: Maturation of the Inchworm technology is currently funded under NASA's Planetary Instrument Definition and Development (PIDD) and Astrobiology Science and Technology for Exploring Planets (ASTEP) programs, managed by the Office of Space Science. The Inchworm concept is highly complex and innovative and currently much research and development (R&D) is required to address the development tall poles, including drill bit design, inchworm mobility method and drill cuttings removal, among others. However, the concept framework is already well supported by years of planetary exploration drilling R&D by Honeybee (under contract to NASA).

Volume and Power: The size of the device is constrained by limits on power, torque, and downforce available for drilling through hard rocks and ices on the upper end and by mechanism miniaturization limits and packaging constraints on the lower end. A current estimate of the Inchworm's dimensions is approximately 4 inches in diameter by 4 feet in length. Such a compact system minimizes force, torque and power requirements while still maintaining the ability to accommodate a science payload and an internal power supply. For a planetary body such as Europa, minimizing power and downforce requirements may improve the Inchworm's capability to maintain the pristine environment. Alteration and contamination of the environment may be minimized by controlling the Inchworm's thermal output (mainly attributed to internal power generation and drilling friction) so that phase change of the ice is avoided.

Mobility. While drilling, the Inchworm Platform reacts torque and thrust into the borehole wall. By keeping one set of borehole wall shoes (on either the forward or aft section) firmly secured to the borehole wall, the other section is able to expand or retract, allowing the drilling system to move up or down the borehole (Figure 1). This method of walking is independent of gravity and allows for the Inchworm to traverse the borehole back up to the surface for cuttings removal.

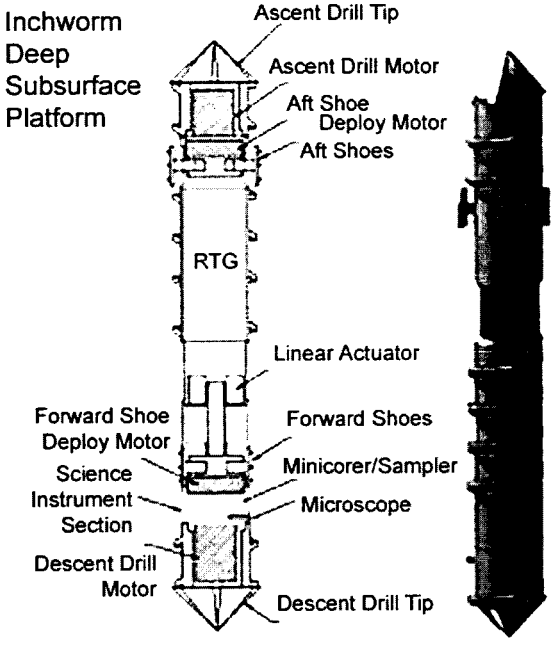

Figure 1: Inchworm Mobility System Schematic

Subsurface Access. Two mission architectures can be accommodated by the Inchworm design, a tethered drill platform capable of accessing a few hundred meters below the surface, or an untethered, fully-autonomous platform that can traverse kilometers in depth. Both configurations are challenging and offer various trades. A tethered system allows the power

supply to remain at the surface, feeding power and data through the tether itself. The Inchworm could then accommodate a larger science payload and/or reduce the overall system volume, which would reduce requirements on force, torque and power. However, the drill's achievable depth would be limited by the length of the tether, which in turn would be limited by the tether management system's mass and volume constraints as well as mission complexity and risk issues. Tether management for a system that travels to depths below a few hundred meters may be an insurmountable engineering problem. Therefore, an Inchworm requiring no tether or umbilical of any kind is desirable since it removes the need for massive tether management systems. The achievable depth by such a system is mechanically unconstrained, although telecom and operation temperature requirements may be limiting factors.

Conclusion: The concept and design of the Inchworm drilling system is supported by years of extensive research, development and testing performed by Honeybee Robotics on related projects. However, the majority of the previous work has focused on drilling and sampling consolidated and unconsolidated rock. Development under the current funding vehicles will focus on deep drilling through rock, although similar Inchworm designs and drilling routines may be used for drilling ices at low temperatures, such as those found on Europa. The Inchworm Platform is an ideal mechanism for deep subsurface access on Europa, since it offers a robust method of drilling and mobility, can accommodate different mission architectures and various science payloads, and can potentially minimize alteration and contamination of the pristine Europan environment.

References: [1] Pappalardo R. T., Head J. W., Greeley R., Sullivan R. J., Pilcher C., Schubert G., Moore W. B., Carrk M. H., Moore J. M., Belton M. J. S., and Goldsby D. L., (1998), Nature, 391, 365-368. [2] Schenk, P. M., (2002), Nature, 417, 419 - 421. [3] Chapelle F. H., O'Neill K., Bradley P. M., Methe B.A., Ciufo S.A., LeRoy L. Knobel and Lovley L. R., (2002) Nature, 415, 312 - 315.

WHAT IS THE YOUNG'S MODULUS OF ICE?. F. Nimmo, *Dept. Earth and Space Sciences, University of California Los Angeles, (nimmo@ess.ucla.edu).*

The Young's modulus E of ice is an important parameter in models of tidal deformation [1, e.g] and in converting flexural rigidities to ice shell thicknesses [2, e.g.]. There is a disagreement of an order of magnitude between measurements of E in the laboratory (9 GPa) and from field observations ($\approx$1 GPa). Here I use a simple yielding model to address this discrepancy, and conclude that $E = 9$ GPa is consistent with the field observations. I also show that flexurally-derived shell thicknesses for icy satellites are insensitive to uncertainties in E.

Lab Measurements Because ice may creep or fracture under an applied stress, it behaves elastically only if the loading frequency is high and stresses are small. Lower temperatures expand the parameter space in which elastic behaviour is expected. The most reliable way of determining E in the laboratory is to measure the sound velocity in ice and thus derive the elastic constants. The values of E found are consistently about 9 GPa [3; 4].

Field Measurements Field techniques rely on observing the response of ice shelves to tidal deformation [5]. In this case, loading frequencies are much lower ($\sim 10^{-5}$ Hz) and stresses much higher ($\sim$1 MPa). Fractures are commonly observed, and creep is also likely to occur [6]; thus, not all of the shelf may respond in an elastic fashion.

The length-scale of the response of an ice shelf to tidal deformation is determined by the parameter β [7], where:

$$\beta^4 = \frac{3\rho g\,(1-\nu^2)}{ET_e^3}. \qquad (1)$$

Here ρ is the density of the sea, g is the acceleration due to gravity, ν is Poisson's ratio and T_e is the effective elastic thickness of the ice shelf. The effective elastic thickness is defined as the thickness of a purely elastic plate which would produce the same response to loading as the actual ice shelf. Note that T_e will be less than the total ice shelf thickness h if ductile creep or fracture are important [8].

Field measurements of ice shelf deformation allow β to be determined [7]. Inspection of equation 1 shows that in order to derive E, a value for T_e must be assumed. One approach is to assume that the elastic thickness T_e is the same as the total ice shelf thickness h, which may be measured directly. Doing so results in values for E which are significantly smaller than the lab values. For instance, Vaughan [7] concluded that the effective Young's modulus from a variety of tidal deformation studies was 0.88 ± 0.35 GPa. [9] used radar observations of tidal flexure to conclude that E varied in both time and space, from 0.8 to 3.5 GPa. They ascribed the variation to viscoplastic effects. Similarly, [10] observed a time-delay between tidal forcing and ice-shelf response, which is also probably due to viscous effects.

Tension fractures are inferred to form at both the top and bottom of ice shelves due to tidal flexure, and may be tens of metres deep [11, p. 204]. The presence of these fractures will reduce the effective elastic thickness T_e of the ice shelf. Furthermore, for typical curvatures of $10^{-6}\ m^{-1}$ and shelf thicknesses of 1 km (see Table 1), the maximum elastic stresses will be O(1) MPa . These stresses are comparable to or exceed the likely elastic limit of ice [12] and suggest that much of the ice shelf will deform in a ductile rather than elastic fashion (see also [9]). It would therefore be surprising if the simple assumption that $T_e = h$ were correct. An alternative [5; 13] is to assume that the *effective* elastic thickness of the ice shelf is some fraction of the total shelf thickness. Doing so results in a larger value of E; equation 1 shows that reducing T_e to 50% of the ice shelf thickness results in an eight-fold increase in E. This increase is sufficient to bring the field results into agreement with the laboratory measurements.

Yielding Model Below I develop a simple model to show the effect of ice yielding on T_e. It will be assumed that the ice is an elastic-perfectly plastic material [14] where the stress increases linearly with strain up to a particular yield stress, σ_y, and remains constant thereafter. The perfectly plastic regime represents the area in which either fracturing or ductile flow occurs.

The first moment of the stress-depth relationship for this rheology may be used to infer the effective elastic thickness T_e of the material [8]. Assuming that stress profile is symmetrical, it can be shown that

$$Te^3 = \frac{\sigma_y(1-\nu^2)}{EK}\left(3h^2 - 4\left[\frac{\sigma_y(1-\nu^2)}{EK}\right]^2\right) \qquad (2)$$

where K is the curvature and it is assumed that $2\sigma_y(1-\nu^2) < EKh$. If this inequality is not satisfied, the whole shelf behaves elastically and $T_e = h$.

The yield stress of ice is not well known, and probably varies with both temperature and strain rate. [12] argues that a yield stress of 0.1 MPa is appropriate for glacier ice. [15] show that the yield stress is independent of pressure, but depends on temperature and strain rate. Extrapolating their results to a strain rate of $10^{-8}\ s^{-1}$ suggests yield stresses of 0.6 MPa at $-5°C$. A fracture depth of 10-100 m implies an effective yield stress of 0.1-1 MPa. I assume that ν=0.3, $\rho = 1000\ kg\ m^{-3}$, $g = 9.8\ m\ s^{-2}$ and generally use E=9 GPa.

Table 1 lists the observational data from [7]. Rather than assuming that $T_e = h$, column 4 lists the implied value of T_e/h assuming that E=9 GPa and using equation 1. Column 5 lists the value of T_e/h obtained using the yielding model (equation 2). The agreement is generally quite good (except for Jakobshavn) and shows that yielding is a valid way of explaining the observations, and is consistent with the laboratory-derived value of E (9 GPa).

In summary, the observed flexure at ice shelves can be reconciled with the laboratory-determined values of E, if some fraction of the shelf experiences yielding (either fracture or creep). Yielding is expected to occur based on the likely behaviour of ice, and a simple elastic-plastic model shows that the amounts of yielding required are reasonable.

REFERENCES

location	$\beta \times 10^{-4}$ m^{-1}	h m	T_e/h (obs.)	Te/h (theor.)
Rutford	2.4 ± 0.4	2000	0.48 ± 0.09	0.47
Ronne	$5.4 \pm^{2.7}_{1.5}$	700	$0.47 \pm^{0.15}_{0.27}$	0.46
Doake	3.4 ± 0.7	1000	0.61 ± 0.15	0.52
Bach	$11.0 \pm^{2.5}_{1.7}$	200?	$0.63 \pm^{0.11}_{0.16}$	0.54
Ekstrom	11.0 ± 0.7	150-200	0.72 ± 0.05	0.51-0.46
Jakobs-havn	$17.0 \pm^{4.0}_{2.0}$	450-800	$0.16 \pm^{0.02}_{0.04}$	0.47-0.38

Table 1: The values of β and h are obtained from [7]. T_e/h (obs.) is the value inferred from equation 1 using the observed β and h and assuming that E=9 GPa. T_e/h (theor.) is the value inferred from equation 2 assuming σ_y=0.3 MPa.

Icy satellites The ice shells of outer solar system satellites differ in several respects from terrestrial ice shelves. Firstly, strain rates are lower: around 10^{-10} s^{-1} on Europa, and less elsewhere. Secondly, surface temperatures are very much lower (typically 100-120 K), indicating that the ice may deform in a brittle fashion. Thirdly, the ice shells are probably 10's-100's km thick, implying that creep, rather than fracture, will occur towards the base of the ice shell. It is therefore more appropriate to use the yield-strength envelope (YSE) approach of [16; 8]. In this model, the near-surface ice deforms in a brittle manner, that at the base deforms in a ductile fashion, and that near the mid-plane elastically. The YSE approach allows us to convert a measurement of rigidity into a shell thickness, given a value for E. The conversion depends on the strain rate and curvature of the feature.

As an example, we will use an apparently flexural feature on Europa studied by [2]. We assume a conductive ice shell in which the thermal conductivity varies as $567/T$ and the top and bottom temperatures are 105 K and 260 K, respectively. The values of ρ,g and the coefficient of friction are 900 $kg\ m^{-3}$, 1.3 $m\ s^{-2}$ and 0.6, respectively. We will use the grain-boundary sliding (n=2.4) rheology of [17] which is grain-size independent. The strain rate is assumed to be $10^{-15}\ s^{-1}$.

[2] obtained a flexural parameter β of $6.25 \times 10^{-5}\ m^{-1}$ and a maximum curvature of $7.5 \times 10^{-7}\ m^{-1}$. Assuming a Young's modulus of 9 GPa, equation 1 gives T_e=2.8 km and the YSE approach gives a conductive ice shell thickness of 11 km. Taking E=1 GPa yields a T_e of 6 km and a shell thickness of 12 km. Increasing strain rate by two orders of magnitude decreases the inferred shell thickness by 1 km. Reducing the friction coefficient by 30% increases the shell thickness by 1 km. Using the grain-boundary sliding ($n = 1.8$) rheology of [17] with a grain-size of 1 mm reduces the shell thickness by 1 km. Thus, uncertainties in most parameters do not significantly affect the final result.

The shell thickness is insensitive to variations in E because the elastic portion of the shell is small. Hence, the YSE approach is a robust way of converting estimates of rigidity into ice shell thicknesses.

References

[1] W. B. Moore and G. Schubert. The tidal response of Europa. *Icarus*, 147:317–319, 2000.

[2] F. Nimmo, B. Giese, and R. T. Pappalardo. Estimates of Europa's ice shell thickness from elastically supported topography. *Geophys. Res. Lett.*, 30:1233, doi:10.1029/2002GL016660, 2003.

[3] V. F. Petrenko and R. W. Whitworth. *Physics of Ice.* Oxford Univ. Press, New York, 1999.

[4] P. H. Gammon, H. Kiefte, M. J. Clouter, and W. W. Denner. Elastic constants of artificial and natural ice samples by Brillouin spectroscopy. *J. Glaciol.*, 29(103):433–460, 1983.

[5] G. Holdsworth. Tidal interaction with ice shelves. *Ann. Geophys.*, 33(1):133–146, 1977.

[6] T. J. Hughes. West Antarctic ice streams. *Rev. Geophys. Space Phys.*, 15(1):1–46, 1977.

[7] D. G. Vaughan. Tidal flexure at ice shell margins. *J. Geophys. Res.-Solid Earth*, 100(B4):6213–6224, 1995.

[8] A. B. Watts. *Isostasy and flexure of the lithosphere.* Cambridge Univ. Press, Cambridge, 2001.

[9] M. Schmeltz, E. Rignot, and D. MacAyeal. Tidal flexure along ice-sheet margins: comparison of insar with an elastic-plate model. *Annals Glaciology*, 34:202–208, 2002.

[10] N. Reeh, C. Mayer, O. B. Olesen, E. L. Christensen, and H. H. Thomsen. Tidal movement of Nioghalvfjerdsfjorden glacier, northeast Greenland: observations and modelling. *Ann. Glaciol.*, 31:111–117, 2000.

[11] T. Hughes. *Ice Sheets.* Oxford Univ. Press, New York, 1998.

[12] W. S. B. Paterson. *The Physics of Glaciers.* Pergamon Press, New York, 1981.

[13] C. S. Lingle, T. J. Hughes, and R. C. Kollmeyer. Tidal flexure of Jakobshavns glacier, West Greenland. *J. Geophys. Res.*, 86(B5):3960–3968, 1981.

[14] D. L. Turcotte and G. Schubert. *Geodynamics.* John Wiley and Sons, New York, 1982.

[15] M. A. Rist and S. A. F. Murrell. Ice triaxial deformation and fracture. *J. Glaciol.*, 40(135):305–318, 1994.

[16] M. K. McNutt. Lithospheric flexure and thermal anomalies. *J. Geophys. Res.*, 89(NB13):11180–11194, 1984.

[17] D. L. Goldsby and D. L. Kohlstedt. Superplastic deformation of ice: Experimental observations. *J. Geophys. Res.-Solid Earth*, 106(B6):11017–11030, 2001.

LATERAL AND VERTICAL MOTIONS IN EUROPA'S ICE SHELL. F. Nimmo, *Dept. Earth and Space Sciences, University of California Los Angeles, (nimmo@ess.ucla.edu).*

Characterizing the lateral and vertical motions that occur within Europa's ice shell is challenging but important. Vertical motions can transport nutrients and thus have astrobiological importance, while lateral movements can cause thinning of the ice shell. Future mission design will be affected by what we think we know about the characteristics of Europa's ice shell. Models and inferences of vertical and lateral motion will help us to constrain the ice shell thickness, and also to estimate the characteristic strain rates and stresses (ie. the shell dynamics).

LATERAL MOTION

Lateral extension is very obvious in bands [1], though minor amounts of strike-slip or compressive motion may also occur [2; 3]. The localized, high stretching factor rifting is very different to the diffuse, lower stretching factor extension seen on Ganymede. Localized extension is favoured by high strain rates and low shell thicknesses. Recent work by [4] suggests that an extensional strain rate $> 10^{-15}\ s^{-1}$ is required to form bands on Europa. The associated stresses are $\approx$0.3 MPa, similar to estimates inferred from flexural studies but several orders of magnitude larger than present day tidal stresses. The fact that bands appear to be elevated relative to their surroundings suggests either compositional or (recent) thermal buoyancy [5].

A less obvious but equally important kind of lateral motion is flow in the lowermost part of the shell. Lateral shell thickness contrasts, *even if isostatically compensated*, produce pressure gradients which drive flow. Thus, topography produced by lateral shell thickness contrasts decays with time [6]. The rate of decay can be very rapid, especially for thick shells. However, the rate of decay is slower for non-Newtonian materials, such as ice, than it is for Newtonian ones. Global shell thickness contrasts can probably be maintained for 50 Myr, but local ($\sim$100 km) variations cannot [7].

Strike slip motion has also been identified on Europa [3] and is almost certainly driven by a "tidal walking" process [8]. It has been proposed that shear-heating at such sites could lead to the formation of double ridges [9]. If shear heating leads to melting, this provides a potential source of near-surface liquid water. Finally, shear heating zones are a source of weakness, which may explain why many bands appear to initiate at double ridges.

Compressional motion is rare on Europa, though folds have been identified in one area [10]. The imbalance between extension and compression is a puzzle. It is possible that compression is being accommodated by diffuse shortening which leaves little geological evidence.

VERTICAL MOTION

The evidence for vertical motion is less clear than that for lateral movements. Features termed pits, spots and domes may be the surface expression of subsurface vertical motion [11], but there is a lack of agreement on this point [12]. Even more controversially, chaos terrains may be the result of either diapiric activity [13] or melt-through caused by hydrothermal plumes [14]. A second kind of vertical motion occurs due to surface, rather than subsurface loads.

Thermal convection suffers from two problems in explaining the surface features. Firstly, it is much harder to initiate convection in Newtonian than non-Newtonian materials [15]. Furthermore, for the likely grain sizes and strain rates, the deformation of ice is controlled by the *slower* of the two relevant mechanisms [16]. The overall result is that convection is unlikely to occur unless the shell thickness exceeds 50 km This is substantially larger than earlier estimates of the critical shell thickness [11; 17].

Secondly, the temperature contrast generated by strongly temperature-dependent convection is determined by the rheological properties of the ice, and is small ($\sim$10 K) [15]. This temperature contrast is probably too small to generate the observed dome amplitudes of several hundred metres [18; 19]. Although a tidal feedback mechanism has been proposed [20], it is not clear that the very long wavelength tidal deformation will couple efficiently with the much shorter wavelength diapiric features [W. Moore, pers. comm.].

Compositional convection is an alternative mechanism for diapir formation. [5] proposed that compositional density contrasts might arise through the preferential loss of brines from warm ice. In this scenario, warm ice near the base of the shell loses salts, is more buoyant than the colder ice overlying it, and becomes gravitationally unstable. This Rayleigh-Taylor instability will grow most rapidly at a characteristic wavelength, which will determine the size of the ascending diapirs [21]. For most systems, the characteristic wavelength is a few times the thickness of the layer above the instability. The rise time of the resulting diapir depends on its radius r, density contrast $\Delta\rho$ and the viscosity structure of the ice. For viscosity which increases exponentially upwards with a characteristic length-scale δ, the rise time τ is given by

$$\tau \approx \frac{\eta_0 \delta}{r^2 \Delta\rho g} \left(\exp(h/\delta) - 1\right) \qquad (1)$$

where g is gravity, η_0 is the viscosity at the base of the shell and h is the shell thickness. For likely diapir radii ($\sim$5 km) and ice viscosities ($\sim 10^{14}\ Pa\ s$), the rise time is O(1 Myr). The nature of the return flow mechanism in the case of compositional convection is not clear, but may involve broad-scale downwards motion.

Vertical motions in response to surface loading also occur. The horizontal distance over which the deformation occurs provides information about the elastic thickness of the ice shell [22; 23]. Frequently, the margins of chaos terrain are a few hundred metres lower than the surrounding areas, and appear to have downdropped along sharp contacts [22]. This downdropping is consistent with scenarios in which the underlying ice is thinned (or even completely melted). While chaos terrain may be elevated with respect to the surroundings at the present day [13], this topography may post-date the original formation of the chaos.

Summary and Future Questions

The availability of topographic data is now allowing us to place quantitative constraints on processes happening within Europa's ice shell. However, as yet neither the *spatial* nor the *temporal* variations in these processes have been properly addressed. Temporal variations are detectable with geological mapping; spatial variations are dependent on data availability. It is therefore critically important to maximize the amount of data available, which in practice will mean increasing reliance on photoclinometric methods [24].

The estimation of stresses and strain rates within Europa's ice shell is at an early stage. However, it is already clear that many of the features observed imply stresses far in excess of the present-day tidal stresses. Other sources of stress, such as those due to compositional or thermal buoyancy, must also be present. Again, whether there are temporal or spatial variations in stress or strain will be the subject of future investigations. Similarly, the reconciliation of global models of tidal dissipation with local geological features has barely begun.

References

[1] L. M. Prockter, J. W. Head, R. T. Pappalardo, R. J. Sullivan, A. E. Clifton, B. Giese, R. Wagner, and G. Neukum. Morphology of Europan bands at high resolution: A mid-ocean ridge-type rift mechanism. *J. Geophys. Res.-Planets*, 107(E5):5028, doi:10.1029/2000JE001458, 2002.

[2] B. R. Tufts, R. Greenberg, G. Hoppa, and P. Geissler. Lithospheric dilation on Europa. *Icarus*, 146(1):75–97, 2000.

[3] A. R. Sarid, R. Greenberg, G. V. Hoppa, T. A. Hurford, B. R. Tufts, and P. Geissler. Polar wander and surface convergence of Europa's ice shell: evidence from a survey of strike-slip displacement. *Icarus*, 158:24–41, 2002.

[4] F. Nimmo. Dynamics of rifting and modes of extension on icy satellites. *J. Geophys. Res. -Planets*, page in press, 2003.

[5] F. Nimmo, R. T. Pappalardo, and B. Giese. On the origins of band topography, Europa. *Icarus*, 166:21–32, 2003.

[6] D. J. Stevenson. Limits on the variation of thickness of europa's ice shell. *Lun. and Planet. Sci. Conf.*, XXXI:art. no. 1506, 2000.

[7] F. Nimmo. Non-Newtonian topographic relaxation on Europa. *Icarus*, page submitted, 2003.

[8] G. V. Hoppa, B. R. Tufts, R. Greenberg, and P. E. Geissler. Strike-slip faults on Europa: global shear patterns driven by tidal stress. *Icarus*, 141:287–298, 1999.

[9] F. Nimmo and E. Gaidos. Strike-slip motion and double ridge formation on Europa. *J. Geophys. Res.-Planets*, 107(E4):5021, doi:10.1029/2000JE001476, 2002.

[10] L. M. Prockter and R. T. Pappalardo. Folds on Europa: implications for crustal cycling and accommodation of extension. *Science*, 289(5481):941–943, 2000.

[11] R. T. Pappalardo and et. al. Geological evidence for solid-state convection in Europa's ice shell. *Nature*, 391:365–368, 1998.

[12] R. Greenberg, M. A. Leake, G. V. Hoppa, and B. R. Tufts. Pits and uplifts on Europa. *Icarus*, 161:102–126, 2003.

[13] P. M. Schenk and R. T. Pappalardo. Stereo and photoclinometric topography of chaos and anarchy on Europa. *Lun. and Planet. Sci. Conf.*, XXXIII:art. no. 2035, 2002.

[14] D. P. O'Brien, P. Geissler, and R. Greenberg. A melt-through model for chaos formation on Europa. *Icarus*, 156(1):152–161, 2002.

[15] F. Nimmo and M. Manga. Causes, characteristics and consequences of convective diapirism on Europa. *Geophys. Res. Lett.*, 29(23):2109, doi:10.1029/2002GL015754, 2002.

[16] D. L. Goldsby and D. L. Kohlstedt. Superplastic deformation of ice: Experimental observations. *J. Geophys. Res.-Solid Earth*, 106(B6):11017–11030, 2001.

[17] W. B. McKinnon. Convective instability in Europa's floating ice shell. *Geophys. Res. Lett.*, 26(7):951–954, 1999.

[18] A. P. Showman and L. Han. Numerical simulations of convection in europa's ice shell: implications for surface features. *Lun. and Planet. Sci. Conf.*, XXXIV:art. no. 1806, 2003.

[19] A.C. Barr and R.T. Pappalardo. Numerical simulations of non-newtonian convecton in ice: application to europa. *Lun. and Planet. Sci. Conf.*, XXXIV:art. no. 1477, 2003.

[20] C. Sotin, J. W. Head, and G. Tobie. Europa: Tidal heating of upwelling thermal plumes and the origin of lenticulae and chaos melting. *Geophys. Res. Lett.*, 29(8):art. no. 1233, 2002.

[21] D. L. Turcotte and G. Schubert. *Geodynamics*. John Wiley and Sons, New York, 1982.

[22] P. Figueredo, R. L. Kirk F. C. Chuang, J. Rathbun, and R. Greeley. Geology and origin of Europa's Mitten feature (Murias Chaos). *J. Geophys. Res.*, 107(E5):5026, doi:10.1029/2001JE001591, 2002.

[23] F. Nimmo, B. Giese, and R. T. Pappalardo. Estimates of Europa's ice shell thickness from elastically supported topography. *Geophys. Res. Lett.*, 30:1233, doi:10.1029/2002GL016660, 2003.

[24] R.L. Kirk, J. M. Barrett, and L. A. Soderblom. Photoclinometry made simple . . ? *Advances in Planetary Mapping*, Houston, 2003.

DOMES ON EUROPA: THE ROLE OF THERMALLY INDUCED COMPOSITIONAL DIAPIRISM. R. T. Pappalardo and A. C. Barr, University of Colorado, Boulder, CO 80309-0397 (robert.pappalardo@colorado.edu).

Overview: The surface of Europa is peppered by topographic domes, interpreted as sites of intrusion and extrusion. Diapirism is consistent with dome morphology, but thermal buoyancy alone cannot produce sufficient driving pressures to create the observed dome elevations. Instead, we suggest that diapirs may initiate by thermal convection that induces compositional segregation within Europa's ice shell. This double-diffusive convection scenario allows sufficient buoyancy for icy plumes to create the observed surface topography, if the ice shell has a very small effective elastic thickness (~0.1 to 0.5 km) and contains low-eutectic-point impurities at the percent level.

Thermal Buoyancy: Thermal diapirism has been proposed as a source of buoyancy for forming Europa's domes [1,2]. Solid-state convection is capable of bringing warm material to shallow (several km) depths within Europa's ice shell [3]; however, stresses due to thermally driven convection are small. The maximum convective stress is

$$P_d \sim 0.1\, \rho_i\, g\, \alpha\, \Delta T\, D \qquad (1)$$

[4], where ρ_i is ice density, g is gravitational acceleration (1.3 m s^{-2} for Europa), α is the coefficient of thermal expansion, ΔT is the temperature difference across the ice shell, and D is the ice shell thickness.

For $\alpha = 10^{-4}$ K^{-1} and $\Delta T = 160$ K, the $P_d \sim 4 \times 10^4$ Pa within an ice shell of $D \approx 20$ km thickness. Numerical modeling of convection and associated thermal diapirism supports this analysis, predicting relief of only ~10 m above convective upwellings [5].

Diffusive cooling can cause diapirs to stall in the subsurface [2]. If warm diapirs reach the surface, thermal diffusion further robs buoyancy, and domes relax as they cool [6] if not supported by dynamic processes or compositional density variations [cf. 7].

Compositional Buoyancy and Double-Diffusive Convection: Differences in impurity levels serve as a potential source of compositional buoyancy to drive diapiric rise, and may be relevant to Europa dome formation (Fig. 1). Galileo NIMS results indicate non-ice materials on Europa, modeled as hydrated sulfate salts [8] or sulfuric acid hydrate [9], but the level of contaminants within the ice is highly uncertain.

A convecting icy shell is expected to have a nearly isothermal adiabatic temperature, T_{ad}, beneath a rigid stagnant lid. For a basally heated pure ice shell, T_{ad} can be as low as ~245 K [3], while for an internally (tidally) heated ice shell, T_{ad} is 250 to 260 K [6,10].

Both sulfate and chloride contaminants are plausible constituents of Europa's icy shell [11]. Hydrated sulfate salts have eutectic temperatures [12] ~270 K, securely above the predicted T_{ad} for Europa; therefore, these salts are expected to be stable against eutectic melting. However, the eutectic temperatures of hydrated chloride salts are in the range ~220 to 250 K, i.e. less than or comparable to the expected T_{ad}. Moreover, the ice-H_2SO_4 system has a eutectic of 211 K [11]. If hydrated chloride salts or sulfuric acid (herein collectively termed "low-eutectic" contaminants) exist within Europa's ice shell, they are expected to melt and produce brines in response to thermal convection. This should be the case throughout the warm base of the ice shell, and wherever a warm ice plume contacts colder contaminant-rich ice.

Melt is expected to drain through the ice at ~10 m yr^{-1} [13], significantly faster than the ~0.1 to 1 m yr^{-1} vertical velocity of convective ice plumes [3]. Therefore, the warm base of the ice shell and the convective plumes that rise from it are expected to be relatively clean of low-eutectic impurities (Fig. 1). In this model, low-eutectic contaminants are expected to become depleted in the ice shell over time unless replenished. It is plausible that Europa's ice shell is not in steady-state, but that instead its youthful surface age (~30 to 80 Myr [14]) reflects a latest incarnation of the ice shell, which began as relatively contaminant-rich and is more recently depleted in contaminants over time.

The warmer ice of a rising diapir will be cleaner and thus compositionally buoyant relative to its surroundings. Assuming isostasy above a column cleaned of low-eutectic contaminants through diapiric rise,

$$P_d = \phi\, (\rho_{le} - \rho_o)\, g\, D \qquad (2)$$

where ρ_{le} is the average density of the low-eutectic solids, ρ_o is the ambient density of the impure ice shell, and ϕ is the volume fraction of low-eutectic contaminants that melt and drain from diapiric plumes.

Choosing $\rho_o = 1000$ kg m^{-3} and $\rho_{le} = 1500$ kg m^{-3}, $\phi \sim 2\%$ can produce $P_d \sim 10^5$ Pa for a range of reasonable ice shell thicknesses, sufficient to upwarp domes to observed (~100 m) heights for intrusions beneath a brittle ice cover of T_e ~0.1 to 0.5 km for Young's modulus $E \sim 10^9$ to 10^{10} Pa The minor amounts of low-eutectic contaminants required are consistent with geochemical models of Europa's evolution [11].

The thermo-compositional buoyancy scenario envisioned here is essentially one of double-diffusive convection (DDC), in which both thermal and compositional gradients exist to trigger fluid motions [e.g., 15], as governed by the standard thermal Rayleigh number

$$\mathrm{Ra} = \rho g \alpha \Delta T D^3 / \kappa \eta \qquad (3)$$

(where α is the coefficient of thermal expansion, ΔT is the temperature drop across the convecting layer, κ is the thermal diffusivity, and η is viscosity), as well as a compositional Rayleigh number

$$\mathrm{Ra}_c = \rho g \beta \Delta C D^3 / \kappa \eta \qquad (4)$$

(where β is a compositional counterpart to α, and ΔC is the vertical composition gradient across the convecting layer).

The system operates in the "finger" regime, where compositionally buoyant material can rise in narrow

upwellings of scale much smaller than the thickness of the convecting system, if

$$Ra_c - Ra > \frac{27}{4}\pi^4 \qquad (5)$$

[16], whereas the system is in the diffusive regime typical of thermal convection for lesser values of (Ra_c – Ra). This relationship can also be expressed in terms of temperature and concentration gradients as

$$\frac{\rho_o g D^4}{\eta}\left[\frac{\beta \Delta C}{\kappa_c D} - \frac{\alpha \Delta T}{\kappa D}\right] > 657 \qquad (6)$$

where κ_c is the compositional diffusivity. For concentrations expressed as volume fraction f, then $\Delta C = \Delta\phi$, and $\beta = (\rho_{le} - \rho_o) / \rho_o$.

For Europa, the value of κ_c can be envisioned as governed by the melt composition, the velocity of melt drainge v_m, and a characteristic length scale for melt drainge L, as

$$\kappa_c \sim \phi_{le} \phi v_m L \qquad (7)$$

where ϕ_{le} is the volume fraction of low-eutectic contaminants in the melt. The length scale L is unknown but may be in the range ~1 to 10% of the scale of a diapir, or ~70 to 700 m. Choosing plausible values of $\phi \sim 0.02, \phi_{le} \sim 0.1$, and $v_m \sim 10$ m yr^{-1}, then $\kappa_c \sim 4 \times 10^{-7}$ to 4×10^{-8} m^2 s^{-1}. Assuming a mean ice viscosity of ~10^{18} Pa s, $\kappa \sim 10^4$ m^2 s^{-1}, $\Delta T \approx 160$ K, and $D \sim 20$ km, then (Ra_c – Ra) ~ 250 to 2500. This suggests that Europa's ice shell may be transitional between the diffusive and finger regimes, but uncertainty in L and κ_c implies that this coarse estimate must be refined.

Summary and Implications: The required buoyancy to account for Europa's domes is difficult to achieve through thermal convection alone but can be produced by percentage level compositional differences between ice diapirs and their surroundings, if low-eutectic contaminants melt and drain from warm ice plumes, and if the effective thickness of the brittle lithosphere is very small (~0.1 to 0.5 km). This implies that convection in Europa's ice shell is best modeled as double-diffusive convection, in which thermal and compositional gradients are both important. Convection in the compositionally dominated finger regime can result in upwelling diapirs that are significantly smaller in scale than the vertical scale of the convecting medium, so attempts to relate lenticula size to Europa's ice shell thickness may not be fruitful.

Thermally induced compositional buoyancy offers a comprehensive and geophysically plausible means for forming Europa's domes. An analogous model has been applied to Europa's bands by [7], and is potentially applicable to the satellite's larger chaos regions as well. The model implies significant compositional inhomogeneity on a local scale within the ice shell, which might be directly detectable by future missions using ground penetrating radar. This process would allow deep interior material to breach the Europa's cold brittle lithosphere, with potential implications for transport of oceanic and astrobiologically relevant materials to the surface.

Acknowledgements: Supported is provided by NASA Exobiology grant NCC2-1340 and GSRP NGT5-50337.

References: [1] Pappalardo, R. T., et al., *Nature, 391*, 365-368, 1998. [2] Rathbun, J. A., et al., *Geophys. Res. Lett., 25*, 4157-4160, 1998. [3] Barr, A. C. and R. T. Pappalardo, *LPSC XXXIV*, # 1477, 2003. [4] McKinnon, W. B., in *Solar System Ices*, pp. 525-550, 1998. [5] Showman, A. P. and L. Han, *LPSC XXXIV*, #1806, 2003. [6] Nimmo, F. and M. Manga, *GRL, 29(23)*, 10.1029/ 2002GL015754, 2002. [7] Nimmo, F., et al., *Icarus, 166*, 21-32, 2003. [8] McCord, T. B., et al., *JGR, 103*, 8603-8626, 1998. [9] Carlson, R. W., et al., *Science, 286*, 97-99, 1999. [10] McKinnon, W. B., *GRL, 26*, 951-954, 1999. [11] Kargel, J. S., et al., *Icarus, 148*, 226-265, 2000. [12] Brass, G. W., *Icarus, 42*, 20-28, 1980. [13] Gaidos, E. and F. Nimmo, *Nature, 405*, 637, 2000. [14] Zahnle, K., et al., *Icarus, 163*, 263-289, 2003. [15] Hansen, U., and D. A. Yuen, , *Earth Sci. Rev., 29*, 385-399, 1990. [16] Kundu, P., *Fluid Mechanics*, Academic Press, 1990.

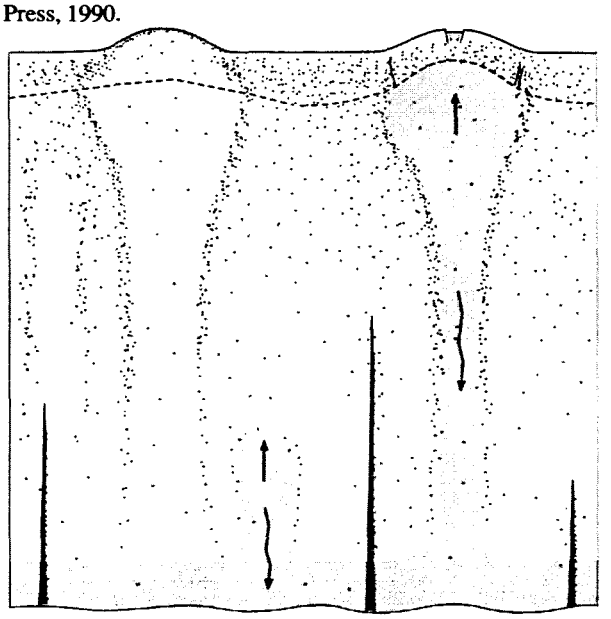

Fig. 1: Schematic illustration of the thermally induced compositional diapirism model. As warm ice (dark gray) near the base of Europa's ice shell begins to rise diapirically, it melts overlying low-eutectic contaminants (stipples) and the brines drain downward (squiggly arrows), allowing compositional buoyancy to aid diapir rise toward the surface. Buoyant diapiric material can breach the cold brittle lithosphere and extrude to form a dome (lefft); contaminants remaining in the diapiric ice are then concentrated by exogenic processes. Alternatively, diapirs can intrude and upwarp the brittle lithosphere to form intrusive domes (right). Low-eutectic contaminant concentration is least in the warmest ice and locally concentrated in halos surrounding diapirs from which they have been expelled. Dome topography and subsurface compositional gradients persist whether the underlying ice column is warm or has cooled (left, lighter gray), until subsequent diapirism redistributes the constituents. Diking might replenish some contaminants from the ocean below, but the ice shell is expected to be overall depleted in low-eutectic contaminants over time.

NUMERICAL MODELING OF PLATE MOTION: UNRAVELING EUROPA'S TECTONIC HISTORY.

G. W. Patterson and J. W. Head III, Department of Geological Sciences, Brown University, Providence, RI , 02912 (Gerald_Patterson@brown.edu).

Introduction: Europa is a highly fractured body broken into plates that have rotated with respect to one another. The effect of these rotations can be seen as regions of extension, strike-slip motion, and possibly compression [1,2,3,4]. Various authors have tried to reconstruct a number of these regions in an effort to gain a better understanding of the tectonic history of the icy satellite [4-8].

The typical approach used to determine a best-fit reconstruction could be described as a 'cut-and-paste' method in which the plates in an image are manually separated and reoriented in an effort to reconstruct preexisting features [4,5,6]. Some authors subsequently determined poles of rotation for the regions reconstructed [7,8]. This step is essential to determining the validity of a reconstruction when the size of a region is such that the curvature of the satellite cannot be ignored.

In those cases that have looked for a pole of rotation, a forward approach is typically used. This method can be used to show that the reconstruction produced has a unique solution but it cannot tell whether or not there were other unique solutions that were not considered. Here we report on the development of an inverse method for determining the Euler pole of a region that has undergone rotation. This method can be used to test all possible rotations of the region and therefore determine all unique solutions (if they exist).

The Model. The inverse model we have developed uses an iterative grid-search method to find an Euler pole of rotation for the region to be reconstructed such that ridges cut and offset will be realigned. The result is a minimized best-fit pole with confidence regions. This is a brute force method that is mathematically simple but computationally cumbersome. The computational requirements of this modelling technique limit the resolution of the grid that can be used to determine the Euler pole but it is sufficient to fully resolve the pole for the resolution of the image used.

$$\begin{aligned} N_x &= \left(A_y * B_z - A_z * B_y\right)/\sin\delta \\ N_y &= \left(A_z * B_x - A_x * B_z\right)/\sin\delta \\ N_z &= \left(A_x * B_y - A_y * B_x\right)/\sin\delta \\ \delta &= \cos^{-1}\left(A_x * B_x + A_y * B_y + A_z * B_z\right) \end{aligned} \quad (1)$$

The model uses two points (A and B) on a fixed plate to form a plane through the body (Fig. 1). The normal to that plane is determined using equation 1 and the distance from that plane to a point (C) on the plate to be reconstructed that corresponds to the offset feature of the fixed plate is determined using equation 2.

$$dist = \left|\overrightarrow{AC}x * N_x + \overrightarrow{AC}y * N_y + \overrightarrow{AC}z * N_z\right| \quad (2)$$

A best-fit reconstruction of the points described involves rotating point C on the plate to be reconstructed about an Euler pole such that it falls in the plane of points A and B on the fixed plate. To accomplish this we use a rotation matrix (equation 3), where R_{ij} is the rotation matrix and it is defined by an Euler pole E = (E_x, E_y, E_z) and an angle of rotation Ω [9].

$$\begin{bmatrix} C_{x'} \\ C_{y'} \\ C_{z'} \end{bmatrix} = \begin{bmatrix} R_{11} & R_{12} & R_{13} \\ R_{21} & R_{22} & R_{23} \\ R_{31} & R_{32} & R_{33} \end{bmatrix} * \begin{bmatrix} C_x \\ C_y \\ C_z \end{bmatrix} \quad (3)$$

Confidence regions for the determined pole were calculated using the following equation [10]:

$$R = R_{\min}\left(1 + \left(N/M - N\right)F\left[N, M - N, 1 - \alpha\right]\right)^{1/2} \quad (4)$$

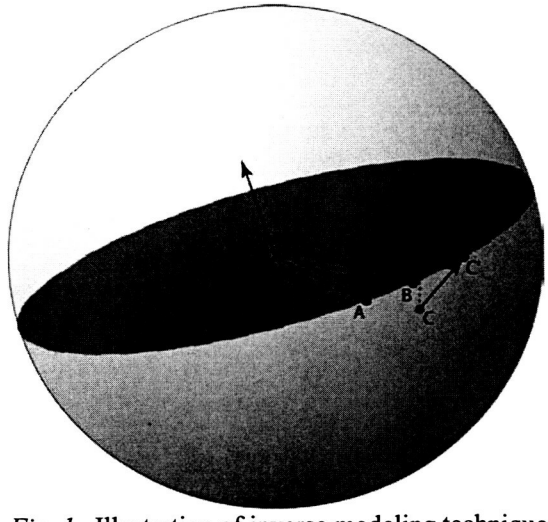

Fig. 1. Illustration of inverse modeling technique. A and B represent points on an offset feature lying on a fixed plate and C represents a point on the same offset

feature lying on the plate to be rotated. C' represents the position of the offset feature after rotation.

A Test Case: The Castalia Macula region was chosen as a test case for the application of this inverse method (Fig. 2). The region in the image is centered about the equator and spans ~800 km. We rotated one plate in this region that is marked by numerous offset features, 27 of which were used in this analysis (the main criterion for choosing these features was clarity of the precise location of each feature across the plate boundary).

The model determined the Euler pole that minimized the distance between the offset features after iterating through every possible combination of pole location and rotation. The resolution of the grid used was increased steadily until we reached the resolution limit of the image. Figure 3 indicates the location of the best-fit pole for this region. The final grid employed was a 1° x 1° latitude/longitude grid with possible rotations tested ranging from -1° to 1° in .01° increments. The pole location is 11° lat. and 253° lon. with –0.43° rotation and the post reconstruction misfit of previously offset features for this reconstruction is within the resolution of the image. This, along with the tightly constrained confidence regions, indicates that a best-fit Euler pole for the region in question has been determined.

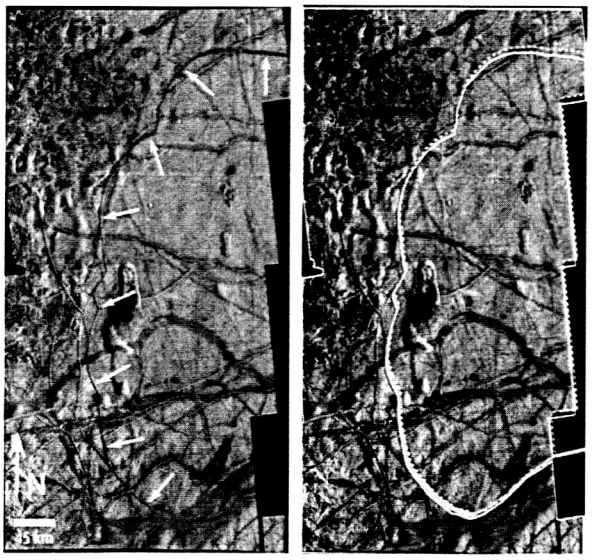

a b

Fig. 2. Castalia Macula region (centered at ~0 lat and 227 lon) as seen in Galileo E17REGMAP01 mosaic (a). Image is transmercator projected with resolution of 220m/pix. Arrows indicate ridge that was reconstructed. Reconstruction of region (b) using Euler pole and rotation shown in Fig. 3. Solid line indicates position of plate before reconstruction and dashed line indicates position after.

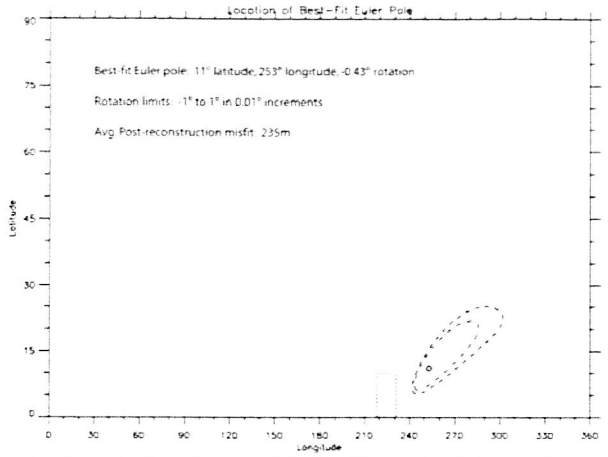

Fig. 2. Plot indicating position of best-fit Euler pole for Castalia Macula region. Dashed lines represent 95% and 99% confidence regions.

Conclusions and Implications: The test case for this method demonstrates that a unique solution for the Euler pole of rotation of this region can be determined. Knowledge of this unique solution allows us to produce a reconstruction of the plate motion in this region with an accuracy that can be quantified. Application of this method to other regions could provide a powerful means of unraveling the tectonic history of Europa.

The application of this model is presently limited by the spatial resolution and coverage available from the Voyager and Galileo missions. Increased image resolution and global comprehensive coverage by future missions will allow us to constrain pole locations and degree of rotation with increased accuracy as well as to consider the broader implications of regional plate rotations on Europa's global tectonic history.

Acknowledgements: We would like to thank Donald Forsyth for his assistance in developing the inverse model.

References: [1] Greeley et al., *Icarus*, 135, 4-24, 1998. [2] Hoppa et al, *Icarus*, 141, 287-298, 1999. [3] Prockter, L.M., and R. T. Pappalardo, *Science*, 289, 941-943, 2000. [4] Patterson, G.W. and R.T. Pappalardo, *Lunar Planet. Sci. Conf. XXXIII,* abstract # 1681 [5] Tufts et al., *Icarus*, 146, 57-75, 2000. [6] Sarid et al., *Icarus*, 158, 24-41, 2002. [7] Schenk, P.M., and W.B. McKinnon, *Icarus*, 79, 75-100, 1989. [8] Pappalardo, R. T. and R. J. Sullivan, *Icarus*, 123, 557-567, 1996. [9] Cox and Hart (1986), *Plate tectonics*, Blackwell Scientific Publications, 51-84 [10] Draper and Smith, *Applied Regression Analysis*, John Wiley and Sons Inc., 1996.

RADAR SOUNDING STUDIES FOR QUANTIFYING REFLECTION AND SCATTERING AT TERRESTRIAL AIR-ICE AND ICE-OCEAN INTERFACES RELEVANT TO EUROPA'S ICY SHELL.
M. E. Peters[1], D. D. Blankenship[1] and D. L. Morse[1], [1]University of Texas, Institute for Geophysics, 4412 Spicewood Springs Rd, Bldg 600, Austin, TX, 78759 (mattp@ig.utexas.edu).

Introduction: Jupiter's moon Europa is characterized by a pervasive icy mantle underlain by a global ocean. The distribution of free water and brines within Europa's icy/watery shell and the processes within the ice that control the exchange of material both with the surface and the ocean will determine Europa's suitability for harboring life. On Earth's ice sheets, radar sounding has proven to be a powerful tool for characterizing the ice-ocean interface as well as the overlying ice up to and including the air-ice interface. We present radar sounding techniques and new results from our recent airborne radar studies over ice-ocean environments in Antarctica.

Geologic Background: Certain processes hypothesized to occur for Europa's icy mantle and ocean have terrestrial analogs in the grounding zones of Antarctic ice streams [1-4]. These dynamic systems involve the interaction of the moving ice mass with the underlying materials, including liquid water (see Figure 1). Surface crevasses at varying levels accompany the ice streams due to high shear stresses at the ice stream margins. Bottom crevasses generally result at the grounding line due to tidal flexure. Once afloat, the ice and its interfaces continue to evolve. Ablation and accretion processes affect the character of the ice-ocean interface. Old bottom crevasses are healed, while new ones can be created, sometimes extending through the full ice thickness (see Figure 2). These processes continue beyond the calving of icebergs at the ice shelf front.

Imaging and characterizing the subglacial environment is fundamental to understanding these complex systems. Our focus has been to characterize the basal interface over the grounding zone of ice stream C and the ice-ocean interface of iceberg B-15 through radar reflection and scattering analyses. We also apply these techniques to the air-ice interface.

Echo Theory and Radar Methods: Echoes from the basal interface generally consist of both specularly reflected and diffusely scattered energy. Subglacial echoes are influenced by physical properties of the interface such as the composition, uniformity and roughness of the materials at the interface. Other important factors include dielectric losses and volumetric scattering losses from propagation through the ice as well as transmission at the air-ice interface. The primary physical factors influencing echoes from the air-ice interface are the surface roughness, the presence of surface crevasses, and the density of the air-ice mixture (firn).

Radar sounding techniques are well-suited to characterizing the reflection and scattering nature of both the ice-ocean and air-ice interfaces [5,6]. For example, unfocussed synthetic aperture radar (SAR) narrows the along-track radar beam, thus increasing resolution and the likelihood of specular reflection from the subglacial interface. Also, echo amplitude statistics can be used to identify reflecting or scattering regions. Fading analyses utilizing both echo and phase can provide estimates of the off-nadir extent of returned echoes, relating to scattering from the interface.

Radar System: Our radar system uses a programmable signal source with a dual-channel coherent down-conversion receiver [7] linked to a 10 kW transmitter. The radar operates in chirped pulse mode at 60 MHz and 15 MHz bandwidth. High and low-gain channels allow for recording both weak bed echoes and strong surface echoes simultaneously and without range-dependent gain control. Coherent data acquisition includes integrations of 16 returned radar signals about every 15 cm along-track. Pulse compression and unfocussed SAR processing using additional along-track integration were significant components of data analysis.

Results: Basal reflection coefficients are computed from these data and then used for inferring the subglacial materials, most notably regions where significant quantities of liquid water are present immediately beneath the ice. However, echo strength statistics based on reflection and scattering theory show that diffuse scattering can still dominate these echoes [8]. Scattering analysis includes imaging of the basal interface at short along-track integration distances to get a low resolution wide look at the basal interface. This is coupled with echo strength statistics (i.e., Rayleigh and Rice criteria) as well as echo amplitude and phase rates of change with distance (i.e., fading). Using the new radar data, we quantify off-nadir scattering from the subglacial interface to infer both the small-scale roughness and the distribution of slopes and facets associated with bottom crevasses and bedrock. We also identify and contrast regions of potential ablation and accretion at the ice-ocean interface.

A similar approach is applied to echoes from the ice-air interface. Reflection and scattering results show regions of heavy surface crevassing, as well as a variation in the surface reflection coefficient consistent with regional changes in firn density. We show that the level of crevassing is also well-quantified by off-nadir surface scattering and/or subsurface volume scattering.

References: [1] Chyba, C. F. et al. (1998) *Icarus, (134)* 292-302. [2] Blankenship, D. D. et al. (1999) *UTIG Tech. Rept. No. 184.* [3] Blankenship, D. D. et al. (2001) *LPSC (32) abstract 1854.* [4] Moore, J. C. (2000) *Icarus (147)* 292-300. [5] Blankenship, D. D. (1989) *EOS, (70)* 1081. [6] Bentley, C. R. et al. (1998) *J. Glaciol., (44)* 149-156. [7] Moussessian, A., et al. (2000) *Proc. IEEE Intl. Geosci. Rem. Sens. Symp., July 24-28, 2002, (2)* 484-486. [8] Peters, M. E. et al. *J. Glaciol.* (submitted).

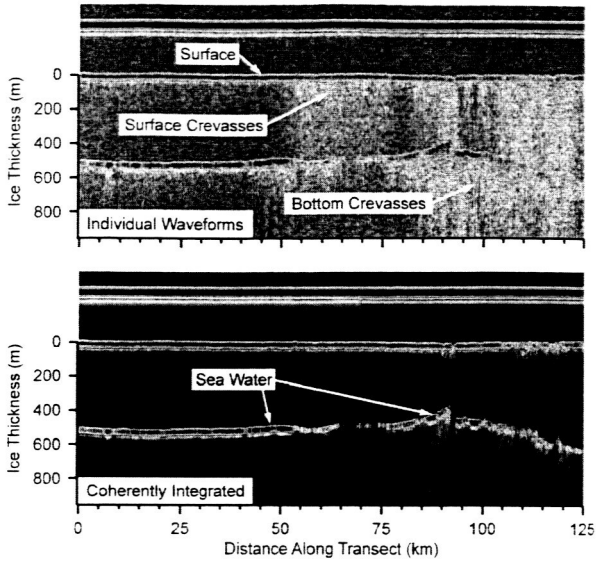

Figure 1. Coherent radar sounding profile at the grounding zone of ice stream C [5,6]. Individual waveforms (top panel) are coherently integrated along-track (bottom panel) implementing unfocussed SAR. Note the crevasse clutter cancellation. The labeled surface crevasses are the relict ice stream C shear margin. The bottom crevasses and overlying surface crevasses are due to tidal flexure at the grounding line.

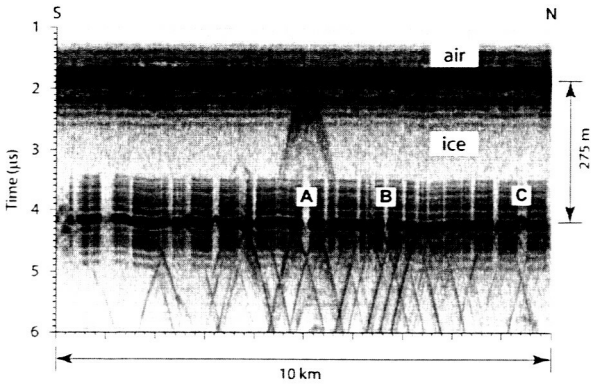

Figure 2. Radar sounding profile across a portion of iceberg B-15. Note the large crevasse (A) *extending through the entire ice thickness. Smaller bottom crevasses are also visible and are characterized by echoes up to 20 dB weaker than those for the adjacent ice-ocean interface.*

IMPACT GARDENING, SPUTTERING, MIXING, AND SURFACE-SUBSURFACE EXCHANGE ON EUROPA. Cynthia B. Phillips and Christopher F. Chyba, Center for the Study of Life in the Universe, SETI Institute, 2035 Landings Drive, Mountain View CA 94043. phillips@seti.org

Introduction: Charged-particle interactions with materials at Europa's surface can produce biologically useful oxidants such as molecular oxygen and hydrogen peroxide, which could help sustain a biosphere on Europa. Irradiation of carbon-containing materials at the surface of Europa should also produce simple organics [1-5]. These oxidants and organics, if transported downward through the ice shell to a liquid water layer, could provide a significant amount of energy to sustain a biosphere. However, irradiation also destroys such materials if they remain exposed on Europa's surface [6]. Sputtering erosion and surface mixing through impact gardening act to change the preservation depth.

If sputtering dominates over gardening, then material is created and destroyed at Europa's surface much faster than it can be buried and preserved by gardening. However, if gardening dominates, this means that irradiation products can be buried beneath the surface by gardening, where they are protected from further radiation processing. We are investigating models of gardening on Europa's surface to determine which regime is most appropriate. The results of this work will also provide the expected regolith depth on Europa, of relevance for future Europa landing spacecraft.

Once material is preserved from the surface irradiation that would destroy it, it must still work its way down through perhaps a kilometer or more of Europa's icy crust before it could become biologically relevant to a putative ocean biosphere. We begin the investigation of the myriad transport mechanisms that would help bring material from the surface to the potential ocean. These mechanisms will also bring up material from the subsurface to the surface, with relevance for the detection of subsurface composition and potential biosignatures.

Previous Gardening Estimates: Previous estimates of the gardening rate on Europa have depended on various assumptions and scalings, often over orders of magnitude. An initial attempt at a gardening estimate [6] based on a lunar analogy resulted in a gardening depth of about 1-10 centimeters over an expected surface age for Europa of about 10 Myr [7,8].

A later estimate of Europa's gardening rate [4] relied heavily on a regolith depth estimate from studies of Voyager images of Ganymede [9]. It also used a mass flux for small particles from studies of planetary rings [10]. This work resulted in a gardening depth of ~1.3 m over a surface age of ~10 Myr [4].

We have previously attempted to update the gardening rate for Europa by using Galileo data. Our initial attempt [11] used the impactor populations in the outer solar system summarized by Zahnle *et al.* [7,8] combined with lunar regolith growth studies of Shoemaker *et al.* [12,13] and Gault [14] as summarized in Melosh [15]. Based on this approach, we estimated a gardening depth on Europa of about 0.67 meters over a surface age of ~10 Myr [11]

To get this initial estimate, we used a value for the slope of the cumulative crater distribution from [9], which came from lunar studies for craters below 1 km in diameter, but is also consistent with fragmentation cascade studies done for small objects [7].

To update this estimate using Galileo data, we attempted to scale down from the large crater distribution of Zahnle et al [7,8] to get a more relevant value for the slope of the crater distribution (a key parameter in our gardening model [11]).

The problem with this approach was that it required us to assume that the slope of the observed large crater distribution on Europa was continued all the way down to the small sub-meter scale craters that are responsible for gardening. Large crater events on Europa are so infrequent compared to Europa's young surface age that they are fairly irrelevant to the gardening depth (by which we mean the mixing depth averaged over the entire surface). Instead, it is the small, more frequent and widespread cratering events which produce the broken surface layer commonly called regolith on small, airless worlds.

New Gardening Approach: Our current approach follows the same gardening depth formalization as our previous work [11], but instead of scaling down from the large crater distribution, we are using the counts of small craters by Bierhaus et al. [16]. These crater counts allow us to determine a small crater distribution from observations rather than by scaling from large craters.

Although we still have to scale down from the craters observed by [16] in the Galileo data (which range in diameter from tens of meters up to a kilometer of so), at least the scaling is over fewer orders of magnitude than was required previously. Also, there appears to be a significant change in slope between small and large craters on Europa, which could be due primarily to the significance of secondary craters on Europa [16]. Since there are so few large primary craters on Europa, Bierhaus et al. [16] found that the majority of

small craters on Europa's surface are actually secondary craters from these large impacts. Whether the small craters are primaries or secondaries, however, should not have a large effect on the mechanics of gardening and regolith formation.

Thus, we believe that our new approach, currently in progress, of applying the observed small crater distribution to the models of gardening and regolith formation developed in our previous work [11], will result in a definitive Galileo-era gardening depth estimate for Europa. Since it seems that the sputtering models are fairly mature at this point [4], once we have a final gardening estimate we can compare it to the sputtering estimates to see what the prospects are for the preservation of radiation products at Europa's surface.

Surface – Subsurface Exchange: Once material has been created through radiation processing at Europa's surface and buried below the radiation processing depth by gardening, the material must then make its way down to the ocean layer before it can become biologically relevant. By considering the number of formation models proposed for various geologic features on Europa's surface, we plan to estimate the amount of material that could be transported from the surface to the subsurface ocean layer, as well as the amount of material that could be brought up from a subsurface ocean to the surface or near-surface. We will present a preliminary overview of this work as well.

References:

[1] Chyba C.F. and Phillips C. B. (2001) *Proc. Natl. Acad. Sci.*.**98**, 801-804.

[2] Chyba C.F. (2000a) *Nature* **403**, 381-382.

[3] Chyba C.F. (2000b) *Nature* **406**, 368.

[4] Cooper J.F. et al. (2001) *Icarus* **149**, 133-159.

[5] Chyba C.F. and Phillips C. B. (2001) LPSC XXXII, abs. 2140.

[6] Varnes E.S. and Jakosky B.M. (1999) *LPSC XXX*, 1082 (CD-ROM).

[7] Zahnle K. et al. (1998) *Icarus* **136**, 202-222.

[8] Zahnle K. et al. (1999) *LPSC XXX*, 1776 (CDROM).

[9] Shoemaker E. M. *et al.* (1982) The Geology of Ganymede, in Satellites of Jupiter, ed. D. Morrison, UA Press, Tucson AZ.

[10] Cuzzi J.N. and Estrada P.R. (1998) *Icarus* **132**, 1-35.

[11]Phillips, C.B., and C.F. Chyba (2001) LPSC XXXII, abs. 2111.

[12] Shoemaker E. M. et al. (1969) *JGR* **74**, 6081-6119.

[13] Shoemaker E.M. et al. (1970) Proc. Apollo 11 Lunar Science Conference, v. 3, 2399-2412.

[14] Gault D.E. (1970) *Radio Science* **5**, 273-291.

[15] Melosh H. J. (1989) Impact Cratering: A Geologic Process. Oxford University Press.

[16] Bierhaus E.B. et al. (2001) Icarus 153, 264-276.

CLATHRATE HYDRATES IN JUPITER'S SATELLITE EUROPA AND THEIR GEOLOGICAL EFFECTS. O. Prieto-Ballesteros[1], J. S. Kargel[2], M. Fernández-Sampedro[1] and D. L. Hogenboom[3] . [1]Centro de Astrobiología. INTA-CSIC. Torrejon de Ardoz, 28850 Madrid. Spain (prietobo@inta.es). [2] Astrogeology Team. USGS. Flagstaff, Arizona. USA (jkargel@usgs.es). Lafayette College, Easton Pensylvania, USA (hogenbod@mail.lafayette.edu)

Introduction: The crust of Europa is dominated by water ice, but some contaminants have been detected on the surface. Several hydrates have been mentioned as part of the composition of the mineralogy of the surface of Europa such as sulfuric acid hydrates [1, 2] and salt hydrates [3, 4, 5, 6]. Clathrate hydrates are also minerals to be considered to be formed in the crust and the possible ocean of Europa.

Physical chemical properties of the hydrates are sometimes substantially different from water ice, so they could locally regulate the final state of the crust and the ocean. Parameters such as thermal conductivity, density and low melting points of these materials are useful to incorporate in the physical geological models of Europa.

Clathrates from brines.

Electrolytes in solution are usually taken as clathrate formation inhibitors. Ions in solution affect the formation of the clathrates in two ways: a) the strong attraction of the water to the electrolytes, and b) the salting-out effect, or the decreasing solubility of the gas molecules into the salty water due to the clustering of the water with the ions. The effects of some chlorides such as NaCl or $CaCl_2$ in the clathrate formation are already quantitatively known. These systems have been extensively studied experimentally and theoretically because they are frequent in the Earth seawater and in many fluid inclusions of terrestrial rocks.

The composition of water reservoirs in Europa have been proposed to be salty from magnetic data analysis and geochemistry modelling [7, 8, 9]. Sulfate-enriched brines for Europa's water reservoirs have been supported by some studies. Since planetary objects generally also contain and release gases from their solid interiors, various gases are also likely constituents of Europa's ocean and floating icy shell. Unlike most planetary objects, which release their gases onto their surfaces, where they form atmospheres or surface condensates, or else escape into space, Europa's ocean is likely to contain vented gases up to the limit of high-pressure saturation. Free fluid phases can form and then may be vented as gases through the icy shell. However, ocean saturation of small apolar gas molecules generally should result in formation of clathrate hydrate phases.

Candidate guest molecules to form clathrates in Europa are CO_2 and SO_2, both observed on the surfaces of some Galilean satellites [10, 11] and are geochemically plausible [5, 12]. Other likely clathrate-forming guest molecules in Europa's ocean and icy shell may include N_2 and perhaps O_2 (the latter from radiolytic processes), and possibly CO and CH_4. CO_2 is especially likely and probably abundant, because it is observed and abundant from Venus to the most distant realms of the Solar System, including comets. SO_2 may be abundant on Europa if Europa's rocky interior and the geochemical processing there is anything like that of Io.

We use a modification of the Hammerschmidt equation (eq. 1) [13, 14] to calculate an approximation of the effect of the magnesium sulfate to the formation of CO_2 clathrates at constant pressure as an example of how salts may affect clathrate stability in Europa:

$$\left(\frac{1}{T_d^0}-\frac{1}{T_d}\right)=\frac{n\cdot\Delta H_{FUS(I)}}{\Delta H_{DIS}}\left(\frac{1}{T_f^0}-\frac{1}{T_f}\right) \qquad \text{(eq. 1)}$$

where: T_d^0 and T_d are the temperatures at which CO_2 dissociates in pure water and in the solution, ΔH_{DIS} is the enthalpy of dissociation of CO_2 clathrate, n is the number of water molecules in hydrate formula, $\Delta H_{FUS(I)}$ is the enthalpy of fusion for pure ice and T_f^0 and T_f are the melting temperatures of ice and the electrolyte solution.

The result (Fig. 1) indicates that dissolved magnesium sulfate decreases the crystallization point of the clathrate in a similar manner to the way the salt itself reduces the melting point of water ice.

Geological implications: The presence of large amounts of hydrates (clathrates, sulfuric acid or salt hydrates) produce some effects on the geology of Europa. Clathrate and salt hydrates have low thermal conductivities, as some experimental analyses indicate [15, 16]. If they are present in the icy crust they would

produce zones of high thermal gradient and perhaps enhanced geological activity of several types.

As has been theoretically predicted, CO_2 clathrates may crystallize from salty water reservoirs at lower temperatures than from pure water. The inhibition of formation only amounts to about 2 K at the eutectic proportions og $MgSO_4$ (17%). On one hand, this means that insofar as clathrates are concerned, the salts do not have a large effect. On the other hand, the introduction of clathrate-forming gases into a salt-saturated or undersaturated ocean may have a large effect on the salts. Formation of clathrates removes water from the solution, so there will be a higher concentration in ions as soon as the clathrates are formed. This property has been used to desalinate terrestrial seawater. If this process occurs in an aqueous magmatic chamber in the crust of Europa, clathration could result in a cryomagmatic differentiation. The formation of clathrates would separate the crystals from the more concentrated brine magma by density. If the destruction of the clathrate layer occurred by any movement or fracturation, clean water ice could ascend through the brine to higher levels.

Destruction of clathrate layers near the surface could produce catastrophic processes because of the fast liberation of gases, and the large negative volume change of the solid phases upon dissociation and loss of the free gas phase. Fracturing and gravitational collapse of terrain could ensue. It could be an autocatalytic, even catastrophic process if fracturing and depressurization causes more clathrate to dissociate and especially if gas-saturated brine from the ocean jets through fractures and erosionally widens them. Chaotic terrain on Europa could conceivably be related to this process, as it may also on Mars, Earth, and Triton [17]. That also could be responsible for explosive cryovolcanic events, as some authors have already pointed out [17, 18, 19].

The transition from a condensed phase (such as clathrate) to a multiphase system containing a free vapor phase is always endothermic if chemical reactivity is not involved (as with clathrate dissociation forming a free vapor phase). Therefore, cooling and crystallization of ice (possibly also salts if the system is already salt-saturated) will occur during dissociation of ice-equilibrated clathrates (as Europa's are expected to be). However, the system includes a negative volume change of the condensed phase assemblage if the free vapor phase is vented; therefore, a continuing fracturing process and collapse of the system can occur in a runaway process of chaotic terrain formation. Energy for the process can be supplied by effervescing oceanic brine gushing through and widening the fractures.

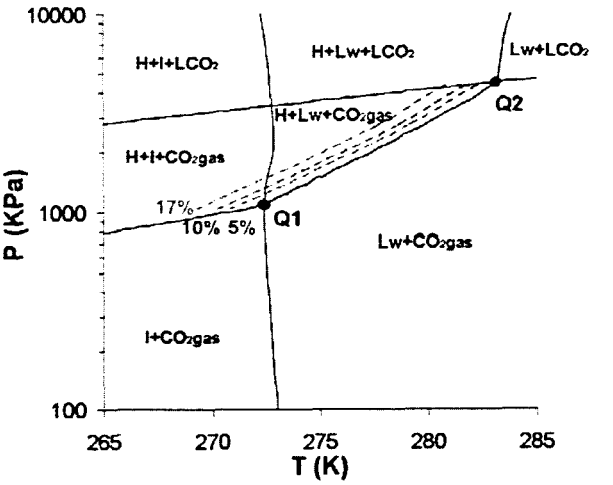

Figure 1. Phase transition diagram of CO2 clathrate. Colors show thedisplacement of the stability line of clathrates, if the indicated proportions of MgSO4 are added to the aqueous solution. H= clathrate hydrate, I = water ice Lw=liquid water, LCO_2= liquid CO_2, Q1 and Q2 are the quadruple points.

References::

[1] Carlson, R.W. et al (1999). *Science* 286, 97-99. [2] Carlson, et al. (2002). *Icarus* 157, 456-463. [3] Fanale, F.P. et al. (2001). *J. Geophys. Res.* 106, 14,595-14,600. [4] Kargel, J. S. (1991). *Icarus* 94, 368-390. [5] Kargel, J. S., et al. (2000). *Icarus* 148, 226-265. [6] McCord, T. B., et al. (1999). *J. Geophys. Res.* 104, 11,827-11,851. [7] Kargel, J. S. and G. J. Consolmagno (1996).*LPSC XXVII*, 643-644. [8] Khurana, K. K., et al. (1998). *Nature* 395, 777-780. [9] Kivelson, K. G., et al. (1999). *J. Geophys. Res.* 104, 4609-4626. [10] Hibbitts, C. A. et al. (2000). *J. Geophys. Res* 105, 22541-22557. [11] Lane, A. L., et al. (1981) *Nature* 292, 38-39. [12] Crawford, G. D. and Stevenson, D. J. (1988). *Icarus* 73, 66-79. [13] Sloan, E. D. (1998) In: Clathrate hydrates of natural gases. Marcelll Dekker Inc., NY. [14] Dickens, G. R. and Quinby-Hunt, M. S. (1997). *J. Geophys. Res.* 102, 773-784. [15] Prieto-Ballesteros, O. and Kargel, J. S. (2002). *LPSC XXXIII*, nº 1726. [16] Ross, R. G. and J. S. Kargel (1998). In *Solar System Ices*, (B. Schmitt, C. De Berg y M. Festou Eds.), pp. 33-62. Kluwer Academic Publishers, Netherlands. [17] J.S. Kargel, et al. (2003) *Geophys. Res. Abstracts*, 5, 14252, 2003,European Geophysical Society. [18] Fagents, S. A. et al. (2000). *Icarus* 144, 54-88. [19] Stevenson, D. J., (1982). *Nature* 298, 142-144.

GEOLOGICAL FEATURES AND RESURFACING HISTORY OF EUROPA. L. M. Prockter[1] and P. H. Figueredo[2], [1]Applied Physics Laboratory, Laurel, MD 20723, Louise.Prockter@jhuapl.edu, [2]Department of Geological Sciences, Arizona State University, Tempe, AZ 85287, figueredo@asu.edu.

Introduction

Many different models have been proposed for the formation of Europa's primary surface features: ridges, bands, chaos and lenticulae. We briefly review the models, evaluating their strengths and weaknesses, and their implications for the thickness of Europa's ice shell. We discuss Europa's stratigraphy, and how the surface may have evolved through time.

Morphological features

Ridges: Double ridges are without doubt the most ubiquitous feature on Europa's surface. They are highly unusual in the solar system, and have only been identified on Triton to date [1]. The Europan ridges constitute an intricate mesh, they have formed throughout Europa's visible history and may still be forming today [e.g., 2]. Ridges appear to form a genetic sequence of different morphological types, ranging from simple troughs, through double ridges, then triple ridges, and finally any number of closely spaced ridges, termed "ridge complexes" [2, 3]. The dominant type by far is the double ridge, which has two crests of largely uniform width and height, separated by a V-shaped trough. Ridges range in size, from ~500 hundred m to ~2 km wide, up to ~200 m high, and up to several thousand km in length, meaning that some are hemispherical in scale. Cycloidal ridges appear to form on relatively rapid timescales resulting from Europa's diurnal cycle [4], but the details of how the majority of Europa's ridges are created are still open to debate.

Several models have been proposed for the formation of the ridges, each of which has its strengths and weaknesses. These include: (1) *Tidal squeezing*, in which fractures penetrate through an ice shell, and open and close as a result of diurnal stresses [5]. The amount of opening and closing is small – about 1 m – and each cycle allows water and icy slush to be pumped toward the surface, forming the characteristic ridge crests and central trough. This process is similar to that which forms terrestrial pressure ridges in lead ice, and the morphology is remarkable similar. (2) *Compression*, in which ridges are proposed to have a compressional origin [6]. This model could help account for the mystery of Europa's surface, which has abundant evidence of extension, but little identified compression. While falling out of favor for a few years, this model has recently been revived by [7]. (3) *Linear volcanism*, in which ridges are proposed to be the result of gas-driven fissure eruptions, resulting in ridge crests comprised of cryoclastic debris [8]. Volatiles SO_2 and CO_2 could drive the eruptions. (4) *Linear diapirism*, a model in which ridges are proposed as the surface expression of linear warm ice diapirs, which rise to the surface, causing cracking and uplift of the surrounding terrain, forming ridge flanks [9]. (5) *Dike intrusion*, in which ridges form by intrusion of melt into vertical cracks, resulting in plastic deformation to form ridge morphology [10]. (6) *Shear heating*, in which heating along cracks from diurnal strike-slip motion causes upwelling of warm ice to form ridges, with possible associated partial melting [11]. To date, none of these models can describe all the features characteristic of ridges, such as uniformity in space and time, forks, and sharp turns.

Bands: Bands are features up to tens of km wide and hundreds of km long, which apparently brighten with age. They have formed through complete separation of the preexisting surface, by extension, shear and/or compression [12, 13]. Two primary models have been proposed for the formation of bands. The first suggests that they are a continuation of the tidal-squeezing ridge forming process [5], and that they result from continuous ratcheting apart of a crack due to diurnal stresses and the possible influence of secular variations [14]. The rising water is proposed to freeze, preventing the crack from closing, and is then pulled further apart during the next tidal cycle, adding more frozen material and widening the band. This model implies that Europa's ice shell is relatively thin. The second model proposes that bands have an origin similar to that of mid-ocean ridges [15], and that they form from solid-state material, possibly ductile warm ice [16]. As with the previous model, new material is added along the band's central axis, but it is solid state, and the resulting band morphology may depend on the rate of band opening. This model does not require a thin shell.

Lenticulae: Lenticulae are the many subcircular areas of disrupted terrain present across Europa's surface. They range in size but are generally agreed to cluster around ~10 km in diameter [e.g., 2, 17]. Lenticulae can be either pits, domes, low albedo plains areas, or some combination of these. Many of them (known as microchaos) have interiors which are broken into small plates of preexisting surface material in a lower albedo matrix [2]. Two primary models have been proposed for their origin. The first, based on their apparently uniform size distribution, suggests that they are the result of diapirism [18, 19], possibly due to thickening of the ice shell to a point at which convection can be initiated. The second, based on the resem-

blence of plates within the lenticulae to terrestrial icebergs, suggests that they result from melting of the surface by liquid water [20, 21] requiring a much thinner shell. Lenticulae may be related to the formation of chaos.

Chaos: Chaos regions are much larger than lenticulae, but are also areas of Europa's surface that appear to have been significantly disrupted by some endogenic (cryo)magmatic process. Although there are morphological variations, chaos terrain is comprised of polygonal plates of preexisting surface material, in a dark, finer grained hummocky matrix [2]. In at least one area, there is evidence that the plates have shifted from their original position [22], and chaos may stand either higher or lower than its surroundings [2, 23]. As with the lenticulae, the two models proposed for chaos formation are that they formed from regions of liquid water melt-through [20, 21], or from single or merged diapirs of warm ice [18]. Each model has significant implications for the thickness of the shell.

Resurfacing history

Image coverage and resolution from the Galileo spacecraft has been sufficient to allow several local and regional areas on Europa to be mapped, and a stratigraphy to be derived [2, 24]. Recent pole-to-pole mapping [25] considerably extends earlier work over a much broader area of coverage, and confirms previous suggestions that there has been an apparent change in the style of resurfacing on Europa over time. The visible history of Europa only goes back as far as the "background ridged plains" which comprise most of Europa. This unit is so heavily tectonized that it is very hard to determine the existence of any preexisting features within it; Europa has either been completely resurfaced prior to background plains formation, or features that existed prior to its formation are so completely tectonized as to be unrecognizable. Either way, the average surface age of Europa is estimated to be ~60 Ma [26].

Postdating the formation of the background plains, the next oldest group of features are the gray bands. Bands have a variety of orientations and commonly cross-cut each other, but none appear to have formed in Europa's recent history. Whether formed from liquid water or warm ice, they suggest a change in resurfacing style to magmatic processes. Chaos and lenticulae commonly postdate bands, although it is impossible to tell whether they themselves formed concurrently. Since chaos-related features are some of the youngest units in Europa's stratigraphic column, it is possible that they are still forming today. This inference has significant implications for Europa's astrobiological potential, since such features may be places where its ocean communicates with the surface. Double ridges and craters are found throughout Europa's visible surface history, although tectonic lineaments have been found to narrow over time, perhaps indicating a change in the thermal state of Europa's ice shell [25].

The change in the formation from bands (lateral tectonics with associated cryomagmatism) to chaos (vertical transport of cryomagmatic materials) has been suggested as evidence that Europa's shell may be undergoing progressive thickening with time, possibly as a result of the "freezing out" of an ocean [16, 24, 25, 27]. Such thickening may explain the change from the inferred earlier mobility of the ice shell, in which lithospheric separation, and hence band formation, was common, to a convective state in which lenticulae and chaos are the norm.

The apparent change in Europa's resurfacing style is not sufficient to place this transition into a longer-term context [25, 27]. Because Europa's surface is so young, on average, we cannot tell from currently available data whether the apparent thickening of the ice shell corresponds to the complete cessation of geological activity, whether both processes coexist in different regions, or whether there are cycles of alternating tectonic and cryovolcanic activity, on geological timescales.

References:

[1] Croft et al. (1995) Neptune and Triton, ed. D.P. Cruikshank, U. of Arizona Press, Tucson, p. 879-948. [2] Greeley, R., et al. (2000) *J. Geophys. Res., 105,* 22,559-22,578. [3] Pappalardo, R.T., et al. (1998) *LPSC XXIX,* 1859. [4] Hoppa, G., et al. (1998), *Science, 285,* 1899-1902. [5] Greenberg et al., *Icarus, 135,* 64-78, 1998. [6] Sullivan, R., et al., (1999) *LPSC XXX,* CD-ROM *1925* [7] Patterson, G. & R. Pappalardo, (2002), *LPSC, XXXIII* CD-ROM 1681. [8] Kadel S. et al., (1998), *LPSC XXX* CD-ROM 1078; Fagents et al., (2000), *Icarus 144,* 54-88. [9] Head J., et al., (1999), *J. Geophys. Res., 104,* 24,223–24,236. [10] Turtle E. et al. (1998), *EOS 79,* F541. [11] Gaidos, E., & F. Nimmo (2000), *Nature 405,* 637. [12] Schenk P. & W. McKinnon, (1989), *Icarus, 79,* 75-100. [13] Sarid, A., et al., (2002), *Icarus, 158,* 24-41. [14] Tufts B. et al., (2000), *Icarus, 141,* 53-64. [15] Sullivan, R. et al., (1998), *Nature, 391,* 371-372. [16] Prockter, L. et al., (2002), *J. Geophys. Res., 107,* 10.1029/2000JE001458. [17] Spaun N., et al., (1999), *LPSC XXX,* CD-ROM 1847. [18] Pappardo R. et al., (1998) *Nature, 391,* 365-366. [19] Rathbun, J. et al., (1998), Geophys. Res. Lett., *25,* 4157-4158. [20] Carr, M. et al., (1998), *Nature, 391,* 363-364. [21] Greenberg R., et al., (1999), *Icarus 141,* 263-286. [22] Spaun N. et al., (1998), *Geophys. Res. Lett., 25,* 4277-4290. [23] Collins G. et al., (2000), *J. Geophys. Res., 105,* 1709-1716; Figueredo P., et al., (2002) *J. Geophys. Res., 107,* 2-12. [24] Prockter L. et al., (1999) *J. Geophys. Res., 104,* 16531-16540; Figueredo P. & R. Greeley (2000), *J. Geophys. Res., 105,* 22629-22646; Kadel S. et al., (2000), *J. Geophys. Res., 105,* 22656-22669. [25] Figueredo P. and R. Greeley, (2003) *Icarus* in press. [26] Schenk P. et al., in "*Jupiter and her Satellites*" ed. F. Bagenal (2003), in press. [27] Pappalardo et al., (1999) *LPSC XXX* CD-ROM 1859.

EUROPAN BANDS FORMED BY STRETCHING THE ICY CRUST: A NUMERICAL PERSPECTIVE.
Ran Qin[1], W. Roger Buck[1], Robert T. Pappalardo[2], [1]Lamont-Doherty Earth Observatory of Columbia University, Palisades, NY 10964, email: rqin@ldeo.columbia.edu; [2]Department of Astrophysical and Planetary Science, University of Colorado at Boulder, CO

High-resolution Galileo images of Europa show linear, curved and wedge-shaped bands crossing the ice surface. These bands are most clearly seen within the region southwest of Europa's anti-Jovian point and make up ~60% of the terrain[1]. It has generally been inferred that bands have formed in response to extension, although Schulson [2]suggests that at least one wedge-shaped band may have formed under compressive stress, analogous to small-scale "wing cracks".

Reconstruction of bands implies that Europa's surface layer has behaved in a brittle or plastic manner, separating and translating atop a low-viscosity subsurface material, with the gap being infilled with relatively dark, mobile material. Two principal models have been proposed for band origin. If Europa's ice shell is very thin (<6 km) and cracks can penetrate through the entire ice shell, then a model of extrusion of water and slush during band opening may be applicable[3][4]. On the other hand, if Europa's ice shell is thicker and ductile subsurface ice plays a significant role in shaping the satellite's geology [5], then bands may have formed from relatively warm ice and would be more analogous to terrestrial mid-ocean ridge rift zones[1][6]

One endmember of Europa's bands commonly exhibit prominent axial troughs, symmetrical spreading from a central axis, large hummocks, tilted fault blocks and bounding ridges (Fig. 1), several kilometers wide and up to 100 meter higher than the surrouding plain. Broadly analogous morphological feature types are also found along terrestrial mid-ocean ridges in the form of axial graben, features of the neovolcanic zone, and abyssal hill normal faults [7]. On the basis of morphology and inferred topography within the bands (such as axial troughs and linear ridges), Prockter et al. [1] proposed that a terrestrial seafloor spreading analog may be appropriate for Europan bands. Furthermore, these authors speculated that if the bands on Europa are analogous to terrestrial mid-ocean ridges and a similar mode of formation applies to both, then analogous processes may be the cause of variations in morphology and topography among the Europan bands.

Terrestrial slow spreading ridges generally exhibit prominent axial troughs, large faults and numerous volcanic edifices as new material is slowly formed then rafted away from the central spreading axis. If on Europa, these characteristic bands (Fig. 1) have opened relatively slowly forming cooler, thicker lithosphere close to the axis, allowing significant topography to be supported, this would be analogous to those slow-spreading mid-ocean ridges such as the Mid-Atlantic Ridge.

We are currently adapting a sophisticated numerical model that exists for modeling rifting phenomena on Earth, as developed and first applied to slow-spreading mid-ocean ridge abyssal hill topography by Buck and Poliakov [8], to quantitatively test the hypothesis of Europan hummocky band formation by stretching its icy crust. The numerical model uses an explicit finite-element method similar to the FLAC (Fast Lagrangian Analysis of Continua) technique of

Cundall [9]. The Lagrangian method allows us to trace the material flow and a remeshing technique is developed to adjust the numerical grid when it's heavily deformed. Advection and diffusion of heat are also included to allow a time varying lithospheric structure. The surface temperature of Europa is around 100 K and increases toward its interior following a proper temperature gradient, probably 5 ~ 40 K/km. The ice of Europa is commonly believed to have elastic-visco-plastic rheology[10][11] which is temperature and strain-rate dependent. In the shallow, cold part of this layer the viscosity is so high that it effectively behaves as a brittle material, approximated with Coulomb elastoplastic rheology, which allows for localization of shear deformation that mimics faults. Warmer regions deform by thermally activated creep. This numerical model will allow us to explore relationships among opening rate, cooling rate, fault initiation, and morphology of rift zones that might be formed by stretching of Europa's icy crust.

Preliminary model runs have been performed with coarse grids to ensure that our algorithms--developed to model faulting in terrestrial rock--will succeed in reproducing tectonic structures in ice. These preliminary runs have successfully produced faults within a thin ice lithosphere with, a transition from brittle to ductile behavior occurring near 0.5 to 3 km (the range constrained observationally [5]), and faults penetrating to near this depth. These results, however, are not yet fully validated. This main goal of our modeling is to produce the surface morphology that will be compared to the morphologies of bands on Europa. Our results will address the first-order question of whether the mid-ocean ridge analog model is an appropriate one to apply to Europa, and if so, will constrain the formation conditions appropriate to formation of bands, notably thermal structure and strain rate.

References: [1]Prockter, L. M. et al. (2002) Morphology of Europan bands at high resolution: A mid-ocean ridge-type rift mechanism, *J. Geophys. Res., 107(E5),* 10.1029/2000JE001458. [2]Schulson, E.M. (2002) On the origin of a wedge crack within the icy crust of Europa, *J. Geophys. Res., 107(E11),* 10.1029/2001JE001586. [3]Greenberg, R. et al. (1998) Tectonic processes on Europa: Tidal stresses, mechanical response, and visible features, *Icarus, 135,* 64-78. [4]Tufts, B. R. et al. (2000) Lithospheric dilation on Europa, *Icarus, 146,* 75-97. [5]Pappalardo, R. T. et al. (1999) Does Europa have a subsurface ocean? Evaluation of the geological evidence, *J. Geophys. Res. 104,* 24015-24055. [6]Sullivan, R. et al. (1998) Episodic plate separation and fracture infill on the surface of Europa, *Nature, 391,* 371-372. [7]MacDonald, K.C. (1982) Mid-ocean ridges: Fine scale tectonic, volcanic, and hydrothermal processes within the plate boundary zone, *Ann. Rev. Earth Planet. Sci., 10,* 155-190. [8]Buck, W. R. and A. N. B. Poliakov (1998) Abyssal hills formed by stretching of oceanic lithosphere, *Nature, 392,* 272-275. [9]Cundall, P.A. (1989) Numerical experiments on localization in frictional materials, *Ingenieur-Archiv, 58,* 148-159. [10]Durham, WB and LA Stern (2001) Rheological properties of water ice – application to satellites of the outer planets, *Annu. Rev. Earth. Planet. Sci., 29,* 295-330. [11]Schulson E.M. (2001) Brittle failure of ice, *Engineering Fracture Mechanics,* 68, 1839-1887.

LIMITS ON THE STRENGTH OF EUROPA'S ICY SHELL FROM TOPOGRAPHIC SPECTRA.

D. T. Sandwell, Scripps Institution of Oceanography, La Jolla, CA, 92093-0225, dsandwell@ucsd.edu

Introduction: Radio echo sounding on Europa may provide estimates of the depth to the brittle-ductile transition. This information should be consistent with the topography spectrum. Here we derive an upper bound on the amplitude and shape of the topographic spectrum that can be supported by the strength of the lithosphere. Topographic features that exceed this upper bound must be supported by local compensation.

Lithospheric Strength: *Byerlee* [1] showed that the frictional resistance on a fault τ depends on the fault normal stress σ_n and the coefficient of friction and is largely independent of material properties. Suppose that the brittle layer of ice has closed fractures oriented in all directions and a differential stress $(\Delta\sigma = \sigma_1 - \sigma_3)$ is applied. Frictional sliding will occur on optimally-oriented fractures when the resolved shear stress exceeds the Byerlee criteria. The magnitude of this differential stress is called the yield strength [2] and it is primarily a function of the overburden pressure as follows:

$\Delta\sigma = -3\rho g z$ (horizontal compression)

$\Delta\sigma = 0.7\rho g z$ (horizontal extension)

For lack of additional information about the ductile layer, we'll assume it has a linear decrease in strength with depth and zero strength is achieved at twice the depth of the brittle ductile transition (Figure 1). One can now calculate the maximum bending moment that can be maintained by the lithosphere before it fails M_s. The saturation bending moment is the integral of the yield strength over depth times the distance to the brittle/ductile transition

$$M_s = \int_0^{2z_b} \Delta\sigma(z)(z - z_b)dz = 0.6\rho g z_b^3$$

where ρ is the density (1000 kg m^{-3}) and g is the acceleration of gravity (1.3 m s^{-2}). The saturation bending moment increases as the cube of the depth to the brittle/ductile transition.

Topographic Moment: This estimate of saturation bending moment provides an upper bound on the amplitude of the topography that is supported by stress in the shell. The vertical load of positive topography must compensated by a nearby negative topographic load. This high to low dipole must be maintained by the strength of the lithosphere. Consider sinusoidal topography of wavelength λ and amplitude w_o. The moment that must be applied at the origin to maintain the topography is given by the following formula.

$$M = g\rho \int_{-\lambda/4}^{\lambda/4} w_o \sin\left(\frac{2\pi x}{\lambda}\right) x dx = \frac{g\rho w_o \lambda^2}{2\pi^2}$$

This topographic moment must be less than the saturation bending moment that can be supported by the strength of the plate M_s. Equating these two moments provides an upper bound on the amplitude of the topography as a function of the characteristic wavelength of the topography.

$$w_o < \frac{2\pi^2 M_s}{g\rho\lambda^2} \cong \frac{\pi^2 z_b^3}{\lambda^2}$$

We see that for a given saturation moment, the maximum amplitude of the topography decreases rapidly with increasing wavelength. The nice feature of this formula is that it contains measurable quantities - the wavelength of the topography and the depth to the brittle/ductile transition. An additional bound on the topographic spectrum is that topographic slopes cannot exceed the angle of repose (~30°). This can be translated into a constraint on topographic amplitude versus wavelength.

$$w_o < \frac{0.57\lambda}{2\pi}$$

Overall the amplitude of the topography must be less than the smaller of the two limiting mechanisms (Figure 2).

Conclusions:

- Saturation bending moment depends on the cube of the depth to the brittle-ductile transition.
- The maximum topography that can be maintained by the strength of the lithosphere decreases as the square of the wavelength of the topography.
- Significant amplitude (>100 m) topography on Europa with wavelength greater than 100 km cannot be supported by lithospheric strength and therefore must be supported by a local compensation mechanism.

References:

[1] Byerlee, J. D. Friction of rocks. *Pageoph* **116**, 615-626 (1978). [2] Brace, W. F. & Kohlstedt, D. L., *J. Geophys. Res.* **85**, 6248-6252 (1980). [3] Prockter, L.M., et al., *J. Geophys. Res.*, 107(E5), 5028, 2002.

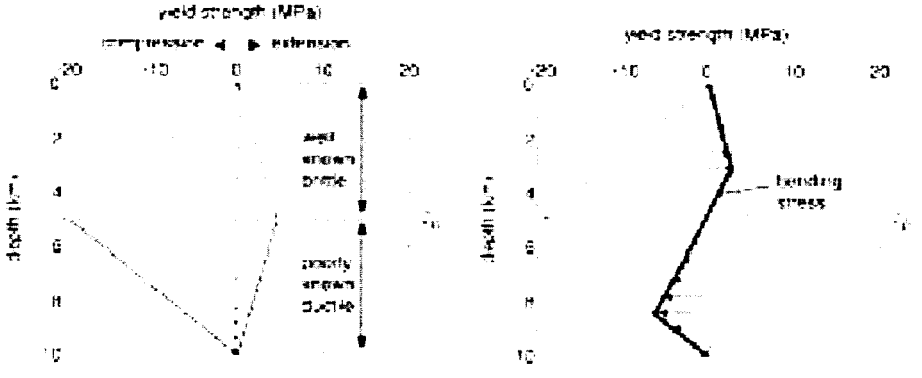

Figure 1. Strength of the lithosphere as a function of depth in tension and compression. (left) Stress is relieved by the lowest-strength deformation mechanism resulting in a yield strength envelope. The strength of the upper brittle layer follows Byerlee's Law while the strength of the lower ductile layer is largely unknown. (right) Concave-up bending of the lithosphere will cause extension in the upper half of the plate and compression in the lower half of the plate.

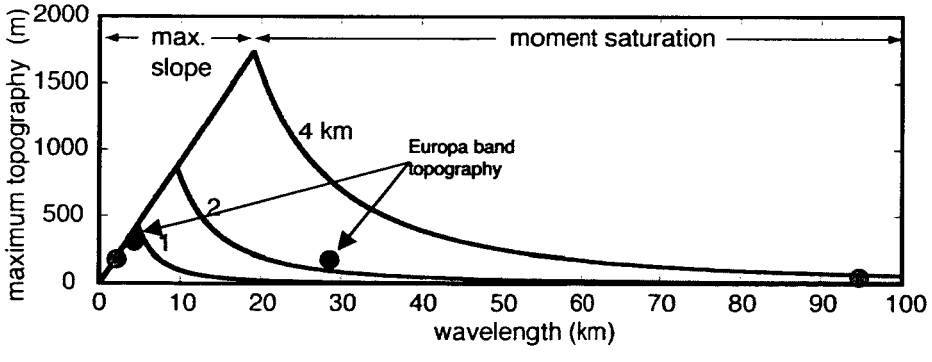

Figure 2. Maximum amplitude topography that can maintained entirely by the strength of an icy shell for brittle/ductile transition depths of 1 km, 2 km and 4 km. The amplitude of the short-wavelength topography is limited by the angle of repose (~30°). The amplitude of the longer wavelength topography is limited by the strength of the lithosphere. The red dots mark the typical amplitude/wavelength of banded topography on Europa [3]. The green dots mark approximate requirements for a new mission.

HIGH-RESOLUTION MAPPING OF EUROPA'S IMPACT CRATERS: COMPARISON WITH GANYMEDE. P. Schenk[1], and J.M. Moore[2], [1]Lunar & Planetary Institute, Houston, TX 77058, [2]SETI Institute, MS 245-3, NASA Ames Research Center, Moffett Field, CA 94035-1000, e-mail: schenk@lpi.usra.edu.

Introduction: Any examination of Europa's unusual impact morphologies is null and void unless detailed comparison can be made to "normal" impact craters on large icy bodies without shallow liquid water oceans. Ganymede and Callisto, with similar surface gravity, lack of recent geologic activity, and relatively deep oceans, come to mind. Here we examine the limited data available for Europan craters and begin the task of comparison with Ganymedean craters of similar size. We focus on impact melt, morphology, and topography (derived from stereo and photoclinometric (PC) analyses).

Europa. Moore et al. [1] performed the first survey of Europan impact craters. High-resolution (better than 100 m/pixel) imaging of large craters on Europa is limited to Manannan (D~23 km, res. 20 m/pixel), and Cilix (D ~19 km, res. 60 m/pixel). The Manannan high-resolution mosaic clear shows flow-like features within the crater rim and onlapping onto the pedestal ejecta deposit (Fig. 1). High-resolution stereo and PC topography (Fig. 1) shows that these features usually occupy local topographic lows, but that these features can also remain on slopes and that intervening areas are very rugged. This would seem to imply that impact melt is not especially voluminous on large Europan craters, and was not invicid.

Additional coverage of Pwyll (D~27 km) and the multiring structures Callanish (D~33 km) and Tyre (D~41 km) was obtained at 125, 170, and 50 m/pixel, respectively. Mapping of ejecta deposits [e.g., 2] shows that the nominal crater rim lies interior to the inner rings, in terrain that is essentially flat. Swirl textures on the floors of both ring structures are reminiscent of features observed in melt sheets on some lunar craters.

Ganymede. The only relatively pristine large impact crater targeted by Galileo on either Ganymede or Callisto is Melkart, a central dome crater on Ganymede (D~107 km, res. 175 m/pixel). The floor of Melkart (and other craters seen at lower resolution) is characterized by large 5-15 km wide rounded hillocks, a morphology reminiscent of melt sheets on some lunar craters. This morphology has not been recognized on Europa (granted that there are no craters this size on Europa). Unfortunately, no other large pristine "normal" impact crater was targeted for either Ganymede or Callisto.

Unusual impact landforms on Ganymede and Callisto include anomalous dome craters, penepalimpsests, and palimpsests. These impact morphologies occur at D>60 km, but generally are relatively ancient structures [3]. A radial image transect was obtained of the 207-km diameter penepalimpsest Epigeous at 90 m effective resolution (our highest such resolution). Despite the relative age of this structure (during or immediately after bright terrain emplacement), these images (Fig. 2) reveal features somewhat reminiscent of flow features seen at Manannan. Another penepalimpsest, Buto Facula (D~157 km) was imaged at too low a resolution (180 m/pixel) to reliably map floor textures. Smooth ponds of impact melt are lacking, however.

Comparisons. Europan craters do share some similarities with those on Ganymede. Evidence for rim slumping is sparse compared to lunar examples, and virtually no unequivocal terrace has been identified on any of the satellites. Evidence for flow in the ejecta on the crater floor is apparent but generally limited on all three satellites. Topographic pedestals commonly forming the inner ejecta deposit of Europan craters are similar to those found around Ganymede craters such as Achelous [e.g., 2]. Europan pedestals are often associated with dark, rather than bright material, however. Ejecta typically consists of shallow-seated excavated crustal material, suggesting that such material on Europa is relatively dark compared with the present surface.

Topography. Detailed mapping of impact crater shapes shows that impact craters follow well-defined depth-diameter (d/D) trends on all three satellites, but that Europa diverges from its sister satellites [4]. Europan craters up to D~9 km across have shapes similar to Ganymedean craters. At D > 9 km, Europan craters become shallower with increasing size. The anomalous interior landforms associated with these craters (disrupted rims, modified or distorted central peaks, rugged floor topography) indicate that these are NOT relaxed "ordinary" Ganymedean craters, but rather craters whose development was arrested or highly modified during crater collapse. At D >30 km, the primary impact crater no longer exists and the "crater" is essentially "flat". These data suggested that larger craters on Europa form in an unusually weak layer, one that may be underlain by liquid water [1, 4]. Modeling of this collapse by Turtle and Ivanov [5, and this workshop] suggests that the liquid layer may be at least 20 km deep [4]. Although dependent on our limited understanding of impact crater formation and modification processes [5], These data provide an independent and relatively

robust constraint on the thickness of Europa's ice shell.

Conclusions. Impact morphology on the icy Galilean satellites provides important lessons for Titan. Comparison to relatively well understood bodies will be important for understanding any large impact features observed on Titan. Crater depths will be important to determine, as well as mapping of interior landforms and ejecta deposits.

References: [1] Moore et al. (1998) Icarus, 135, 127-145. Moore et al., (2001) Icarus, 151, 93-111. [2] Schenk, P., and F. Ridolfi, (2002) Geophys. Res. Lett. 29, 12, 31. [3] Schenk, P., Chapman, C., Zahnle, K., and J. Moore, (2004) Ages and Interiors, in Jupiter, Cambridge U. Press, in press. [4] Schenk, P. (2002), Nature, 417, 419-421. [5] Turtle, E., and B. Ivanov, (2002) Lunar Planet. Sci. XXXIII, abstract no. 1431.

Figure 1. Portion of high-resolution mosaic and stereo DEM (color-coding) of interior and rim of Mananan, Europa. Flow-like features are indicated by arrows.

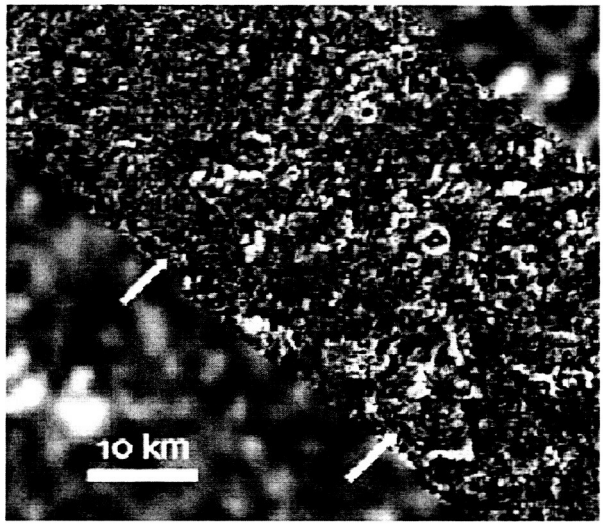

Figure 2. Portion of high-resolution mosaic across Epigeus, Ganymede. Arrows indicate radial flow-like features.

SINKING TO NEW LOWS & RISING TO NEW HEIGHTS: THE TOPOGRAPHY OF EUROPA.
Paul M. Schenk, Lunar and Planetary Institute, Houston, TX 77058 (schenk@lpi.usra.edu).

"Neither can the weak ice support high mountains. Topography is at most a few hundred meters high."

Introduction: The perception of a "flat" Europa dates to Voyager days, when terminator images showed little relief except ridges and a few knobs [1]. While ridges rarely exceed such heights, Galileo has shown that topography on longer scales (kilometers to 100's of km) is decidedly variable. Topographic measurements of selected features have been reported [e.g., 2-4] but no systematic description or appraisal of Europa's topography has been attempted, until now.

Topography of a planet is one of its most fundamental characteristics (witness the Mars revolution wrought by MOLA), and is a direct expression of the response of the lithosphere to external and internal forces. The resulting topographic expression is in turn directly related to the properties of that lithosphere, and this is especially true in the case of a floating ice shell.

Tools: Tools for the production of 2-dimensional topographic maps (DEM's) are stereogrammetry (3D) and 2-D photoclinometry (PC). These tools have been described elsewhere [e.g., 4]: here I focus on the advantages and limitations of each technique. Stereo DEMs can be treated as rigid plates, except for linear mosaics where "bending" of the mosaic and resulting DEM can occur if image registration is not done with care. As there is no global topographic net for Europa tied to the center of mass, all DEM's "float" with respect to the true surface, but a reasonable approximation to the true tilt can be had by proper image registration. Stereo DEM registration is also limited to no better than 3 times worse than the lowest resolution image in the stereo pair. PC can achieve full pixel DEM resolution but accumulated errors and uncertainties degrade the reliability of measurements at length-scales of more than 50 pixels or so. Use of low-phase angle images to model local albedo partially reduces this problem. We are fortunate that on Europa many PC sites are coincident with stereo coverage, which I use to control long-wavelength deviations in the PC, while preserving high-resolution fidelity.

Topographic mapping coverage is highly variable in quality and decidedly limited (perhaps the most significant loss due to the LGA failure). Vertical precision ranging from 5 to 50 meters. Stereo coverage, including untargetted stereo pairs, is available for <2% of the surface (except for low resolution coverage of ~15%). PC mapping is more extensive (~20%), with pixel resolution ranging from 10 m to 1.4 km.

Often only one or two examples of a geologic feature or terrain type are available. Thus the observed properties of one example may not necessarily be representative of all such features. Even when we can characterize a given feature, because imaging coverage is so limited, topographic mapping often does not extend far from the target features. Knowledge of the regional topographic characteristics can be very important for the interpretation of some features, and these limitations must be acknowledged.

Focus on the Dark Spot:. A few features on Europa were targeted for multiple observations, allowing for detailed topographic mapping at various scales. One of these, Castalia Macula (aka., The Dark Spot) is revealed as a broad depression 350 m deep [5], sandwiched between two large domical rises, the largest of which is fault-bounded and rises a whoppin' 900 m, for total relief of 1250 m. Dark material is mostly confined to this depression, although some patches lie on the domes. Remnant ridges are preserved on the dark floor, such that if due to volcanism, dark material burial was not deep.

Other negative topographic expressions include pits typically 10-20 km across, and up to 400 m deep. Irregular and curved troughs can be 500 m deep (and in one case >1 km deep! These may constrain the shell to no less than 6 km thickness [6].

Focus on Chaos: Conamara is by far the best studied site on Europa. Stereo coverage of Conamara is possible at 4 different scales: 180 m (regional), 180 m (medium-resolution swath), 55m, and 9 m. Low-sun PC topography is coincident with the first 3 of these, providing controlled full resolution pixel-scale mapping of all Conamara at 180 m, and selected higher resolution patches of the interior.

The matrix component of Conamara Chaos is

generally elevated 200-300 m above surrounding plains, but is also variable by a similar amount [7]. Highest elevations are correlated with areas dominated by matrix. Locally, older blocks can be 200-300 m high (effectively doubling block thickness estimates [2]). Some blocks, however, are lower than matrix only a few km away, suggesting that matrix was rather viscous as blocks were rotated.

Several other chaos sites were observed in stereo. Some chaos units are elevated above surrounding terrains, others are not, suggesting that chaos evolution is complex or can respond to post emplacement modification. Lenticulae (oval chaos-textured domes) also appear to be variable in elevation. Several have been observed in excess of 150 m local relief, placing tight constraints on convection dynamics [8]. Others have no positive topographic expression. In several instances, moats form within chaos or lenticulae along their border with ridged plains. Although elevated and variable relief for chaos and lenticulae tends to favor a diapiric origin [7], these data provide key constraints for any model of chaos origin.

Having an Impact: Impact crater morphology is discussed in detail elsewhere, but the few large impact craters identified are important as they penetrate deeply into the shell. Initial and subsequent Galileo observations [2, 11] show that most craters <8 km across are similar to Ganymedean craters, but that larger craters are shallower. The observed changes in morphology suggest that larger craters are penetrating into unusually soft material, and may sense the ocean. Inferred depths to the ocean are on the order of 20 km [2]. High resolution topography (vertical precision ~15 m) is available only for Manannan. Here, mappable melt deposits are correlated with isolated depressions, but most of the floor is rugged and probably comprised of uplift disrupted crust.

Learning to Relax: The icy shell also responds to vertical or horizontal stresses. Evidence for folding has been found at a few locations [9], but limited topographic coverage prevents a global search. However, stereo mapping several of these sites indicates amplitudes of 200-300 meters. One site reaches at least 1 km amplitude but its origin as folding is uncertain. These broad undulations are difficult to characterize with current data.

Evidence for flexure due to surface loads is found at double ridges [e.g., 10]. Using bent-plate models, the shape of the bending can be used to constrain elastic plate thickness. Flexure associated with an elevated rise has also been suggested near the crater Cilix [3]. Analysis of the topographic form suggests a thick shell, but the lack of regional topographic mapping precludes confirmation that this is truly flexure and not regional warping. Ridge and band topography will also examined.

Regional Characteristics: Of 15 stereo sites analyzed to date, only 4 have total relief of less than 500 meters. None off these sites are greater than 300 km across, however. Larger areas can be mapped using PC but the long-wavelength characteristics are not reliable, and global coverage is incomplete. Nonetheless, provinces of distinct topographic characteristics are obvious. Mottled terrain is the most rugged. Ridged plains have variable relief but at longer wavelengths, with pits and domes predominating in some areas, absent in others. These patterns suggest that internal dynamics within the shell has strong regional control.

Despite the limitations, the topographic variability of Europa is much greater than expected, and the total dynamic range may approach 2 km. Large vertical fault movements of 300-500 m (and as high as 900m) are also not uncommon. The impression is of a lithosphere that is able to support large variations in topography, at least as great as those on Ganymede. These variations in relief are not consistent with a shell only a few kilometers thick, but more analyses are required to quantify this conclusion with confidence.

References: [1] Lucchitta, B., and L. Soderblom, in Satellites of Jupiter, 1982. [2] Williams, K., and R. Greeley, GRL, 25, 4273, 1998. [3] Nimmo, F., B. Giese, and R. Pappalardo, GRL, 29, 5, 1233, 2003. [4] Schenk, Nature, 417, 41, 2002. [5] Prockter, L., and P. Schenk, manuscript in preparation. [6] Schenk, P., and W. McKinnon, LPSC XXXIII, 2002. [7] Schenk, P., and R. Pappalardo, Jupiter Conf. (abstract), 2001. [8] Showman, A., and L. Han, LPSC XXIV, 2003. [9] Prockter, L., and R. Pappalardo, Science, 289, 941, 2000. [10] Billing, S., and S. Kattenhorn., LPSC XXXIII, 2002. [11] Moore, J., et al., Icarus, 151, 93, 2001.

THERMAL EVOLUTION OF EUROPA'S ICY CRUST C. Sotin[1], G. Choblet[1], J.W. Head[2], A. Mocquet[1] and G. Tobie[1], [1]Universite de Nantes, 2 rue de la Houssiniere, BP 92208, 44322 Nantes, France, sotin@chimie.univ-nantes.fr, [2]Department of geological sciences, Brown university, 02912 Providence, RI, USA.

Introduction: The Galileo mission revealed that Europa is a differentiated body with surface features including domes, faults and chaotic terrains suggesting the presence of an ocean in between the icy surface and the silicate core. The presence of domes suggests some forms of upwelling (thermal or/and chemical) linked to heat transfer by subsolidus convection in Europa's icy crust. This situation makes Europa a very appealing place for exobiology because life may develop at the interface between the deep water and the silicate core. For the last 5 years, we have developed models of Europa's internal structure and have obtained the following results :

- tidal forces produce very small amount of heat in the silicate layer and very large amount of heat in an ice shell close to its melting temperature [1].
- tidal heating varies in time, latitude and longitude resulting in strongly time dependent convection [2].
- tidal heating in the ice layer is large enough to prevent a complete freezing of the ocean without invoking the presence of ammonia [2].
- although tidal heating is an internal heating source, hot icy plumes can form at the interface with the ocean due to the strong temperature dependence of ice viscosity [3].
- For viscosities in agreement with those measured on terrestrial glaciers, tidal heating may heat up hot plumes leading to partial melting, which may explain the formation of chaotic terrains [4].
- Doppler shift measurements on a Europa orbiter should allow us to determine the presence of an ocean and to constrain the thickness of the ice crust [5]

Thermal convection models: The models use temperature-dependent viscosity for the ice and include viscosity dependent tidal heating. There has been some discussion about the viscous behavior of ice at stresses relevant to thermal convection models. One major issue is the stress exponent one must use. Figure 1 shows how viscosity varies as a function of differential stress : the lower the stress, the smaller the stress exponent. Thermal convection stresses are smaller than 10 kPa and deformation measurements of polar glaciers[6] suggest that below 10 kPa, ice behaves like a Newtonian material. The viscosity of ice at its melting point is on the order of 10^{14} Pa.s with upper and lower bounds equal to 10^{15} Pa.s and 10^{13} Pa.s, respectively.

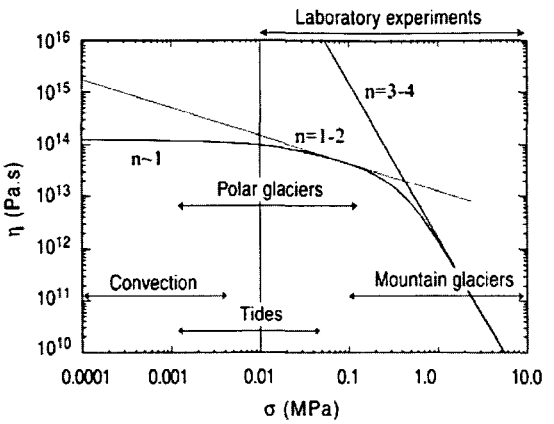

Figure 1 : viscosity versus differential stress at temperature close to melting temperature. The stress domain of different processes is indicated. The larger the stress, the larger the stress exponent.

The dynamics of convection is controlled by instabilities that form at the water-ice interface. These instabilities are time-dependent. The amount of heat, which can be removed from the base of the ice-crust, depends on the amount of internal (tidal) heating (Figure 2). An equilibrium is obtained for a thickness of 20 km for reasonable parameters of radiogenic heating in the silicate core and ice viscosity. One must note that the surface heat flux does not depend on the amount of tidal heating because it is controlled primarily by the viscous characteristics of the ice, which drive the instabilities in the conductive lid regime.

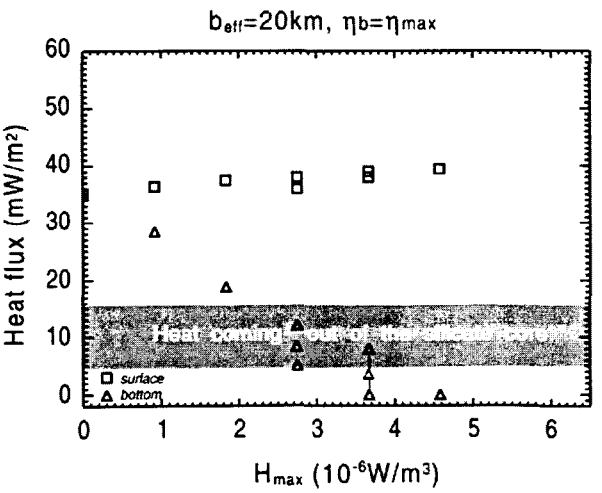

Figure 2 : Surface heat-flux versus tidal heating.

Tidal heating: Tidal heating is computed assuming that the material behaves like a Maxwell solid. If the viscosity of the material is larger than the Maxwell viscosity (ratio of shear modulus by orbital frequency), then tidal heating is negligible. Taking the present time values of the orbital parameters for Europa, the Maxwell viscosity is 3 10^{15} Pa.s and 1.5 10^{14} Pa.s for silicates and ice, respectively. Because the viscosity of partially molten silicates is at least 10^{18} Pa.s (value of mantle viscosity at mid-oceanic spreading centers), the amount of tidal heating deposited in the silicate core is likely to be negligible compare to radiogenic heating rate. On the other hand, the viscosity of ice close to its melting point is on the order of the Maxwell viscosity. Consequently, tidal heating is a major source of internal heating in the ice shell (Figure 3).

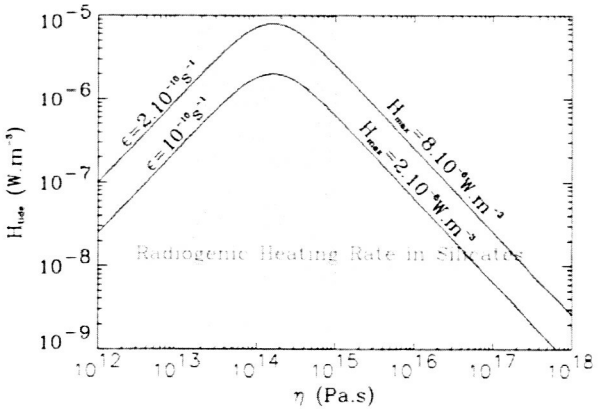

Figure 3 : Tidal heating in the ice shell versus viscosity. The radiogenic heating rate per unit volume is represented for comparison.

For viscosities in between 10^{13} and 10^{15} Pa.s, the amount of tidal heating is 2 orders of magnitude larger than heating produced by the decay of long-lived radiogenic elements in the silicate core. As it can be seen on Figure 2, an equilibrium thickness of 20 km is obtained if a value of 3 10^{-6} W/m3 is used according to Figure 3. When the radiogenic heating rate was larger, the equilibrium thickness was smaller. A large range of parameters is investigated in Tobie et al., 2003 [2].

Because tidal heating depends on latitude and longitude, the equilibrium thickness may vary from place to place [7]. In the model described in Figure 4, it is found that the thickness varies between 17 km at the poles up to 29 km at the equator at the sub-jovian and anti-jovian points. The depth of any given isotherm varies also. For example, the 200 K isotherm, which is sometimes the one used for the definition of the lithosphere, varies from 13 km deep at the poles to 9 km deep at the equator. Variations of the lithosphere thickness may have implications on surface tectonics.

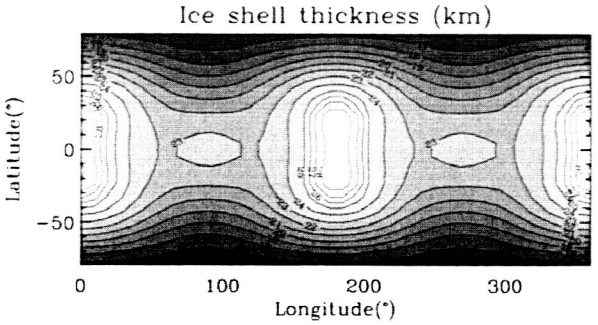

Figure 4 : Variations of the equilibrium thickness for a mean value of 22 km.

Another result of these models is that tidal heating may lead to melting in the upwelling plumes [4]. Because the density of water is larger than that of ice, subsidence may result in the formation of chaotic regions. The formation of partial melt is predicted if the ice viscosity at its melting point is equal to 10^{14} Pa.s, a value in agreement with available data (Fig. 1).

Conclusion and perspectives : The present study confirms that tidal heating plays a major role in the thermal history and dynamics of Europa. However, several problems remain. For example the topography of domes is difficult to explain due to the very thick conductive lid overlying the convective ice shell. In a companion paper (Tobie et al.), we investigate the interaction between the convective shell and the brittle elastic outer shell using damage rheology.

Although the results of Galileo and theoretical studies such as this one strongly suggest the presence of an ocean, one must admit that there is no direct measurement that such an ocean exists. An orbiter around Europa could achieve this goal and put constraints on the thickness of the ice crust.

References:

[1] Tobie et al. (submitted), *Icarus* [2] Tobie et al. (in press), *JGR*. [3] Deschamps F. and Sotin C. (2000) *JGR, 90,* 1151–1154. [4] Sotin C. et al. (2002) *GRL., 32,* A74. [5] Castillo et al. (2000) *C.R.A.S., 90,* 1151–1154. [6] Montagnat and Duval (2000) *EPSL*, 183, 179-186 [7] Ojakangas G.W. and D.J. Stevenson (1989), *Icarus*, 81, 220-241.

THERMAL PROPERTIES OF EUROPA'S ICE SHELL. J. R. Spencer[1], [1]Lowell Observatory, 1400 W. Mars Hill Rd., Flagstaff, AZ 86001, spencer@lowell.edu.

I will review our current knowledge of surface and subsurface temperatures on Europa. Daytime and nighttime surface temperatures have been extensively mapped by the Galileo Photopolarimeter-Radiometer (PPR) instrument, and vary between 130 and 80 K at low latitudes. Nighttime temperatures show complex and poorly-understood spatial variations, including a remarkable temperature minimum centered on and parallel to the equator on the leading hemisphere. Comparison with daytime temperatures indicates that these patterns are controlled by spatial variations in thermal inertia rather than by warming of the surface by endogenic heat, but the cause of the thermal inertia variations is not understood.

The amplitude of the diurnal temperature variations is matched with a thermal inertia of about 5×10^4 erg cm^{-2} $s^{-1/2}$ K^{-1}, fifty times lower than the value for solid ice, indicating that much of the uppermost few centimeters of Europa's surface has high porosity and thus low thermal conductivity. Daytime temperatures are high enough that significant sublimation of H_2O ice is likely on geological timescales, leading to thermal segregation of ice into high-albedo patches that are colder than the average surface.

Less is known about subsurface temperatures in Europa's ice shell, though it is likely that there is an upper conducting layer, with a steep thermal gradient, overlying a lower convecting layer that is almost isothermal at temperatures slightly below the melting temperature of the ice.

Localized endogenic resurfacing may produce long-lived passive or active anomalies in surface temperature, providing a promising technique for detecting regions of recent resurfacing from Europa orbit. No such anomalies were definitively identified in the Galileo PPR data, however.

CONSTRAINTS ON THE OPENING RATE OF BANDS ON EUROPA. M. M. Stempel, A. C. Barr, R. T. Pappalardo. Laboratory for Atmospheric and Space Physics (LASP), University of Colorado at Boulder, Campus Box 392, Boulder CO, 80309-0392 (stempel@colorado.edu).

Introduction: The opening rates of two bands on Europa, inferred to be sites of spreading of the icy lithosphere, are constrained based on a mid-ocean-ridge analog model. Estimates of brittle-ductile transition depth combined with a conductive cooling model limit active band lifetimes to 0.24 - 35 Myr and strain rates of $8.1 \times 10^{-13} - 8.2 \times 10^{-15}$ s^{-1}. These values suggest tensile strengths for ice on Europa of 0.46 – 2.3 MPa, consistent with nonsynchronous rotation as the dominant driving mechanism for band opening.

Background. Europa exhibits varied surface morphology, including long linear features of a variety of types and a range of widths [1, 2]. The most narrow (~500 m) linear features are troughs. Double ridges are ridge pairs ~2-5 km wide with an axial trough. The widest linear features are bands up to 25 km across, some of which are inferred to be sites of separation and spreading of the icy lithosphere [3, 4, 5]. It is inferred that troughs develop to form ridges, which in turn can develop into bands [6].

Bands themselves are not all alike: some appear to be a complex interweaving of double ridges, some are relatively smooth, and some express both characteristics [7]. *Prockter et al.* [8] examined several Europan bands and ascertained a continuum of morphologies, interpreted to perhaps represent varying rates of spreading. Fast spreading rates may create smooth bands, whereas slower spreading rates might produce features analogous to that of mid-ocean-ridge (MOR) spreading on Earth, where extensional stresses produce block faults, in turn straddling a neovolcanic zone adjacent to the central trough.

Two bands are explored in this study, Yelland and Ino Lineae, are both located at approximately -16 latitude and 196 longitude, where Yelland crosscuts Ino. Both display a prominent axial trough straddled by a hummocky zone, in turn flanked by subparallel ridges and troughs with clearly defined boundaries against the surrounding terrain. These morphologies may be indicative of "slow-spreading" bands [8], where extension and faulting occur slowly enough for the icy lithosphere to cool and fault as opening proceeds, in contrast to smooth "fast-spreading" bands which may open too rapidly for lithospheric cooling to support internal band deformation.

Given the width of the hummocky zone and the width of fault blocks within a band, a simple lithospheric cooling model can be used to constrain the band opening rate. From the inferred spreading rate and width of a band, its active lifetime can be estimated and driving mechanisms inferred.

The Model: MOR spreading on Earth can be modeled as instantaneous cooling of the oceanic lithosphere in a semi-infinite half-space, with the surface held at a constant temperature [12]. This model is useful as an analog to band spreading on Europa, where analogous tectonic features are observed [8].

In the MOR cooling model, isotherms, including that describing the brittle-ductile transition (BDT) temperature, fall off like the square root of distance from the spreading center. The cooling model is coupled to a description of the BDT isotherm, and self-consistent values for the BDT temperature and the spreading rate of the bands are constrained. Measured parameters are average observed fault block width x_b, the width w from the central trough to the edge of the band, and the width from the central trough to the edge of the hummocky zone x_L. The distance x_L is measured from the axial trough to the first high albedo lineation. Block width x_b is the average distance between lineations. Estimates of fault block width-to-depth ratios provide a range of possible depths of faulting y_l, assumed to equal the local BDT depth.

Although the MOR model defines the depth at the spreading center as zero, in reality a thin shell of brittle material would exist in the vicinity. Solving the heat equation for both conduction and advection, and assuming the system is in steady state, the minimum depth of this thin shell is on order 10 m, which is much less than the relevant dimentions of Yelland Linea: x_L = 700 m, x_b = 350 m, w = 3600 m. Measured dimentions of Ino Lineae are of similar orders of magnitude: x_L = 860 m, x_b = 530 m, w = 7800 m. Thus, our MOR model provides a sufficient first-order representation of the shape and depth of the BDT isotherm.

For a cooling oceanic lithosphere in an infinite half space, the relationship between depth y_l, horizontal distance x_L from a spreading center, and half spreading rate u can be expressed as

$$u = [\ x_L\,(2\ \mathrm{erfinv}\,(\,(T_{BDT} - T_s)\,/\,(T_w - T_s)\,)\ /\,y_L)^2\ ] \quad (1)$$

[12] where erfinv is the inverse error function, T_{BDT} is the temperature at the BDT, T_s is the surface temperature (which we take as 110 K for Europa), T_w is the temperature of the ductile ice (260 K), and is thermal

diffusivity (1×10^{-6} m^2 s^{-1} for ice). The half spreading rate is used to obtain the strain rate $\dot{\varepsilon} = u/x_L$.

A "Byerlee's law" for ice [13] describes the strength of the brittle lithosphere as $\sigma = \sigma_1 - \sigma_3$, where σ_1 is greatest compressional stress (lithostatic in the extensional case: $\sigma_1 = \rho g y_L$), σ_3 is least compressive stress (here horizontal: $\sigma_3 = \sigma_1 / \{ 2 [(\mu^2 + 1)^{1/2} + \mu] + 1 \}$), μ is the coefficient of internal friction (0.69 [13]), ρ is density of ice (920 kg m^{-3}), and g is gravitational acceleration for Europa (1.3 m s^{-2}). To describe the strength of the lower ductile lithosphere, we adopt the flow law for ice creep in the grain boundary sliding regime [14]:

$$\dot{\varepsilon} = ((\sigma_1 - \sigma_3)^p / A)^{1/n} \exp (Q / (n R T_{BDT})) \quad (2)$$

where d is grain size (assumed to be 1 mm), p, A, and n are experimentally determined constants (1.4, 3.9 x 10^{-3} [need to include the bizarre-looking units of A], and 1.8 respectively), Q is the activation energy for creep (49 kJ mol^{-1}), and R is the gas constant. The BDT occurs at a depth where the brittle and ductile failure strengths are equal:

$$T_{BDT} = Q \{ n R \ln [(\sigma_1 - \sigma_3) ((\dot{\varepsilon}_{dot} d^p) / A)^{1/n}] \}^{-1}. \quad (3)$$

For each band, we solve iteratively for T_{BDT} and u, for a variety of fault block width-to-depth ratios. We choose 1/10 as a reasonable lower limit, and 1/2 as an upper limit based correspondence to the upper limit for reasonable T_{BDT} of 190 K [15].

Results: Estimates of BDT depth combined with a conductive cooling model limit active band lifetimes to 0.24 - 35 Myr and strain rates of 8.1 x 10^{-13} – 8.2 x 10^{-15} s^{-1} (see figure). These ranges correspond to half-spreading rates between 22 and 0.22 mm yr^{-1}.

The above values also suggest tensile strengths for ice on Europa of 0.46 – 2.3 MPa (= ($\rho g y_L$) / 3). These stress levels are consistent with nonsynchronous rotation as the dominant driving mechanism for band opening [2].

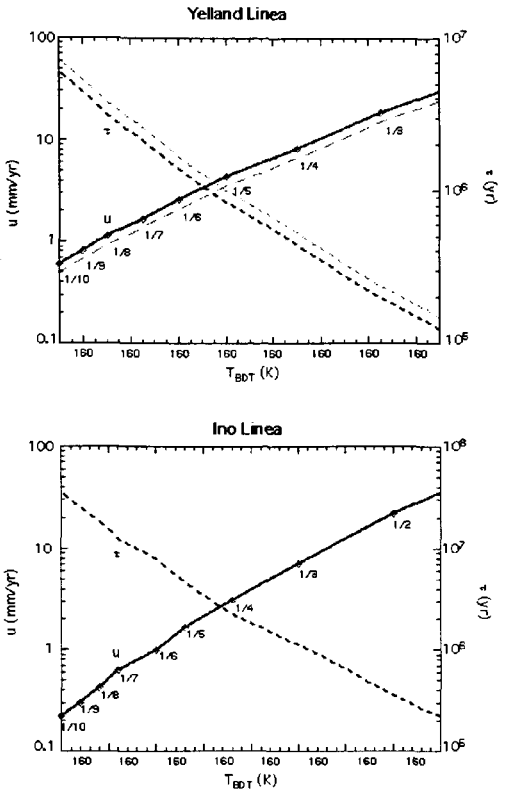

Figure 1: Half spreading rate u and active lifetime are plotted versus T_{BDT} for Yelland and Ino Lineae. The relationship changes with the width-to-depth ratio of fault blocks, as labeled along the curves. The lighter dashed lines in the plot for Yelland Linea are the model results when using x_L = 580 m [as per 8].

References: [1] Greeley R. et al. (1998b) *Icarus* 135, 4-24. [2] Greeley R. et al. (submitted) *Geology of Europa*, in Jupiter: The Planet, Satellites & Magnetosphere (F. Bagenal et al., eds.), Cambridge Univ. Press, in press. [3] Schenk P. M. and W. B. McKinnon (1989) *Icarus* 79, 75-100. [4] Sullivan et al. (1998) *Nature* 391, 371-372. [5] Tufts B. R. et al. (2000) *Icarus* 146, 75-97. [6] Pappalardo R. T. et al. (1999) *JGR* 104, 24015-24055. [7] Figueredo P. H. and R. Greeley (2000) *JGR* 105, 22629-22646. [8] Prockter L. M. et al. (2002) *JGR* 107, (4-1) - (4-25). [9] Turtle and Pierazzo (2002) *Science* 294, 1326-1328. [10] Shenck P. M. (2002) *Nature* 417, 419-421. [11] Pappalardo and Head 2001 [12] Turcotte D. L. and G. Schubert (2002) Geodynamics, 2nd ed., 153-159. [13] Beeman M. et al. (1988) *JGR* 93, 7625-7633. [14] Goldsby D. L. and D. L. Kohlstedt (2001) *JGR* 106, 11017-11030. [15] Nimmo F. et al. (2002) *GRL* 29, (62-1) - (62-4).

Acknowledgements: Support for this work is provided by NASA Planetary Geology and Geophysics grant NAG5-11616.

INTERACTION BETWEEN THE CONVECTIVE SUBLAYER AND THE COLD FRACTURED SURFACE OF EUROPA'S ICE SHELL. G. Tobie[1,2], G. Choblet[2], J. Lunine[1] and C. Sotin[2] [1]Lunar and Planeary Laboratory, (1629 University Bvld, Tucson, AZ; e-mail: gtobie@lpl.arizona.edu),[2] Laboratoire de Planetologie et Geodynamique (2, rue de la houssiniere, 44322 NANTES cedex, France).

Introduction: As it travels around Jupiter on a synchronous orbit, Europa is subjected to periodic deformation due to its high orbital eccentricity (e=1%). The tidal response of its ice shell is almost uniquely controlled by the radial displacement of the underlying ocean [1]. At the base of the ice shell, ice, close to its melting point behaves like a viscoelastic medium, whereas the elastic/brittle response progressively dominates when the cold surface is approached.

Tidal stress field and brittle failure: The periodic radial displacement of the ocean induces a large tidal flexing of the ice shell. The resulting stress field would be responsible for the highly fractured appearance of Europa's surface. Usually, tidal stress is computed assuming the superficial ice shell is elastic. From the elastic response, one can show that the brittle strength of ice is exceeded at the surface of Europa [e.g., 2, 3, 4]. The downward propagation of cracks initiated at the surface is more problematic. Experimentally, the brittle and ductile domains of a material are defined from change in stress-strain curve behaviors. The transition between the two domains occurs at the train rate $\dot{e}_t$ where the brittle stress σ_b is equal to the ductile strength σ_d. Several factors can modify this transition, notably temperature, grain size, confined pressure [5].

On Europa, tidal forcing imposed in the ice shell strain rates of 10^{-10}-$2.10^{-10}.s^{-1}$, depending mainly on longitude, [6, 7]. Near the surface where the temperature is far from the melting point value, the brittle strength σ_b is weaker than the viscous strength σ_d at these strain rates, whereas $\sigma_b > \sigma_d$ toward the base of the layer. As mentionned above, the exact transition depth between the brittle layer and the ductile one depends on several parameters and on the type of crack mechanism. The lateral variations of the strain rate and of the temperature at the surface ($\dot{e}_t = 2.10^{-10}.s^{-1}$ and T_{surf}= 50K at the poles, $\dot{e}_t = 10^{-10}.s^{-1}$ and T_{surf}= 110K at the equator) modify the depth transition to some extent.

Crack nucleation and propagation are firstly limited by confined pressure, which avoids fault propagation to depth more than 1km for the elastic tidal stress value (~0.1MPa). However, the existence of cracks in the upper icy crust would modify significantly the stress field compared to the elastic case, amplifying locally the magnitude of stress. This would help the crack nucleation and propagation deeper in the ice shell.

Furthermore, the periodic forcing creates progressive fatigue of the icy material, which modifies its brittle strength [5, 6]. Simultaneously, tidal friction along activated fault creates a heat source elevating locally the temperature of the ice and making it more ductile.

Thermal convection and ductile creep: The low viscosity of ice near its melting point (~10^{13}-10^{14} Pa.s) creates large dissipation in the bottom part of the layer and can initiate convective instabilities for ice thickness as thin as 10 km. Once thermal convection occurs, almost half of the bottom part of the layer becomes dissipative. The high power dissipated by body tide in the ice shell is thus able to prevent the freezing of the ocean even if the layer is convecting. For its current eccentricity, tidal dissipation in the silicate mantle is probably negligible, and the ice layer is stabilized to a thickness of about 20-30 km [8,9]. The ice shell thus consists of an isothermal convective sublayer overlaid by a thick rigid conductive lid of around 5-10 km.

Tidal heating in the ice shell is so high that it raises the temperature in hot plumes up to the melting point temperature. This creates episodic upwelling of partially molten ice up to the base of the conductive lid [8]. The ascent of warm ice would add supplementary stress and then help the formation of fractured zone. Reciprocally, the existence of fractured zone would help the rise of partially molten ice near the surface.

Toward a self-consitent model - preliminary results: Modeling the dynamics of Europa's ice shell from the ocean to the surface required the inclusion of tidal heating due to viscous dissipation, fault formation, strain localization and heating resulting from friction along faults, and partial melting in a self-consistent way. The model developement is based on the 2D thermal convection model described in [9]. At a first attempt, we model the fractured zone in the conductive lid using simple damage parameterization. We suppose that the local viscosity of ice depends on temperature T, on partial melting x_m, and on a parameter d characterizing the degree of ice damage:

$$\eta(x,z)=\eta_0 \exp(-\gamma_T T) \exp(-\gamma_m x_m) \exp(-\gamma_d d), \quad (1)$$

η_o being the viscosity of pure ice near its melting. Tidal heating is computing directly from the effective viscosity field [8]:

$$H_{tide}(x,z)=2\, H_{max}/(\eta_{max}/\eta + \eta / \eta_{max}), \qquad (2)$$

where H_{max} *is the maximum dissipation value that occurs for viscosity equal to* $\eta_{max} = \mu/\omega = 1.5\text{x}10^{14}$ Pa.s on Europa (μ =3.3x10^9 Pa, w=2.10^{-5} rad.s^{-1}).

For the example presented on Figure 1, we suppose a constant distribution of damage d localized in the conductive lid, at x=20km. This simulates a zone of weakness in the rigid lid extending from the surface down to a depth of 5 km. At the middle of this zone (x=20 km), the parameter d is equal to 1 and it decreases exponentially on both sides. In this weakness zone, the effective viscosity is reduced by a factor of 10. The fall of the effective viscosity increases locally the amount of tidal heating and favors the rise of warm ice up to shallow depths (< 2 km) (Figure 1). The rise of this hot plume increases locally the heat flux up to about 100-150 mW.m^{-2}. It also generates locally an upward stress of around 0.1 MPa, inducing a bump of around 50m magnitude.

This preliminary result indicates the importance of tidal strain localization in the conductive lid on convective instabilities, and the strong mechanical and thermal coupling that exists between tidal deformation and thermal convection. We are currently incorporating these different aspects in our numerical model in order to better understand the link between the convective instabilites in the icy layer and the highly fractured surface of Europa.

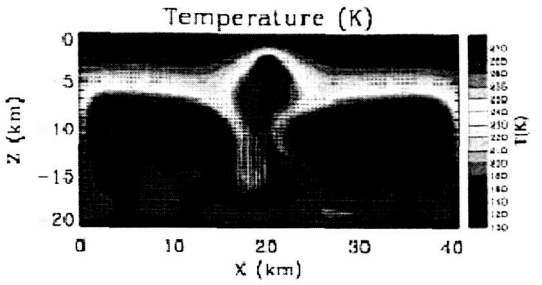

Figure 1: Temperature field obtained with our 2D thermal convection model including a weakness zone in the conductive lid and viscosity dependent tidal heating. (model parameter: Ra=6.10^6, $\Delta\eta$ =1.2x10^6, h0=3.75x10^{13} Pa.s, b=20 km)

References:

[1] Tobie G., Mocquet A. and Sotin C. (2003a) Icarus, submitted. [2] Helfenstein and Parmentier (1983) Icarus, 53, 415-430. [3] Greenberg et al. (1998) Icarus, 135, 64-78. [4] Schulson (2002), J. Geophys. Res., 107, 17-1. [5] Schulson (2001), Eng. Frac. Mech., 68, 1839-1887. [6] Weber and Nixon (1997) Cold Reg. Sci. Tech., 26, 153-164. [7] Ojakangas and Stevenson (1989), Icarus, 81, 220-241. [8] Tobie G., Choblet G. and C. Sotin (2003), J. Geophys. Res., in press. [9] Hussmann H. et al. (2002) Icarus, 156, 143-151.

WHAT EUROPA'S IMPACT CRATERS REVEAL: RESULTS OF NUMERICAL SIMULATIONS.

E. P. Turtle[1,2], [1]Lunar and Planetary Lab., Univ. of Arizona, Tucson, AZ, 85721-0092; turtle@lpl.arizona.edu, [2]Planetary Science Institute, 1700 E. Fort Lowell, Suite 106, Tucson, AZ, 85719-2395; turtle@psi.edu.

Introduction: Europa's surface is only lightly cratered; 28 primary impact structures larger than 4 km in diameter have been identified [1]. Nonetheless, the craters span a wide range of sizes (up to ~50 km diameter) and exhibit morphologies similar to those observed on other planets, following a progression generally correlated with crater size [1-3]. Primary craters less than ~5 km in diameter, have the bowl shape typical of simple craters. Craters ~5-24 km in diameter have flat floors and several have central peaks [1-4], characteristics typical of complex craters, although Europa's craters tend to be shallower [1-3]. Two larger impact structures, Tegid and Taliesin, appear to have unusual morphologies, but have been imaged only at low resolution and so are poorly understood. The two largest impact structures, Callanish and Tyre, consist of disrupted centers ringed by numerous concentric graben with diameters of up to 100 km.

The morphology of a crater is influenced by the energy of the impact event (related to crater size) as well as by the gravity, material properties and near-surface structure of the target. So, the characteristics of impact craters can be used to infer information about the target. For example, the diameter of the simple-to-complex transition depends upon the strength of the target material [*e.g.*, 5]; Europa's anomalously shallow craters [1-3] may be a result of the collapse process itself under Europan conditions or of post-impact viscous relaxation; and the concentric fractures around the two largest impact structures may have formed as a result of Europa's near-surface structure [*e.g.*, 6]. Therefore, careful study of craters can reveal much about the nature of Europa's near-surface.

One approach to investigating the constraints that the observed crater morphologies put on Europa's near-surface structure is to use numerical methods (*e.g.*, hydrocode and finite-element modeling) to simulate impact cratering under Europan conditions. By reproducing the observed crater morphologies it is possible to constrain the near-surface structure and conditions.

Several discrete lines of evidence [*e.g.*, 7-10] suggest that Europa's icy surface is but a thin shell overlying a liquid water ocean. Although the total thickness of Europa's outer H_2O layer is constrained by gravity measurements to be 80-170 km [11], estimates for the thickness of the solid ice range from only a few [*e.g.*, 12-15] to a few tens of kilometers [*e.g.*, 16-18].

Although Europan complex craters are shallow, they otherwise resemble complex craters found elsewhere in the solar system; their central peaks are morphologically similar to those observed on other planets. Therefore, the simplest explanation is that they formed by the same mechanism. In lunar and terrestrial craters central peaks consist of deeply buried material that was uplifted during crater formation [19,20]. Therefore, their occurrence on Europa requires that the ice shell not be breached during crater formation. So, numerical simulations of impact cratering in ice layers of various thicknesses overlying liquid water can provide constraints on the thickness of Europa's ice shell.

Modeling impact-induced melting and vaporization: Turtle and Pierazzo [4] conducted hydrocode simulations of vapor and melt production during impacts into ice layers with various thicknesses and thermal gradients overlying liquid water; complete vaporization or melting penetrating to liquid water or warm ice would preclude the formation and preservation of central peaks, therefore these models can constrain the thickness of Europa's crust. Turtle and Pierazzo [4] simulated impacts that would produce transient craters with diameters of ~12 and ~21 km (Fig. 1), lower limits for the transient crater diameters predicted for Europa's largest central peak crater (Pwyll) and the multiple-ring craters, respectively [1]. Their simulations demonstrated that at the times and locations of complex crater formation on Europa, the cold ice layer had to exceed 3-4 km [4]. Impacts disrupt target material well beyond the zone of partial melting [*e.g.*, 5], so these simulations put a lower limit on the thickness of the ice.

Modeling crater collapse: Turtle and Ivanov [21] conducted hydrocode simulations of the excavation and collapse of 10-km-diameter transient craters (within the range expected for Europa's central peak craters [1]) in ice layers 5-11 km thick with linear thermal gradients. They found a strong dependence of crater morphology on ice thickness (Fig. 2). For ice less than ~8 km thick, liquid water penetrated to the surface as the transient crater collapsed, precluding central peak formation. Therefore, these simulations provided a lower limit for the thickness of the Europan ice at the times and locations of central peak crater formation. To prevent craters from penetrating to an ocean, the ice shell thickness must be comparable to of greater than the transient crater diameter: 10-15 km thick. This range is consistent with Schenk's [2] results based on the diameters at which Europa's craters are observed to undergo morphologic transitions.

Conclusions: Numerical modeling of impact cratering is a powerful tool for constraining the prop-

erties of Europa's near-surface. Further modeling to investigate the later stages of cratering, including the formation of rings around Callanish and Tyre, as well as longer term modification due to viscous creep is currently underway and promises to reveal yet more information about Europa's near-surface.

References: [1] Moore J.M. *et al.* (2001) *Icarus, 151*, 93-111. [2] Schenk P.M. (2002) *Nature, 417*, 419-421. [3] Schenk P.M. *et al.* (2003) in *Jupiter: Planet, Satellites and Magnetosphere*, F. Bagenal *et al.*, Eds., Cambridge Univ. Press, in press. [4] Turtle E.P. and Pierazzo E. (2001) *Science, 294*, 1326-1328. [5] Melosh H.J. (1982) *JGR, 87*, 371-380. [6] Melosh H.J. and McKinnon W.B. (1978) *GRL, 5*, 985-988. [7] Ojakangas G.W. and Stevenson D.J. (1989) *Icarus, 81*, 220-241. [8] Carr M.H. *et al.* (1998) *Nature, 391*, 363-365. [9] Geissler P.E. *et al.* (1998) *Nature, 391*, 368-370. [10] Kivelson M.G. *et al.* (2000) *Science, 289*, 1340-1343. [11] Anderson J.D. *et al.* (1998) *Science, 281*, 2019-2022. [12] Hoppa G.V. *et al.* (1999) *Science, 285*, 1899. [13] Greenberg R. *et al.* (2000) *JGR, 105*, 17551-17562. [14] Geissler P.E. *et al.* (2001) *LPSC, XXXII*, #2068. [15] O'Brien D.P. *et al.* (2002) *Icarus, 156*, 152-161. [16] Rathbun J.A. *et al.* (1998) *GRL, 25*, 4157-4160. [17] Pappalardo R.T. *et al.* (1999) *JGR, 104*, 24015-24055. [18] Prockter L.M. and Pappalardo R.T. (2000) *Science, 289*, 941. [19] Grieve R.A.F. *et al.* (1981) in *Multiring Basins*, P.H. Schultz, R.B. Merrill, Eds., *Proc. Lunar Planet. Sci. Conf., 12A*, 37-57. [20] Pieters C.M. (1982) *Science, 215*, 59-61. [21] Turtle E.P. and Ivanov B.A., (2002) *LPSC, XXXIII*, #1431.

Fig. 1: Melting and vaporization [from 4] in large (A, B, C) and small craters (D, E, F) in: 9 km of ice over liquid water (A, D); 5 km of ice over liquid water (B, E); and a 3 km thick conductive lid over convecting ice (C, F). Solid, dotted, and dashed lines circumscribe the regions of complete vaporization, complete melting, and 50% melting.

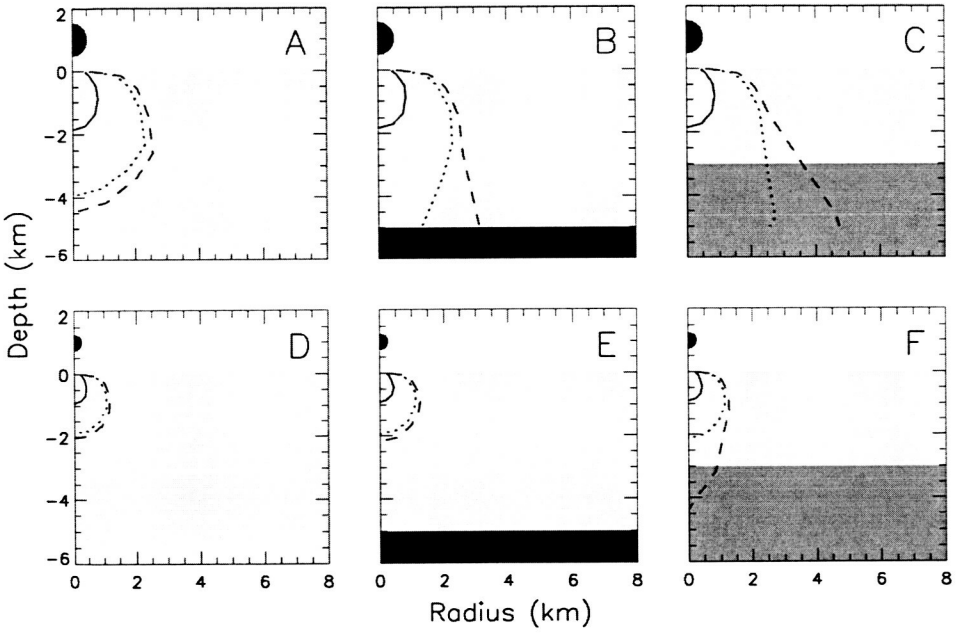

Fig. 2: Cross-sections of the final stages of simulations of impacts in ice 5, 6, 7, 8, 9, and 11 km thick (from upper left to lower right) illustrating penetration of water to the surface during crater collapse in ice ≤7 km thick [from 21].

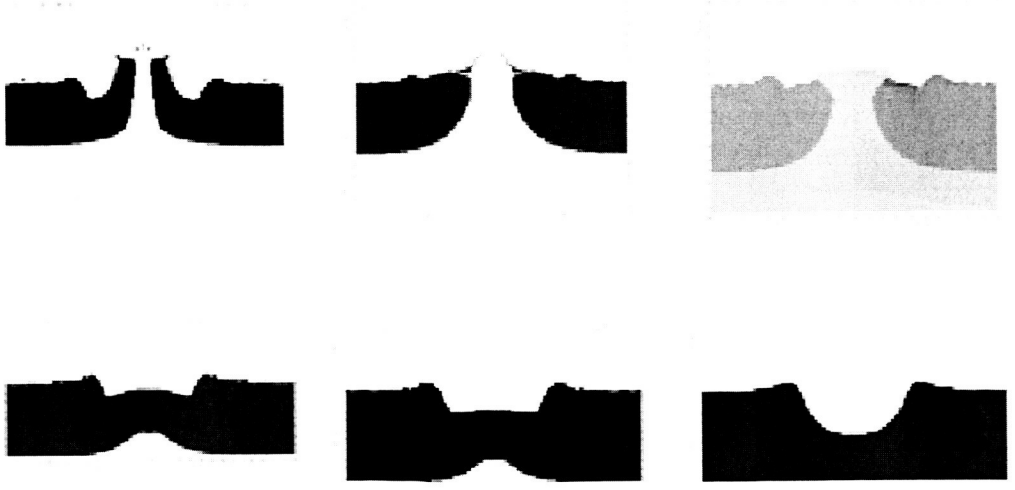

SUBSURFACE ACTION IN EUROPA'S OCEAN. [1]S. D. Vance, [1]J. M. Brown, [2]T. Spohn and [3]E. Shock, [1]NASA Astrobiology Institute, University of Washington, Seattle, svance@ess.washington.edu, [2]Institut für Planetologie, Münster, Germany, Chemistry Department, University of Arizona

Subsurface processes may have created observed surface features on Europa's ice. A key question is whether plumes originating from the rocky crust can reach the surface. Kimura and Kurita [1] treat a mechanically created plume while Thompson and Delaney [2] look at buoyancy and circulation after such a plume has formed. In addition to the obvious aspect of mechanical driving forces for fluid motion, the issue is intimately linked to composition, relative salinity, and heat distribution throughout the ocean. Since publication of [1] and [2], Hussman and Spohn have assessed tidal heating and dissipation in a more thorough manner. We tested the accuracy of chemical models in accounting for pressure effects and find supcrt92 sufficient for pressures in Europa's ocean (max 2000 atm) for predicting sulfate volumes at 50 °C while FREZCHEM has yet to incorporate pressure effects. The recent discovery of peridotite hydrothermal opens the possibility that a marriage of tidal and compositional effects may bears further activity in Europa's ocean.

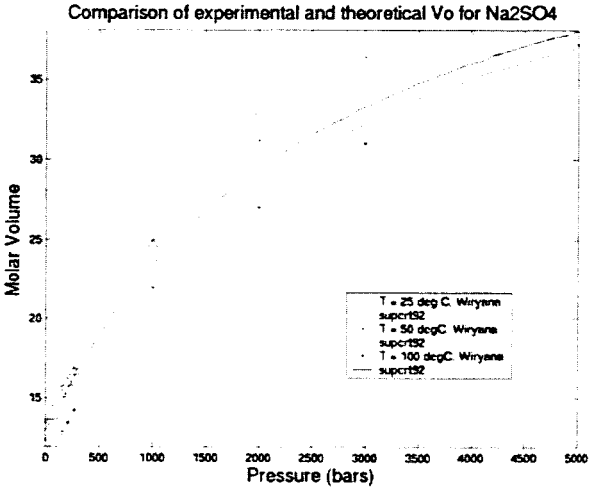

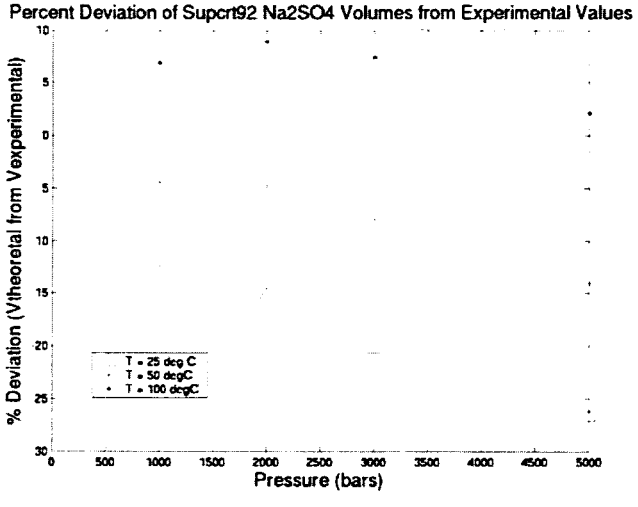

Figures 1 and 2: Volume change of a pure water sample with addition of an infinitesimal amount of Na_2SO_4. Points represent experimental data from present authors. Plotted curves are comparison of predicted values from supcrt92. Figure 2 shows that there is less than 5% deviation at 50 °C up to a pressure of 2000 atm.

If peridotite was exposed in Europa's early days, hydrothermal systems certainly existed. Non-synchronous rotation of the europan crust may keep fresh peridotite exposed, leaving the possibility that such activity persists to the current time.

References: [1] Kimura, J. and Kurita, K. (2002) LPS XXXIII, Abstract #1492. [2] Thomson R.E. and Delaney J.R. (2001) JGR, 106, 12,355-12,365. [3] Hussman, H. (2003) Dissertation Thesis, Institut für Planetologie, University of Münster.

PHYSICAL BASIS FOR THE RADAR OBSERVATION OF GEOLOGICAL STRUCTURE IN THE ICE SHELL ON EUROPA. D.P. Winebrenner[1], D.D. Blankenship[2], B.A. Campbell[3], [1]University of Washington, Applied Physics Laboratory and Department of Earth and Space Sciences, Box 355640, Seattle, WA 98195 USA, dpw@apl.washington.edu, [2]Institute for Geophysics, University of Texas, Austin, TX 78759 USA, blank@ig.utexas.edu, [3]Center for Earth and Planetary Studies, Smithsonian Institution, Washington, DC 20560 USA, Campbellb@nasm.si.edu.

Introduction: Radar sounding of Europa has been discussed primarily as a means to measure the depth of a prospective ice/ocean interface [e.g. 1-4]. On terrestrial ice sheets, however, radar sounding commonly maps internal structure associated with compositional and structural horizons, i.e., by radar-reflective stratigraphic boundaries (depth variations of which encode information about ice dynamics and climate history).

Several types of radar-reflecting horizons other than an ice/ocean interface may occur on Europa [2-4]. In particular, where temperature varies in the transition between cold, brittle (impure) ice and warm, convecting ice, sharp dielectric contrasts will occur where temperatures pass through eutectic points of the impurities, thus creating a reflecting boundary [5]. Relict diapirs in cold (no-longer-convecting) ice [6], as well as buried crater floors [7], would differ sharply from surrounding ice in their bulk density and impurity content, thus also creating dielectric boundaries. Intermittent eruptions of low-viscosity material can create compositional, and thus dielectric, stratification wth depth. Finally, faults may be marked by discontinuities in density or crystallographic structure, which also translate to dielectric variations.

Understanding the surface expression of geological structure will be improved by tracking stratigraphic boundaries in the near-subsurface. Radar mapping of such boundaries may prove to be as important as the knowledge of ice thickness for understanding any interchange between the Europan surface and an underlying ocean.

These considerations motivate our examination of the dielectric properties of impure ice (Ih) at the low temperatures characteristic of Europa (75 to perhaps 250 K). We examine dielectric propertiesas function of temperature and of the concentrations of geologically plausible, dielectrically significant impurities. The latter include especially acid [8], chloride [2], subeutectic hydrated salts [1,2,9], and chondritic soils [1]. We focus initially on the effective conductivity, both because this property is fundamental to estimating how deeply radar can probe and because terrestrial experience suggests that conductivity variations may be the primary sources of reflection beneath the (poorly known [7]) annealing depth on Europa.

Effective Conductivity Due to Acid and Chloride Impurities: The effective conductivity of ice with ionic impurities, at typical radar sounding frequencies (tens of MHz), consists of a sum of contributions from resonances at much lower frequencies. The net effect at small impurity concentrations is a linear dependence of effective conductivity on each separate concentration, with coefficients, i.e., molar conductivities, which depend on temperature differently for each impurity via an Arrhenius relationship [2,10]. The dependence for a given impurity is smooth except at the eutectic temperature for that impurity – at the eutectic, the coefficient decreases abruptly with decreasing temperature, by a factor of 2-5 [3].

Figure 1 shows replotted data for molar conductivities of the two most dielectrically effective impurities, acid and chloride, assembled from various sources by Moore and Fujita [10]. The chloride data span two cases, one in which concentrations were below that where macroscopic brine pockets appear in the ice, the other above; they therefore bracket the range of possibilities at a given temperature. Also shown in figure 1 are extrapolations to Europan temperatures based on the pertinent Arrhenius relationship, with parameters determined by a fit to the data. The extrapolations are upper bounds on the true molar conductivities because the data from which they result were all acquired above the respective eutectics.

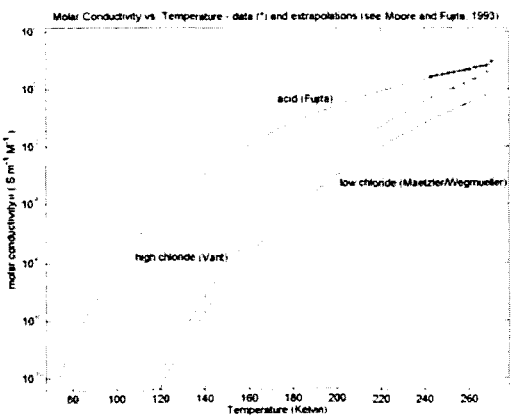

Figure 1. Semi-log plot of molar conductivity in Siemens per meter per mole versus temperature, according to tabulated data [8] and extrapolation. Data points are again denoted by asterisks, theoretical curves by solid lines. Legends on theoretical curves indicate first authors of papers in which the original data were presented.

The extrapolations indicate conductivities many orders of magnitude lower than those that occur in terrestrial ice environments. The required extrapolation far outside the range of observations, however, points up the need for new, low-temperature measurements [c.f., 1].

Effective Conductivity Due to Sub-Eutectic Salts or Chondritic Soils: Effective conductivities due to lunar or chondritic soil and to hydrated, sub-eutectic salts are much less well-known that those for ionic impurities. However, the synthesis of observations and empirical relations by Chyba et al. [1] strongly indicates that losses due to such impurities dominate those of ionic impurities at low temperatures, and that solid salt and soil impurities are roughly equivalent in their dielectric effects (see also [2]). Figure 2 shows one-way attenuation in dB/km for a radar sounding frequency of 50 MHz, and for effective conductivities derived as follows. For ionic impurities, we assumed, for purposes of illustration, equal volumetric concentrations of 300 micromoles per liter – concentrations close to or below those at which macroscopic brine or acid pockets appear. The acid and chloride curves in figure 2 are thus simply rescaled version of those in figure 1. For soil/salt impurities, we have tentatively adopted the density and empirical relations given by Chyba et al. [1] and assumed a volumetric concentration of impuritiesof1%.

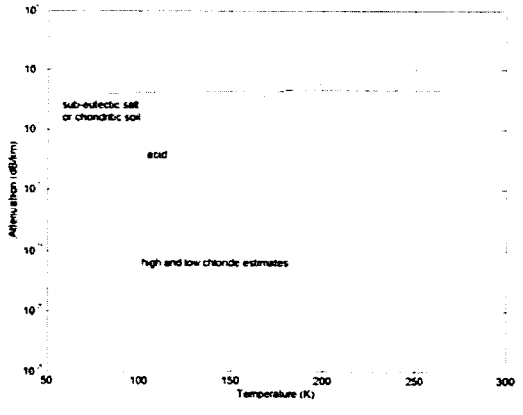

Figure 2. Semi-log plot of attenuation, in dB/km for various impurity species, using the fits in figure 1 with ionic species concentrations of 300 micromoles per liter, and the parameters and relations of Chyba et al. [1], assuming a volumetric impurity concentration of 1%.

The very low temperature sensitivity of conductivity in soil/salt impurities leads to their complete dominance of total dielectric loss at temperatures below ~180 K. While the relations given here must be regarded as very significantly uncertain, reversal of this latter conclusion would require that they be incorrect by many orders of magnitude.

Discussion: The computations in figures 1 and 2 must be regarded as significantly uncertain, given the range of extrapolation and scattered data on which they are based [1-3]. Our first conclusion is therefore that new observations are needed to narrow this uncertainty. However, even with the uncertainty, it seems clear that: (1) soil/salt impurities will dominate 50 MHz absorption at temperatures below about 180 K, which translates to more than half of the non-convecting ice thickness; (2) at higher temperatures, acid impurities quickly become dominant; (3) compostional radar horizons within upper half of the non-convecting ice will likely be caused by abrupt changes in soil or salt concentrations, the latter possibly derived from surface lag deposits – we will estimate the strength of such radar horizons based on the calculations presented here; and (5) because absorption is so low, we must consider limits on penetration depth due to scattering processes, both those due to stratication itself (i.e., 1-D inhomogeneities) and those due to scattering from 3-dimensional inhomogeneities and structure.

References:

[1] Chyba, C.F., Ostro, S.J., and Edwards, B.C., *Icarus 134,* 292-302. [2] Blankenship et al. (1999) University of Texas Institute of Geophysics, *Report No. 184.* [3] Moore, J.C. (2000) *Icarus 147,* 292-300. [4] Blankenship et al. (2001) *LPSC XXXII,* abstract 1854. [5] Matsuoka, T., Fujita, S., and Mae, S. (1997) *J. Phys. Chem. B 101,* 6219-6222. [6] Pappalardo, R. et al. (1998) *Nature 391,* 365-368. [7] Ostro, S.J., and E.M. Shoemaker. (1990) *Icarus 85,* 335-345. [8] Carlson, R.W, Johnson, R.E, and Anderson, M.S. (1999) *Science (286),* 97-99. [9] McCord, T. et al. (1998) *Science 280,* 1242-1245. [10] Moore, J.C., and Fujita, S. (1993) *JGR 98,* 9767-9780.

A HIGHLY MINIATURISED LASER ABLATION TIME–OF–FLIGHT MASS SPECTROMETER FOR PLANETARY EXPLORATION. Peter Wurz, Urs Rohner, and James A. Whitby, Physics Institute, University of Bern, Sidlerstrasse 5, CH-3012 Bern, Switzerland (email: peter.wurz@phim.unibe.ch).

Introduction: We report the development and testing of two highly miniaturised mass spectrometers intended to be deployed on an airless planetary surface to measure the elemental and isotopic composition of solids. We designed and built two instruments, a larger unit for use on a fixed landing spacecraft and a smaller unit intended for use in a small mobile platform roving on a planetary surface. Both instruments were designed and built with the intention for implementation in the Mercury Surface Element (MSE) of the proposed BepiColombo mission to the planet Mercury [1], either in the landing spacecraft itself or on the rover. Both mass spectrometers are time-of-flight instruments using ion mirrors to increase the ion path length and increase the mass resolution by time-focussing.

Laser Ion Source: The ion sources for these mass spectrometers utilise in both cases a laser induced plasma, which is directly coupled into the mass analyser. When using a time-of-flight spectrometer the use of a pulsed laser is obvious and we histogram many individual spectra to obtain a mass spectrum with high dynamic range. For example, by accumulating 10'000 spectra (which can be done in about 1 s with our system) a mass spectrum with a dynamic range exceeding six decades can be obtained in principle, and at least five decades in an real instrument. Laser ablation gives high spatial resolution and potentially depth resolution [2], and avoids the need for sample preparation [3]. Laser ablation and ionisation is a common method in the laboratory for mass spectroscopic analysis of surfaces [4]. Once a critical power density of approximately 10^9 W/cm^2 is exceeded during the laser pulse the ionisation of released surface material is more or less independent of the element, i.e., minimal inter-element fractionation in the ionisation process occurs [4, 5]. We use a commercial passively Q-switched Nd:YAG laser system, either with the fundamental wavelength of 1064 nm or the second harmonic at 532 nm. Once available, we will test operation with the higher harmonic wavelengths as well before we decide what to use in the flight application. Of course, with a suitable laser system our mass spectrometers can be operated as laser desorption instruments for chemical analysis of the surface and possibly even as MALDI system given that the sample preparation can be realised with robotic means.

Lander Instrument: The instrument for the landing spacecraft is a simple time-of-flight instrument using a grid-less reflectron as ion mirror. The ions removed from the target surface are accelerated into the mass spectrometer through a small hole and focussed through a narrow tunnel in the centre of the detector toward the reflectron. The ions pass the time-of-flight tube and are reflected by the ion mirror back onto the MCP detector. Mass resolution is typically $m/\Delta m$ = 600 FWHM. The resolution can be adjusted ion-optically; a higher mass resolution can be set at the expense of ion-optical transmission and vice-versa. The total dimension of the instrument, as displayed in Figure 1, is 120 mm x Ø60 mm. The flight instrument will be somewhat taller since the laser electronics will be accommodated in a compartment above the ion mirror. The anticipated weight of the flight unit would be about 500 g including all electronics [6].

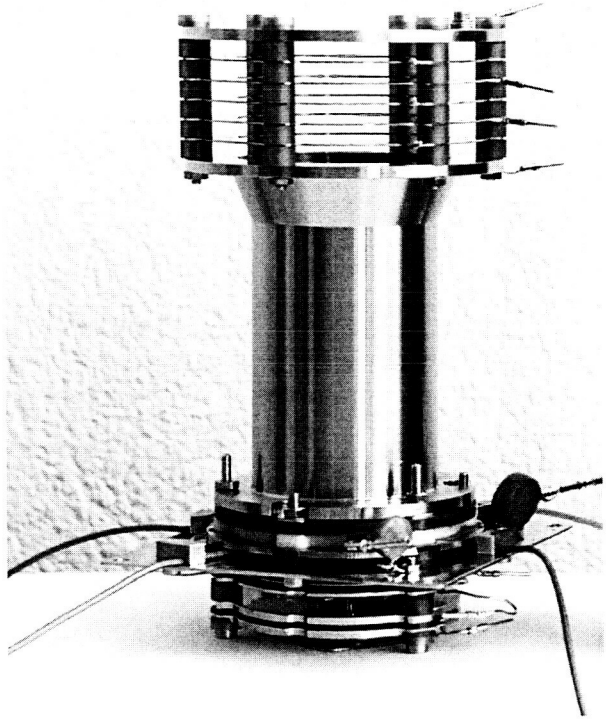

Figure 1: LMS Prototype for the landing spacecraft [6]: Topmost is the reflectron built from a set of potential rings, in the centre is the actual flight tube with the MCP detector below; further down are the ion optical elements for collecting and focussing the ions removed from the investigated surface.

Rover Instrument: The instrument for the rover is also of the time-of-flight type, but using a novel combination of an electrostatic analyser and grid-less reflectron [7]. The time-of-flight path is folded two times to make it sufficiently long for decent mass analysis. The prototype instrument, as shown in Figure 2, has a demonstrated mass resolution m/Δm in excess of 180 (FWHM) and a predicted dynamic range of better than five orders of magnitude. The ion-optical system itself has a mass resolution of 400, as seen from single shot spectra, which is in good agreement with the ion-optical design. As with all time-of-flight instruments, covering a large mass range is not a problem here and elements from hydrogen up uranium have been detected with this instrument. When aiming for the detection chemical compounds of higher mass we have to improve the mass resolution during routine operations to the single-shot value, which is about the theoretical limit of an instrument of that size. We estimate that a flight instrument would have a mass of 280 g (including laser and all electronics) and a total volume of 7 x 4 x 3 cm^3 including all electronics. For full operation only 3 W power will be needed making use of local energy storage to accommodate the short-term power needs of the laser system.

References: [1] Balogh, A., M. Bird, L. Blomberg, P. Bochsler, J.-L. Bougeret, J. Brückner, L. Iess, J. Guest, Y. Langevin, A. Milani, J.-A. Sauvaud, W. Schmidt, T. Spohn, R. von Steiger, N. Thomas, K. Torkar, H. Wänke and P. Wurz, BepiColombo - An interdisciplinary cornerstone mission to the planet Mercury. ESA-SCI(2000)1, Noordwijk, The Netherlands, European Space Agency (2000). [2] J.A. Whitby, U. Rohner, W. Benz, and P. Wurz, "A laser-ablation mass spectrometer for the surface of Mercury," proceedings of the 34th Lunar and Planetary Science Conference, March 17–21, (2003), abstract no.1624. [3] J.S. Becker, and H.-J. Dietze, State-of-the-art in inorganice mass spectrometry for analysis of high-purity materials, Int. J. Mass Spectr. 228 (2003) 127–150. [4] A.Vertes, R. Gijbels, and F. Adams, "Laser Ionisation Mass Analysis" (1993) Wiley, New York. [5] W.B. Brinckerhoff, , G.G. Managadze, R.W. McEntire, A.F. Cheng and W.J. Green, "Laser time-of-flight mass spectrometry for space." *Rev. Sci. Instr.* 71(2), (2000) 536–545. [6] U. Rohner, J. Whitby, and P. Wurz, "A miniature laser ablation time-of-flight mass spectrometer for in situ planetary exploration," *Meas. Sci. Technol.*, 14 (2003), 2159–2164. [7] U. Rohner, J.A. Whitby, P. Wurz, and S. Barabash, A highly miniaturised laser ablation time–of–flight mass spectrometer for a planetary rover, *Rev. Sci. Instr.* (2003) submitted.

Acknowledgement The authors are grateful to J. Fischer, H. Mischler and J. Jost with their teams for their contributions in the areas of design, fabrication and electronics, respectively. The Swiss National Science Foundation supported this work.

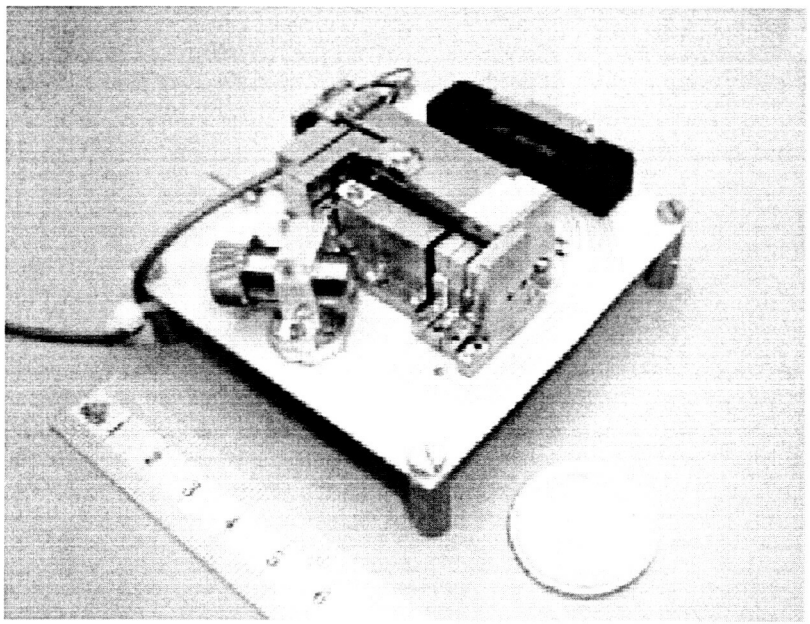

Figure 2: LMS prototype for the planetary rover [7]. In the foreground is the lens holder for focusing the laser radiation onto the sample. The sample will be placed in front of the spectrometer, at the small hole. The ruler is in cm.

CRATERING RATES IN THE JOVIAN SYSTEM. K. Zahnle[1], P. Schenk[2], L. Dones[3] and H. Levison[3] [1]NASA Ames Research Center (MS 245-3 Moffett Field CA 94035), [2]LPI, [3]SWRI.

We use several independent constraints on the number of ecliptic comets to estimate impact cratering rates on the Jupiter moons. The impact rate on Jupiter by 1.5-km diameter ecliptic comets is currently $\dot{N}(d>1.5\text{km}) = 0.005^{+0.006}_{-0.003}$ per annum [1]. Asteroids and long period comets are currently unimportant. The size-number distribution of ecliptic comets smaller than 20 km is inferred from size-number distributions of impact craters on Europa, Ganymede, and Triton. For comets bigger than 50 km we use the size-number distribution of Kuiper Belt Objects.

Figure 1 gives the overview of the impact rate at Jupiter in general and at Europa in particular [1]. These impact rates imply cratering rates on Europa of 0.5 per Ma per 10^6 km^2 for impact craters bigger than 1 km, and of 0.015 per Ma per 10^6 km^2 for impact craters bigger than 20 km. The latter corresponds to an average recurrence time of 2.2 Ma for 20 km craters. The best current estimates for the number of 20 km craters on Europa appear to range between about twelve to thirty. This implies that the average age of Europa's surface is between 30 and 70 Ma. The average density of craters with diameter greater than 1 km on well-mapped swaths on Europa is 30 per 10^6 km^2. The corresponding nominal surface age would be 60 Ma. These two estimates are not truly independent because we have used size-number distribution of the Europan craters to help generate the size-number distribution of comets. The uncertainty of the best estimate—call it 42 Ma for specificity—is at least a factor of 3.

Discussion: By placing a heavy weight on the historical record of close encounters with Jupiter we favor generally high impact rates, especially for comets larger than a few km diameter. But we also conclude that comets smaller than a km or so are relatively rare at Jupiter, and hence that small primary craters (smaller than 10 km or so) are produced less frequently than one might expect.

Among the questions addressed by our study, the depletion of small comets and whether this depletion is characteristic of the Kuiper Belt source seems most worth additional discussion.

The Kuiper Belt size-number distribution allows us to exploit the observed number of Centaurs as a constraint on the number of ecliptic comets, provided that are free to interpolate the slope between 20 and 50 km. It is an imperfect solution because the source of the ecliptic comets—the "scattered disk"—is a dynamical subset of the Kuiper Belt as more generally defined, and because the size-number distribution of Kuiper Belt objects smaller than 50 km is currently at the edge of knowledge. Indeed, the authors of the deepest survey to date have suggested that the size-number distribution in the Kuiper Belt turns over for objects smaller than 50 km [2] (their best fitting curve is shown on Fig 1). The slope of the deduced size-number distribution seems to be in conflict with that set by the Ganymedean craters, but it is premature to draw any conclusions as of yet—observational astronomy has a long history of underestimating what has not yet been seen.

At the other end of the size spectrum, sub-kilometer comets are going missing at Jupiter. This parallels the depletion of small comets seen in the historical record of comet discovery in the inner solar system [3]. Missing sub-km comets in the inner solar system could be explained by their absence in the Kuiper Belt, by disintegration (true loss), or by extinction (becoming asteroids). Missing craters on Europa and Ganymede show that extinction is relatively unimportant. The existential question is harder to address. Abundant small craters on Triton imply that at Neptune the comets may be a collisional population rich in small bodies, but it is unclear whether the craters on Triton are of heliocentric (i.e. intruders from outside the Neptune system) or planetocentric (internal to the Neptune system, perhaps generated by a moon's disruption) origin.

There is an older view that the Kuiper Belt must have been collisionally evolved at its current location. The argument presumes that Pluto and Quaoar etc. were formed where they are now. Given this presumption, it can be shown that disk surface densities two or three orders of magnitude higher than they are now are needed to make worlds as big as Pluto and Quaoar in a reasonable amount of time [4]. Such a thick swarm of bodies inevitably generates a lot of debris. If thereafter the Kuiper Belt evolved in a way that preserved the size-number distribution, small KBOs would now be abundant. If all the ifs are granted—if we accept formation of large bodies in place, no preferential loss of small bodies, and if the classical Kuiper Belt is the source of ecliptic comets—then the absence of small comets at Jupiter poses a problem. To solve this problem would then require that most small comets vanish before they reach Jupiter, and perhaps even before they reach Neptune. Near Jupiter one might ask whether CO2 or NH3 vaporization could be disruptive; at greater distances one might ask the same of CO, N2, or CH4. Comets are known to contain volatiles that can erupt beyond Saturn. Chiron is known to have been active at 13 AU and P/Halley had an outburst at 14 AU.

A second possibility is that in the course of losing the greater part of its primordial mass the Kuiper Belt shed its smaller comets preferentially. How this might have happened is open to speculation, but the presence of gas would seem the most hopeful option. Perhaps smaller fragments were carried off with the gas, or spiralled into the inner solar system because of gas drag, leaving only the larger bodies in place. Given that more than 99% of the big objects are also lost if Pluto formed *in situ,* a bit of mass fractionation is not unreasonable.

A third choice (not necessarily inconsistent with the second) is to suggest that the larger bodies in the Kuiper Belt formed nearer the Sun, in rough analogy to how Neptune and Uranus may have formed in the vicinity of Jupiter and Saturn, only later to be scattered to greater distances [5,6]. Such a model directly accounts for the low mass of the Kuiper Belt and the rarity of Pluto-class objects [6]. Migration obviates the need for *in situ* collisional evolution in the Kuiper Belt, and so no large population of small comets need form at the Kuiper Belt's distance in the first place. The model is therefore agnostic with respect to small comets. We note that, in this model, whether a planetesimal joins the classical cold Kuiper Belt or the dynamically hot scattered disk becomes a matter of chance rather than a fate strongly tied to place of origin.

REFERENCES

[1] Zahnle et al (2003), *Icarus 163,* 263. [2] Bernstein et al (1988) *A.J. 93,* 13776. [3] Shoemaker & Wolfe (1982) *Moons of Jupiter* D. Morrison, Ed., Univ. Ariz. Press, 277. [4] Stern S.A. (1995) *A.J. 110,* 856; Kenyon S. (2002) *P.A.S.P. 114,* 265. [5] Thommes, E. et al. (2002) *A.J. 123,* 2862. [6] Gomes (2003) *Icarus 161,* 404; Levison & Morbidelli, *Nature* 2003.

Figure caption. Data points refer to various estimates of the impact rate at Jupiter, with the exception of the Centaurs, which scales from the impact rate at Saturn [1]. Generous error bars are reminders that uncertainties are large. The labeled intermittent curves give the slopes of the size-frequency distributions as obtained from craters on Europa and Ganymede, and from the observed populations of Kuiper Belt objects (plotted through the Centaurs). The curve labeled "Bernstein et al" [2] gives a different observational account of the Kuiper Belt size distribution. Also shown are current impact rates on Jupiter by Trojan asteroids and nearly isotropic comets (NICs; these include Halley-type comets and Long Period comets). The "Trojans" is a lower limit because it considers only dynamical loss from the L4 and L5 swarms; if collisional losses are important the impact rate at Jupiter is increased proportionately.

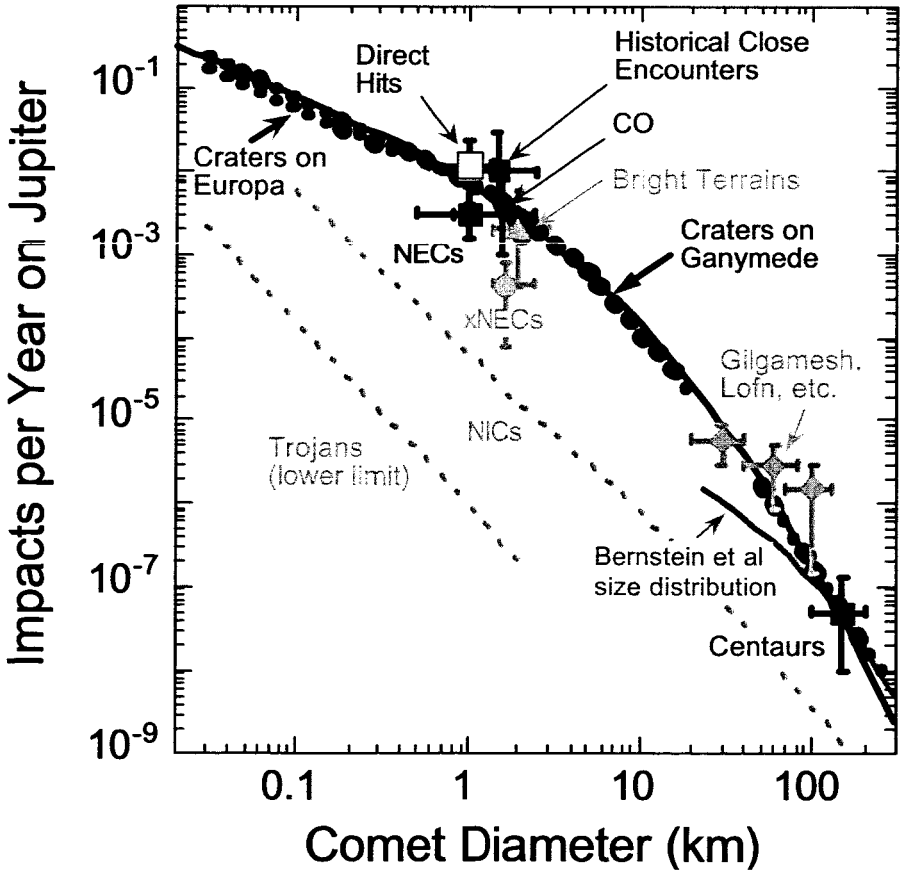

BRINE POCKETS IN THE ICY SHELL ON EUROPA: DISTRIBUTION, CHEMISTRY, AND HABITABILITY. M. Yu. Zolotov[1], E. L. Shock[1,2], A. C. Barr[3], and R. T. Pappalardo[3]. [1]Department of Geological Sciences, [2]Department of Chemistry and Biochemistry, Arizona State University, Tempe, AZ 85287. [3]Laboratory for Atmospheric and Space Physics, University of Colorado, Boulder, CO 80309. E-mail: zolotov@asu.edu.

Introduction: On Earth, sea ice is rich in brine, salt, and gas inclusions that form through capturing of seawater during ice formation [1, 2]. Cooling of the ice over time leads to sequential freezing of captured seawater, precipitation of salts, exsolution of gases, and formation of brine channels and pockets. Distribution and composition of brines in sea ice depend on the rate of ice formation, vertical temperature gradient, and the age of the ice. With aging, the abundance of brine pockets decreases through downward migration. Despite low temperatures and elevated salinities, brines in sea ice provide a habitat for photosynthetic and chemosynthetic organisms [1-3].

On Europa, brine pockets and channels could exist in the icy shell that may be from a few km to a few tens of km thick [4,5] and is probably underlain by a water ocean [4,6]. If the icy shell is relatively thick, convection could develop, affecting the temperature pattern in the ice [7-9]. To predict the distribution and chemistry of brine pockets in the icy shell we have combined numerical models of the temperature distribution within a convecting shell [8,9], a model for oceanic chemistry [10], and a model for freezing of Europan oceanic water [10]. Possible effects of brine and gas inclusions on ice rheology and tectonics are discussed.

Modeling: Brine composition is modeled in the framework of temperature distributions within a convective icy shell 20 km thick. The temperature field is calculated using the numerical finite element model Citcom [11] with a Newtonian rheology for ice I and neglecting the effects of tidal heating inside the shell. We use a Reyleigh number of 3.3×10^6, which is calculated using a melting point viscosity at the base of the icy shell of 5×10^{13} Pa s, appropriate to the temperature at the base of an icy shell of 272.85 K. The surface of the shell is held at a constant temperature of 100 K, consistent with Galileo data [12] and earlier models [13], and the oceanic temperature is derived from our chemical model [10]. We neglect the effect of pressure on the temperature of freezing, which is only ~2° at the depth of 20 km at ~24 MPa. Note that results will change as a more accurate representation of the rheology of ice (i.e., non-Newtonian) is implemented in the convection model.

The calculated distribution of temperature is used to evaluate chemical composition of brine pockets with the FREZCHEM 5.2 program (written by Giles Marion), which uses the Pitzer model for activities of solutes and water activity [e.g., 14]. At each temperature and bulk composition of the Mg-Na-Ca-K-SO_4-Cl-H_2O system, concentrations and activities of ions and water were calculated together with amounts of brines, precipitated salts, and ice. Slow convection rates obtained in the physical modeling (see next section) make the equilibrium chemical model highly applicable.

Results: Modeling with the Citcom code shows that the icy shell is slowly (~10^{-9} m s^{-1}) convecting with the exception of the upper 3-7 km where T < 215 K and a "stagnant lid" is formed. Below this "lid", the shell is mixed in ~10^5 years, and the swiftly convecting interior is mixed in ~10^3 years. In central parts of convecting cells, temperature variations are small and T > ~260 K, as shown in Fig. 1. The eutectic temperature of 237 K for the chosen chemical system (see [10]) is shown by the red isothermal curve. In upwelling parts of convective cells, that eutectic temperature represents conditions of complete freezing. In downwellings, it is the temperature at which brines form. The smallest depth of brine existence at 5.8 km corresponds to upwelling. Salinities of brine pockets are in the range of 200-240 g/kg H_2O in the central parts of convective cells (Fig. 2). Typically, the pockets contain only 5-0.5 % of the initially captured water (Fig. 3). Concentrations of ions increase as temperature decreases, as can be seen for Cl^- in Fig. 4. However, the composition of brines is different from that of the oceanic water owing to precipitation or dissolution of salts. For example, brines in the upper part of convective cells have an elevated Cl^-/SO_4^{2-} ratio (Fig. 5). Major salts precipitated from brines are hydrated sulfates of Ca, Na, and Mg, and chlorides of Na and K.

Discussion: *Gas inclusions.* Expelling of distilled gases from growing ice crystals and lowering water activity in brines with decreasing temperature can lead to resolution of gases (e.g., CO_2) that were dissolved in oceanic water. In addition, precipitation of carbonates, which should occur close to the ocean-ice interface, can result in formation of CO_2, which condenses closer to the surface where brines are completely frozen. Presence of gas inclusions decreases ice density and facilitates its buoyancy.

Formation and redistribution of brine pockets. The distribution and amount of brine pockets in the icy shell should be affected by water capturing mechanisms and downward migration of brine. Slow ice convection and correspondingly sluggish formation of ice

at the base of the shell do not favor capturing of oceanic water. Even if captured in local high-velocity upwellings, water pockets can move down into the ocean, as observed in terrestrial sea ice. The temperature gradient and density differences between ice and captured water could be the major factors influencing downward migration. Disruptions of the icy shell through cracking followed by upwelling and freezing of oceanic water (i.e., diking) [15] could be a more effective mechanism of water capturing, at least near the base of the icy shell. Later, convection should disrupt the frozen dikes leading to redistribution of brine, gas, and salt inclusions in lower parts of the shell.

Tidal heating, if it occurs in the ice shell, could be localized in parts of the shell that are weaker due to higher content of brine and gas inclusions. However, the size and geometry of the weak zone, migration of brine pockets from surrounding ice in the temperature gradient and corresponding changes in ice density and in heat release must be taken into account. A coupled compositional-tidal-convective model is needed to best explore the links between the tidal forcing and the observed surface features.

Over time, large ice crystals might grow in the icy shell [16] causing brine, salt, and gas inclusions to be concentrated at grain boundaries. In the downwellings, melting should occur at the grain boundaries where impurities are concentrated. Redistribution of inclusions to the boundaries of large crystals may affect the rheology of the shell and make non-Newtonian flows of ice more likely, especially in downwellings.

Habitability of brine pockets. Neither low temperature nor high salinity forbids habitability of brine pockets. However, in contrast to Earth's sea ice, photosynthetic life probably does not exist on Europa. It has been proposed that organisms on Europa could produce methane and acetate from dissolved CO_2 and H_2, and/or reduce sulfate by H_2 and organic compounds to get energy for metabolism [17,18]. To survive in brine pockets, captured oceanic organisms would have to adapt to low temperatures and high salinities. Limited sources of chemical energy and nutrients during a 10^5 year journey in convective cells also make survivability difficult. Radiolytically-produced oxidants would be harmful rather than useful for captured oceanic organisms that have developed in relatively reduced conditions. If they were to survive in brine pockets, organisms would likely be in a dormant state, except perhaps in the lowest parts of the shell.

Summary: Convection in a thick icy shell creates large zones with temperatures above ~240 K in which highly concentrated brines could exist. Brines can be present in the lower and middle parts of the ice shell, depending on the location in the convective pattern. Although the ocean would be a more habitable place than the ice shell, brine pockets could provide the only habitable niches close to Europa's surface.

Acknowledgements: This work is supported by NASA Exobiology grants NAG5-7696 & NCC2-1340.

References: [1] Thomas D. N. and Dieckmann G. S. (Eds.) (2003) *Sea Ice*, Blackwell. [2] Horner R. A. (Ed.) (1985) *Sea Ice Biota*, CRC Press. [3] Thomas D. N. and Dieckmann G. S. (2002) *Science, 295*, 641-644. [4] Pappalardo R. T. et al. (1999) *JGR, 104*, 24015-24055. [5] Greenberg R. et al. (1998) *Icarus, 135*, 64-78. [6] Kivelson M. G. et al. (2000) *Science, 289*, 1340-1342. [7] McKinnon W. B. (1999) *GRL, 26*, 951-954. [8] Barr A. C. (2002) *LPS XXXIII*, Abstract 1545. [9] Barr A. C. and Pappalardo R. T. (2003) *LPS XXXVI*, Abstract 1477. [10] Zolotov M. Yu. and Shock E. L. (2001) *JGR, 106*, 32815-32828. [11] Zhong S. M. et al. (1998) *JGR, 103*, 15255-15268. [12] Spencer J. R. et al. (1999) *Science, 284*, 1514-1516. [13] Ojakangas G. W. and Stevenson D. J. (1989) *Icarus, 81*, 220-241. [14] Marion G. M. and Farren R. E. (1999) *GCA, 63*, 1305-1318. [15] Crawford G. D. and Stevenson D. J. (1988) *Icarus, 73*, 66-79. [16] Schmidt K. G. and Dahl-Jensen D. (2002) *LPS XXXIII*, Abstract 1469. [17] McCollom T. M. (1999) *JGR, 104*, 30729-30742. [18] Zolotov M. Yu. and Shock E. L. (2004) *JGR*, submitted.